ISTANBUL TECHNICAL UNIVERSITY ★ INSTITUTE OF SCIENCE AND TECHNOLOGY

THE PREPARATION OF H-SHAPED POLYMERS USING CLICK CHEMISTRY

Ph. D. Thesis by
Eda GÜNGÖR

Department : Polymer Science and Technology

Programme : Polymer Science and Technology

FEBRUARY 2011

ISTANBUL TECHNICAL UNIVERSITY ★ INSTITUTE OF SCIENCE AND TECHNOLOGY

THE PREPARATION OF H-SHAPED POLYMERS USING CLICK CHEMISTRY

Ph.D. Thesis by
Eda GÜNGÖR
(515052005)

Date of submission : 29 November 2010
Date of defence examination : 09 February 2011

Supervisor (Chairman) : Prof. Dr. Ümit TUNCA (ITU)
Members of the Examining Committee : Prof. Dr. Gürkan HIZAL (ITU)
Assoc. Dr. A. Ersin ACAR (BU)
Prof. Dr. Yusuf YAĞCI (ITU)
Prof. Dr. A. Levent DEMİREL (KU)

FEBRUARY 2011

İSTANBUL TEKNİK ÜNİVERSİTESİ ★ FEN BİLİMLERİ ENSTİTÜSÜ

CLİCK KİMYASI KULLANILARAK H ŞEKİLLİ POLİMERLERİN HAZIRLANMASI

DOKTORA TEZİ
Eda GÜNGÖR
(515052005)

Tezin Enstitüye Verildiği Tarih : 29 Kasım 2010
Tezin Savunulduğu Tarih : 09 Şubat 2011

Tez Danışmanı : Prof. Dr. Ümit TUNCA (İTÜ)
Diğer Jüri Üyeleri : Prof. Dr. Gürkan HIZAL (İTÜ)
Doç. Dr. A.Ersin ACAR (BÜ)
Prof. Dr. Yusuf YAĞCI (İTÜ)
Prof. Dr. A. Levent DEMİREL (KÜ)

ŞUBAT 2011

To my family,

FOREWORD

I would like to acknowledge first and foremost, Prof. Dr. Ümit Tunca. He has been an incredible advisor and mentor who always gave unwaivering support and guidance for which I will always be grateful. His enthusiasm and commitment becomes contagious and is a catalyst for success.

I would also like to acknowledge the guidance and recommendations of Prof. Dr. Gürkan Hızal in directing this thesis. Besides, I am honored to have Prof. Dr. Yusuf Yağcı, Prof. Dr. A. Levent Demirel and Assoc. Dr. A. Ersin Acar in the committee. I would like to express special thanks to Prof. Dr. A. Levent Demirel for measuring AFM of my samples.

Special thanks to my great friends Aydan Dağ and Dr. Hakan Durmaz. They have all been wonderful colleagues to work with throughout the years and we had a lot of good times. I hope we will always keep in touch with each other and I wish them all the best of luck in their future endeavors.

I would like to thank my friends from outside of group for all their help. In particular, İpek Ösken, Dr. Şebnem İnceoğlu, Dr. Yasemin Yüksel Durmaz, Dr. Binnur Aydoğan, Dr. Abdullah Aydoğan, Muhammet U. Kahveci, Dr. Mehmet Atilla Taşdelen, and Dr. Bünyamin Karagöz. It was really a great pleasure for me to know all of them.

Finally, I would like to thank my parents, Erbil Güngör and Fatma Güngör, my sisters Merve Güngör and Seda Günay and her husband Zahid Günay. I am thankful for supporting me through thick and thin and for always motivating me to get the job done. I am very grateful for their love, parental guidance, without which this would have been impossible. Their support has kept me alive and put me where I am today.

This work is supported by ITU Institute of Science and Technology.

February 2011 Eda GÜNGÖR

TABLE OF CONTENTS

Page

ABBREVIATIONS

AFM : Atomic Force Microscopy
ATRP : Atom Transfer Radical Polymerization
$CDCl_3$: Deuterated chloroform
CH_2Cl_2 : Dichloromethane
C/LRP : Controlled/Living Radical Polymerization
CuAAC : Copper catalyzed azide-alkyne cycloaddition
DA : Diels-Alder
DMF : *N*,*N*-dimehthylformamide
DSC : Differential Scanning Calorimetry
DVB : Divinyl benzene
EtOAc : Ethyl acetate
FRP : Free Radical Polymerization
FT-IR : Fourier Transform Infrared Spectrophotometer
GPC : Gel Permeation Chromatography
^{1}H NMR : Hydrogen Nuclear Magnetic Resonance Spectroscopy
MMA : Methyl Methacrylate
MWD : Molecular Weight Distribution
NMP : Nitroxide Mediated Polymerization
PCL : Poly(ε-caprolactone)
PEG : Poly(ethylene glycol)
PDI : Polydispersity Index
PMDETA : *N, N, N',N'', N''*-Pentamethyldiethylenetriamine
PMMA : Poly(methyl metacrylate)
PS : Poly(styrene)
P*t*BA : Poly(*tert*-butyl acrylate)
RAFT : Reversible Addition Fragmentation Chain Transfer
ROP : Ring Opening Polymerization
St : Styrene
***t*BA** : *tert*-Butylacrylate
TD-GPC : Triple Detector-Gel Permeation Chromatography
TEA : Triethylamine
TEMPO : 2,2,6,6-Tetramethylpiperidine-*N*-oxyl
THF : Tetrahydrofuran
UV : Ultra Violet
ε-CL : ε-caprolactone

LIST OF TABLES

Page

LIST OF FIGURES

Page

LIST OF SYMBOLS

dn/dc	**:** Refractive index increment
k_{act}	**:** Activation rate constant
k_{deact}	**:** Deactivation rate constant
M_n	**:** The number average molecular weight
M_w	**:** The weight average molecular weight
M_w/M_n	**:** The molecular weight distribution
ppm	**:** Parts per million
$R^{\cdot}$	**:** Radical
R_p	**:** Rate of polymerization
^oC	**:** Celsius
T_g	**:** Glass-transition temperature

THE PREPARATION OF H-SHAPED POLYMERS USING CLICK CHEMISTRY

SUMMARY

Complex macromolecules have been prepared in the search for polymers with developed mechanical and physical properties. H-shaped polymer is a good example of complex macromolecular architectures. H-shaped polymers are defined as two side chains attached to the each end of a polymer backbone (main chain), inspite of their broad applications, the synthesis of H-shaped polymers with well-defined structure remains a challenge.

The ionic polymerizations (anionic or cationic) were the only living systems available until last decade. These systems provide polymers with controlled molecular weight, well-defined chain ends, and low polydispersity. In recent years, the use of controlled/living radical polymerization (C/LRP) methods for the synthesis of complex macromolecules has fast increased because of the variety of applicable monomers and more tolerant experimental conditions than the living ionic polymerization routes require. Reversible addition fragmentation chain transfer (RAFT) polymerization, nitroxide-mediated free radical polymerization (NMP), and metal mediated living radical polymerization often called atom transfer radical polymerization (ATRP) are versatile methods for living radical polymerizations.

Meanwhile, the development of the click reactions particularly, copper (I) catalyzed azide-alkyne cycloaddition (CuAAC) and Diels–Alder (DA) reactions have provided new synthetic pathways for the preparation of H-shaped polymers. From this point of view, in this thesis, we described the synthesis of H-shaped polymers using different controlled/living polymerization techniques and CuAAC or the combination of DA and CuAAC click reactions.

In the first study, we investigated the CuAAC click reaction for the preparation of H-shaped polymer that has two thermodynamically incompatible arms (PS and PMMA) on either side of the central unit (P*t*BA or PEG). Using this strategy, diazide end functionalized P*t*BA or PEG (main chain) and PS-*b*-PMMA copolymer (side chains) with an alkyne functional group at the junction point were linked to give (PS)(PMMA)-P*t*BA-(PMMA)(PS) and (PS)(PMMA)-PEG-(PMMA)(PS) heteroarm H-shaped terpolymers (Figure 1).

Second, we extended CuAAC modular approach to the first time preparation of fully heteroarm H-shaped (ABCDE type) quintopolymer consisting of P*t*BA block as a main chain and poly(ε-caprolactone) (PCL), PS, PEG, and PMMA blocks as side chains. CuAAC click reaction of azide end-functionalized miktoarm star terpolymer with block copolymer having alkyne at the junction point was carried out for the preparation of target H-shaped quintopolymer (Figure 2).

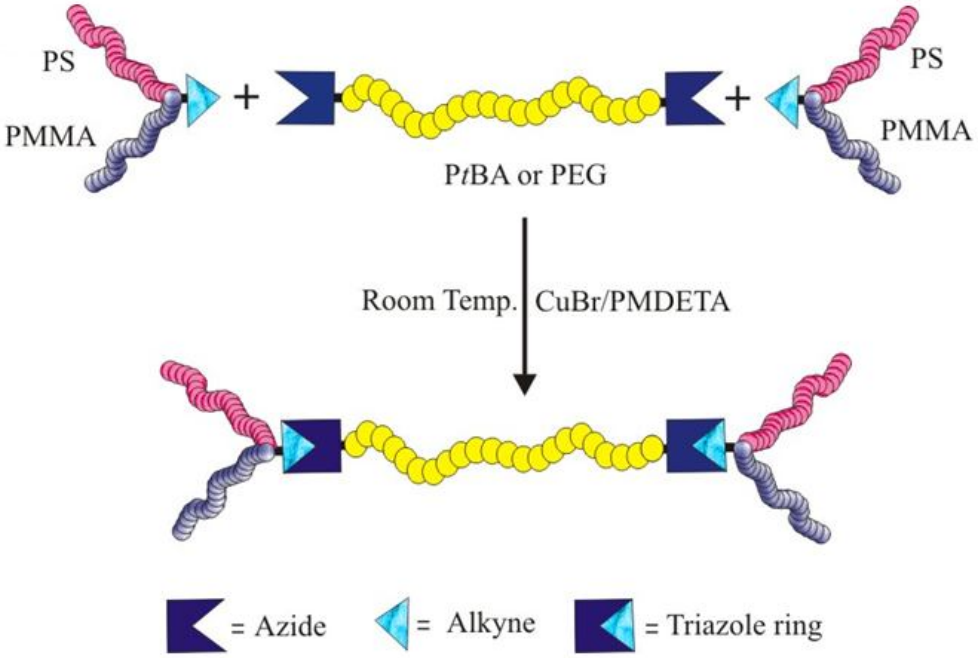

Figure 1: Synthesis of heteroarm H-shaped terpolymers via CuAAC click reaction.

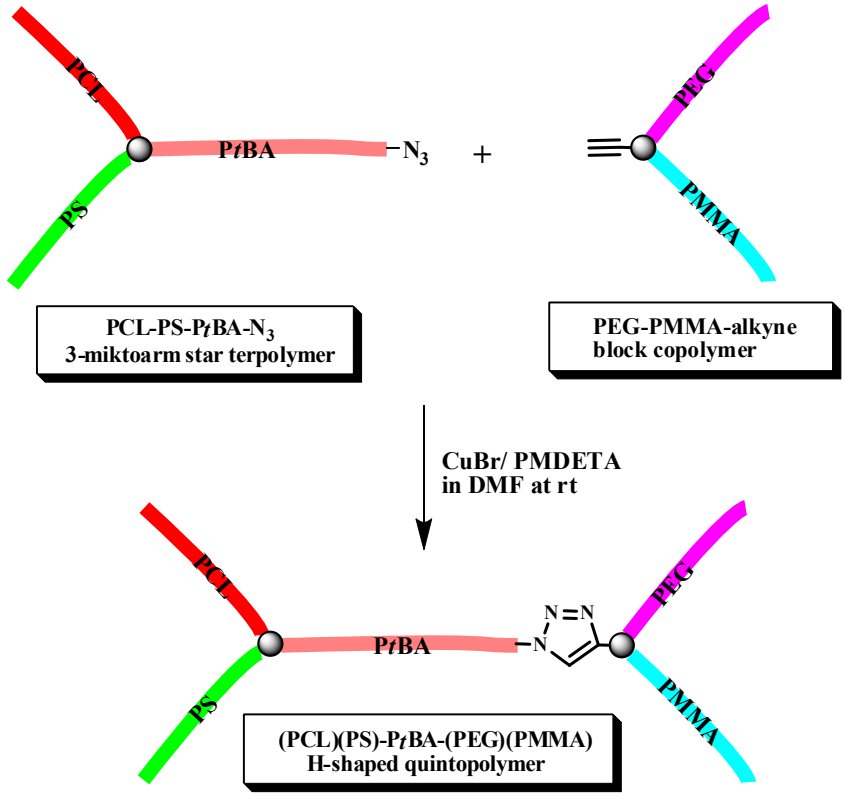

Figure 2: Synthesis of ABCDE type H-shaped quintopolymer via CuAAC click reaction.

Finally, the effective use of double click reactions involving the CuAAC and DA double click reactions for the preparation of H-shaped polymer possessing pentablocks with different chemical nature, which, contains well-defined PEG-*b*-PMMA and PCL-*b*-PS side chains and a P*t*BA main chain. The first time using double click reactions in a one-pot manner enabled us to provide an alternative and a simple way for the preparation of well-defined H-shaped quintopolymer (Figure 3).

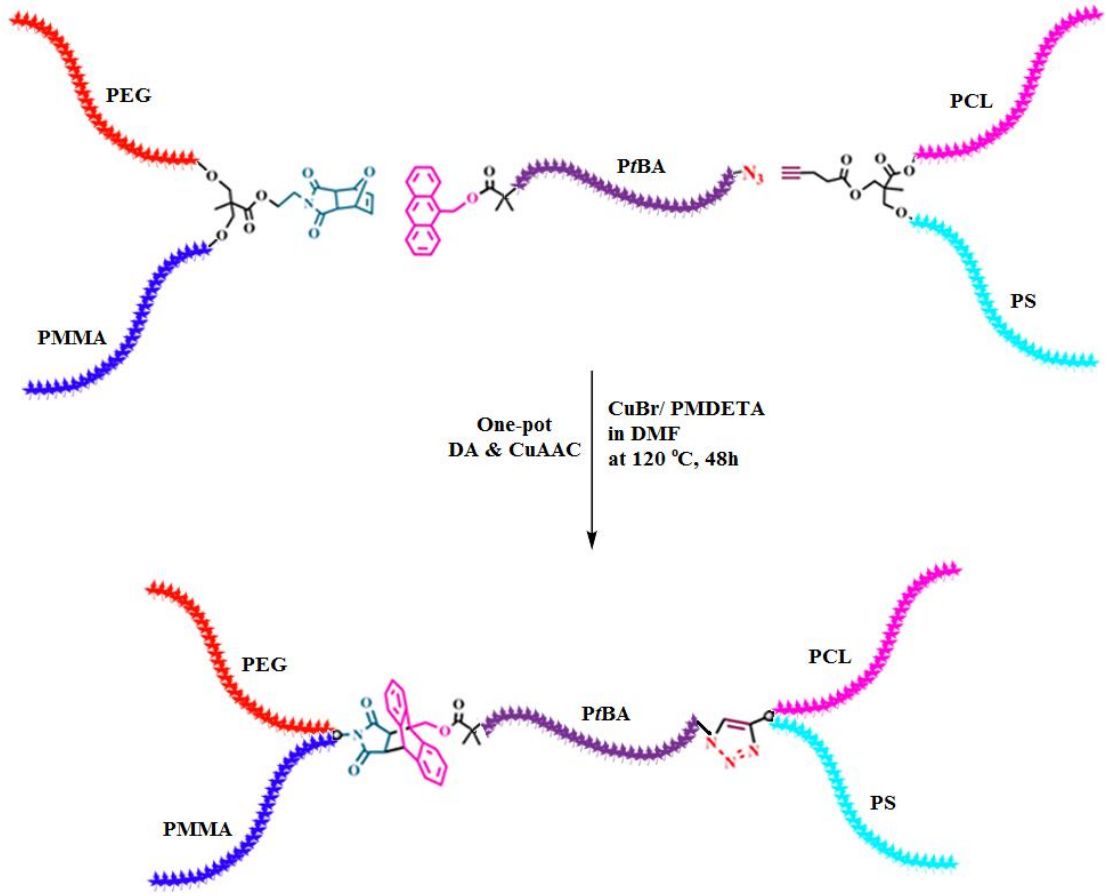

Figure 3: Synthesis of ABCDE type H-shaped quintopolymer via one-pot CuAAC and Diels-Alder click reactions.

CLİCK KİMYASINI KULLANARAK H TİPİ POLİMERLERİN SENTEZİ

ÖZET

Kompleks makromoleküller, polimerlerin mekanik ve fiziksel özelliklerinin geliştirilmesi araştırmaları için sentezlenmektedir. H şeklindeki polimerler, kompleks makromoleküller için iyi bir örnektir. H şeklindeki polimerler, polimer ana zincirinin her iki ucuna iki yan zincirin bağlanması olarak tanımlanır ve geniş bir uygulama alanına sahip olmalarına rağmen iyi tanımlanmış H şekilli polimerlerin sentezi oldukça zordur.

Son on yıla kadar, iyonik polimerizasyon (anyonik veya katyonik), yaşayan sistemler içinde mevcut tek yöntemdi. Bu sistemler, polimerlerin kontrollü molekül ağırlığına, iyi tanımlanmış zincir uçlarına ve düşük molekül ağırlığı dağılımına sahip olmalarını sağlar. Ancak son yıllarda, kontrollü/yaşayan radikal polimerleşme yöntemleri, çok fazla monomere uygulanabilmesi ve yaşayan iyonik polimerizasyon yöntemlerine göre deneysel koşullarının daha toleranslı olması, kompleks makromoleküllerin sentezlenmesinde kullanımı hızlı bir şekilde artmıştır. Tersinir ekleme-ayrılma zincir transfer polimerizasyonu (RAFT), nitroksit ortamlı radikal polimerizasyonu (NMP) ve genellikle atom transfer radikal polimerizasyonu (ATRP) olarak bilinen metal ortamlı yaşayan radikal polimerizasyonu en yaygın olarak kullanılan yaşayan radikal polimerizasyon yöntemlerindendir.

Bu arada ‘’click reaksiyonlarının’’ gelişmesi, özellikle bakır(I) katalizli azid-alkin siklokatılma (CuAAC) ve Diels-Alder reaksiyonları H şekilli polimerlerin hazırlanması için yeni sentetik yollar sağlamıştır. Bu noktadan hareketle bu tezde, farklı kontrollü/yaşayan radikal polimerizasyon teknikleri ve sadece bakır(I) katalizli azid-alkin siklokatılma (CuAAC) veya CuAAC ve Da click reaksiyonlarının birlikte kullanılmasıyla H şekilli polimerlerin sentezi gerçekleştirilmiştir.

İlk çalışmada, merkezi birimin (P*t*BA veya PEG) her iki tarafında termodinamik olarak uyumlu iki farklı kollara (PS ve PMMA) sahip H şekilli polimerler sentezlenmiştir. Bu stratejiyi kullanarak, diazid uç gruplu P*t*BA veya PEG (ana zincir) ve alkin uç gruplu PS-*b*-PMMA kopolimer (yan zincirler) arasında gerçekleşen CuAAC click reaksiyonu ile (PS)(PMMA)-P*t*BA-(PMMA)(PS) ve (PS)(PMMA)-PEG-(PMMA)(PS) farklı kollara sahip H şekilli terpolimerler sentezlenmiştir (Şekil 1).

İkinci olarak, farklı kollara sahip, ana zinciri P*t*BA olan ve poli(ε-kaprolakton) (PCL), PS, PEG, and PMMA yan zincirli H şekilli (ABCDE tipi) pentapolimer, CuAAC modüler yaklaşımı kullanılarak hazırlanmıştır. Azid uç gruplu farklı kollu yıldız polimer ile alkin fonksiyonelitesine sahip blok kopolimer arasında gerçekleşen CuAAC click reaksiyonu ile amaçlanan H şekilli pentapolimer sentezlenmiştir (Şekil 2).

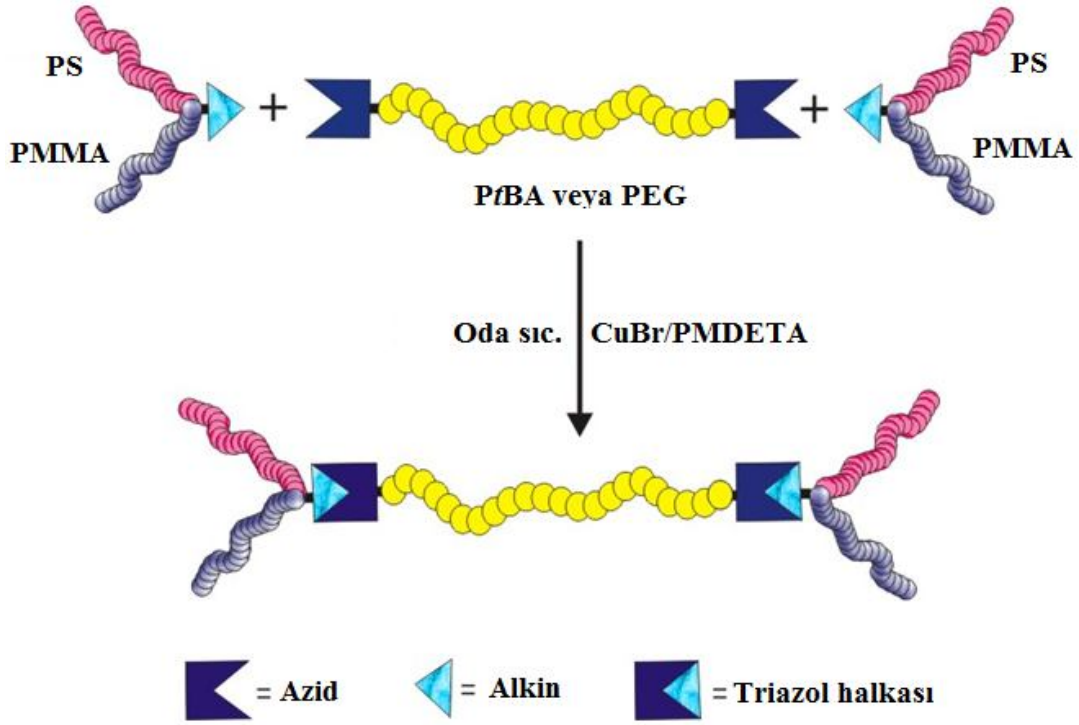

Şekil 1: CuAAC click reaksiyonu ile hetero kollu H şekilli terpolimerlerin sentezi.

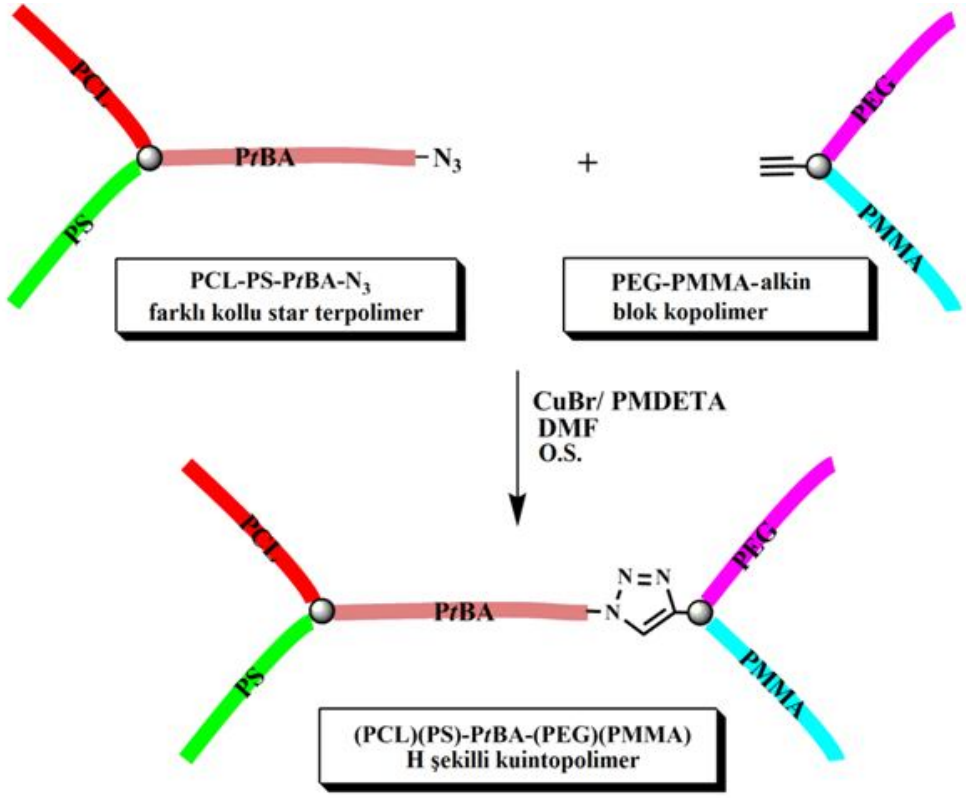

Şekil 2: CuAAC click reaksiyonu ile H şekilli ABCDE tip pentapolimerin sentezi.

Son olarak, etkin bir biçimde CuAAC ve DA çift click reaksiyonları kullanılarak farklı kimyasal yapılara sahip pentablok H şekilli polimer sentezlenmiştir. H şekilli kuintopolimerde ana zincir olarak antrasen ve azid uç gruplarına sahip P*t*BA ve iyi tanımlanmış maleimid fonksiyonlu PEG-*b*-PMMA ve alkin fonksiyonlu PCL-*b*-PS, yan zincirlirinin arasında tek adımda gerçekleşen çift click reaksiyonları ile hazırlanmıştır ve H şekilli ABCDE tipi pentapolimerinin sentezlenmesi için alternatif bir yol sağlamıştır (Şekil 3).

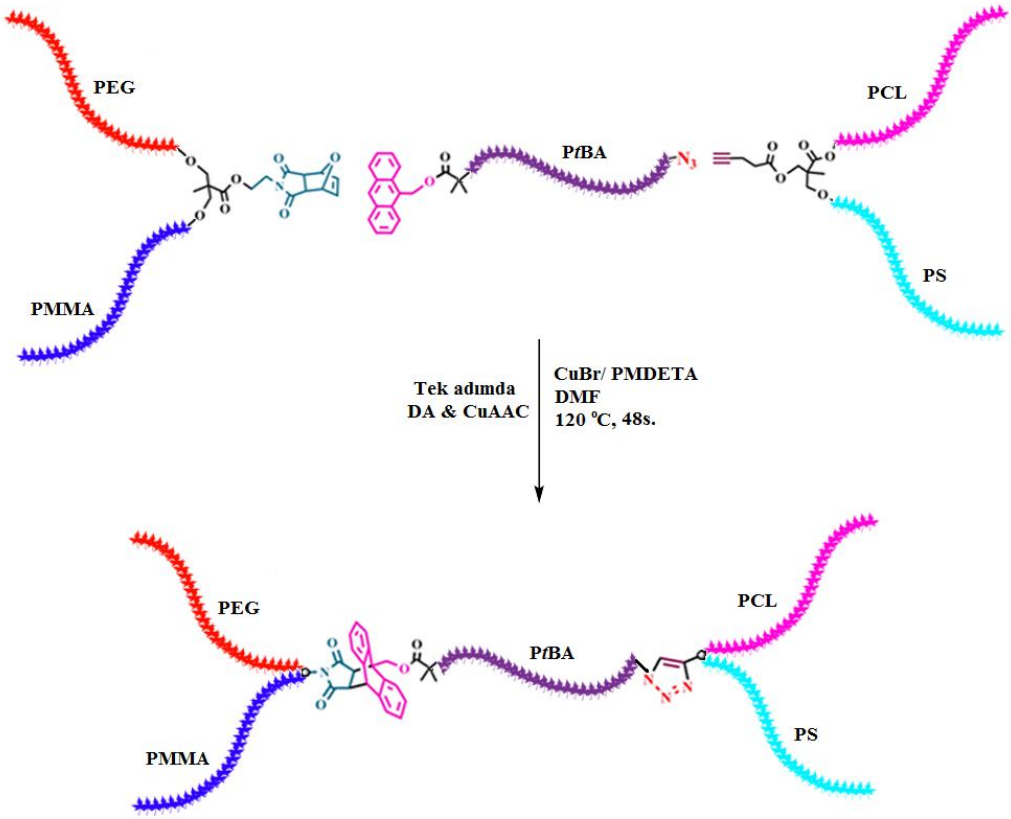

Şekil 3: Tek adımda CuAAC ve Diels-Alder click reaksiyonları ile H şekilli ABCDE tip pentapolimerin sentezi.

1. INTRODUCTION

The ionic polymerizations (anionic or cationic) were the only living systems available until recently. These systems provide the polymers with the controlled molecular weight, well-defined chain ends and low polydispersity. In recent years, the controlled/living radical polymerization (C/LRP) techniques for the synthesis of complex macromolecules has fast increased because of the variety of applicable monomers and more tolerant experimental conditions than the living ionic polymerization techniques require [1-3]. The reversible addition fragmentation chain transfer [4] (RAFT) polymerization, the nitroxide-mediated radical polymerization [5] (NMP), and the metal mediated living radical polymerization often called atom transfer radical polymerization [6-8] (ATRP) are versatile methods for the living radical polymerizations.

The "click chemistry" concept was introduced by Sharpless and coworkers in 2001 [9]. Selected reactions were classifield as click chemistry if they were modular, stereospecific, wide in scope, resulted in high yields, and generated only safe byproducts. Several efficient reactions such as copper (I) catalyzed azide-alkyne cycloaddition (CuAAC), Diels-Alder (DA) and thiol additions to double bond (thiol-ene), can be classified under this term. Since their fast growth, click chemistry strategies have been rapidly integrated into the field of macromolecular engineering and extensively been used in the synthesis of polymers ranging from linear to complex structures.

A branched polymer structure is elucidated as a nonlinear polymer with multiple backbone chains growing from junction points [10]. It has been shown that branching results in a more compact structure in comparison with linear analogs of similar molecular weight, due to its high segment density, which changes the melt, solution, and solid-state properties of the polymer [10]. Nonlinear polymers primarily include star, miktoarm star, hyperbranched, dendrimers, dendrimer like star, and H-shaped polymers.

H-shaped polymers defined as two side chains linked to the each end of a polymer backbone (main chain) have been generally prepared through anionic polymerization technique starting from chlorosilane or aromatic diolefins as coupling agents [11-15]. Various types of H-shaped homo- and copolymers have been successfully prepared using this technique. Because of its architectural difference, H-shaped polymers show different rheological and micellar properties and self-assembled structures compared to analogous linear or branched block copolymers. H-shaped polymers are important as model materials in understanding the rheology of branched polymers such as low density polyethylene (LDPE) [16-18]. H-shaped copolymers form micelles with lower aggregation numbers, which results in smaller micellar structures, compared to linear block copolymers [19, 20]. The self-assembly of H-shaped copolymers show a variety of morphologies depending on the preparation conditions [21]. The synthesis of H-shaped polymers, having various chemical structures, is thus important to thoroughly understand the above-mentioned physical properties.

In this thesis, we developed novel approaches for the synthesis of various H-shaped polymers using different kinds of C/LRP polymerization techniques and CuAAC or the combination of DA and CuAAC click reactions. For this purpose, first, the preparation of H-shaped polymer that has two thermodynamically compatible arms (PS and PMMA) on either side of the central unit (P*t*BA or PEG). Using this strategy, diazide end-functionalized P*t*BA or PEG (main chain) and PS-*b*-PMMA copolymer (side chains) with an alkyne functional group at the junction point were linked to give (PS)(PMMA)-P*t*BA-(PMMA)(PS) and (PS)(PMMA)-PEG-(PMMA)(PS) heteroarm H-shaped terpolymers.

Subsequently, CuAAC click reaction was applied to the preparation of fully heteroarm H-shaped (ABCDE type) quintopolymer consisting of P*t*BA block as a main chain and poly(ε-caprolactone) (PCL), PS, PEG, and PMMA blocks as side chains. A click reaction of azide end-functionalized miktoarm star terpolymer with block copolymer having alkyne at the junction point was carried out for the preparation of target H-shaped quintopolymer.

In addition, the combination of CuAAC and DA double click reactions were first time employed for the synthesis of H-shaped quintopolymer (PCL)(PS)-P*t*BA-(PEG)(PMMA) using one-pot technique.

2. THEORETICAL PART

2.1 Controlled/Living Radical Polymerization (C/LRP)

Macromolecular engineering of polymers with well-defined and applications through composition, size (molecular weight), uniformity (polydispersity), topology and end-functionality is essential to modern synthetic polymer chemistry research and advanced technological applications [22-28].

Nearly vast part of commercial synthetic polymers is made by using conventional free radical polymerization (FRP), which has so many advantages such as the polymerization of numerous vinyl monomers under mild reaction conditions, requiring an oxygen free medium, also tolerant to water, and a large temperature range (-80 to 250^{o}C) [29]. But it has some limitations, particularly in comparison with living processes [30, 31].

The term of living polymerization is a chain growth polymerization. An ‘’ideal’’ living system is that the growing chain end propagates without chain transfer and termination. Szwarc et al. reported the first living polymerization in 1956, which was the anionic polymerization of styrene with sodium naphthalenide [32, 33]. Well-defined polymers with uniform size, desired functionalities and various architectures have been increasingly achieved via living ionic polymerization. However, ionic polymerizations typically require stringent reaction conditions and have a limited range of (co)polymerizable monomers [34]. Following developments in living anionic polymerization by Michael Szwarc, new approaches towards synthesis of macromolecular engineered materials termed as controlled/’living” radical polymerizations (C/LRP) have been developed [35-37].

Mechanistically, C/LRPs are similar to FRP and proceed through the same intermediates. However, in C/LRPs the equilibrium between active and dormant species allows steadily growth of polymer chains via near instantaneous initiation and chain breaking reactions is minimized [36, 38]. There are three classes of C/LRP, i.e. nitroxide mediated polymerization (NMP) [39, 40] atom transfer radical

polymerization (ATRP) [41-44], and reversible addition-fragmentation chain transfer (RAFT) polymerization [45, 46]. These methods have been known as powerful tools for preparing polymers with predetermined molecular weights, narrow molecular weight distributions, specific end functionalities, and well- defined architectures [40].

2.1.1 Nitroxide mediated radical polymerization (NMP)

In 1982, Otsu et al. were the first to attempt to use a stable radical as a mediating agent in free radical polymerization (reaction 2.1) [47]. This process proceed with an *iniferter* compound which is capable of *ini*tiation, trans*fer*, and *ter*mination. Different from common initiators that homolytically cleave to yield two identical primary radicals, iniferters also cleave homolytically to give two radicals but one initiate the system and the other one reversibly terminates a propagating chain. The iniferter process was limited control because the initiating radical generally was too unreactive and/or the stable free radical also initiated chains. The most favorable iniferter processes have leaned on thioiniferters, which can control molecular weight with low polydispersities (M_w/M_n) (reaction 2.4) [48].

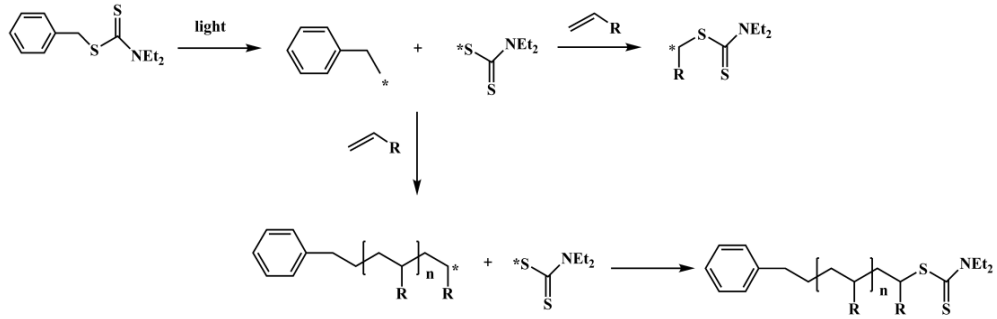

(2.1)

Building on the limited success of the iniferter process, NMP was introduced in 1986 by Solomon, Rizzardo and Moad. They were the first to demonstrate the reversible end capping of the propagating chain ends by alkoxyamines, as 2,2,6,6-tetramethylpiperidinyl 1-oxy (TEMPO). At temperatures typically associated with the process (40-60 °C), the TEMPO capped molecules were stable and did not participate further in the reaction. Further work investigate the same concept at slightly elevated temperatures (80-100 °C), which yielded low molecular weight oligomers. This initial NMP process was successful to control only styrenics, and like the iniferter process, limited control was obtained [5].

The use of TEMPO in C/LRP was a report from the group of Georges [5] who demonstrated that polystyrene with narrow MWD can be prepared using a mixture of benzoyl peroxide (BPO) and TEMPO as an initiating system [49]. The key feature of this work was the realization that, while nitroxides are polymerization inhibitors at low temperatures, hence their use by Solomon to trap polymerization intermediates, at elevated temperatures they may act as polymerization mediators, not inhibitors. TEMPO is employed to contribute to the simultaneous initiation of all the polymer chains by promoting the dissociation of peroxide initiators. These two seminal reports resulted in developments of the modern of C/LRP era (reaction 2.2).

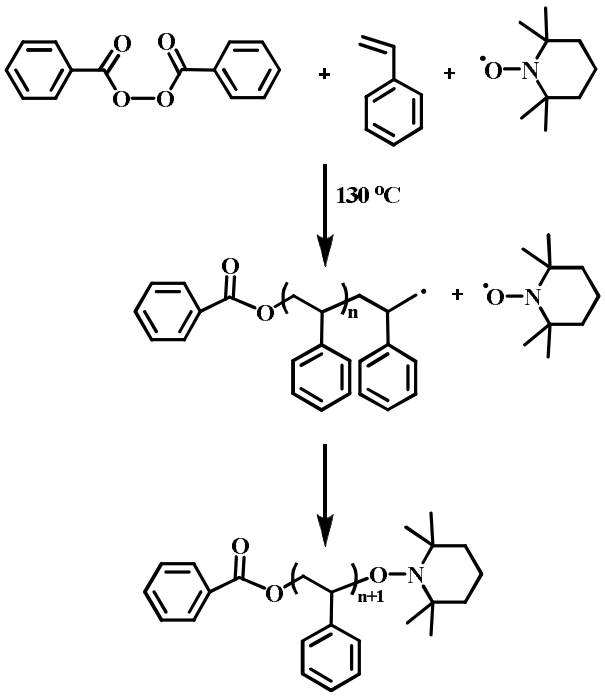

(2.2)

In addition to the bimolecular systems described above, the unimolecular processes have offered some advantages over bimolecular systems. In these processes, the unimolecular alkoxyamine initiators are shelf-stable and the polymerization can be induced with simple monomer addition and heating. More importantly, the decomposition of these initiators yields a stoichiometric amount of nitroxide relative to the initiating radical. This is important, as each polymer chain initiated will be capped by nitroxide leading to controlled living polymerization and ultimately polymers with low MWD. The amount of initiator added to the polymerization can be accurately weighed, and consequently, the resulting polymer chain length can be determined by the monomer to initiator ratio. The structure of the typically used unimolecular initiators for NMP can be seen in 2.3.

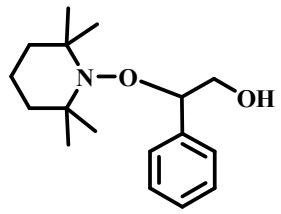
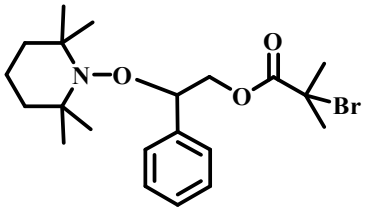

(2.3)

If it is needed to explain briefly from NMP type process, the propagating species ($P_n\cdot$) reacts with a stable radical ($X\cdot$) as seen in mechanism 2.4 . The resulting dormant species (P_n-X) can then reversibly cleave to regenerate the free radicals once again. Once $P_n\cdot$ forms it can then react with a monomer, M, and propagate further (reaction 2.4).

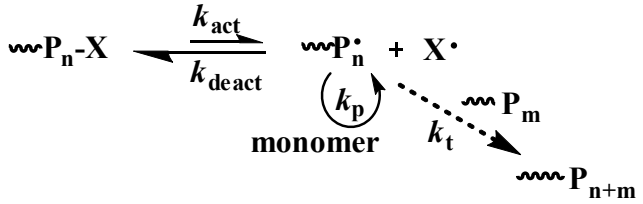

(2.4)

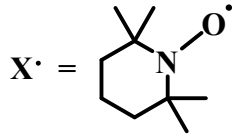

TEMPO (2,2,6,6 tetramethyl-piperidinyloxy)

Several researchers have investigated alternative nitroxide mediators, a quest for new and better nitroxides began. Originally, NMP mediated by TEMPO was limited by slow polymerization (25-70 h), high polymerization temperature (125-145 °C), and a limited range of suitable monomers, mainly styrene and derivatives [5, 50]. The discovery of new types of nitroxides (such as *N*-*tert*-butyl-*N*-(1-diethylphosphono-2,2-dimethylpropyl)-*N*-oxyl or DEPN, 2,2,5,5-tetramethyl-4-phenyl-3-azahexane-3-oxyl or TIPNO, and *N*-*tert*-butyl-(1-*tert*-butyl-2-ethylsulfinyl)propyl nitroxide or BESN) [34, 36, 40, 51, 52] also contributed to overcoming the original limitations (2.5). These nitroxides have been used successfully in the controlled polymerizations of acrylates, acrylamides, dienes, and acrylonitriles. Their improved ability compared to TEMPO has been attributed to several factors. They are more sterically crowded than TEMPO, which decreases the rate of combination and increases the rate of dissociation from carbon-centered radicals. This shift in the homolysis equilibrium leads to faster rates of polymerization and makes these nitroxides more effective as mediators in NMP.

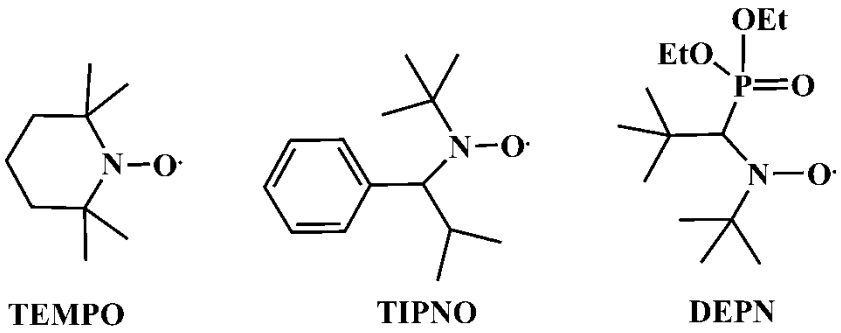

TEMPO TIPNO DEPN (2.5)

As a result, NMP system is achieved to control with dynamic equilibration between dormant alkoxyamines and active propagating radicals, so it has become popular method in polymer chemistry for preparing living polymers under mild, chemoselective conditions with good control over both the polydispersity and molecular weight [40].

2.1.2 Atom transfer radical polymerization (ATRP)

The name of atom transfer radical polymerization (ATRP) comes from the atom transfer step. In 1995, Matyjaszewski [53] and Sawamoto [54] reported independently that metal-catalyzed atom transfer radical addition (ATRA) can be successfully applied to radical polymerization processes to control the growth of chains.

ATRP is also related to transition metal initiated redox processes and inhibition with transition metal compounds [55]. These two techniques allow for either an activation or deactivation process. A general mechanism for ATRP is shown in reaction 2.6.

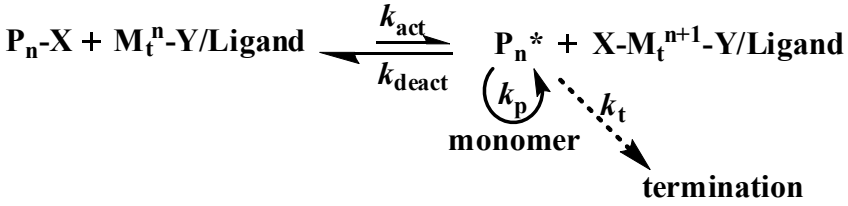

(2.6)

The propagating species P_n^* , are generated during a reversible redox process catalyzed by a transition metal complex (activator, M_t^n –Y/ ligand, where Y may be another ligand or a counterion) which undergoes a one-electron oxidation with concomitant abstraction of a (pseudo)halogen atom, X, from a dormant species, P_n–X. Radicals react reversibly with the oxidized metal complexes, $X–M_t^{n+1}$/ligand, the deactivator, to reform the dormant species and the activator. This process occurs with

a rate constant of activation, k_{act}, and deactivation k_{deact}, respectively and the dynamic equilibrium favors the dormant species. Polymer chains grow by the addition of the free radicals to monomers like a conventional radical polymerization, with the rate constant of propagation, k_p. Termination reactions (k_t) also occur in ATRP, mainly through radical coupling and disproportionation; however, in a well-controlled ATRP, no more than a few percent of the polymer chains undergo termination. So linear first-order kinetic plot, which is accompanied by a linear increase in polymer molecular weights with conversion confirm the "livingness" character of ATRP process.

ATRP, which is the most versatile method of the controlled radical polymerization system, uses a wide variety of monomers, catalysts, solvents, and reaction temperature. ATRP was improved by designing a proper catalyst, using an appropriate initiator, and adapting the polymerization conditions. This provides to control over the topology (stars, combs, branched), the composition (block, gradient, alternating, statistical), and the end functionality [56-58].

ATRP process has many advantages compared with other C/LRP processes. First of all, commercially available reagents (alkyl halides, ligands and transition metals) are using. Moreover, the dynamic equilibrium between dormant and active species can be easily and appropriately adjusted for a given system by modifying the complexing ligand of the catalyst [59]. However, there are drawbacks, which are intolerance to water and acidic species, the necessity of removing the often cytotoxic catalyst.

In ATRP process can be used a variety of monomers, allowing control during the polymerization of styrenics [59], (meth)acrylates [60], acrylamides [61, 62], vinylpyridines [63, 64], and acrylonitrile [65]. Additionally, ATRP has tolerance to many functional groups such as amido, amino, ester, ether, hydroxy, siloxy and others. Having 'free' carboxylic acid funtional monomers are not used for ATRP, since they potentially complexes with the catalyst and disables ATRP, and therefore, presently, it has to be protected. Recent work has shown that monomers bearing ionic substituents such as sodium 4-vinylbenzoate, sodium 4-vinylbenzylsulfonate and 2-trimethylammonioethyl methacrylate methanesulfonate and triflate, and dimethylaminoethyl methacryate can be polymerized directly [66].

The initiator posses an important role to determine the number of growing chains. In ATRP, alkyl halides (RX) are typically used as initiators. For the successful polymerization, initiation should be quantitative and faster than propagation. To obtain best controlled polymers over narrow PDI and molecular weight, the halide group, X, should transfer fast between the growing chain and the transition metal complex. So, X must be either bromine or chlorine. Iodine works well for acrylate polymerizations in copper-mediated ATRP [67] but fluorine is not suitable because The carbon–fluorine bond strength is too strong for the fast activation–deactivation.

The catalyst has the main role in ATRP since it determines the position of the atom transfer equilibrium and the dynamics of exchange between the dormant and active species. There are some requirements, using a catalyst in ATRP process [67]. 26 First, the metal center must have at least two oxidation states. Second, the metal center should have enough affinity toward a halogen, also the ligand should complex the metal relatively strongly. ATRP has been successfully worked by a variety of metals, including those from Groups 4 (Ti [68]), 6 (Mo [69-71]), 7 (Re [72]), 8 (Fe [73-76], Ru [77], Os [69]), 9 (Rh [78], Co [60]), 10 (Ni [79, 80], Pd[81]), and 11 (Cu [59, 82]). But complexes of Cu have been found to be the most efficient catalysts in the ATRP.

Ligand is the other important component for ATRP system. It helps to solubilize the transition metal salt in the organic media and to adapt the redox potential and dynamics of exchange between the dormant and active species with atom transfer [83]. The ligand should complex strongly with the transition metal, and also allow expansion of the coordination sphere and selective atom transfer without any side reactions. Commonly employed nitrogen-based ligands used in conjunction with Cu ATRP catalysts include derivatives of bidentate bipyridine (bpy) [82, 84] and pyridine imine [85], tridentate diethylenetriamine (DETA) [86], and tetradentate tris[2-aminoethyl]amine (TREN) [87] and tetraazacyclotetradecane (CYCLAM) [88].

2.1.3 Reversible addition–fragmentation chain transfer process (RAFT)

The reversible-addition fragmentation chain transfer (RAFT) is the most recent process of the living/controlled radical polymerization. It was introduced in 1998 by the Common-wealth scientific and Industrial Research Organization (CSIRO) in Melbourne, Australia [4]. The RAFT technique relies on the principle of degenerative

chain transfer between active and dormant species and varies fundamentally from NMP and ATRP. This key component in the RAFT process is a so-called RAFT agent or chain transfer agent (CTA). Thiolcarbonylthio species are usually used as a CTA. Depending on the nature of the Z group, thiolcarbonylthio RAFT agents are divided into four classes i.e. dithioester, xanthates, dithiocarbamates, and trithiocarbonate (2.7).

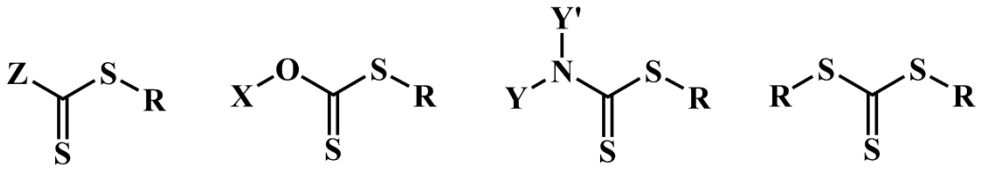

(2.7)

The RAFT polymerization has important advantages. Polymerization is successfully realized from a wide range of monomers in varying solvents, including water, using only chain transfer agents and common free radical initiators (without needing any component such as metal catalysts) [4, 89-92]. It also show tolerance to a wide variety of functional groups, namely –OH, -COOH, -$CONR_2$, -NR_2, - SO_3Na etc., in monomer and solvent [93-99]. A wide variety of architectures such as telechelic, block copolymers, graft copolymers, gradient copolymers, nanogels, stars, and dendritic structures can be synthesized by using RAFT technique [100-109]. Moreover, RAFT can be carried out in bulk, in solution, and in heterogeneous system (e.g.,suspension, emulsion) [110-113].

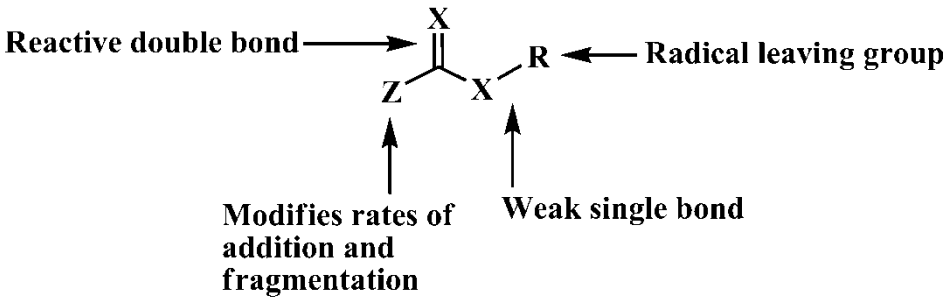

Figure 2.1: General representation of RAFT agents.

For successful RAFT polymerization, the structures of RAFT agent (Figure 2.1) should crefully be designed. The Z group of a RAFT agent is highly influential in determining its reactivity and consequently its effectiveness at mediating polymerization. The Z group should be chosen so that it will activate the C=S bond

toward radical addition and then impart minimal stabilization of the adduct radical formed. It is necessary to choose a Z group that is suitable for mediating the polymerization of a specific monomer. More reactive monomers are better controlled by RAFT agents that have a lesser activating effect on the thiocarbonyl group and, therefore, a greater destabilizing effect on the adduct radical, thus favoring fragmentation. The adduct radical formed by a more reactive monomer is more stable and less likely to undergo fragmentation. Thus, a Z group that destabilizes the adduct radical is required so that fragmentation can occur.

Two parameters influence to the selection of R group. First, the R group should be a better leaving group compared with the propagating radical. Second, it must efficiently reinitiate monomer. Steric factors, radical stability, and polar effects have main roles to determine the leaving/reinitiating ability of an R group [111, 114]. Design of RAFT agents so that the R group is structurally similar to the monomer being polymerized is occasionally employed. This allows the R group to have similar structural and electronic properties to the propagating radical, thus increasing reinitiation ability. The commonly accepted mechanism of the RAFT polymerization with the thiocarbonylthio-based RAFT agents involves a series of addition–fragmentation steps as depicted below (reaction 2.8 a-e).

The method for radical generation is identical to that used in conventional free radical polymerization (e.g., thermoinitiator, photoinitiator, and gamma irradiation). In early stages, the primary radical reacts with monomer to form a propagating radical Pn• (reaction 2.8a). The addition of Pn• to the RAFT CTA followed by the formation of dormant species (macroCTA) and a new fragment radical, R• (reaction 2.8b) which reinitiates the polymerization to form a new propagating chain (Pm•) (reaction 2.8c). In the presence of monomer, the equilibrium between the active propagating species (Pn• and Pm•) with the dormant polymeric RAFT compound leads to an equal probability growing for all chains (reaction 2.8d). At the very early stage of the polymerization, RAFT CTAs are consumed to insure that all chains are initiated before propagation. Following addition-fragmentation steps allow a dynamic equilibrium to be established between the active propagating radicals (Pn• and Pm•) and the dormant polymeric dithioester compounds [Pn-S-C(Z)=S and Pm-S C(Z)=S].

A fast equilibrium is necessary for all the polymeric radicals to propagate with the same probability and achieve low polydispersity polymers. When the polymerization is complete, the great part of the chains contain end-functionality.

Initiation and propagation

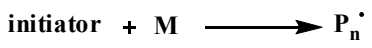

(2.8a)

Addition to RAFT agent

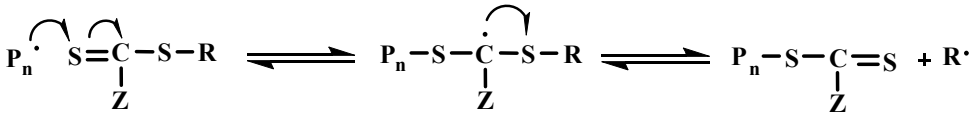

(2.8b)

(A)

Reinitiation

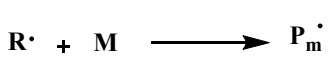

(2.8c)

Chain equilibration by reversible addition fragmentation

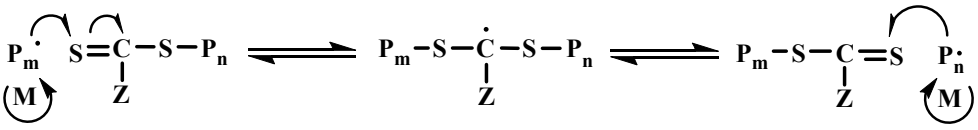

(2.8d)

(B)

Overall

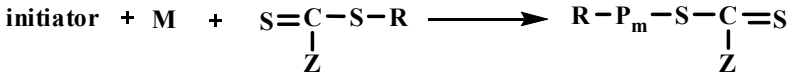

(2.8e)

2.2 Ring-Opening Polymerization (ROP)

Aliphatic poly(ester)s receive increasing attention nowadays due to their biodegradable property. Poly(ester)s can be prepared from a wide range of materials with judicious choice of monomer feedstock able to modulate the physio-chemical properties including glass transition temperatures, toughness, stiffness and degradability.

Aliphatic poly(ester)s are prepared through one of two routes: the first is step-growth polycondensation of a hydroxy acid or between a diacid and a diol. The second route is ring-opening polymerization (ROP). It is a unique polymerization process, in which a cyclic monomer is opened to generate a linear polymer, e.g., ROP of ε-caprolactone (CL) (reaction 2.9). ROP is a chain polymerization, comprise of a

sequence of initiation, propagation and termination, so different from step polymerization. Altough ROP like as living polymerization because of increasing molecular weigth linearly with conversion [115], it differs from chain polymerizations due to reaction kinetics. By this methodology the preparation of high molecular weight aliphatic poly(ester)s is possible while maintaining high levels of control over their molecular characteristics under relatively mild conditions.

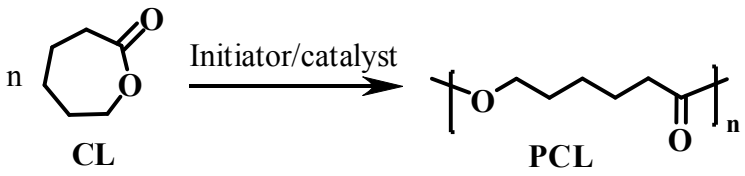

(2.9)

The thermodynamic factors (ΔH, ΔS, ΔG) affecting the ring opening of a cyclic monomer will be due to the relative stability of the linear polymer in comparison to its corresponding monomer [115]. Four or seven membered rings have greater ring strain in comparison with five or six membered rings and hence there is a greater thermodynamic driving force for their ROP. A series of simple lactones of varying ring size and strain have been investigated. Generally, substituents on the rings decrease the ring strain and thereby the polymerizability of the rings.

2.2.1 Coordination-insertion ring-opening polymerization

There are different types of ROP processes, including anionic, cationic, organocatalytic and coordination-insertion [116]. But the latter one has gained increasing attention, which is the most efficient method for the production of well-controlled polyesters in terms of molecular weight, narrow PDI and different compositions.

The commercially available tin(II) bis(2-ethylhexanoate) $Sn(Oct)_2$, zinc(II) lactate and aluminium(III) isopropoxide ($AlOiPr_3$) [117, 118] metal-based initiating systems are widely used for the controlled ring-opening polymerization of cyclic esters and brought important contributions for the mechanism understanding.

The ROP proceeds mainly via two major polymerization mechanisms depending on the used organometallics. Some of them acts as catalysts, and activate the monomer by complexation with the carbonyl group e.g.,$Al(Oi\text{-}Pr)_3$ (reaction 2.10).

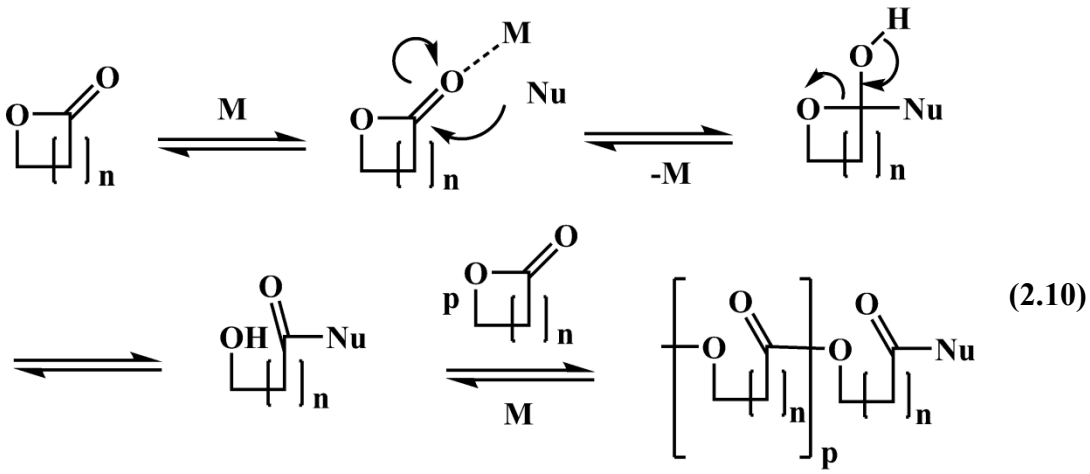

(2.10)

M=Metal Nu=Nucleophile

Tin (II) 2-ethylhexanoate is the most commonly prefered catalyst for ROP. It is a very effective and versatile catalyst, which is easy to handle and is soluble in common organic solvents. The Food and Drug Administration has accepted it as a food additive. It is also known as stannous octoate $(SnOct)_2$.

$Sn(Oct)_2$ is intrinsically more active than $Al(O\textit{i}\text{-}Pr)_3$, also the polymerization was found to be even faster and better controlled when $Sn(Oct)_2$ was combined with a protic reagent such as an alcohol (reaction 2.11). The second mechanism for $Sn(Oct)_2$-catalyzed ROP has been the subject of much more arguments. Though it is usually accepted that protic reagents react with $Sn(Oct)_2$ to form covalent tin(II) alkoxides, and the reaction conditions suh as temperature, alcohol-to-tin ratio, solvent are believed to strongly influence these processes.

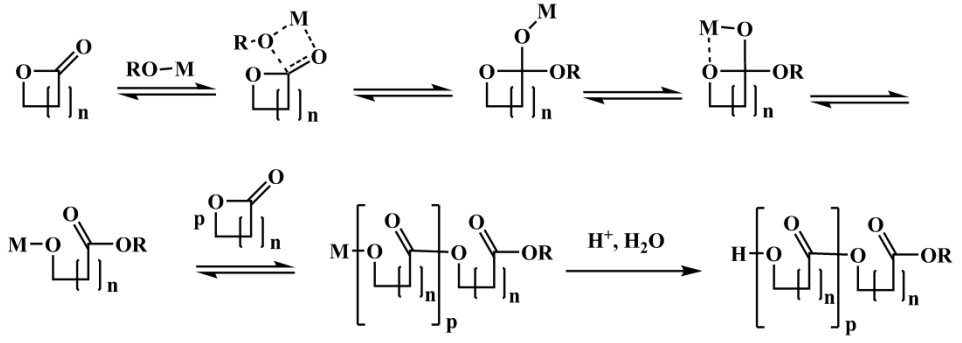

(2.11)

2.3 Click Chemistry

The term "click chemistry" concept encompasses a wide range of highly efficient and specific organic reactions that can be conducted in a range of environments. Click reactions are characterized by being modular, wide in scope, giving very high yields, generating only inoffensive byproducts that are capable of removal by nonchromatographic methods, and contain regiospecificity. The chemical process must include simple reaction conditions, readily available starting materials, the use of without solvent or a benign solvent, simple product isolation, and a thermodynamic driving force of at least 20 kcal/mol [9].

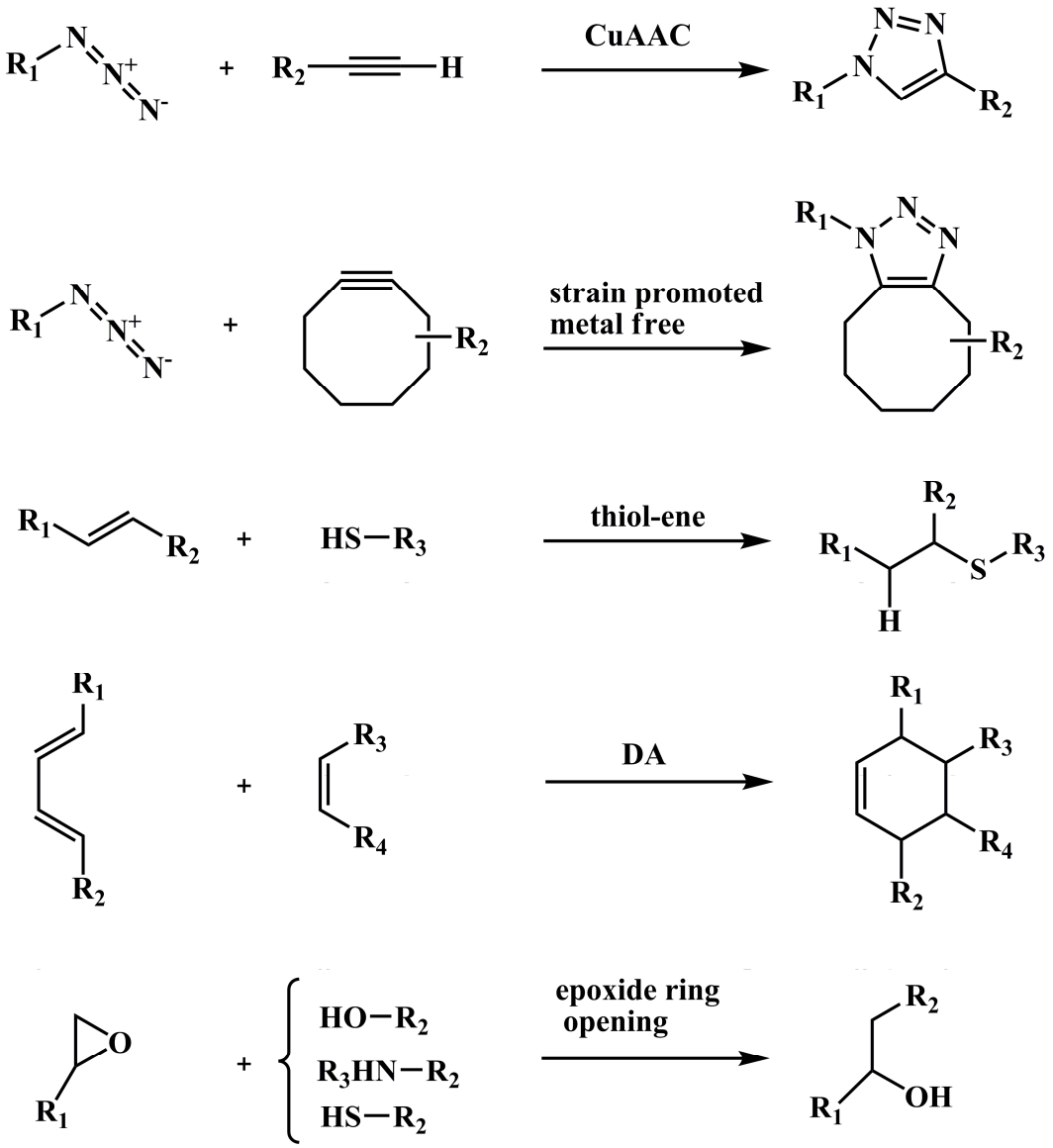

Figure 2.2: General representation click reactions.

The click reactions commonly include to form a carbon-heteroatom bond such as: *nucleophilic substitution chemistry* - especially ring opening reactions of strained heterocyclics such as epoxides, aziridines, aziridinium ions, and episulfonium ions; *nonaldol carbonyl chemistry* – formation of ureas, thioureas, aromatic heterocycles, oxime ethers, hydrazones, and amides; *additions to carbon-carbon multiple bonds* – epoxidation, dihydroxylation, aziridination, sulfenyl halide addition, and Michael additions; *cycloadditions of unsaturated species* – 1,3-dipolar cycloaddition reactions, and Diels-Alder type reactions. These reactions have been employed for many years to bring about a range of chemical transformations. But nowadays Cu(I) catalyzed azide–alkyne cycloaddition, Diels–Alder cycloaddition and the thiol-ene reaction receive particular attention as they are easy and elegant synthetic approaches to the coupling of chemical compounds (Figure 2.1).

2.3.1 Copper(I)-catalyzed azide-alkyne cycloaddition (CuAAC)

The thermal reaction of organic azides with terminal or internal alkynes has been known for more than a century, the first 1,2,3-triazole being synthesized by A. Michael from phenyl azide and diethyl acetylenedicarboxylate in 1893. The reaction has been investigated in detail by Huisgen and coworkers during 1950s–70s in the course of their studies of the larger family of 1,3-dipolar cycloaddition reactions [119]. The Huisgen 1,3-dipolar cycloaddition reaction of alkynes and organic azides [120] has gained considerable the most attention of any click reaction since 2001, the copper-catalyzed azide-alkyne cycloaddition (CuAAC) was realized independently by the Meldal and the Sharpless laboratories [121, 122]. The conventional Huisgen cycloaddition of azides and alkynes is not appropriate the criterion of a click reaction, by reason of the high temperatures necessary (>110 °C) and the lack of regiospecificity, with a racemic mixture of 1,4- and 1,5-triazole products (2.12) [119]. The copper catalyzed reaction allows to proceed much faster under much milder conditions and produces only the 1,4-regiosomer triazole [123, 124]. The great success of the Cu(I) catalyzed reaction is actually a virtually quantitative, very robust, insensitive, general, and orthogonal ligation reaction.

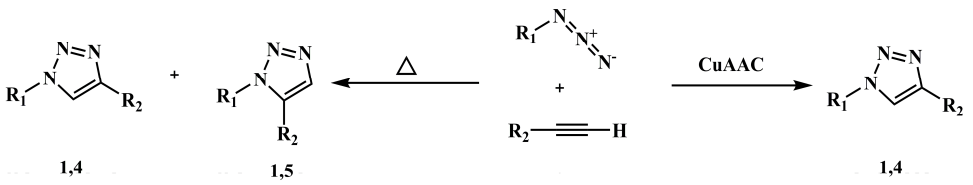

(2.12)

The CuAAC rate is increased by a factor of 10^7 relative to the Huisgen 1,3-dipolar cycloaddition [125], so it considerably fast at and below room temperature. The reaction is not significantly affected by the steric and electronic properties of the groups attached to the azide and alkyne centers, and primary, secondary, and even tertiary, electron-withdrawing and electron-donating, aliphatic, aromatic, and heteroaromatic azides usually react well with variously substituted terminal alkynes. The reaction realizes in many protic and aprotic solvents, including water, and is unaffected by most organic and inorganic functional groups. The 1,2,3-triazole has the advantageous properties of high chemical stability, strong dipole moment (4.8–5.6 Debye), aromatic character, and hydrogen bond accepting ability [126].

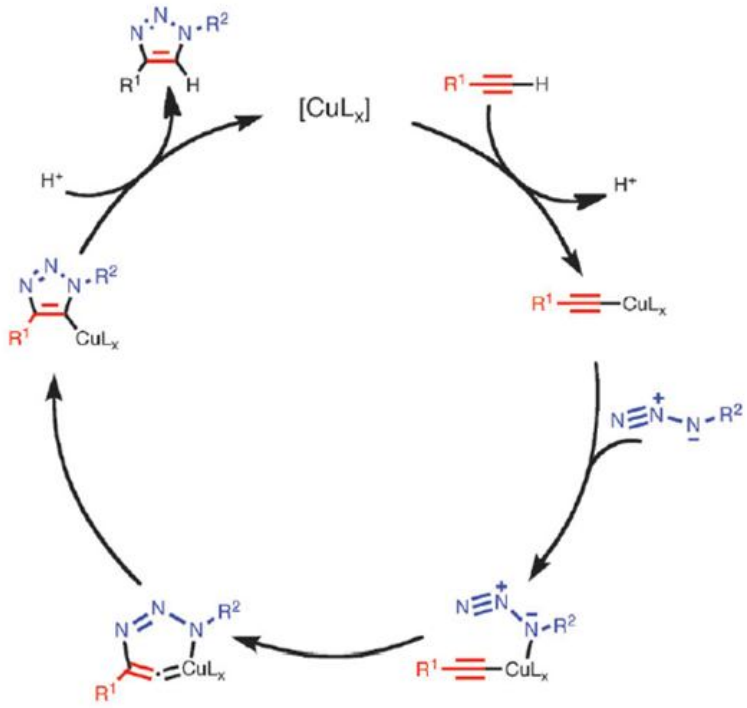

(2.13)

A stepwise mechanism [122, 125] of CuAAC (2.13) consist of three key steps [127]:

(1) activation of a terminal alkyne as copper acetylide

(2) formal cycloaddition to produce cuprated triazole

(3) protiolysis of to release triazole.

The alkyne first coordinates to copper(I), forming a π-complex in which the acetylenic proton is more acidic by up to 9.8 units [125]. Coordination of the azide's nearby nitrogen to copper establishes the regiochemistry of the overall reaction and produces cupracycle. Ring contraction of forms (1,2,3-triazol-5-yl) copper species, which undergoes protiolysis to form triazole. Protonation of triazole-copper derivative followed by dissociation of the product ends the reaction and regenerates the catalyst.

To date, copper is noticeable as the only metal for the dependable, easy, and 1,4-regiospecific catalysis of the azide–alkyne cycloaddition. Indeed, other metals known to catalyze various transformations of alkynes have not so far provided efficient catalysts for producing to 1,4-triazoles. Investigatios of complexes of all of the first-row transition elements as well as complexes of Ag(I), Pd(0/II), Pt(II), Au(I/III), and Hg(II), among others, have all failed to produce triazoles in synthetically useful yields; their effect on the rate and selectivity of the cycloaddition was at best marginally noticeable. Only ruthenium cyclopentadienyl complexes were found to catalyze the formation of the 1,5-disubstituted triazole from azides and terminal alkynes, and also to engage internal alkynes in the cycloaddition.

2.3.2 Diels-Alder reaction (DA)

The Diels-Alder (DA) reaction is a concerted [4π+2π] cycloaddition reaction of a conjugated diene and a dienophile, which [128-136] has been one of the best methods for the preparation of six-membered carbocycles. The typical [4+2]-cycloaddition condenses a diene moiety onto an alkene or alkyne system (dienophile) to afford a cyclohexene or cyclohexadiene derivative. The Diels-Alder reaction's name comes form Professor Otto Diels [137] and his student, Kurt Alder [138]. DA reaction was arising from the reaction of cyclopentadiene with quinone denotes a historic event in the field of chemistry [128].

According to the Woodward-Hoffmann rules, the concerted suprafacial [π4s + π2s] cycloaddition of a diene and a dienophile is thermally allowed. The theory predicts that the rate and regioselectivity of cycloadditions are controlled by either the HOMO of the diene and the LUMO of the dienophile in the normal Diels-Alder and by the HOMO of the dienophile and the LUMO of the diene in the inverse electron-demand Diels-Alder [139]. In Diels-Alder reactions, the stereoselectivity is generally

high due to the "*cis* principle", which states that Diels-Alder reactions require a cisoid conformation for the diene and suprafacial-suprafacial mode of reaction, meaning that both ends of the diene attack from the same face of the dienophile in a *syn* fashion. The Diels-Alder addition of dienophiles to dienes quite often gives the *endo* adducts [129, 130]. This is the "*endo* rule", first proposed by Alder and Stein [140]. The "*endo* rule" is usually rationalized as a result of the principle of "maximum accumulation of unsaturation" (2.14).

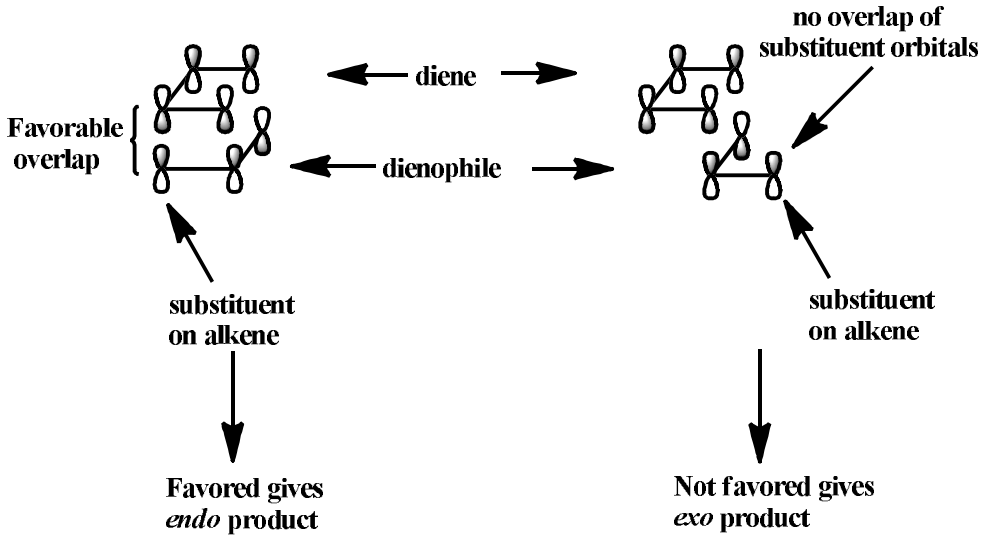

(2.14)

The polarizability of the diene and dienophile creates dispersive forces making the *endo* transition state more stable than the *exo* transition state. Secondary orbital overlaps are possible, leading to secondary binding forces that stabilize this transition state [141-143]. Solvents other than water have little effect on the *endo* selectivity [144-147], however, temperature and/or the presence of a Lewis acid catalyst can affect it [148].

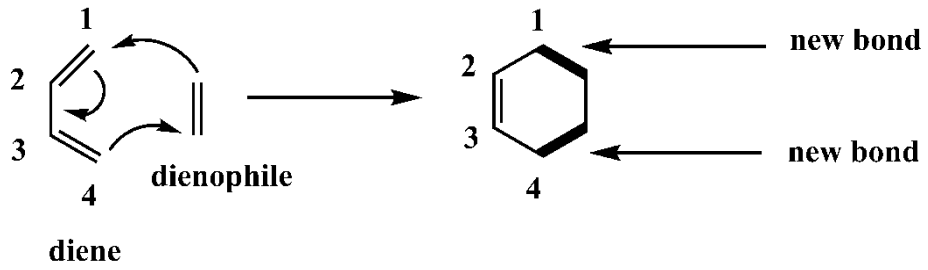

(2.15)

Diels-Alder reaction possess characteristics of click techniques like being specific, atom-economical, and highly efficient. This reaction has been employed in organic chemistry for many years, but its increased use in the area of macromolecular

structures has led to the emergence of click chemistry concepts. In contrast to the majority of click reactions that create carbon-heteroatom bonds formation, traditional Diels-Alder reactions form new carbon-carbon bond between dienes and electron-deficient dienophiles (2.15).

2.3.3 Thiol-ene reaction

The thiol-ene click reaction has realized between a thiol and an alkene to form a thioether linkage. More specifically, the sulfur–carbon bond formation follows an anti-Markonikov process, which can be promoted by UV light radiation or by radical initiators.

Thiol-ene click reactions are not new discovered chemistry, but have been rather extensively studied over the last century [149-151] and were depicted as early as 1926 by Braun and Murjahn [152]. During the time that thiol-ene polymerizations utilize for the formation of networks [153, 154] or for the purpose of controlling molecular weight in radical polymerizations, thiol-ene reaction is more recently also referred to as a click reaction [155].

Among the three ‘‘click’’ methodologies, thiol-ene click is considered the most encouraging the green aspects of these reactions. Additionally, this metal-free reaction can be performed in the absence of solvents in some cases, and can be photochemically controlled (even in the absence of a photoinitiator). According to recent reports has indicated that the thiol-ene click reaction is more efficient when initiated by light than by thermally [156]. Another advantage is that water- tolerant and oxygen makes it even more attractive.

Radicalic thiol-ene click proceeds by the same mechanism with chain transfer polymerization mechanism. Firstly, a thiyl radical is generated from a thiol-functionalized molecule by hydrogen abstraction from an initiator-derived radical, which subsequently reacts with carbon–carbon double bond. This reaction is like propagation step. And then, the radical abstracts a proton from another thiol to form the reaction product and recover a thiyl radical (reaction 2.16). But unfortunately, thiol-ene chemistry shows significant side reactions [157], the whole process might not be considered a click reaction, as this is a direct paradox to the click concept. One known side reaction is disulfide formation; another is head-to-head coupling of the carbon centered radicals. These two reactions are arguably the most prominent

reactions terminating the thiol-ene cycle. Thus, thiol-ene may only serve as an efficient conjugation tool if such reactions can be largely avoided.

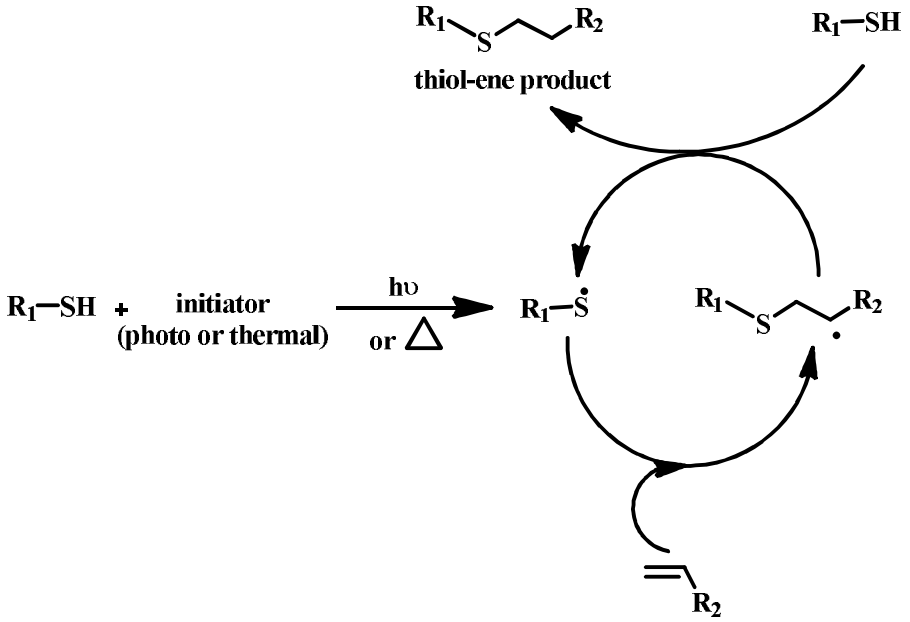

(2.16)

2.4 Click Chemistry on Polymer Science

The modification of polymers after the successful achievement of a polymerization techniques represents an important issue in macromolecular science. Materials have gained dramatically different properties with functional groups and chain architecture. Despite there is a variety of progress for the preparation of new organic molecules, not all of these are always readily transferable from the molecular scale to the macromolecular scale [158]. Many of the most chemistries are limited by lack of starting materials, complex experiment, or a scarcity of specificity. The primary goal of polymer science should be to arrive at the necessary structure by the simplest, cleanest, and most efficient means possible throughout polymer synthesis and functionalization. All of these requirements are supplied by the "click chemistry" which pioneers to the modification of polymers and synthesis of different architectural macromolecules.

Click chemistry strategies have been exponential joined into the field of macromolecular engineering. It could be argued that the marriage of click chemistry with polymer science is a gentle one, a temporary movement relying on revisiting and rebranding well-known reactions to capitalize on a fashionable concept.

The copper (I) catalyzed azides-alkynes cycloaddition (CuAAC), Diels-Alder cycloaddition and thiol-ene click reactions allow wide possibilities of macromolecular engineering, for instance, the synthesis of telechelic polymers, functionalized block copolymers and the synthesis of complex architecture macromolecules (Figure 2.3) [159, 160].

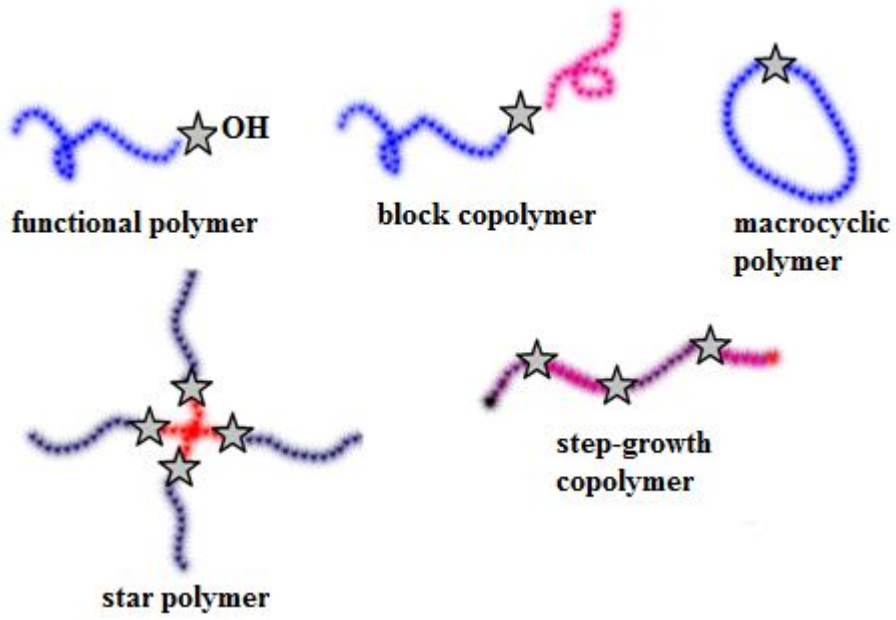

Figure 2.3: General representation of synthesis of different polymer topologies via click reactions.

Despite CuAAC was firstly assumed as a concept for organic synthesis, this strategy also has an enormous potential in materials science [161, 162]. In mid-2004 Hawker, Fokin, Sharpless, et al. employed this reaction during convergent dendrimer preparation [163], and it was likely this approach that originally brought click chemistry to the attention of the polymer community. As a result, the number of publications in this field has increased dramatically within the last six years.

The application of click chemistry together with C/LRP has contributed to rapid improvement in polymer architectures and functional materials because of the ease with which these two synthetic techniques are combined. ATRP has been utilized most extensively in conjuction with the CuACC to prepared end-functionalized polymers. Terminal functionality can be easily introduced on polymers prepared via ATRP by substitution of the halogen end group with azide and then click reaction with alkyne species. Opsteen and van Hest first demonstrated it was possible to

prepare a library of AB [164] or ABC [165] block copolymers by coupling various combinations of azido- or alkyne-terminated polymers by CuAAC. CuAAC has also been effectively combined with other controlled polymerization methods, including RAFT [166-178], NMP [179-183], cationic polymerization [174, 184-186], anionic polymerization [187-190], and ring-opening metathesis polymerization [191-193].

Since this momentous discovery, the CuAAC has been subject to a variety of mechanistic investigations [125, 194-196] and has received widespread application in polymer and materials science [161, 197, 198]. It has been used for the conjugation of biological polymers to viruses [199, 200], synthetic polymers [201-203], and solid surfaces [204-206]; the preparation of cyclodextrin [207] and cyclopeptide [208, 209] analogues; polymer functionalization [210-212], and the preparation of macromonomers [213, 214], block copolymers [164, 173, 215], star polymers [216, 217], dendrimers [163, 218, 219], brushes [220, 221], shell cross-linked nanoparticles [222], and organometallic polymers [223].

Due to efficiency and facile work-up, Diels-Alder reactions have been extensively evaluated for the synthesis of dendrimers [224-228] stars [229-232] graft copolymers [233], and other highly dense macromolecular architectures. Our group has reported many of these examples, demonstrating that a different type of structures can be synthesized with using Diels –Alder cycloaddition.

For example, maleimide-terminated polymers were reacted with trianthracene cores to yield PEG, poly(methyl methacrylate), or poly(tert-butyl acrylate) (PtBA) stars with very high click efficiency [230]. Miktoarm stars with PEG, polystyrene, and PtBA chains were prepared by Diels-Alder click reaction of maleimide-terminated PEG to an anthracene functional initiator capable of both ATRP and NMP [232]. The orthogonality of Diels-Alder and CuAAC reactions was demonstrated by preparing modular ABC triblock copolymers from maleimide-functional P*t*BA, alkyne-functional PEG, and R-anthracene-ω-azide-terminated polystyrene [215]. At high temperatures in the presence of a Cu(I) catalyst, both reactions took place simultaneously, and the triblock copolymer was obtained with high efficiencies. A similar one-pot "double-click" approach was employed to prepare three-arm stars [229] and H-shaped ABCDE quintopolymers [181].

Barner-Kowollik, Stenzel, and co-workers recently reported a unique functionalization procedure that relies on hetero-Diels-Alder reactions of dienes with thiocarbonylthio functional groups on RAFT-generated polymers [234].170 Chain transfer agents with electron-withdrawing Z groups result in polymers capable of highly efficient cycloaddition reactions to yield modular block copolymers [234, 235], polymer-functionalized microspheres [236], and star block copolymers [237, 238].

There have been several studies for a successful functionalization of polymers with small molecules via radical-initiated thiol-ene reaction. However, no example exists where two polymer chains were coupled. DuPrez and Barner-Kowollik and coworkers demostrated that thiol-ene click reaction between two polymers with low molecular weight occurs to some extent [239].

2.5 Complex Macromolecular Architecture

The improvement of controlled/living polymerization techniques resulted in definitely management many aspects of complex macromolecular architecture in terms of topology, composition and functionality [240-242]. Anionic polymerization is the most precise and powerful methodology [243], but recent progress in C/LRP additionally has opened the possibility of using many unprotected functional monomers [244, 245].

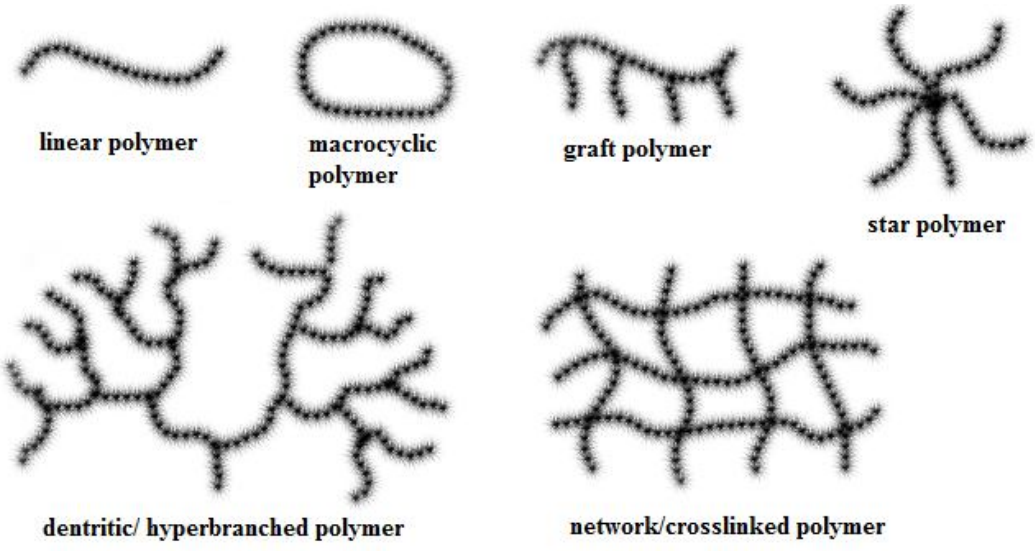

Figure 2.4: Illustration of polymers with various topologies.

The various C/LRP techniques allow the synthesis of well-defined polymeric materials with different topology, including linear, star, cylic, brush, branched polymers, and cross-linked networks (gels) (Figure 2.4).

2.5.1 Star polymers

Among the complex macromolecules, star polymers yield one of the simplest arrangement of linked macromolecules because a well-defined star polymer contains several identical linear chains linked together at one end of each chain. Aroused interest of many scientists because they constitute the simplest form of branching [246].

The earliest attempt to synthesize star molecules was that of Schaefgen and Flory in 1948,1 who by the polymerization of ε-caprolactam in the presence of either cyclohexanonetetrapropionic or dicyclohexanoneoctacarboxylic acid formed tetra- and octachain star-shaped polyamides.

The synthesis of well-defined star polymers with various numbers of arms and compositions were continued in the 1960's using living anionic polymerization techniques. Shortly after, polymer physical chemists and polymer physicists worked on the synthesized polymer materials to discover the unique properties of star polymers in either solution or bulk when compared to the linear analogs, and to develop new theories regarding the properties of polymers. Eventhough star polymers synthesized by living anionic polymerization have been established as the best defined standards, it loses its popularity due to the stringent experimental conditions [247]. The development of C/LRP techniques supplied a promising solution for synthesis of star polymers via an easier and more economic process.

The preparation of star polymers by using controlled polymerization systems can be divided into three general synthetic routes:

The 'core-first' or divergent approach, in which a multifunctional initiator is capable of simultaneously initiating the polymerization of vinylic monomers, thus forming the arms of the star polymer (Figure 2.5a).

The ‘arm-first’ or convergent approach involves the synthesis of a living macroinitiator (or macromonomer), the arm, and reaction with a difunctional (or higher) vinylic cross-linker to form a densely cross-linked core from which the arms radiate (Figure 2.5b).

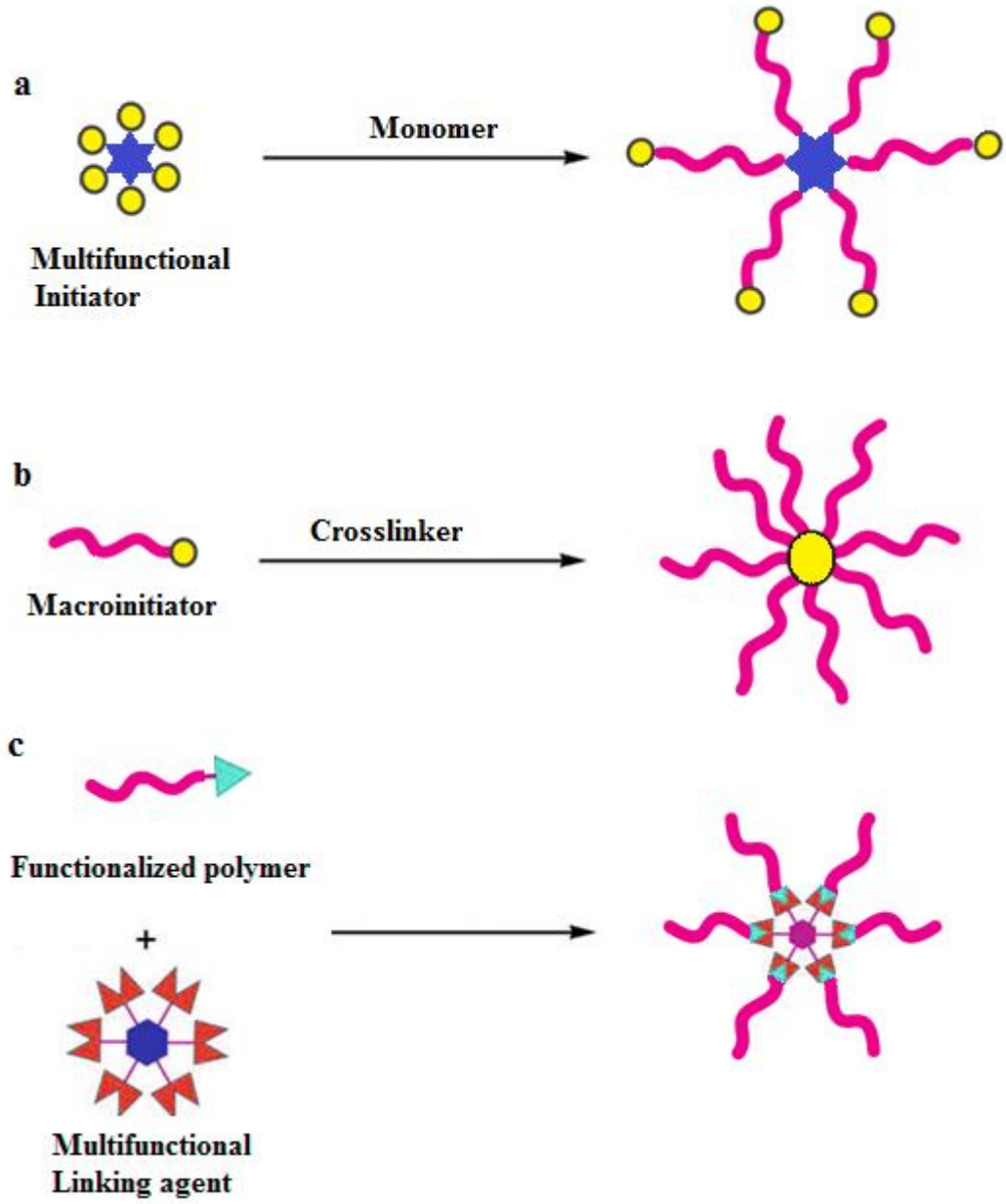

Figure 2.5: Synthetic approaches for the preparation of star polymers via controlled polymerisation techniques; (a) the core-first approach, (b) the arm-first approach and c) grafting to-approach.

The third method, namely the 'grafting to' approach, can be considered as a combination of controlled polymerization and coupling reactions; initially, a well-defined arm is prepared via C/LRP and coupled to a multifunctional linking agent. (Figure 2.5c). This method is similar to the ''arm-first'' approach but the same technique can be applied as a ''core-first'' approach. However, it should be noted that it is usually necessary to appropriately modify the terminal group of arms to enable coupling with the multifunctional linking agent.

Star polymers can be classified into two categories according to the chemical compositions of arms species: homoarm star polymers and heteroarm (or miktoarm) star polymers. Homoarm star polymers consist of a symmetric structure comprising radiating arms with similar molecular weight and identical chemical composition. In contrast, a miktoarm star polymer contains two or more arm species with different chemical compositions and/or molecular weight, which will be described in detail (Figure 2.6).

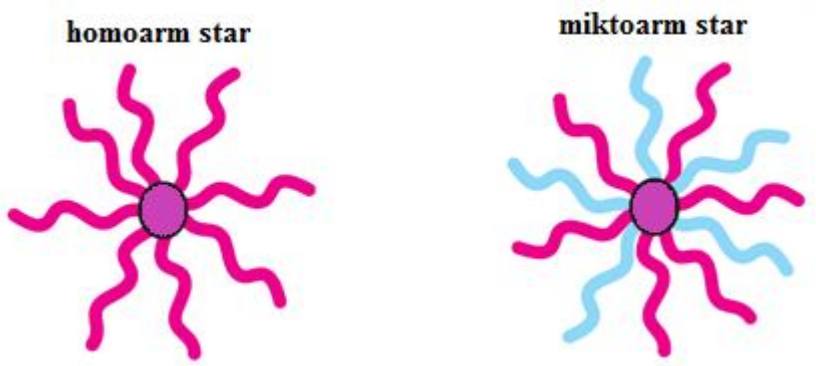

Figure 2.6: Illustration of star polymer categories.

2.5.1.1 Miktoarm star (μ-star) polymer

Miktoarm star polymers are a novel type of nonlinear polymers consisted of a central core with various kinds of arms of different nature. Compared with linear block copolymers, miktoarm star polymers demostrate intense differences in morphology [248-252] and properties [253-256], etc. The synthesis and properties of miktoarm star polymers were extensively reviewed by Hadjichristidis [257-259].

Miktoarm star polymers (mikto defined by Hadjichristidis, meaning mixed), which contain two or more arm species linking to one central core, have attracted considerable attention due to their branched architectures, globular shapes and segmented block structures [259]. The different chemical compositions of the arms in miktoarm star molecules led to interesting microphase separation behavior in bulk [260, 261], in solution [262] and at different interfaces. Stars with molecular weight asymmetry can be considered miktoarm homopolymers. Star polymers having arms of similar chemical nature but different end groups also belong to this category. Finally, topologically asymmetric stars are also μ-stars. They consist of diblock copolymer arms that are connected by different ends to the star center [263]. Although the large number of reports on synthesis of homoarm star polymers by using various type of C/LRP techniques, the synthesis of miktoarm star polymers was more difficult because of that there are fewer reports. The most commonly used methods for the synthesis of miktoarm star polymers via C/LRP techniques involved the use of a miktofunctional initiator that combined various C/LRP techniques with other living polymerization methods, specially ROP. Different types of arms grow sequentially from the corresponding initiating sites via polymerization of various monomer species using different polymerization methods. The composition and numbers of the arms in the miktoarm star polymer are determined by the number and type of initiating sites on the miktoinitiator [264, 265].

Many synhtetic strategies to create a wide variety of miktoarm star polymers are possible. One of the most established synthetic strategies for miktoarm stars with reactive chain ends involves linking chlorosilane compounds as a core, synthesized via living anionic polymerization. Hadjichristidis and coworkers have used tetrachlorosilane to synthesize an $A(AB)_3$-type miktoarm star polymer, composed of polystyrene (PS) and polystyrene-*b*-polyisoprene (Figure 2.7) [266].

There are so many kinds of miktoarm star polymers, some of them are A_2B, A_3B, A_2B_2, ABC, ABCD, π-shaped (AB)B(AB), H-shaped A_2BA_2, H-shaped (AB)C(AB), H-shaped ABCDE, super H-shaped A_3BA_3, super H-shaped A_5BA_5.

There are so many examples throughout the literature where synthesized μ-stars via C/LRP techniques. A miktofunctional initiator was used in a large part of these studies. From this initiator, each arm is grown outwards through a combination of different polymerization techniques, such as living anionic polymerization, ring-

opening polymerization (ROP) [259, 267], or a variety of C/LRP [35] techniques. Because of the [268] combination of different polymerization methods, it is easy to introduce a wide variety of monomers into the final polymeric structure. Our group synthesized many different types of miktofunctional initiator to obtain miktoarm star polymers with ‘’core-first’’ approach. If it is needed to give examples, one of them has three different initiating sites for ATRP, ROP, and NMP to create an ABC [217] miktoarm star polymer where each polymerization step does not require end-group modification for subsequent polymerization reactions (Figure 2.8)[269].

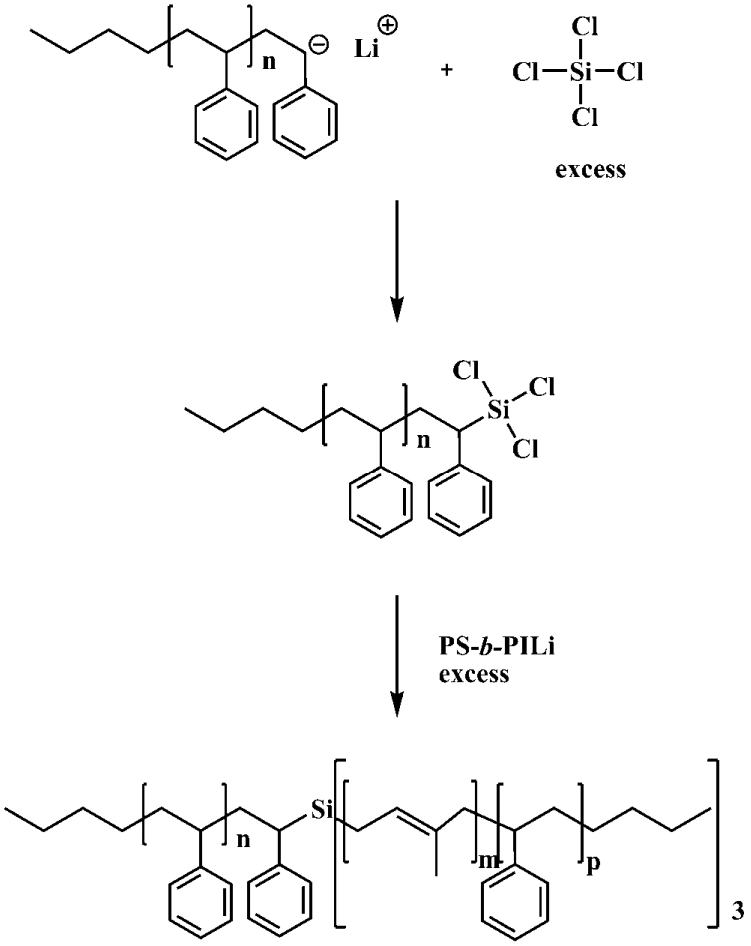

Figure 2.7: Synthesis of $A(AB)_3$ miktoarm polymer using living anionic polymerization and a chlorosilane linking agent.

ABC-type miktoarm star polymer was composed of polycaprolactone (PCL), polystyrene (PS), and poly(*tert*-butyl acrylate) (P*t*BA) arms. Because of the variety of [270] polymerization methods and their accompanying choice of monomers, it is easy to see why the core-first approach is a versatile and efficient synthetic strategy, and it has been widely used [271-280].

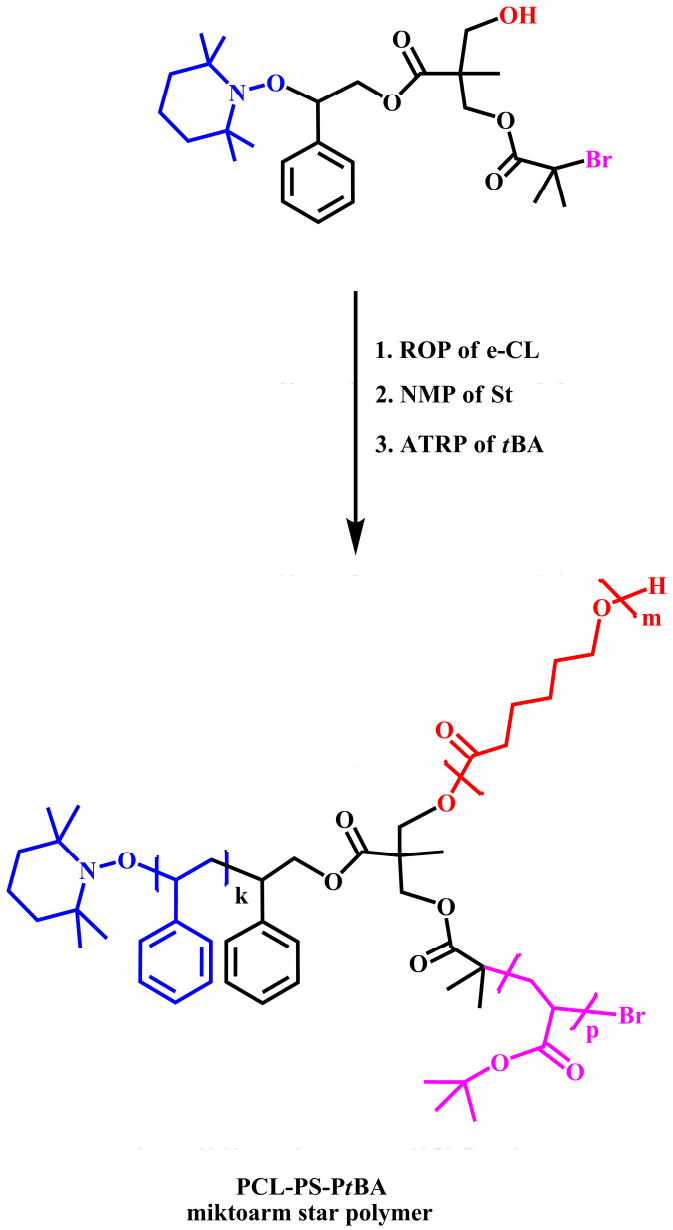

Figure 2.8: Synthesis of ABC miktoarm polymer made with the ‘’core-first’’ method by three different polymerization methods.

Although the ‘’arm-first’’ technique had typically been used to generate homoarm star polymers [216], Gao and Matyjaszewski were the first to use it to exhibit the synthesis of miktoarm star polymers, synthesized using either two or five different types of arms [221]. Generally, in this methodology, the chain ends of many linear macroinitiators are used to polymerize a divinyl compound, typically divinylbenzene (DVB). Many polymers were used to initiate this polymerization in a one-pot [281] method to obtain miktoarm stars in high yields.

The final miktoarm polymer consisted of a crosslinked core composed of DVB, and many polymer chains, connected together by the core (Figure 2.9).

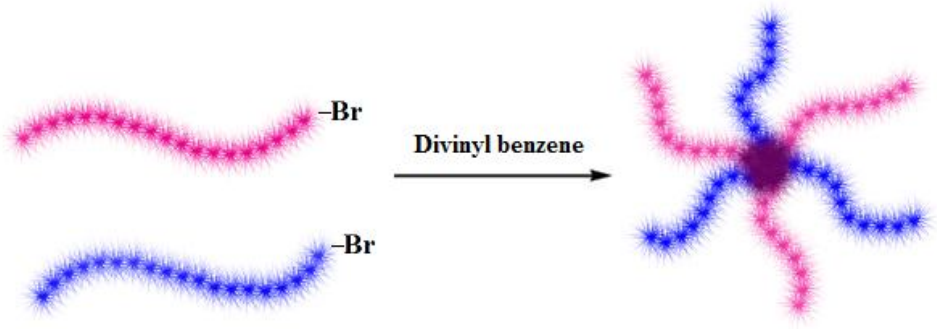

Figure 2.9: General synthesis of a miktoarm star polymer by the ‘’arm-first’’ method.

Our group have also worked on this subject and presented a nice example [282-284]. We employed sequential double click reactions involving CuAAC and DA for the preparation of multi-miktoarm star block copolymers by using the arm-first approach. Multiarm star PS with both alkyne and anthracene moieties at the periphery, (alkyne-PS)–polyDVB–(PS-anthracene), was simply obtained via ATRP of DVB concurrently initiated with linear α-silyl protected alkyne- and α-anthracene-terminated PS macroinitiators. It is followed by sequential CuAAC and DA click reactions with P*t*BA–N_3 and α-maleimide terminated PMMA, respectively, resulting in formation of the target multi-miktoarm star block copolymer P*t*BA–PS–polyDVB–PS–PMMA [285].

Recently,‘’click reactions’’ have become very trendy for the synthesis of miktoarm star polymers due to easy synthetic methodologies [286-288]. This method is highlighted by coupling of the reactive end of polymer arm to a multifunctional core using highly efficient reactions. This specific click reaction has found widespread use throughout the synthesis of miktoarm star polymers.

One of the most standard examples of the click technique arises from our group. In this study, first, PMMA-*b*-PS with alkyne functional group at the junction point was obtained from successive ATRP and NMP routes. Furthermore, P*t*BA obtained from ATRP of *t*BA and commercially available monohydroxyl PEG were efficiently converted to the azide end-functionalized polymers.

As a second step, the alkyne and azide functional polymers were reacted to give ABC-type star polymers, PMMA-PS-P*t*BA and PMMA-PS-PEG, using CuAAC strategy between azide and alkyne functional groups of the polymeric precursors [289].

The DA reaction has also been used to make ABC miktoarm star polymers. Another study of our group was achieved by combining DA reaction of maleimide-end functionalized PEG (PEG-maleimide), NMP of St, and ATRP of *t*BA routes the preparation of ABC type miktoarm star [232].

Other examples of the synthesis of even more challenging miktoarm stars have been reported. The same strategy of coupling two block copolymers together through click chemistry to create the final miktoarm star was employed to yield a very unique H-shaped miktoarm star composed of five different arms (PS, PCL, P*t*BA, PEG, and PMMA) in moderately high yield [180]. Other popular variants of the click reaction that are widespread in macromolecular synthesis include Diels-Alder reaction [181].

Though alkyne-alkyne homocoupling method for the synthesis of miktoarm star polymers due to easy synthetic methodologies are rather rare, one notable example arose recently from our group where an A_2B_2 miktoarm star polymer was made by coupling two diblock copolymers together at their junction points in an alkyne-alkyne homocoupling reaction [290].

2.5.2 H-shaped polymers

H-shaped polymer is an example of complex macromolecular structures. The general definition of H-shaped polymers are based on two arms attached to the each end of the polymer backbone. Due to their architectural differences, H-shaped polymers show different rheological properties, micellar properties, and self-assembled structures when compared with linear or branched block copolymers. H-shaped polymers are important as model materials in understanding the rheology of branched polymers such as LDPE [16-18]. H-shaped copolymers form micelles with lower aggregation numbers, which results in smaller micellar structures compared with linear block copolymers [19, 20]. The self-assembly of H-shaped block copolymers shows a variety of morphologies depending on the preparation conditions [21].

The synthesis of H-shaped polymers having various chemical structures is thus important to thoroughly understand the aforementioned physical properties.

The first H-shaped polymer was synthesized from styrene by Roovers and Toporowski [11] via anionic polymerization; two eqiuvalents of poly(styryllithium) reacted with methyltrichlorosilane, and the resulting $(PS)_2Si(CH_3)Cl$ subsequently condensed with α,ω-difunctional poly(styryllithium).

Generally, H-shaped copolymers have been prepared by anionic polymerization technique [11-13, 15, 291]. Hadjichristidis et al. [246, 292] and Knauss et al. [293, 294] have worked widely on this subject and presented some nice examples [13, 295, 296]. However, because of the critical experiment condition and the limitation in monomers that can be applied in the living anionic polymerization, only a few kinds of polymers have been prepared successfully. In addition, the coupling reaction is often time-consuming, and the troublesome purification is inevitable because the coupling reactions cannot go to completion and some byproducts will be generated.

With the advent of C/LRP, [40, 46, 53, 67] the synthesis of H-shaped polymers can be conducted in a much simpler manner with well-defined structures. Besides these, some combinations of living anionic, cationic polymerization and C/LRP have been extensively used to prepare this type complex polymers [277, 297-303].

Gnanou and coworkers [49] prepared successfully H-shaped copolymer where poly(ethylene oxide) (PEO) as a main chain and polystyrene (PS) as a side chains $[(PS)_2\text{-PEO-}(PS)_2]$ respectively, by integrating ATRP and anionic polymerization (Figure 2.10).

Subsequently, Pan and coworkers [304, 305] published the synthesis of H-shaped copolymer $(PS)_2$-poly(ethylene glycol) (PEG)-$(PS)_2$ by using ATRP route and $[\text{poly(L-lactide)}]_2\text{-PS-}[\text{poly(L-lactide)}]_2$ and $[(PLLA)_2\text{-PS-}(PLLA)_2]$ using ATRP and ROP systems (Figure 2.11).

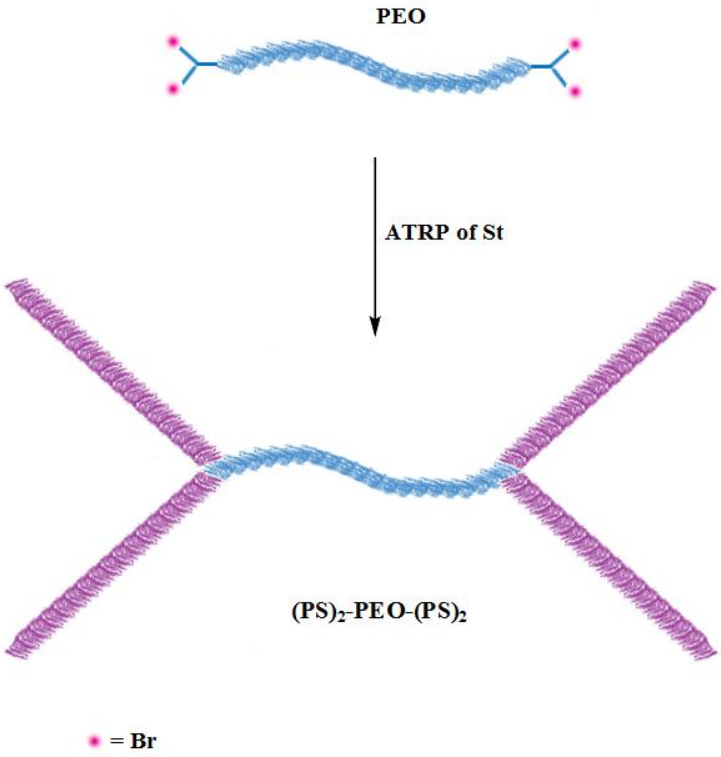

Figure 2.10: Synthesis of $(PS)_2$-PEO-$(PS)_2$ H-shaped polymer by Gnanou and coworkers.

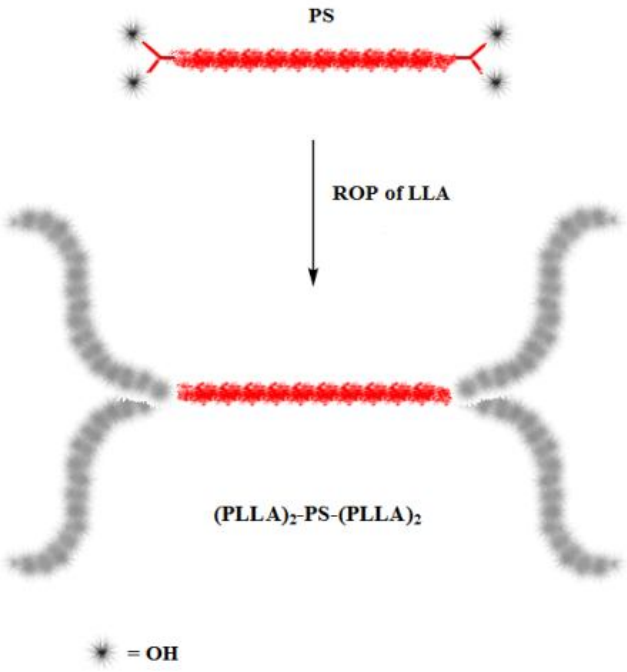

Figure 2.11: Synthesis of $(PLLA)_2$-PS-$(PLLA)_2$ H-shaped polymer by Pan and coworkers.

More recently, Pan and coworkers [306] synthesized heteroarm H-shaped terpolymer (PS)(PLLA)-PEG-(PS)(PLLA) where PEG served as the main chain and PS and PLLA as the side chains by the combination of RAFT and ROP (Figure 2.12).

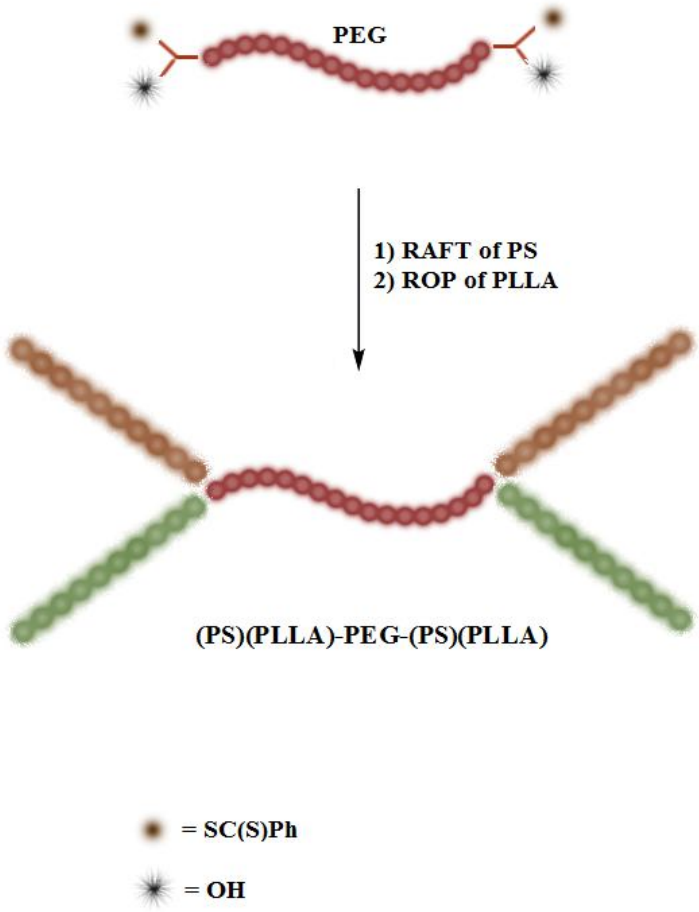

Figure 2.12: Synthesis of (PS)(PLLA)-PEG-(PLLA)(PS) H-shaped polymer by Pan and coworkers.

Zhang and coworkers designed and prepared an asymmetric H-shaped copolymer $(PS)_2$-PEO-$(PMMA)_2$ via the combination of ATRP and anionic polymerization. Meanwhile, click chemistry [9] generated a novel way to construct polymer architecture, and it was extensively used for the preparation of H-shaped polymers [198]. Just recently, Monteiro and coworkers [307] successfully obtained H-shaped block copolymer using a combination of ATRP and click chemistry, which provided to be a more straightforward approach for the preparation of block copolymers with different chain architectures (Figure 2.13).

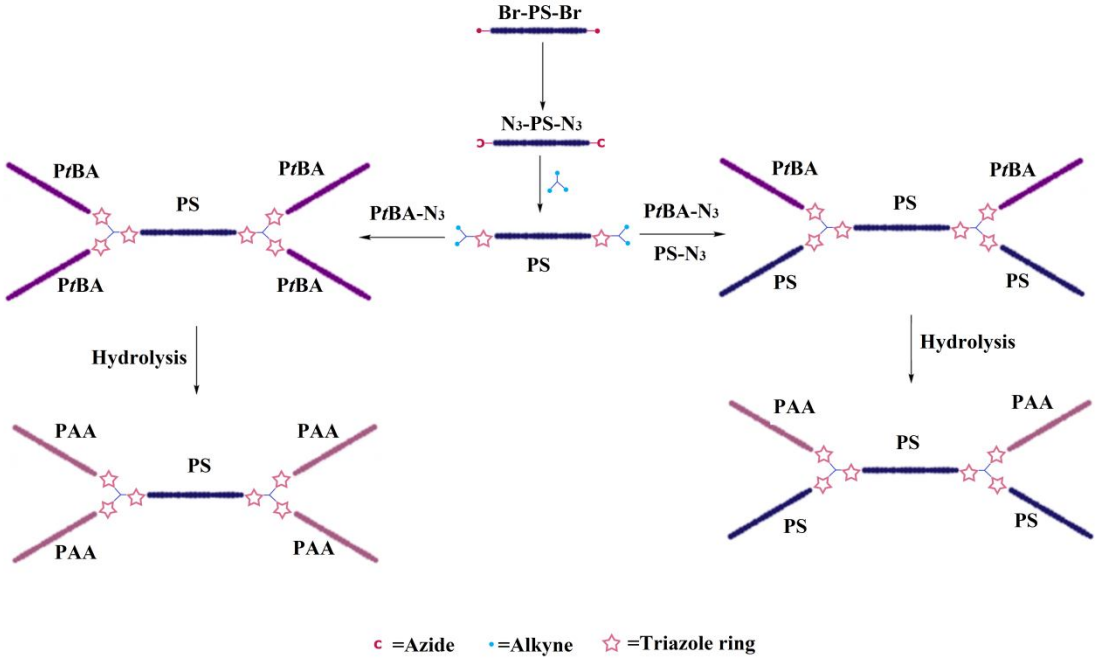

Figure 2.13: Synthesis of H-shaped polymer by Monteiro and coworkers.

3. EXPERIMENTAL WORK

3.1 Materials

Styrene (St, 99%, Merck), methyl methacrylate (MMA, 99%, Aldrich) and *tert*-butylacrylate (*t*BA, 99%, Aldrich) were passed through basic alumina column to remove inhibitor and then distilled from CaH_2 in vacuum prior to use. ε-Caprolactone (ε-CL, 99%, Aldrich) was dried over CaH_2 and distilled in vacuum prior to use. Furan (99%, Aldrich), maleic anhydride (99%, Aldrich), ethanolamine (99.5%, Aldrich), succinic anhydride (97%, Aldrich), 9-anthracenemethanol (97%, Aldrich), Merifield's resin (1% crosslinked chloromethylated PS, Aldrich), 2,2-bis(hydroxymethyl)propanoic acid (bis-MPA, 99% Acros), *p*-toluenesulfonic acid monohydrate (*p*-TSA, Merck), 2,2,6,6-Tetramethylpiperidinyl-1-oxy (TEMPO, 98% Acros), 2,2-dimethoxypropane (98%, Acros), benzoyl peroxide (BPO, 77% Fluka), 2-bromoisobutryl bromide (98%, Aldrich), triethylamine (Et_3N, 99.5%, Aldrich), propargyl alcohol (99%, Aldrich), *N,N'*-dicyclohexylcarbodiimide (DCC, 99%, Aldrich), 4-dimethylaminopyridine (DMAP, 99%, Aldrich), 4-pentynoic acid (98%, Aldrich), sodium azide (99%, Aldrich), tin(II)-2-ethylhexanoate (Aldrich, 98%), CuBr (99.9%, Aldrich), and CuCl (99.9%, Aldrich) were used as received. *N*, *N*, *N*', *N*", *N*"-pentamethyldiethylenetriamine (PMDETA, 99%, Aldrich) was distilled over NaOH prior to use. Poly(ethylene glycol) (HO-PEG-OH M_n = 6000, Acros), poly(ethylene glycol) monomethylether (Me-PEG-OH, M_n = 2000, Fluka) were dried by azeotropic distillation with anhydrous toluene. Tetrahydrofuran (THF, 99.8%, J.T. Baker) was dried and distilled from benzophenone-Na. *N,N*-dimethylformamide (DMF, 99.8%, Aldrich) was dried and distilled under vacuum over CaH_2. Dichloromethane (CH_2Cl_2, 99%, J. T. Baker) was dried and distilled over and P_2O_5. Diethyl ether (99.7%, Aldrich), toluene (99.8%, Aldrich), methanol (99.8%, Aldrich), and acetone (99.8%, Aldrich) were used without further purification. Ethyl acetate (EtOAc) and hexane were in technical grade and distilled prior to use.

3.2 Instrumentation

The ^{1}H (250 MHz) and ^{13}C NMR (62.89 MHz) spectra were recorded on a Bruker NMR AC 250 Spectrometer in $CDCl_3$. The conventional Gel Permeation Chromatography (GPC) measurements were carried out with an Agilent instrument (Model 1100) consisting of a pump, refractive index, and UV detectors. Four Waters Styragel columns (HR 5E, HR 4E, HR 3, HR 2), (4.6 mm internal diameter, 300 mm length, packed with 5 μm particles) were used in series. The effective molecular weight ranges were 2000- 4.000.000, 50-100.000, 500-30.000, and 500–20.000, respectively. THF was used as eluent at a flow rate of 0.3 mL/min at 30 °C. Toluene was used as an internal standard. The molecular weight of the polymers were calculated on the basis of linear PS standards (Polymer Laboratories), whereas linear PMMA standards (Polymer Laboratories) were only used for the molecular weight determination of the PMMA homopolymer using PL Caliber Software from Polymer Laboratories. The second GPC system with an Agilent model isocratic pump, four Waters Styragel columns (guard, HR 5E, HR 4, HR 3, and HR 2), a Viscotek TDA 302 triple detector (RI, dual laser light scattering (LS) (λ = 670 nm, 90° and 7°) and a differential pressure viscometer) (TD-GPC) was conducted to measure the absolute molecular weights in THF with a flow rate of 0.5 mL/min at 35 °C. All three detectors were calibrated with a PS standard having narrow molecular weight distribution (M_n = 115,000 g/mol, M_w/M_n = 1.02, [η] = 0.519 dL/g at 35 °C in THF, dn/dc = 0.185 mL/g) provided by Viscotek company. Typical sample concentrations for GPC-analysis were in the range of 2–8 mg/mL depending on molecular weight of analyzed polymers. Data analyses were performed with OmniSec 4.5 software from Viscotek Company.

UV spectra were recorded on a Shimadzu UV-1601 spectrophotometer in CH_2Cl_2. FT-IR spectra were recorded on a Perkin Elmer FTIR Spectrum One B spectrometer. Differential scanning calorimeter (DSC) was performed on a Perkin Elmer Diamond DSC with a heating rate of 10 ^{o}C min^{-1} under nitrogen flow.

Atomic Force Microscopy (AFM) images were taken by NT-MDT Solver P47 in tapping mode. Ultra sharp Si cantilevers having force constant of 48 N/m were used.

3.3 Synthesis Methods

Benzoic acid-2-phenyl-2-(2,2,6,6-tetramethylpiperidin-1-yloxy)ethyl ester (**1**) [308], 2-phenyl-2-(2,2,6,6-tetramethyl-piperidin-1-yloxy) ethanol (**2**) [308], 1,2-bis (bromoisobutyrloxy) ethane (**8**) [309], 4,10-dioxatricyclo[5.2.1.$0^{2,6}$]dec-8-ene-3,5-dione (**12**) [310], 4-(2-hydroxyethyl)-10-oxa-4-azatricyclo[5.2.1.$0^{2,6}$]dec-8-ene-3,5-dione (**13**) [310], 9-anthyrylmethyl 2-bromo-2-methyl propanoate (**18**) [311], and monocarboxylic acid terminated PEG (PEG-COOH) [312] were prepared according to published procedures.

3.3.1 Synthesis of benzoic acid-2-phenyl-2-(2,2,6,6-tetramethylpiperidin-1-yloxy)ethyl ester (1)

In a 1000 mL of two-necked round bottom flask, equipped with a magnetic stirrer, TEMPO (2,2,6,6-tetramethylpiperidinyl-1-oxy) (6.0 g, 19.2 mmol) and BPO (benzoyl peroxide) (9.4 g, 38.8 mmol) were dissolved in 600 mL of freshly distilled styrene, then flask conducted three times evacuation and subsequent nitrogen purging. The solution was kept for 30 minutes stirring at 90 ^{o}C in an oil bath. After that period the excess of styrene removed via back distillation and flask dissolved in 200 mL of ethyl acetate then extracted two portions (100 mL) of NaOH (1%). The combined organic phase was dried with Na_2SO_4 and solvent evaporated. The crude product purified by column chromatography over silica gel eluting just with dichloromethane, and the product was purified by recrystallization from cold hexane to yield 4.44 g (11.64 mmol, 60 %) as white needles. ^{1}H NMR ($CDCl_3$, δ): 8.2 (q, 2H, Ar*H*), 7.25-8 (m, 8H, Ar*H*), 5.06 (t, 1H, C*H*Ar), 4.83 (q, 1H, CH*H*CHAr), 4.53 (q, 1H, C*H*HCHAr), 0.75-1.8 (m, aliphatic protons).

3.3.2 Synthesis of 2-phenyl-2-(2,2,6,6-tetramethyl-piperidin-1-yloxy) ethanol (2)

Benzoic acid 2-phenyl-2-(2,2,6,6-tetramethyl-piperidin-1-yloxy)ethyl ester (4.44 g, 11.64 mmol) was dissolved in 70 mL of absolute ethanol and 17 mL of 2 N KOH and kept for 5 h to reflux. The product was extracted with water and dichloromethane (1:1). The combined liquid phase was again extracted with dichloromethane and combined organic phase was dried with Na_2SO_4, evaporation of the solvent yielded 2.8 g (10.11 mmol, 87 %) as yellow viscous liquid without further purification. ^{1}H

NMR ($CDCl_3$, δ): 7.3-7.4 (m, 5H, Ar*H*), 5.9 (br, O*H*), 5.31 (dd, 1H, C*H*Ar), 4.22 (dd, 1H, C*H*HOH), 3.72 (dd, 1H, CH*H*OH), 1.15-1.8 (m, 18H). ^{13}C NMR ($CDCl_3$, δ) : 17.25, 20.66, 25.64, 32.30, 34.21, 39.99, 40.52, 61.03, 67.93, 69.18, 84.23, 126.96, 127.83, 128.31, 139.10.

3.3.3 Synthesis of 2,2,5-trimethyl-[1,3]dioxane-5-carboxylic acid (3)

2,2-Bis(hydroxymethyl)propanoic acid (bis-MPA), (4.0 g, 29.8 mmol) along with *p*-TSA (0.1 g, 0.6 mmol), and 2,2-dimethoxypropane (5.6 mL, 44.8 mmol) was dissolved in 20 mL of dry acetone , and stirred 2 h at room temperature. In the vicinity of 2 h, while stirring continued the reaction mixture was neutralized with 3 mL of totally NH_4OH (25 %), and absolute ethanol (1:1), filtered off by-products and subsequent dilution with dichloromethane (80 mL) , and once extracted with distilled water (20 mL). The organic phase was dried with Na_2SO_4, concentrated to yield 4.01 g (77.3 %) as white solid after evaporation of solvent. ^1H NMR ($CDCl_3$, δ): 4.20 and 3.62 (dd, 4 H, C(CH_2O-)$_2$), 1.43-1.39 (d, 6H, -C(CH_3)$_2$), 1.17 (s, 3H, -CH_3).

3.3.4 Synthesis of 2,2,5-trimethyl-[1,3]dioxane-5-carboxylic acid 2-phenyl-2-(2,2,6,6-tetramethyl-piperidin-1-yloxy)ethyl ester (4)

2-Phenyl-2-(2,2,6,6-tetramethyl-piperidin-1-yloxy) ethanol (2.8 g, 10.1 mmol), was dissolved in 20 mL of dry CH_2Cl_2 along with 2,2,5-trimethyl-[1,3]dioxane-5-carboxylic acid (1.9 g, 10.7 mmol), and DMAP (0.5 g, 1.5 mmol) were added in that order. Dicyclohexylcarbodiimide (DCC) (2.6 g, 12.5 mmol) dissolved in CH_2Cl_2 (5 mL) was then immediately added and the mixture was stirred at room temperature for 24 h. The precipitated dicyclohexylurea was filtered off, the solvent was evaporated, and the remaining product was purified by column chromatography (silica gel) eluting with hexane then gradually increasing to 1:4 (EtOAc/hexane) to give the final product as pale yellow oil. Yield 3.68 g (84 %). ^1H NMR ($CDCl_3$, δ): 7.30-7.23 (m, 5H, Ar*H*), 4.93 and 4.91 (dd, 1H, ArC*H*), 4.57 and 4.52 (dd, 1H, ArCHC*H*H), 4.41 (dd, 1H, ArCHCH*H*), 3.98 (dd, 2H, CH_2O), 3.47 (dd, 2H, CH_2O), 1.73-0.72 (m, 21H).

3.3.5 Synthesis of 3-hydroxy-2-hydroxymethyl-2-methyl-propionic acid 2-phenyl -2-(2,2,6,6-tetramethyl-piperidin-1-yloxy)ethyl ester (5)

2,2,5-Trimethyl-[1,3]dioxane-5-carboxylic acid 2-phenyl-2-(2,2,6-trimethyl-piperidin-1-yloxy)ethyl ester (3.7 g, 8.5 mmol) was dissolved in a mixture of 22.2 mL of THF and 11.1 mL of 1 M HCl (aq). The reaction mixture was stirred for 4 h. The precipitated product was filtered off and washed with THF and evaporated at 45 °C to dryness. The crude product was dissolved in CH_2Cl_2 and washed with water. The combined organic phases were dried over Na_2SO_4, filtered and evaporated. The product was isolated as white solid. Yield: 3.14 g (94 %). ^{1}H NMR ($CDCl_3$, δ): 7.4-7.27 (m, 5H, Ar*H*), 5.0 (t, 1H, ArC*H*), 4.51 (d, 2H, ArCHC*H*$_2$), 3.80-3.50 (m, 4H, C*H*$_2$OH), 2.74 (br, 1H, CH_2O*H*), 2.61 (br, 1H, CH_2O*H*), 1.65-0.55 (m, 21H).

3.3.6 Synthesis of 2-(2-bromo-2-methyl-propionyloxymethyl)-3-hydroxy-2-methyl propionic acid 2-phenyl-2-(2,2,6,6-tetramethyl-piperidin-1-yloxy) ethyl ester (6)

3-Hydroxy-2-hydroxymethyl-2-methyl-propionic acid 2-phenyl-2-(2,2,6,6-tetramethyl-piperidin-1-yloxy)ethyl ester (4.2 g, 10.7 mmol) was dissolved in dry TEA (3.3 mL, 23 mmol) and CH_2Cl_2 (20 mL) and cooled to 0 ^{o}C. 2-bromoisobutyrylbromide (1.3 mL, 10.7 mmol) was added dropwise to the reaction mixture within 30 minutes. It was then stirred for 4 h at room temperature. After dilution with 200 mL of CH_2Cl_2, the mixture was extracted three times with 50 mL of saturated aqueous solution of $NaHCO_3$. The organic phase was dried over Na_2SO_4. The solution was purified by column chromatography on silica gel with 1:10 (ethylacetate/ hexane) to give 4.37 g (75 % yield) of product as pale yellow. ^{1}H NMR ($CDCl_3$, δ): 7.45-7.2 (m, 5H, Ar*H*), 4.97 (t, 1H, ArC*H*), 4.4-4.6 (m, 2H, ArCHC*H*$_2$), 4.3 and 4.1 (dd, 2H, C*H*$_2$OCO), 3.55 (dd, 2H, C*H*$_2$OH), 2.3 (br, 1H, CH_2O*H*), 1.85 (d, 6H, CBr(C*H*$_3$)$_2$), 1.60-0.6 (m, 21H). ^{13}C NMR ($CDCl_3$, δ): 17.0, 17.2, 20.3, 28.3, 29.6, 30.5, 33.8, 40.1, 48.4, 55.3, 60.1, 64.9, 66.9, 83.5, 127.15, 127.18, 127.7, 128.14, 128.15, 140.0, 171.3, 173.6. Anal. Calc. for $C_{26}H_{40}BrNO_6$: C, 57.56%; H, 7.43; N, 2.58%. Found: C, 57.52%; H, 7.40%, N, 2.60%.

3.3.7 Synthesis of pent-4-ynoic acid 3-(2-bromo-2-methyl-propionyloxy)-2-methyl-2-[2-phenyl-2-(2,2,6,6-tetramethylpiperidin-1-yloxy)-ethoxy carbonyl] propyl ester (7)

About 0.9 g, 1.6 mmol of **6** was dissolved in 15 mL of dichloromethane. To this solution, DMAP (0.2 g, 1.6 mmol) and 4-pentynoic acid (0.2 g, 2.0 mmol) were added in that order. After stirring for 5 min at room temperature, DCC (0.5 g, 2.3 mmol) dissolved in 10 mL CH_2Cl_2 was added to the reaction medium. The reaction mixture was then stirred overnight at room temperature. After filtration of the byproduct, urea was removed from the solvent, and the remaining product was purified by column chromatography over silica gel eluting with hexane/ethylacetate (4:1) yielding **7** (0.765 g; 90%). ^{1}H NMR ($CDCl_3$, δ) 7.32–7.26 (m, 5H, Ar*H*), 4.94 and 4.91 (dd, 1H, ArC*H*), 4.57 and 4.52 (dd, 1H, ArCHC*H*H), 4.42 and 4.37 (dd, 1H, ArCHCH*H*), 4.18–4.11 (m, 4H, CH_2OC=O), 2.45–2.40 (m, 4H, C=OCH_2CH_2CCH), 1.95 (t, 1H, *H*C≡CCH_2), 1.83 (6H, CBr(CH_3)$_2$), 1.58–0.74 (m, 21H). Anal. Calcd for $C_{31}H_{44}NO_7Br$: C, 59.80%; H, 7.12%; N, 2.25%. Found: C, 59.75%; H, 7.06%; N, 2.20%.

3.3.8 Synthesis of 1,2-bis(bromoisobutryloxy)ethane (8)

1,2-Bis(bromoisobutryloxy)ethane was synthesized by dropwise addition of 2-bromoisobutyryl bromide (2.25 mL, 42 mmol) to ethylene gylcol (1.25 mL, 21.15 mmol) and TEA (6.3 mL, 45.05 mmol) solution in CH_2I_2 (50 mL) at 0 °C under an nitrogen atmosphere. After addition, the reaction mixture was stirred overnight at room temperature. The reaction mixture was extracted with $NaHCO_3$ and NaCl solution and organic phase was dried with Na_2SO_4. The solution was concentrated and the crude product was purified by column chromatography over silica gel eluting with Hexane/Ethyl acetate (10/1) to give the product as white solid (yield: 4.5 g, 65 %). ^{1}H NMR ($CDCl_3$, δ) 4.43 (s, 4H, O=CO*C*H_2*C*H_2OC=O) 1.94 (s, 6H, OC=OCC(*C*H_3)$_2$.

3.3.9 General procedure for the synthesis of PS macroinitiator by NMP of St

St (2.0 mL, 17.4 mmol) and **7** (0.054 g, 0.087 mmol) were added to a schlenk tube and the reaction mixture was degassed by three freeze-pump-thaw (FPT) cycles and then placed in a thermostated oil bath at 125 ^{o}C for 17 h. The polymerization mixture was diluted with THF, and precipitated in methanol. The polymer was dried for 24 h

in a vacuum oven at 25 °C ($M_{n,GPC}$ = 9800; $M_{n,theo}$ = 9300;$M_{n,NMR}$ =10000;M_w/M_n = 1.2). ^{1}H NMR ($CDCl_3$, δ) 7.5-6.2 (br, Ar*H* of PS), 4.2 (br, 1H, C*H*(Ph)-Br), 2.4 (t, 1H, *H*C≡CCH_2), 2.2-1 (br, aliphatic protons of PS, other aliphatic protons).

3.3.10 General procedure for the synthesis of PS-*b*-PMMA by ATRP of MMA (PS-PMMA-Alkyne)

To a schlenk tube equipped with a magnetic stirring bar, MMA (1.00 mL, 9.35 mmol), PMDETA (6.50 μL, 0.03 mmol), CuCl (3.00 mg, 0.03 mmol), toluene (1 mL), and PS macroinitiator (0.31 g, 0.03 mmol, based on $M_{n,NMR}$) were added in that order and the reaction mixture was degassed by three FPT cycles. The polymerization was carried out at 60 °C under degassed conditions for 1 h. After the polymerization, the reaction mixture was diluted with THF and then passed through a column of neutral alumina to remove metal salt. The polymerization mixture was diluted with THF and precipitated in methanol. The block copolymer was dried for 24 h in a vacuum oven at 25 °C ($M_{n,GPC}$ = 17,000; $M_{n,NMR}$ = 17,800; $M_{n,theo}$ = 16,000; M_w/M_n = 1.17). ^{1}H NMR ($CDCl_3$, δ) 7.2-6.3 (Ar*H* of PS), 3.58 (br, OCH_3 of PMMA), 2.4 (t, 1H, *H*C≡CCH_2), 2.2-0.6 (aliphatic protons of PMMA and PS).

3.3.11 General procedure for the synthesis of dibromo end-functionalized P*t*BA by ATRP (Br-P*t*BA-Br)

Dibromo end-functionalized P*t*BA was prepared by the ATRP of *t*BA in bulk with CuBr/PMDETA as catalyst and difunctional initiator (**8**). To a schlenk tube equipped with a magnetic stirring bar, the *t*BA, (10.0 mL, 68.3 mmol), ligand, (PMDETA, 95.00 μL, 0.46 mmol), CuBr (65 mg, 0.46 mmol), and difunctional initiator (0.08 g, 0.23 mmol) were added in this order and the reaction mixture was degassed by three FPT cycles. The polymerization was carried out at 80 °C under degassed conditions for 20 min. After the polymerization, the reaction mixture was diluted with THF and then passed through a column of neutral alumina to remove metal salt. The excess of THF and the unreacted monomer were evaporated under reduced pressure. The polymer was dissolved in THF and precipitated into excess amount of cold methanol/water (80/20; v/v). After decantation, the polymer was dissolved in CH_2Cl_2, extracted with water and dried over Na_2SO_4. Finally, the organic phase was evaporated to give dibromo end-functionalized P*t*BA ($M_{n,GPC}$ = 5100; $M_{n,theo}$ = 4970; $M_{n,NMR}$=4300;M_w/M_n=1.29).^{1}H NMR ($CDCl_3$, δ) 4.29 (s, 4H, O=COCH_2CH_2OC=O),

4.2-4.0 (m, and C*H*Br end group of P*t*BA), 2.2 (br, C*H* of P*t*BA), 2.0-1.0 (br, aliphatic protons of P*t*BA).

3.3.12 General procedure for the synthesis of diazide end functionalized P*t*BA (N_3-P*t*BA-N_3)

To a solution of dibromo end-functionalized P*t*BA (Br-P*t*BA-Br) (0.76 g, 0.18 mmol, based on $M_{n,NMR}$) in dimethylformamide (DMF) (10 mL), NaN_3 (0.2 g, 3.0 mmol) was added. Stirring the reaction mixture overnight at room temperature, CH_2Cl_2 and water were added and the organic layer was extracted three times with water and dried over Na_2SO_4. The purification procedure was the same as described for the preparation of Br-P*t*BA-Br. Yield: 0.72 g (95 %). FTIR (cm^{-1}): 2109 (s) (azide stretching). ($M_{n,GPC}$ = 5250; $M_{n,theo}$ = 4970; $M_{n,NMR}$ = 4300; M_w/M_n = 1.27). ^{1}H NMR ($CDCl_3$, δ) 4.29 (s, 4H, O=COCH_2CH_2OC=O), 3.7-3.6 (m, C*H*N_3 end group of P*t*BA), 2.2 (br, C*H* of P*t*BA), 2.0-1.0 (br, aliphatic protons of P*t*BA).

3.3.13 General procedure for the synthesis of ditosylated PEG

HO-PEG-OH (M_n = 6000 g/mol) (3 g, 0.5 mmol) is dissolved in 5 mL of CH_2Cl_2. To this solution, DMAP (0.0305 g, 0.25 mmol), TEA (0.416 mL, 3 mmol), and toluene-4-sulfonyl chloride (tosyl chloride) (0.572 g, 3 mmol) were added. Reaction mixture was stirred overnight at room temperature. First, it was extracted with cold 4 M HCl, then with distilled water and dried over Na_2SO_4. The organic phase was evaporated to 1/4 of its volume and precipitated into diethyl ether. The product was obtained as white solid. Yield: 2.93 g (97 %). ^{1}H NMR ($CDCl_3$, δ) 7.80 and 7.34 (8H, PEG-$OSO_2C_6H_4CH_3$), 4.16 (4H, CH_2CH_2-$OSO_2C_6H_4CH_3$), 3.63 (OCH_2CH_2 repeating unit of PEG), 2.44 (6H, PEG$OSO_2C_6H_4CH_3$).

3.3.14 General procedure for synthesis of diazide end fuctionalized PEG (N_3-PEG-N_3)

Ditosylated-PEG (2.93 g, 0.46 mmol) was dissolved in DMF (15 mL) and sodium azide (NaN_3) (0.299 g, 4.6 mmol) was added to this solution. After stirring the reaction mixture overnight at room temperature, CH_2Cl_2 and water were added and the organic layer was extracted three times with water and dried over Na_2SO_4. The polymer was precipitated in diethyl ether. The polymer was dried for 24 h in a

vacuum oven at 25 ^{o}C. Yield: 2.8 g (96 %). ^{1}H NMR ($CDCl_3$, δ) 3.63 (m, OCH_2CH_2 repeating unit of PEG and CH_2CH_2O-N_3).

3.3.15 Synthesis of heteroarm H-shaped polymer via copper(I) catalyzed azide-alkyne cycloaddtion (CuAAC) reaction between PS-*b*-PMMA and N_3-P*t*BA-N_3

Alkyne functionalized PS-*b*-PMMA copolymer (0.19 g, 0.01 mmol, based on $M_{n,NMR}$) and N_3-P*t*BA-N_3 (0.022 g, 0.005 mmol, based on $M_{n,NMR}$) were dissolved in nitrogen-purged DMF (5 mL) in a schlenk tube equipped with magnetic stirring bar. CuBr (3.5 mg, 0.025 mmol) and PMDETA (5.2 μL, 0.025 mmol) were added and the reaction mixture was degassed by three FPT cycles, left in argon and stirred at room temperature for 24 h. Reaction mixture was passed through alumina column to remove copper salt, precipitated into methanol and dried in vacuum oven at 25 ^{o}C. Yield: 0.175 g. ($M_{n,GPC}$ = 32,000; $M_{n,theo}$ = 39900; $M_{n,NMR}$ = 4300; $M_{n,NMR}$ = 34800; M_w/M_n = 1.33). ^{1}H NMR ($CDCl_3$, δ) 7.2-6.3 (Ar*H* of PS), 3.58 (br, OCH_3 of PMMA), 2.2 (br, C*H* of P*t*BA), 2.1-0.6 (aliphatic protons of P*t*BA, PMMA and PS).

3.3.16 Synthesis of heteroarm H-shaped polymer via CuAAC reaction between PS-*b*-PMMA and N_3-PEG-N_3

Alkyne functionalized PS-*b*-PMMA copolymer (0.150 g, 0.008 mmol, based on $M_{n,NMR}$) and N_3-PEG-N_3 (0.025 g, 0.004 mmol, based on $M_{n,NMR}$) were dissolved in nitrogen-purged DMF (5 mL) in a schlenk tube. CuBr (0.003 g, 0.020 mmol) and PMDETA (4.4 μL, 0.020 mmol) were added and the reaction mixture was degassed by three FPT cycles, left in argon and stirred at room temperature for 24 h. The purification step was the same as described above. Yield: 0.14 g. ($M_{n,GPC}$ = 22,000; $M_{n,theo}$ = 41600; $M_{n,NMR}$ = 36500; M_w/M_n = 1.16). ^{1}H NMR ($CDCl_3$, δ) 7.2-6.3 (Ar*H* of PS), 3.62 (br, OCH_2CH_2 of PEG) 3.58 (br, OCH_3 of PMMA), 2.1-0.6 (aliphatic protons of PMMA and PS).

3.3.17 Preparation of merrifield's resin with alkyne functionality (merrifield's resin-alkyne)

Merifield's resin (1 g, 1 mmol), K_2CO_3 (6.9 g, 0.050 mol), and propargyl alcohol (2.8 g, 0.050 mol) were added in 40 mL of DMF and the resulting solution was

stirred at 110 °C for 48 h. The obtained resin was washed several times with water and THF, respectively. FTIR (cm^{-1}): 2330 ($HC{\equiv}CCH_2$) and 3300 ($HC{\equiv}CCH_2$).

3.3.18 Preparation of azide-functionalized merrifield's resin (merrifield's resin-azide)

Merrifield's resin (1 g, 1 mmol) was suspended in DMF (30 mL), and sodium azide (2.6 g, 40 mmol) was added to the mixture. The reaction mixture was stirred overnight at 80 °C, then filtered, washed three times with distilled water, methanol, and acetone to give Merrifield's resin with azidomethyl functionality and dried in vacuum oven at 25 °C. FTIR (cm^{-1}): 2109 (s) (azide stretching).

3.3.19 Synthesis of PCL macroinitiator with TEMPO and bromide functionality by ROP of ε-CL

Degassed ε-CL (5 mL, 45 mmol), $Sn(Oct)_2$ (9 mg, 0.02 mmol), and **6** (0.245g, 0.45 mmol) were added to a previously flamed Schlenk tube in that order. The tube was degassed with three FPT cycles, left in vacuum, and placed in a thermostated oil bath at 110 °C for 10.5 h. After a specified polymerization time, the mixture was diluted with THF, precipitated in an excess amount of methanol, and then isolated by filtration and dried at room temperature in a vacuum oven. ($M_{n,GPC}$ = 15000; $M_{n,PCL}$ = 7800; $M_{n,theo}$ = 8600; $M_{n,NMR}$ = 6500; M_w/M_n = 1.13).^{1}H NMR ($CDCl_3$, δ) 4.04 (t, 2H, $CH_2OC{=}O$ of PCL), 3.65 (t, 2H, CH_2OH, end-group of PCL), 2.3 (t, 2H, $C{=}OCH_2$ of PCL), 1.91 (6H, $CBr(CH_3)_2$), 1.8-1.2 (m, 6H, CH_2 of PCL).

3.3.20 Synthesis of PCL-*b* -PS copolymer with bromide functionality by NMP of St

St (5.0 mL, 43.6 mmol) and PCL macroinitiator (1.42 g, 0.22 mmol, based on $M_{n,NMR}$) were added to a schlenk tube and the reaction mixture was degassed by three freeze-pump-thaw (FPT) cycles and then placed in a thermostated oil bath at 125 °C for 3h. Next, The polymerization mixture was diluted with THF, precipitated in methanol, isolated by filtration, and dried in a vacuum oven at room temperature ($M_{n,GPC}$ = 22900; $M_{n,theo}$ = 12750; $M_{n,NMR}$ = 13000; M_w/M_n = 1.13). ^{1}H NMR ($CDCl_3$, δ) 7.2-6.3 (Ar-*H* of PS), 4.07-4.01 ($CH_2CH_2CH_2CH_2CH_2OC{=}O$, repeating unit of PCL), 2.5-2.2 ($C{=}OCH_2CH_2CH_2CH_2CH_2O$), 0.6-2.2 (aliphatic protons).

3.3.21 General procedure for the synthesis of bromide end-functionalized miktoarm star polymer (PCL-PS-P*t*BA-Br) by ATRP of *t*BA

To a schlenk tube equipped with a magnetic stirring bar, *t*BA (3.00 mL, 21 mmol), PMDETA (14 μL, 0.07 mmol), CuBr (1.00 mg, 0.07 mmol), toluene (3 mL), and PCL-PS macroinitiator (0.9 g, 0.07 mmol, based on $M_{n,NMR}$) were added in that order and the reaction mixture was degassed by three FPT cycles. The polymerization was carried out at 60 ^{o}C under degassed conditions for 1 h. After the polymerization, the reaction mixture was diluted with THF and then passed through a column of neutral alumina to remove metal salt. The polymerization mixture was diluted with THF and precipitated in methanol, then isolated by filtration. The block copolymer was dried for 24 h in a vacuum oven at 25 ^{o}C ($M_{n,GPC}$ = 28000; $M_{n,NMR}$ = 17600; $M_{n,theo}$ = 18400; M_w/M_n = 1.18). ^{1}H NMR ($CDCl_3$, δ) 7.2-6.3 (Ar*H* of PS), 4.07-4.01 ($CH_2CH_2CH_2CH_2CH_2OC$=O, repeating unit of PCL), 2.5-2.2 (C=O$CH_2CH_2CH_2CH_2CH_2$O of PCL and C*H* of P*t*BA), 2.0-0.6 (aliphatic protons).

3.3.22 Preparation of azide end-functionalized PCL-PS-P*t*BA miktoarm star polymer (PCL-PS-P*t*BA-N_3)

To a solution of PCL-PS-P*t*BA-Br (1.3 g, 0.071 mmol, based on $M_{n,NMR}$) (entry 4 in Table 4.3) in 10 mL of DMF, NaN_3 (0.185 g, 2.84 mmol) was added. After stirring the reaction mixture overnight at room temperature, DMF was evaporated and remaining polymer was dissolved in THF and precipitated in methanol then isolated by filtration. The block copolymer was dried for 24 h in a vacuum oven at 25 ^{o}C. (Yield: 1.1 g, 85%). FTIR (cm^{-1}): 2109 (s) (azide stretching).

3.3.23 Synthesis of propargyl-2,2,5-trimethyl-1,3-dioxane-5-carboxylate (9)

Propargyl alcohol (4.9 mL, 85.0 mmol) was dissolved in 70 mL of CH_2Cl_2 and 2,2,5-trimethyl-[1,3]dioxane-5-carboxylic acid (9.9 g, 57.0 mmol), and DMAP (3.4 g, 28.0 mmol) was added to the reaction mixture in that order. After stirring 5 min at room temperature, DCC (14 g, 68 mmol) dissolved in 30 mL of CH_2Cl_2 was added. Reaction mixture was stirred overnight at room temperature and urea byproduct was filtered. Reaction mixture was extracted with water/ CH_2Cl_2 (1:4) two times, and combined organic phases were dried with Na_2SO_4. Solvent was evaporated and the remaining product was purified by column chromatography over silica gel eluting with hexane/ethyl acetate (9:1) to give pale yellow oil (yield = 8.1 g; 67%). ^{1}H NMR

($CDCl_3$, δ) 4.72 (d, 2H, CH≡CC*H*$_2$O), 4.18 (d, 2H, CC*H*$_2$O), 3.63 (d, 2H, CC*H*$_2$O), 2.45 (t, 1H, C*H*≡CCH$_2$O), 1.40 (s, 3H, *CCH*$_3$*)* 1.36 (s, 3H, *CCH*$_3$*),* 1.18 (s, 3H, C=OC(CH$_2$O)$_2$C*H*$_3$). ^{13}C NMR (CDCl3, δ*)* 173.47, 98.11, 76.58, 73.03, 65.84, 52.35, 49.96, 25.68, 23.66, 17.37.

3.3.24 Synthesis of propargyl-3-hydroxy-2-(hydroxymethyl)-2-methyl propanoate (10)

Propargyl-2,2,5-trimethyl-1,3-dioxane-5-carboxylate (**9**) (4.0 g, 19 mmol) was dissolved in a mixture of 10 mL of THF and 10 mL of 1 M HCl. The reaction mixture was stirred for 2 h at room temperature. The precipitated product was filtered off, the reaction mixture was concentrated and extracted with 160 mL of CH_2Cl_2 and 40 mL of water. The combined organic phase was dried with Na_2SO_4 and conc. Hexane was added to the reaction mixture, and it was kept in deep freeze overnight to give white solid, M_p = 50 °C (yield = 3.1 g, 95%). ^{1}H NMR ($CDCl_3$, δ*)* 4.72 (d, 2H, CH≡CC*H*$_2$O), 3.88 (d, 2H, C*H*$_2$OH), 3.69 (d, 2H, C*H*$_2$OH), 2.93 (br, 2H, O*H*), 2.48 (s, 1H, C*H*=CCH$_2$O), 1.07 (s, 3H, *CCH*$_3$*)*. ^{13}C NMR ($CDCl_3$, δ) 175.08, 76.56, 73.28, 67.70, 52.52, 50.04, 18.05.

3.3.25 Synthesis of propargyl-3-[(2-bromo-2-methylpropanoyl)oxy]-2-(hydroxy methyl)-2-methylpropanoate (11)

Propargyl-3-hydroxy-2-(hydroxymethyl)-2-methylpropanoate (**10**) (0.9 g, 5.2 mmol) was dissolved in 15 mL of CH_2Cl_2, and TEA (1.6 mL, 11.5 mmol) was added to the mixture, followed by cooling to 0 °C. 2-Bromo isobutrylbromide (0.65 mL, 5.2 mmol) in 5 mL of CH_2Cl_2 was added dropwise within 30 min. The reaction mixture was further stirred 4 h at room temperature. After filtration, the mixture was extracted with CH_2Cl_2 and saturated aq. $NaHCO_3$. The aqueous phase was again extracted with CH_2Cl_2, and organic phase was dried with Na_2SO_4. The solution was concentrated, and the crude product was purified by column chromatography over silica gel eluting with hexane/ethyl acetate (4:1) to give pale yellow oil (yield = 1.25 g, 75%). ^{1}H NMR ($CDCl_3$, δ) 4.72 (d, 2H, CH= CC*H*$_2$O), 4.43 and 4.30 (dd, 2H, C*H*$_2$OC=O), 3.75 (d, 2H, C*H*$_2$OH), 2.47 (t, 1H, C*H*≡CCH$_2$O), 2.33 (br, 1H, O*H*), 1.91 (6H, CBr(C*H*$_3$)$_2$), 1.27 (s, 3H, (s, 3H, CC*H*$_3$). ^{13}C NMR ($CDCl_3$, δ) 173.28, 171.50, 76.53, 75.29, 66.93, 64.93, 55.42, 52.54, 48.54, 30.66, 17.26.

3.3.26 Synthesis of alkyne end functionalized PEG macroinitiator

PEG-COOH (2.0 g, 0.95 mmol, based on $M_{n,NMR}$) was dissolved in 40 mL of CH_2Cl_2. **11** (1.2 g, 3.8 mmol) and DMAP (0.2 g, 1.9 mmol) were added to the reaction mixture in that order. After stirring for 5 min at room temperature, DCC (0.6 g, 5.7 mmol) dissolved in 10 mL of CH_2Cl_2 was added. Reaction mixture was stirred overnight at room temperature. After filtration, the solution was concentrated and precipitated in cold diethyl ether and the product was dissolved in CH_2Cl_2. This dissolution-precipitation was repeated two times. Yield: 1.68 g (73%); M_{ntheo} = 2400; M_{nNMR} = 2600; $M_{n\ GPC}$ = 3500; M_w/M_n = 1.02). ^{1}H NMR ($CDCl_3$, δ): 4.7 (s, 2H, CH≡CCH_2O), 4.4–4.2 (m, 6H, PEG-OCH_2CH_2OC=O and CH_2OC=O), 3.9 (t, 2H, PEG-OCH$_2$CH_2OC=O), 3.8–3.5 (m, 4H, OCH_2CH_2O, repeating unit of PEG), 3.4 (s, 3H, OCH_3 end group of PEG), 2.6 (s, 2H, C=OCH_2CH_2C=O), 2.5 (s, 1H, CH≡CCH$_2$O), 1.9 (s, 6H, C(Br)(CH_3)$_2$), 1.3 (s, 3H, C=OCCH_3).

3.3.27 Preparation of PEG-*b*-PMMA copolymer with alkyne at the junction point (PEG-PMMA-Alkyne) via ATRP of MMA

MMA (3.0 mL, 28 mmol), PMDETA (29 µL, 0.14 mmol), CuCl (14 mg, 0.14 mmol), toluene (3 mL), and PEG-macroinitiator (0.36 g, 0.14 mmol, $M_{n,NMR}$) were added in that order to a schlenk tube equipped with a magnetic stirring bar. The polymerization was carried out at 60 ^{o}C under degassed conditions for 1 h. After this specified time, the reaction mixture was diluted with THF and then passed through a column of neutral alumina to remove metal salt. Next, the mixture was diluted with THF and precipitated in hexane. The block copolymer was dried for 24 h in a vacuum oven at 25 ^{o}C ($M_{n,theo}$ = 8800; $M_{n,NMR}$ = 11300; $M_{n,GPC}$ = 13700; M_w/M_n= 1.08, relative to PS standards). ^{1}H NMR ($CDCl_3$, δ) 4.71 (s, 2H, CH≡CCH_2O), 4.22 (m, 6H, PEG-OCH_2CH_2OC=O and CH_2OC=O), 3.89 (t, 2H, PEG-OCH$_2$CH_2OC=O), 3.7-3.5 (br, OCH_2CH_2O, repeating unit of PEG and OCH_3 of PMMA), 3.4 (s, 3H, OCH_3 end group of PEG), 2.62 (s, 4H, C=OCH_2CH_2C=O), 2.52 (s, 1H, CH≡CCH$_2$O), 2.0–0.6 (aliphatic protons).

3.3.28 Synthesis of ABCDE H-shaped quintopolymer by click reaction of miktoarm star polymer (PS–PCL–P*t*BA-N_3) with block copolymer (PEG–PMMA–Alkyne)

Azide end-functionalized PS-PCL-PtBA miktoarm star terpolymer (0.42 g, 0.023 mmol, based on $M_{n,NMR}$) and PEG–PMMA copolymer with alkyne at the junction point (0.36 g, 0.032 mmol, based on $M_{n,NMR}$) were dissolved in nitrogen-purged DMF (15 mL) in a schlenk tube. CuBr (0.0165 g, 0.115 mmol) and PMDETA (0.0240 mL, 0.115 mmol) were added, and the reaction mixture was degassed by three FPT cycles and left in argon and stirred at room temperature for 20 h. After that time, reaction mixture was passed through alumina column to remove copper salt, precipitated into methanol, and dried in a vacuum oven at 25 ^{o}C (yield = 0.60 g, 89%). Thus, obtained H-shaped quintopolymer was sequentially treated with Merrifield's azide and alkyne resin to remove precursors ($M_{n,theo}$ = 29700; $M_{n,NMR}$ = 22400; $M_{n,GPC}$ = 32100; M_w/M_n= 1.2, relative to PS standards). ^{1}H NMR ($CDCl_3$, δ) 7.2–6.2 (br, 5H, Ar*H* of PS), 4.04 (br, 2H, CH_2OC =O of PCL), 3.63 (br, 4H, OCH_2CH_2 of PEG), 3.58 (br, OCH_3 of PMMA), 2.32–2.1 (br, 2H, C=OCH_2 of PCL and 1H, backbone C*H*(C=O) of P*t*BA), 2–0.7 (br, aliphatic protons).

3.3.29 General procedure for treatment of H-shaped quintopolymer with merrifield's resin-azide to remove unreacted PEG–PMMA–Alkyne copolymer

H-shaped quintopolymer (0.60 g, 0.019 mmol) was dissolved in DMF (15 mL) in a schlenk tube. CuBr (0.0136 g, 0.095 mmol), PMDETA (0.0198 mL, 0.095 mmol), and Merrifield's resin-azide (0.1 g) were added, and the reaction mixture was degassed by three FPT cycles and left in argon and stirred at room temperature for 2 days. Reaction mixture was passed through alumina column to remove copper salt and the resin, precipitated into methanol, and dried in vacuum oven at 25 ^{o}C (Yield : 0.58 g) ($M_{n,GPC}$= 31,700, M_w/M_n = 1.22).

3.3.30 General procedure for the treatment of H-Shaped quintopolymer with merrifield's resin-alkyne to remove unreacted PCL–PS–P*t*BA–N_3 miktoarm star terpolymer

After a treatment described earlier, H-shaped polymer (0.58 g, 0.018 mmol) was dissolved in DMF (15 mL) in a schlenk tube. CuBr (0.013 g, 0.09 mmol), PMDETA

(0.019 mL, 0.09 mmol), and Merrifield's resin-alkyne (0.1 g) were added, and the reaction mixture was degassed by three FPT cycles and left in argon and stirred at room temperature for 2 days. Reaction mixture was passed through alumina column to remove copper salt and the resin, precipitated into methanol, and dried in vacuum oven at 25 ^{o}C (Yield: 0.58 g) (M_{nGPC} = 32,100, M_w/M_n = 1.20).

3.3.31 Synthesis of 4,10-dioxatricyclo[5.2.1.0^{2,6}]dec-8-ene-3,5-dione (12)

Maleic anhydride (60.0 g, 0.6 mol) was suspended in 150 mL of toluene and the mixture warmed to 80 °C. Furan (66.8 mL, 0.9 mol) was added via syringe and the turbid solution was stirred for 6 h. The mixture was then cooled to ambient temperature white solids formed during standing were collected by filtration and washed with 2 × 30 mL of petroleum ether and once with diethyl ether (50 mL) afforded **12** as white needless. Yield: 80.2 g (80%). Mp: 114-115 ^{o}C (DSC). ^{1}H NMR ($CDCl_3$, δ) 6.57 (s, 2H, C*H*=C*H*, bridge protons), 5.45 (s, 2H, -C*H*O, bridge-head protons), 3.17 (s, 2H, C*H*-C*H*, bridge protons). ^{13}C NMR ($CDCl_3$, δ) 170.18, 137.29, 82.46, 48.88.

3.3.32 Synthesis of 4-(2-hydroxyethyl)-10-oxa-4-azatricyclo[5.2.1.0^{2,6}]dec-8-ene-3,5-dione (13)

The adduct **12** (10.0 g, 60.0 mmol) was suspended in methanol (150 mL) and the mixture was cooled to 0 °C. A solution of ethanolamine (3.6 mL, 60 mmol) in 30 mL of methanol was added dropwise (10 min) to the reaction mixture, and the resulting solution was stirred for 5 min at 0 °C, then 30 min at ambient temperature, and finally refluxed for 6 h. After cooling the mixture to ambient temperature, solvent was removed under reduced pressure, and residue was dissolved in 150 mL of CH_2Cl_2 and washed with 3 × 100 mL of water. The organic layer was separated, dried over Na_2SO_4 and filtered. Removal of the solvent under reduced pressure gave white-off solid which was further purified by flash chromatography eluting with ethylacetate (EtOAc) to give the product as a white solid. Yield: 5 g (41%). Mp = 138-139 °C (DSC). ^{1}H NMR ($CDCl_3$, δ) 6.51 (s, 2H, C*H*=C*H*, bridge protons), 5.26 (s, 2H, -C*H*O, bridge-head protons), 3.74-3.68 (m, 4H, NC*H*$_2$C*H*$_2$OH), 2.88 (s, 2H, C*H*-C*H*, bridge protons). ^{13}C NMR ($CDCl_3$, δ) 177.03, 136.60, 81.09, 60.53, 47.74, 42.03.

3.3.33 Synthesis of 2,2,5-trimethyl-[1,3]dioxane-5-carboxylic acid 4-(2-ethyl)-10-oxa-4-azatricyclo[5.2.1.$0^{2,6}$] dec-8-ene-3,5-dione ester (14)

4-(2-Hydroxyethyl)-10-oxa-4-azatricyclo[5.2.1.$0^{2,6}$] dec-8-ene-3,5-dione (5.0 g, 24 mmol) was dissolved in 50 mL of CH_2Cl_2 and 2,2,5-trimethyl-[1,3]dioxane-5-carboxylic acid (4.2 g, 24.0 mmol), and DMAP (1.5 g, 12.0 mmol) were added to the reaction mixture in that order. After stirring 5 minutes at room temperature, DCC (5 g, 24.0 mmol) dissolved in 30 mL of CH_2Cl_2 was added. The reaction mixture was stirred overnight at room temperature, than filtered and evaporated. The remaining product was extracted two times with water/CH_2Cl_2 (1:4) and finally dried with Na_2SO_4. The raw product was further purified by column chromatography over silica gel eluting with hexane/ EtOAc (9:1) to give **14** as a cream colored solid. Yield : 8.3 g (95 %). ^{1}H NMR ($CDCl_3$, δ) 6.50 (s, 2H, C*H*=C*H*, bridge protons), 5.24 (s, 2H, C*H*O, bridge-head protons), 4.25 (t, 2H, -CH_2OC=O), 4.19-4.00 (m, 2H, C=O(CH_3)CH_2O), 3.74 (t, 2H, -NCH_2), 3.7-3.5 (m, 2H, C=OC(CH_3)CH_2O), 2.86 (s, 2H, C*H*-C*H*, bridge protons), 1.37 (s, 3H, CCH_3) 1.34 (s, 3H, CCH_3), 1.15 (s, 3H, C=OC(CH_2O)$_2$CH_3).

3.3.34 Synthesis of 3-hydroxy-2-hydroxymethyl-2-methyl-propionic acid 4-(2-ethyl)-10-oxa-4-azatricyclo [5.2.1.$0^{2,6}$]dec-8-ene-3,5-dione ester (15)

14 (6.0 g, 16 mmol) was dissolved in a mixture of 30 mL of THF and 30 mL of 1 M HCl. The reaction mixture was stirred for 2 h at room temperature, than mixture was filtered, concentrated and extracted two times with 160 mL of CH_2Cl_2 and 40 mL of water. The combined organic phase was dried with Na_2SO_4 and concentrated. Hexane was added to the solution and the mixture was stored in a deep freeze overnight to give white solid **15**. Yield: 5 g (94 %). ^{1}H NMR ($CDCl_3$, δ) 6.50 (s, 2H, C*H*=C*H*, bridge protons), 5.26 (s, 2H, C*H*O, bridge-head protons), 4.29 (m, 2H, -CH_2OC=O), 4.4-3.5 (m, 6H, -NCH_2 and CH_2OH), 2.87 (s, 2H, C*H*-C*H*, bridge protons), 2.67 (bs, 2H, O*H*), 1.0 (s, 3H, CH_3).

3.3.35 Synthesis of 2-(2-bromo-2-methyl-propionyloxymethyl)-3-hydroxy-2-methyl propionic acid 4-(2-ethyl)-10-oxa-4-azatricyclo [5.2.1.$0^{2,6}$]dec-8-ene-3,5-dione ester (16)

15 (3.0 g, 9.2 mmol) was dissolved in 15 mL of CH_2Cl_2 and TEA (2.8 mL, 20.3 mmol) was added to the mixture, followed by cooling to 0 ^{o}C. 2-bromoisobutryl

bromide (1.1 mL, 9.2 mmol) in 10 mL of CH_2Cl_2 was added dropwise within 30 minutes to the solution. The reaction mixture was further stirred 4 h at room temperature. After filtration the mixture was extracted with CH_2Cl_2/ saturated aq. $NaHCO_3$. The aqueous phase was again extracted with CH_2Cl_2 and the combined organic phase was dried with Na_2SO_4. The solution was concentrated and the crude product was further purified by column chromatography over silica gel eluting with hexane/EtOAc (4:1) to give yellow oil **16.** Yield: 3.1 g (70 %). ^{1}H NMR ($CDCl_3$, δ) 6.50 (s, 2H, C*H*=C*H*, bridge protons), 5.27 (s, 2H, C*H*O, bridge-head protons), 4.26 (m, 4H, -NCH$_2$C*H*$_2$OC=O and C*H*$_2$OC=O), 3.77 (t, 2H, -NC*H*$_2$), 3.65 (s, C*H*$_2$OH), 2.88 (s, 2H, C*H*-C*H*, bridge protons), 1.88 (s, 6H, CBr(C*H*$_3$)$_2$), 1.19 (s, 3H, CC*H*$_3$). ^{13}C NMR ($CDCl_3$, δ) 176.3, 173.7, 171.4, 136.5, 80.9, 67.0, 65.1, 61.7, 55.6, 48.7, 47.5, 38.0, 30.7, 17.3.

3.3.36 Synthesis of 2-(hydroxymethyl)-2-methyl-3-oxo-3-(2-phenyl-2-(2,2,6,6-tetramethylpiperidin -1-yloxy)ethoxy)propyl pent-4-ynoate (17)

5 (1.7 g, 4.3 mmol), 4-pentynoic acid (0.42 g, 4.3 mmol), DCC (0.9 g, 4.3 mmol) and DMAP (0.26 g, 2.1 mmol) were dissolved in 20 mL of CH_2Cl_2. The reaction mixture was stirred overnight at room temperature, then filtered, evaporated and the remaining product was purified by column chromatography over silica gel eluting with hexane/ EtOAc (8:2) to obtain pure viscous colorless product. Yield: 0.86 g (43%). ^{1}H NMR ($CDCl_3$, δ) 7.33–7.22 (m, 5H, Ar*H*), 4.98–4.94 (m, 1H, ArC*H*), 4.51–4.42 (m, 2H, ArCHC*H*$_2$), 4.14 (d, 2H, C*H*$_2$OC=O), 3.6–3.42 (m, 2H, C*H*$_2$OH), 2.45–2.40 (m, 4H, C=OC*H*$_2$C*H*$_2$C≡CH), 2.38–2.20 (m, 1H, O*H*), 1.95 (t, 1H, *H*C≡CCH$_2$), 1.60–0.70 (m, 21H). Anal. Calc. for $C_{27}H_{39}NO_6$: C, 68.47; H,8.30; N, 2.96; Found C, 68.46; H, 8.28; N, 2.93.

3.3.37 Synthesis of 9-anthyrylmethyl-2-bromo-2-methyl propanoate (18)

9-Anthracene methanol (1.5 g, 7.2 mmol) and DMAP (0.18 g, 1.5 mmol) were dissolved in 50 mL of CH_2Cl_2, and TEA (1.2 mL, 8.6 mmol) was added to the solution, followed by cooling to 0 ^{o}C. 2-bromo isobutyryl bromide (1.8 g, 7.9 mmol) was added dropwise within 30 minutes to this solution. The reaction mixture was stirred for 15 min. at 0 ^{o}C then for overnight at room tempeature. The ammonium salt was filtered off and the solvent was evaporated under reduced pressure. The remaining residue was extracted with CH_2Cl_2, and saturated aqueous $NaHCO_3$. The

aqueous phase was again extracted with CH_2Cl_2, and combined organic phases were dried over Na_2SO_4. The solution was concentrated, and the crude product was purified by column chromatography over silica gel eluting with hexane/EtOAc (10:1) to give **18** as yellow solid. Yield: 1.78 g (70%). M.p. = 83-84 ^oC (DSC). ^1H NMR ($CDCl_3$, δ) 8.51 (s, 1H, Ar*H* of anthracene), 8.33 (d, 2H, Ar*H* of anthracene), 8.03 (d, 2H, Ar*H* of anthracene), 7.60-7.45 (m, 4H, Ar*H* of anthracene), 6.21 (s, 2H, CH_2-anthracene), 1.86 (s, 6H, C(CH_3)$_2$-Br). ^{13}C NMR ($CDCl_3$, δ) 172.01, 131.57, 131.11, 129.29, 129.07, 127.01, 126.05, 125.41, 124.04, 60.99, 56.19, 30.83.

3.3.38 Preparation of PEG macroinitiator with maleimide (PEG-MI)

PEG-COOH (3.4 g, 1.6 mmol, based on $M_{n,NMR}$) was dissolved in 60 mL of CH_2Cl_2 in a round bottom flask. **16** (1.9 g, 4.0 mmol) and DMAP (0.2 g, 1.6 mmol) were added to the reaction mixture in that order. After stirring 5 minutes at room temperature, DCC (1.0 g, 4.8 mmol) dissolved in 20 mL of CH_2Cl_2 was added to this solution and next, the mixture was stirred overnight at room temperature. After removing insoluble parts, the solution was concentrated and precipitated in cold diethyl ether. The above dissolution-precipitation cycle was repeated two times affording PEG-macroinitiator. Yield: 3 g (71%). $M_{n,theo}$ = 2620; $M_{n,NMR}$ = 2590; $M_{n,GPC}$ = 1870, M_w/M_n = 1.19; relative to PS standards). ^1H NMR ($CDCl_3$, δ) 6.50 (s, 2H, C*H*=C*H*, bridge protons), 5.28 (s, 2H, C*H*O, bridge-head protons), 4.22 (m, 6H, -NCH$_2$C*H*$_2$OC=O and C*H*$_2$OC=O), 3.6-3.5 (m, OC*H*$_2$C*H*$_2$, PEG repeating unit and C=ONC*H*$_2$), 3.36 (s, 3H, OC*H*$_3$, end-group of PEG), 2.88 (s, 2H, C*H*-C*H*, bridge protons), 2.62 (s, 4H, C=OC*H*$_2$C*H*$_2$C=O), 1.88 (s, 6H, C(C*H*$_3$)$_2$Br), 1.24 (s, 3H, C*H*$_3$).

3.3.39 Preparation of PEG-*b*-PMMA copolymer side chain with maleimide at its center (PEG-*b*-PMMA-MI)

MMA (5.0 mL, 46.7 mmol), PMDETA (48 μL, 0.23 mmol), CuCl (23 mg, 0.23 mmol), toluene (5 mL), and PEG-macroinitiator (0.60 g, 0.23 mmol, based on $M_{n,NMR}$) were added in that order to a schlenk tube equipped with a magnetic stirring bar. The polymerization was carried out at 50 ^oC under degassed conditions for 1.5 h. After this specified time, the reaction mixture was diluted with THF and then passed through a column of neutral alumina to remove metal salt. Next, the mixture was diluted with THF and precipitated in cold methanol. The recovered block

copolymer (PEG-*b*-PMMA-MI) was dried for 24 h in a vacuum oven at 25 °C ($[M]_0/[I]_0$ = 200; conv. % = 20; $M_{n,theo}$ = 6590; $M_{n,NMR}$ = 8090; $M_{n,GPC}$ = 9860; M_w/M_n= 1.10, relative to PS standards). ^{1}H NMR ($CDCl_3$, δ) 6.50 (s, 2H, C*H*=C*H*, bridge protons), 5.28 (s, 2H, C*H*O, bridge-head protons), 4.22 (m, 6H, -NCH_2CH_2OC=O and CH_2OC=O), 3.91-3.4 (br, -OCH_2CH_2 repeating unit of PEG, OCH_3 of PMMA and NCH_2CH_2OC=O), 3.36 (s, 3H, OCH_3, end-group of PEG), 2.88 (s, 2H, C*H*-C*H*, bridge protons), 2.62 (s, 4H, C=OCH_2CH_2C=O), 2.2-0.6 (aliphatic protons of PMMA).

3.3.40 Synthesis of alkyne end functionalized PCL-macroinitiator by ROP of ε-CL

Degassed ε-CL (2.7 mL, 24 mmol), $Sn(Oct)_2$ (0.0050 g, 0.012 mmol), and initiator **17** (0.115 g, 0.240 mmol) were added to a previously flamed schlenk tube in that order. The tube was degassed with three FPT cycles, left in vacuum, placed in a thermostated oil bath at 110 °C and stirred for 2 h. After this specified time, the mixture was diluted with THF, precipitated into an excess amount of methanol, then isolated by filtration and dried at room temperature in a vacuum oven for 24h ($[M]_0/[I]_0$ = 100; $[I]_0/[Sn(Oct)_2]_0$ = 20; conv. % = 53; $M_{n,theo}$ = 6520; $M_{n,NMR}$ = 5040; $M_{n,GPC}$ = 8500; M_w/M_n = 1.03 relative to PS standards; $M_{n,PCL}$ = 4260 obtained from $M_{n,PCL}$ = 0.259 X $M_{n,GPC}^{1.073}$). ^{1}H NMR ($CDCl_3$, δ) 4.9 (t, H, C*H*Ar), 4.04 (t, 2H, $CH_2CH_2CH_2CH_2CH_2OC$=O, repeating unit of PCL), 3.65 (t, 2H, CH_2OH, end-group of PCL), 2.7-2.2 (t, 2H, C=OCH_2 of PCL), 1.8-1.2 (m, 6H, CH_2 of PCL).

3.3.41 Synthesis of PCL-*b*-PS copolymer with alkyne functionality at the junction point by NMP of St (PCL-*b*-PS-alkyne)

St (2 mL, 17.45 mmol) and PCL-macroinitiator (0.44 g, 0.09 mmol, based on $M_{n,NMR}$) were placed in a schlenk tube. The reaction mixture was degassed with three FPT cycles, left in vacuum, placed in an oil bath at 125 °C and stirred for 15 h. After that given time, the polymerization mixture was diluted with THF, precipitated into methanol, isolated by filtration, and dried in a vacuum oven at room temperature ($[M]_0/[I]_0$ = 200; conv.% = 33 %; $M_{n,theo}$ = 12000; $M_{n,NMR}$ = 12840; $M_{n,GPC}$ = 19000; M_w/M_n = 1.26, relative to PS standards). ^{1}H NMR ($CDCl_3$, δ) 7.2-6.3 (Ar*H* of PS), 4.07-4.01 ($CH_2CH_2CH_2CH_2CH_2OC$=O, repeating unit of PCL), 2.5-2.2 (C=$OCH_2CH_2CH_2CH_2CH_2O$), 2.2-1 (aliphatic protons).

3.3.42 Preparation of P*t*BA with α-anthracene-ω-azide (Anth-P*t*BA-N_3)

*t*BA (10.0 mL, 68.27 mmol), PMDETA (0.048 mL, 0.23 mmol), CuBr (0.033 g, 0.23 mmol), **18** (0.082 g, 0.23 mmol) and ethylene carbonate (0.88 g 1/10; w/w; *t*BA/solvent) were added in a schlenk tube and the reaction mixture was degassed by FPT. The tube was then placed in a thermostated oil bath at 80 ^{o}C for 2 h. After that specified time, the polymerization mixture was diluted with THF, passed through alumina column to remove the catalyst, and precipitated in cold water/methanol mixture (20/80; v/v). The product was dried in a vacuum oven at 25 ^{o}C for 24 h ($[M]_0/[I]_0$ = 300; conv. % = 11; $M_{n,theo}$ = 4600; $M_{n,NMR}$ = 8700; $M_{n,GPC}$ = 5000; M_w/M_n= 1.10, relative to PS standards). ^{1}H NMR ($CDCl_3$, δ) 8.4 (bs, 1H, Ar*H* of anthracene), 8.3 (bs, 2H, Ar*H* of anthracene), 7.9 (bs, 2H, Ar*H* of anthracene), 7.5 (bs, 4H, Ar*H* of anthracene), 6.1 (CH_2-anthracene), 4.05 (b, C*H*-Br end group of P*t*BA), 2.2 (bs, C*H* of P*t*BA), 2.0-1.0 (m, CH_2 and CH_3 of P*t*BA).

To a solution of Anth-P*t*BA-Br (0.96 g, 0.11 mmol) dissolved in DMF (5 mL), NaN_3 (0.29 g, 4.4 mmol) was added. After stirring the reaction mixture overnight at room temperature, CH_2Cl_2 and water were added and the organic layer was further extracted with water three times and dried over Na_2SO_4. A similar purification procedure for the synthesis of Ant-P*t*BA-N_3 was performed as described for that of Anth-P*t*BA-Br. ^{1}H NMR ($CDCl_3$, δ) 8.4 (bs, 1H, Ar*H* of anthracene), 8.3 (bs, 2H, Ar*H* of anthracene), 7.9 (bs, 2H, Ar*H* of anthracene), 7.5 (bs, 4H, Ar*H* of anthracene), 6.1 (CH_2-anthracene), 3.7-3.6 (br, C*H*-N_3 of P*t*BA), 2.2 (bs, C*H* of P*t*BA), 2.0-1.0 (m, CH_2 and CH_3 of P*t*BA).

3.3.43 One-pot preparation of (PEG)(PMMA)-P*t*BA-(PCL)(PS) H-shaped ABCDE quintopolymer by double click reactions

PEG-*b*-PMMA-MI (0.18 g, 0.023 mmol, based on $M_{n,NMR}$), PCL-*b*-PS-alkyne (0.25 g, 0.019 mmol, based on $M_{n,NMR}$), and Anth-P*t*BA-N_3 (0.20 g, 0.023 mmol, based on $M_{n,NMR}$) were dissolved in nitrogen-purged DMF (5 mL) in a schlenk tube. PMDETA (0.020 mL, 0.095 mmol) and CuBr (0.014 g, 0.095 mmol) were added and the reaction mixture was degassed by three FPT cycles, left in argon and then stirred at 120 ^{o}C for 48 h. After that time, the polymer solution was passed through neutral alumina column to remove copper salt, precipitated in methanol, and dried in a vacuum oven at 25 ^{o}C. Yield: 0.49 g (86 %). $M_{n,TD\text{-}GPC}$ = 39400, M_w/M_n = 1.26). ^{1}H

NMR ($CDCl_3$, δ) 7.2-6.2 (br, 5H, Ar*H* of PS), 4.04 (br, 2H, CH_2OC=O of PCL), 3.59 (br, 4H, OCH_2CH_2 of PEG and OCH_3 of PMMA), 2.33-2.27 (br, 2H, C=OCH_2 of PCL and 1H, backbone C*H* of P*t*BA), 1.2-1.8 (br, aliphatic protons).

4. RESULTS AND DISCUSSION

4.1 Heteroarm H-Shaped Terpolymers through CuAAC

Heteroarm H-shaped terpolymers, (PS)(PMMA)-P*t*BA-(PMMA)(PS), and (PS)(PMMA)-(PEG)-(PMMA)(PS), were prepared through CuAAC strategy between PS-PMMA copolymer (as side chains) with an alkyne functional group at the junction point and diazide-terminated P*t*BA or PEG (as a main chain).

4.1.1 Synthesis of ABC type miktofunctional initiator

For heteroarm H-shaped polymers two kinds of initiator systems were synthesized. First initiator is ABC type miktofunctional initiator, and produced by six steps. First two steps were synthesized according to procedure reported by Hawker et al. [308]. The synthesis of 2-phenyl-2-(2,2,6,6-tetramethyl-piperidin-1-yloxy)-ethyl ester (**1**) was carried out by heating styrene in the presence of benzoyl peroxide and TEMPO for 30 minutes (reaction 4.1). **1** was then hydrolyzed with aqueous KOH to give 2-phenyl-2-[(2,2,6,6-tetramethylpiperidino)oxy]-1-ethanol, **2** (reaction 4.2). The characteristic peak of aromatic protons adjacent to ester group at 8.2 ppm completely disappeared after hydrolysis. Moreover, the new signals appeared at 5.9 ppm of -O*H* and the shifts of the –CH_2 protons adjacent to hydroxyl group and –C*H* proton adjacent to aromatic group, at 4.3-3.6 ppm and 5.3 ppm respectively, were confirmed the successful hydrolysis by ^{1}H NMR. The ^{1}H NMR spectra of the corresponding ester and alcohol precursors are presented in Figures 4.1 and Figure 4.2, respectively.

In order to convert the hydroxyl functionality of compound **2** into two hydroxyl functionalities, successive protection, esterification and deprotection reactions were realized. For this purpose, 2,2-bis(hydroxymethyl)propionic acid, protected by conversion to acetonide by reaction with 2,2-dimethoxypropane and catalytic amount of *p*-toluene sulfonic acid (*p*-TSA) in dry acetone, [313] leading to 2,2,5-trimethyl-[1,3]dioxane-5-carboxylic acid, **(3)** (reaction 4.3).

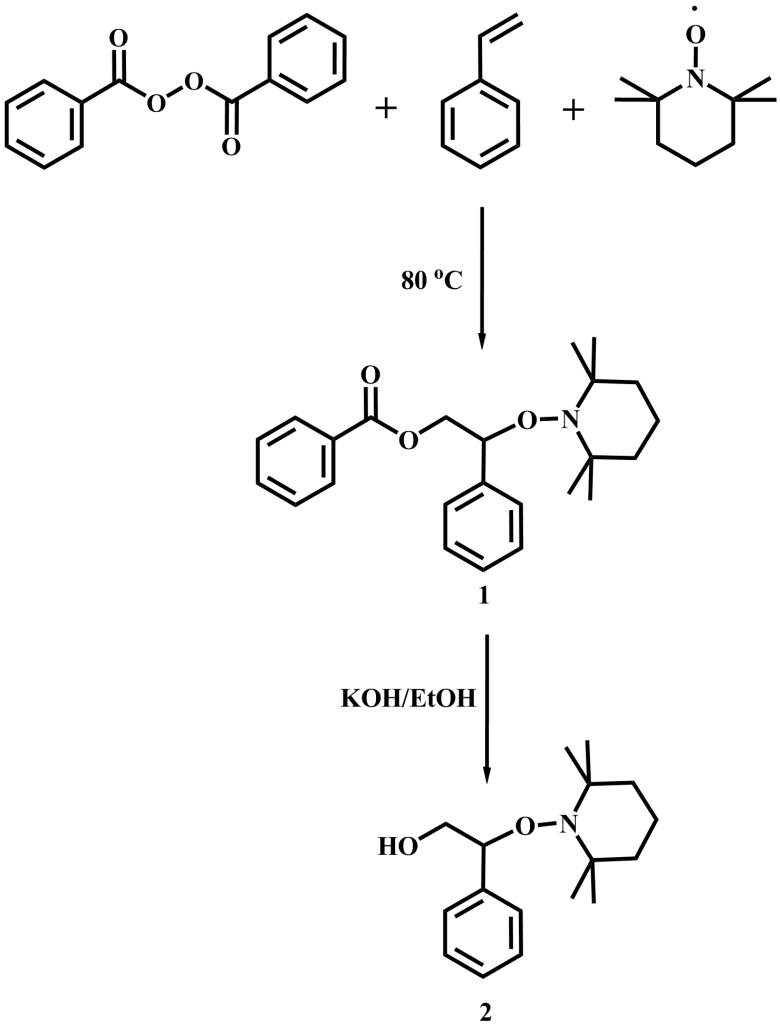

(4.1)

(4.2)

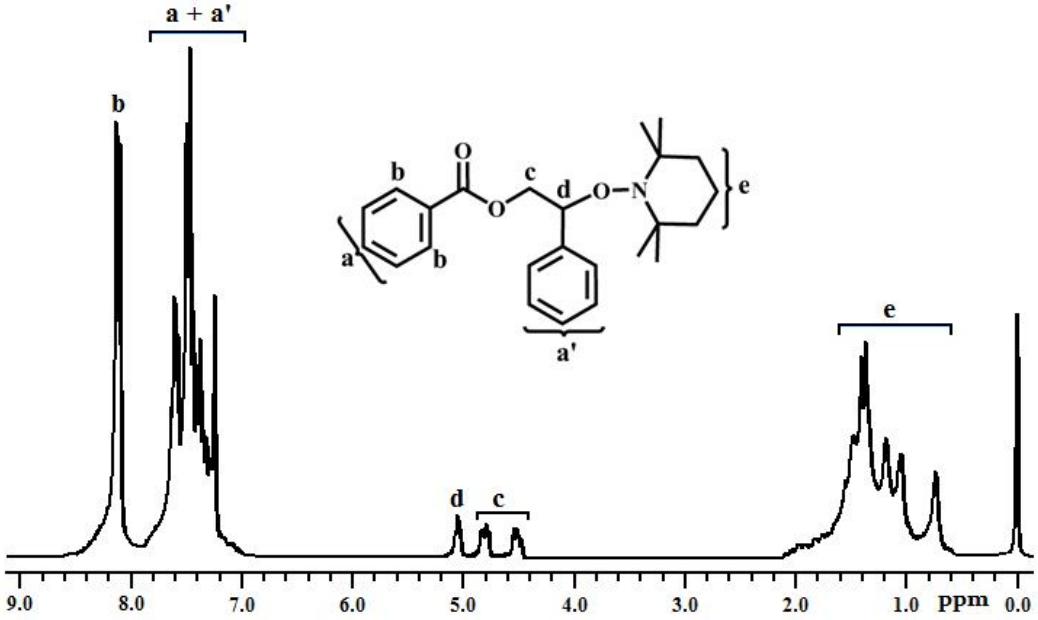

Figure 4.1: ^{1}H NMR spectrum of benzoic acid 2-phenyl-2-(2,2,6,6-tetramethyl-piperin-1-yloxy)-ethyl (**1**) in $CDCl_3$.

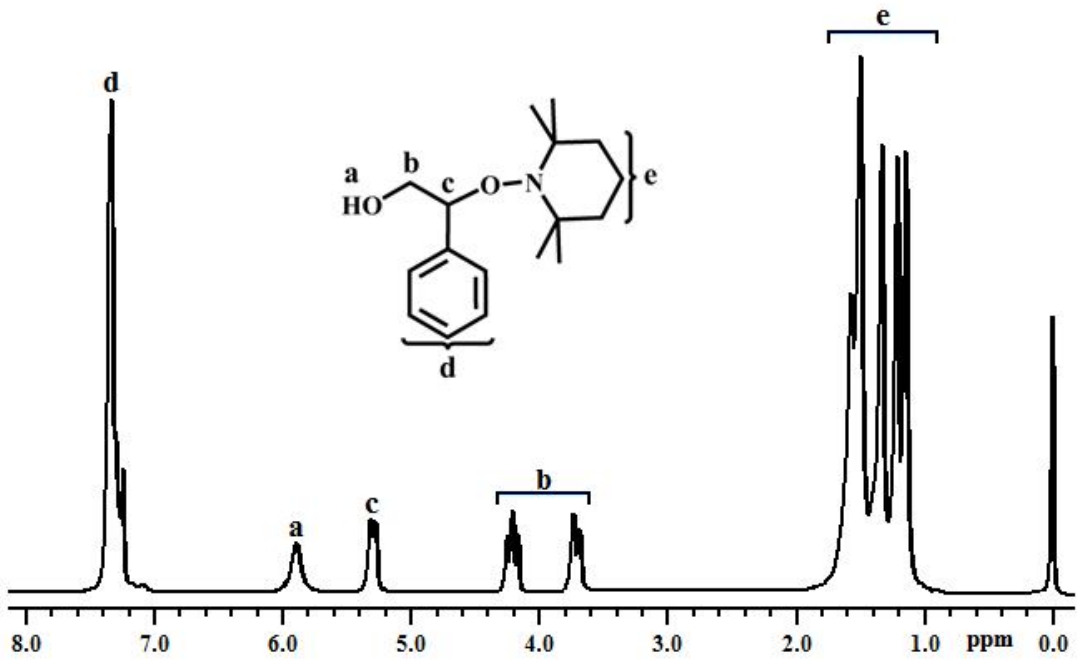

Figure 4.2: ^{1}H NMR spectrum of 2-phenyl-2-(2,2,6,6-tetramethyl-piperin-1-yloxy)-ethanol (**2**) in $CDCl_3$.

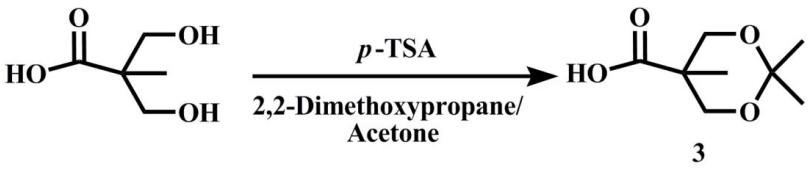

(4.3)

Figure 4.3 depicts the ^{1}H NMR spectrum of 2,2,5-trimethyl-[1,3]dioxane-5-carboxylic acid **(3)** showing resonances corresponding to -COO*H* proton at 11.2 ppm, methylene groups at 4.2 and 3.6, the methyl protons adjacent to ketal group and the methylene groups at 1.2 ppm and 1.4 ppm respectively.

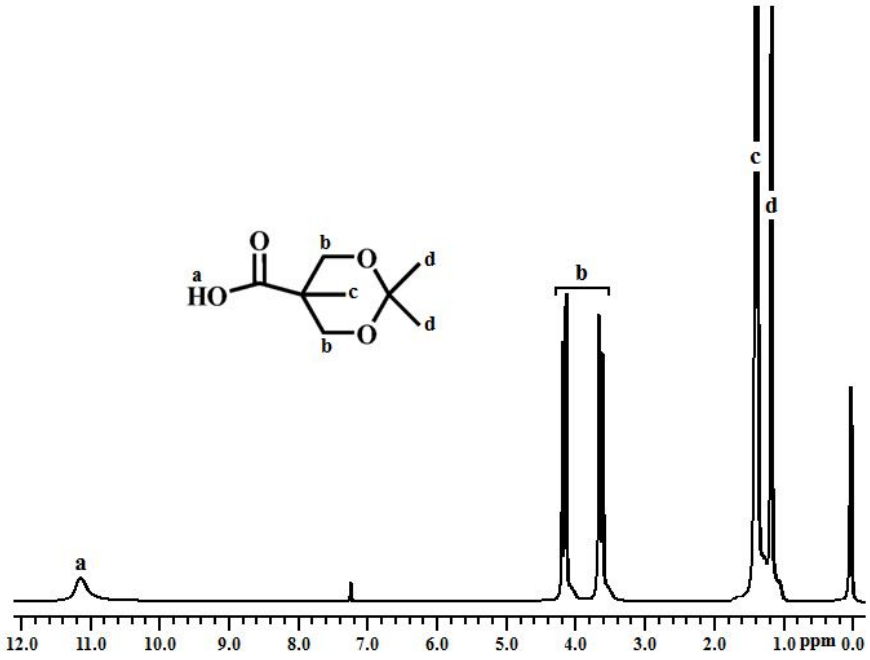

Figure 4.3: ^{1}H NMR spectrum of 2,2,5-trimethyl-[1,3]dioxane-5-carboxylic acid (**3**) in $CDCl_3$.

Then esterification of **3** with 2-phenyl-2-[(2,2,6,6-tetramethylpiperidino)oxy]-1-ethanol (**2**) produced the TEMPO functional compound **4** using DCC and DMAP in high yields after column chromatography purification (reaction 4.4). Although this procedure was reported to be a suitable method for the esterification reaction [314], the main drawback of this system is related to the difficulties arising from the removal of formed urea with product. However, this was overcomed by further precipitation followed by filtration method.

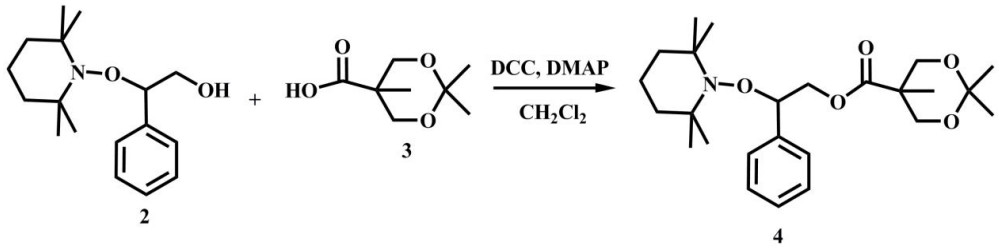

(4.4)

The esterification was monitored by ^{1}H NMR spectroscopy by observing the dissappearance of carboxylic acid protons at 11.2 ppm and the appearance of the new protons, methylene protons adjacent to acetonide groups at 4.0 ppm and 3.5 ppm. Also, the signals of aromatic hydrogens appeared at 7.3 ppm and the methylene protons (c) next to the ester linkage shifted from 4.2-3.7 ppm to 4.6-4.3 ppm and methine proton adjacent to the phenyl group shifted from 5.3 ppm to 4.9 ppm (Figure 4.4).

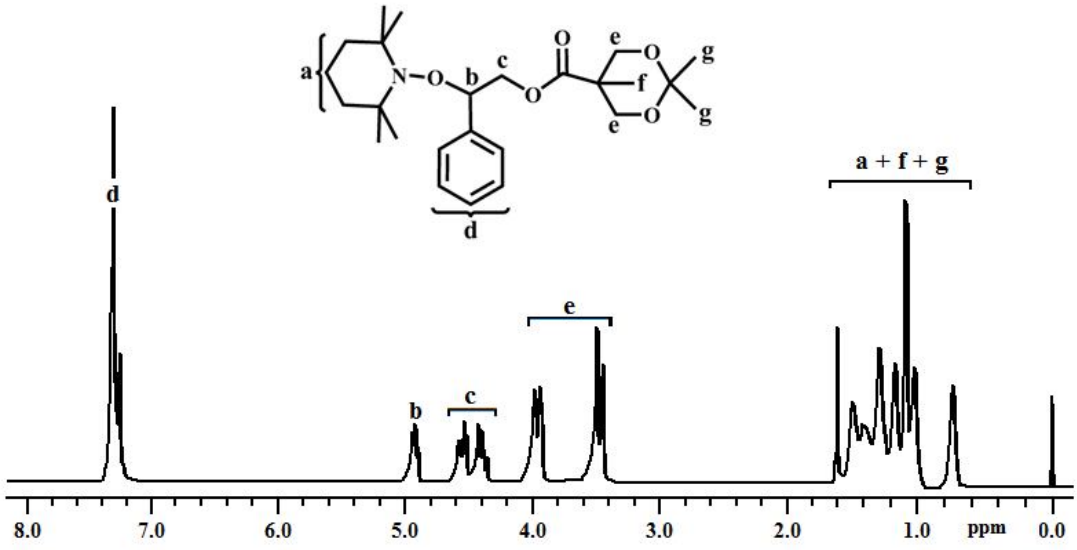

Figure 4.4: ^{1}H-NMR spectrum of 2,2,5-trimethyl-[1,3]dioxane-5-carboxylic acid 2-phenyl-2-(2,2,6,6-tetramethyl-piperidin-1-yloxy)-ethyl ester (**4**) in $CDCl_3$.

Deprotection of the acetonide groups of compound **4** can easily be accomplished quantitatively in the presence of 1 M HCl in THF to yield **5** (reaction 4.5).

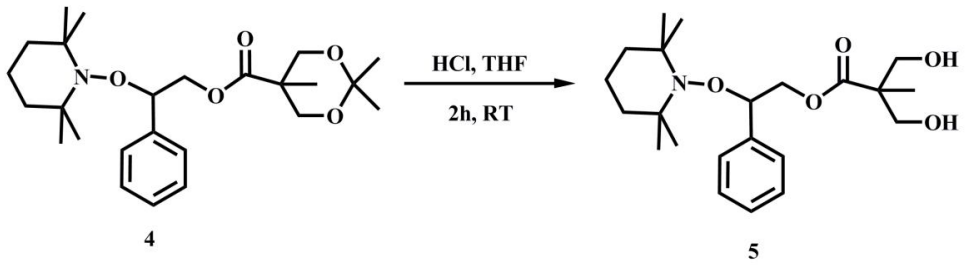

(4.5)

The hydroxyl groups of **5** can clearly be seen from δ = 2.61 and 2.74 ppm together with the signals associated with TEMPO functionality and core compound (Figure 4.5). Those signals disappeared after D_2O treatment.

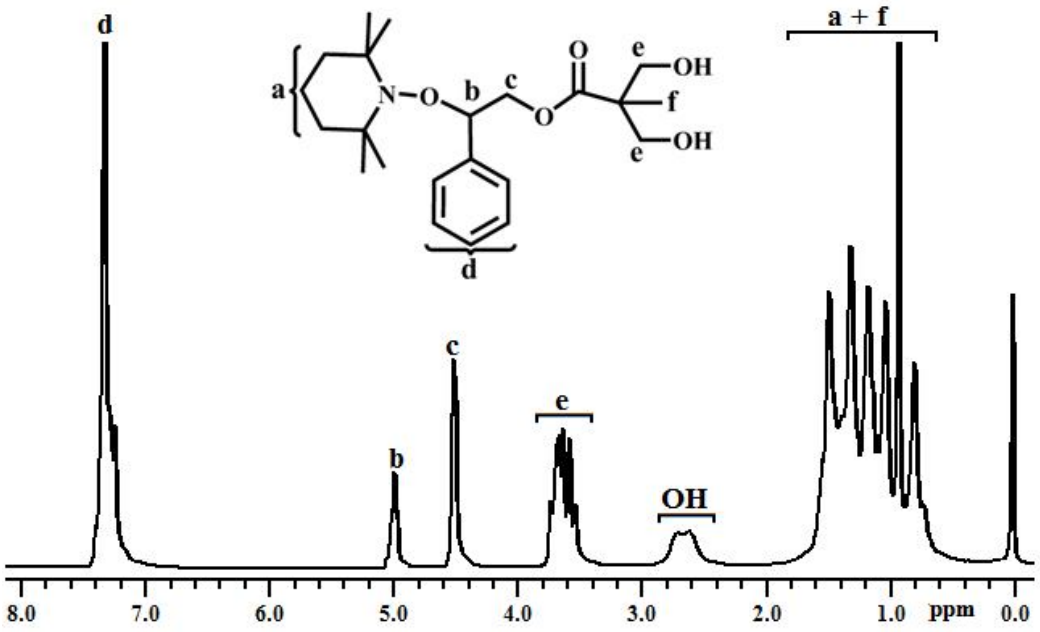

Figure 4.5: ^{1}H NMR spectrum of 3-hydroxy-2-hydroxymethyl-2-methylpropionic acid 2-phenyl-2-(2,2,6,6-tetramethyl-piperidin-1-yloxy)-ethyl ester (**5**) in $CDCl_3$.

The bromide functionality serving as ATRP initiator was introduced into the core by esterification reaction of one hydroxyl group of **5** with one equivalent of 2-bromoisobutyrylbromide. It should be pointed out that at this step severe reaction conditions may cause the hydrolysis of the ester groups present in the structure and/or disubstituted ester product. Therefore, the esterification process was performed at room temperature and 2-bromoisobutryl bromide was added in a dropwise manner. Thus, the disubstituted product did not occur, so that tri miktofunctional initiator **6** is obtained in high yields (reaction 4.6).

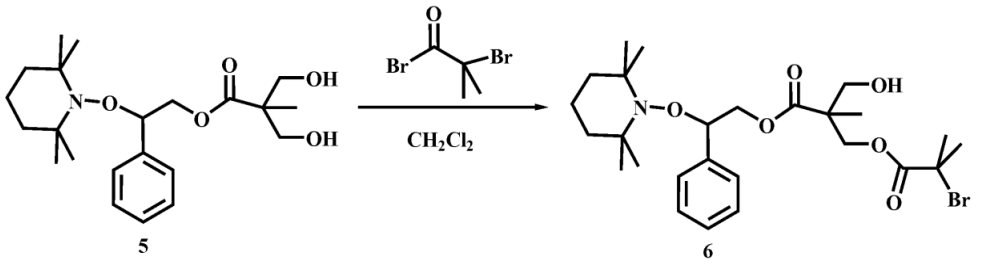

(4.6)

The ^{1}H NMR spectrum of the compound **6** clearly shows that the intensity of –O*H* protons decreased and the signals ((C*H*$_3$)$_2$CBr) arisen from ATRP initiator appeared at 1.85 ppm. Moreover, monofunctional hydroxyl groups (2.28 ppm) together with the shift of the -C*H*$_2$ protons adjacent to bromine functionality to 4.1 ppm indicate that esterification reaction was carried out successfully. The ^{1}H NMR spectrum of the resulting compound **6** is shown in Figure 4.6.

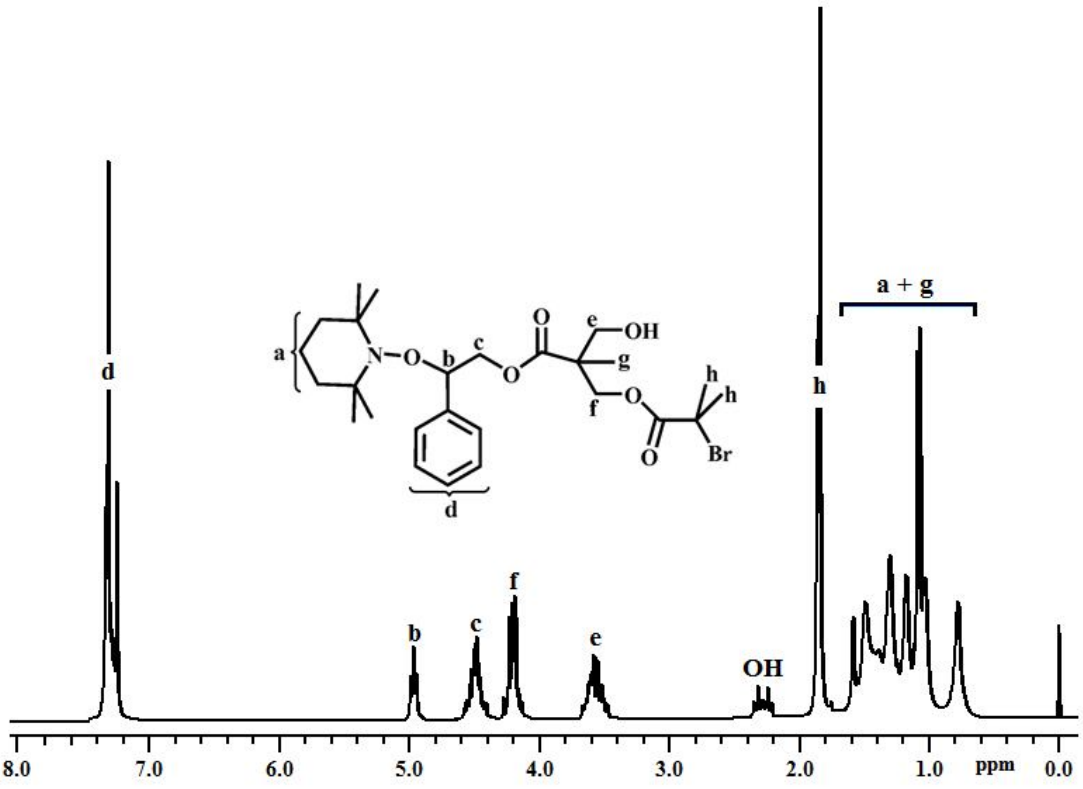

Figure 4.6: ^{1}H NMR spectrum of 2-(2-bromo-2-methyl-propionyloxymethyl)-3-hydroxy-2-methyl propionic acid 2-phenyl-2-(2,2,6,6-tetramethyl-piperidin-1-yloxy)-ethyl ester (**6**) in $CDCl_3$.

Last esterification reaction was realized to gain alkyne functionality for initiator system using DCC and DMAP as mentioned before between **6** with 4-pentynoic acid and compound **7** was obtained with very high yield (reaction 4.7).

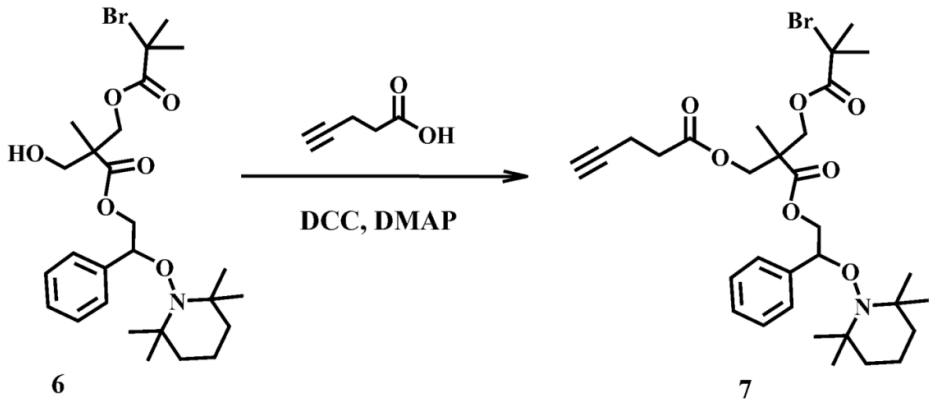

(4.7)

A broad peak of -CH_2OH at 3.6 ppm disappeared and a corresponding ester (CH_2OC=O) signal came out at around 4.10 ppm together with another CH_2 ester linkage of **7**. Furthermore, from the spectrum, CH_2-C*H* protons adjacent to TEMPO, *H*C≡C- hydrogen of alkyne, and CH_3 protons of *tert*–bromide functionality could easily be detected at 4.93-4.36, 1.95, and 1.83 ppm, respectively (Figure 4.7). Successive synthesis of compound **7** was confirmed by ^{1}H NMR.

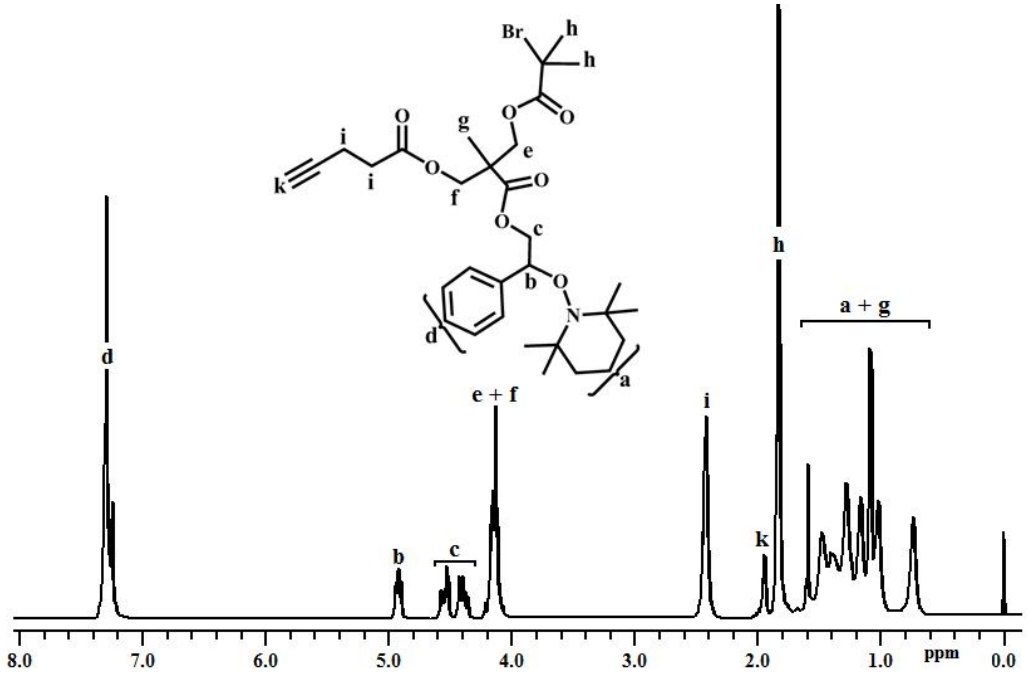

Figure 4.7: ^{1}H NMR spectrum of Pent-4-ynoic Acid 3-(2-Bromo-2-methyl-propionyloxy)-2-methyl-2-[2-phenyl-2-(2,2,6,6-tetramethylpiperidin-1-yloxy)-ethoxycarbonyl]-propyl ester (**7**) in $CDCl_3$.

4.1.2 Synthesis of 1,2-bis (bromoisobutyrl-oxy)-ethane (8)

The choice of bromine initiator was due to the easy synthetic accessibility of the difunctional bromine initiator by a simple coupling reaction between ethylene glycol and 2-bromoisobutyryl bromide (**8**) (reaction 4.8).

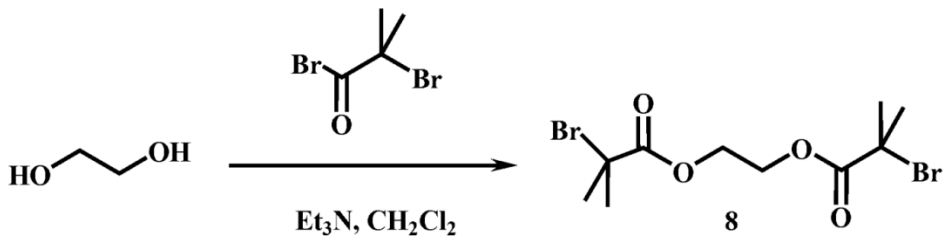

(4.8)

Figure 4.8 depicts the ^{1}H NMR spectrum of compound **8** showing resonances corresponding to methylene protons at 4.4 ppm and methyl porotons at 1.9 ppm.

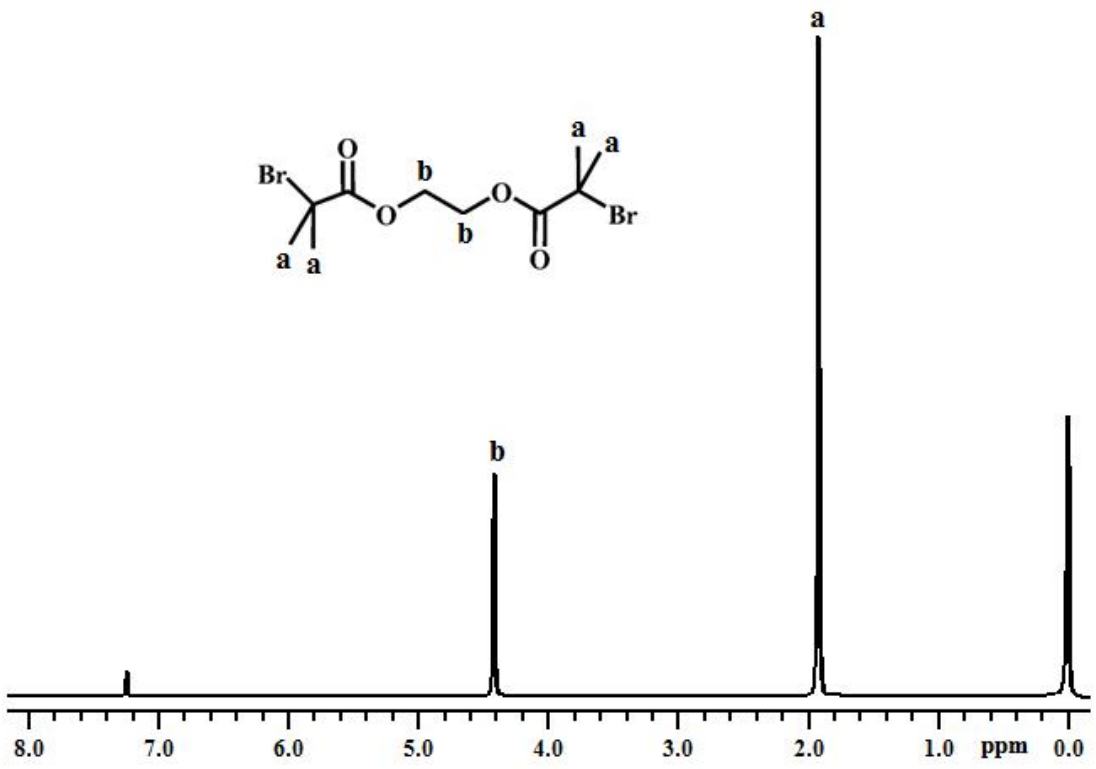

Figure 4.8: ^{1}H NMR spectrum of 1,2-bis (bromoisobutyrl-oxy)-ethane (**8**) in $CDCl_3$.

4.1.3 Synthesis of PS macroinitiator by NMP

NMP of St from TEMPO group of **7** was accomplished at 125 °C in bulk (reaction 4.9). The number average molecular weight calculated by GPC ($M_{n,GPC}$) was consistent with that of $M_{n,theo}$ (Table 4.1).

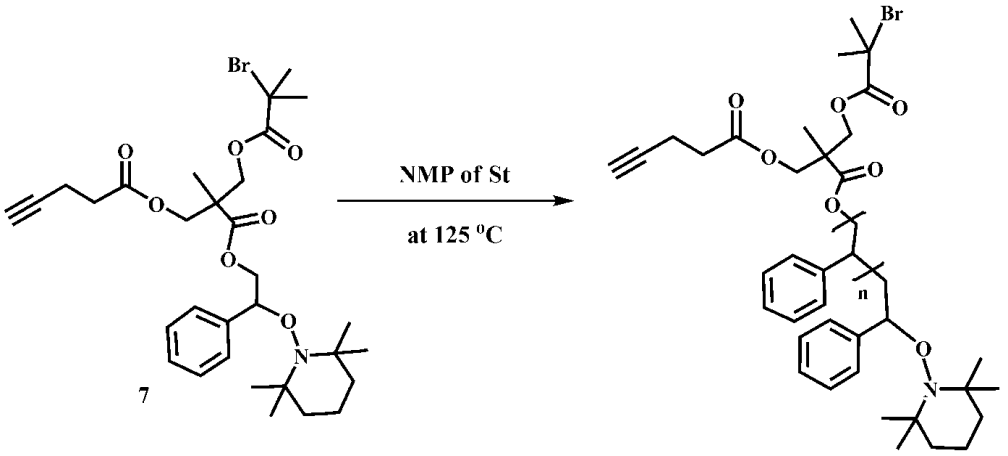

(4.9)

The NMR number average molecular weight of the polymer ($M_{n,NMR}$ = 10000) was determined by comparing the integral of C=OCH_2CH_2C≡C*H* end group signal (2.4 ppm) to that of repeating unit of PS (6.3–7.5 ppm) (Figure 4.9), while including the MW of **7** (622.6 g/mol).

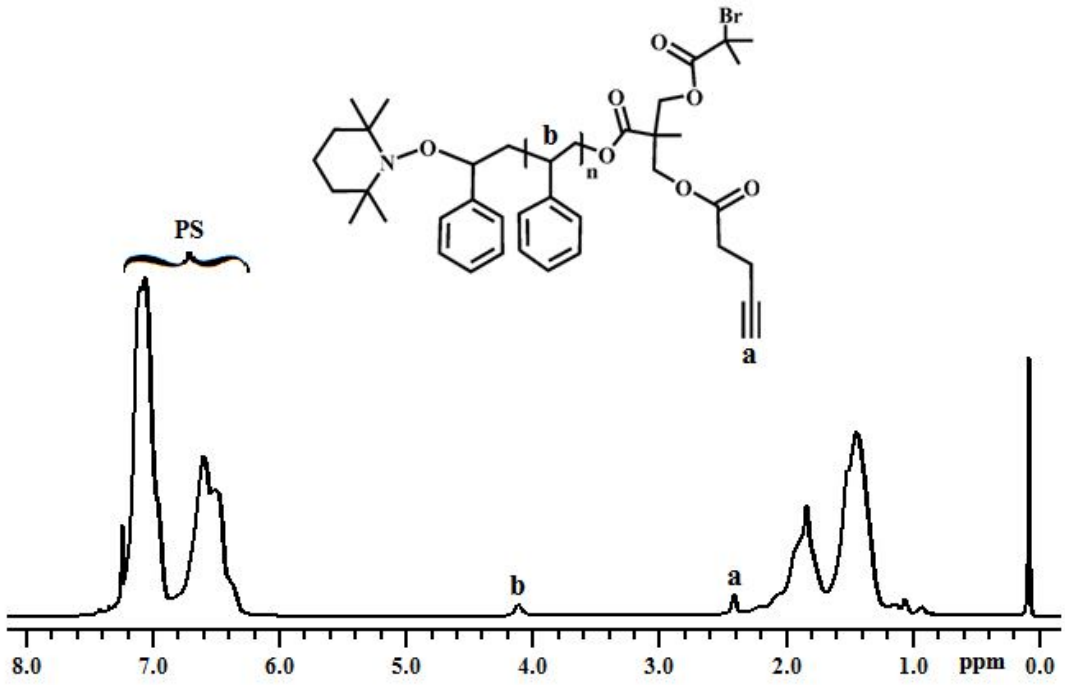

Figure 4.9: ^{1}H NMR spectrum of PS macroinitiator in $CDCl_3$.

The PS macroinitiator was obtained with $M_{n,GPC}$ of 9800 and low polydispersity index (M_w/M_n) 1.2 as determined by GPC in THF relative to PS standards. It should be pointed out that $M_{n,theo}$, $M_{n,NMR}$ and $M_{n,GPC}$ values of PS macroinitiator fit well.

4.1.4 Synthesis of PS-*b*-PMMA by ATRP

Then PS precursor containing *tert*-bromide functionality was used as a macroinitiator in ATRP of MMA in the presence of CuBr/PMDETA as a catalyst in toluene at 60 ^oC (reaction 4.10). The signals of OCH_3 protons of PMMA were assigned by ^1H NMR and confirmed the incorporation of PMMA segments into the block copolymer (Figure 4.11)

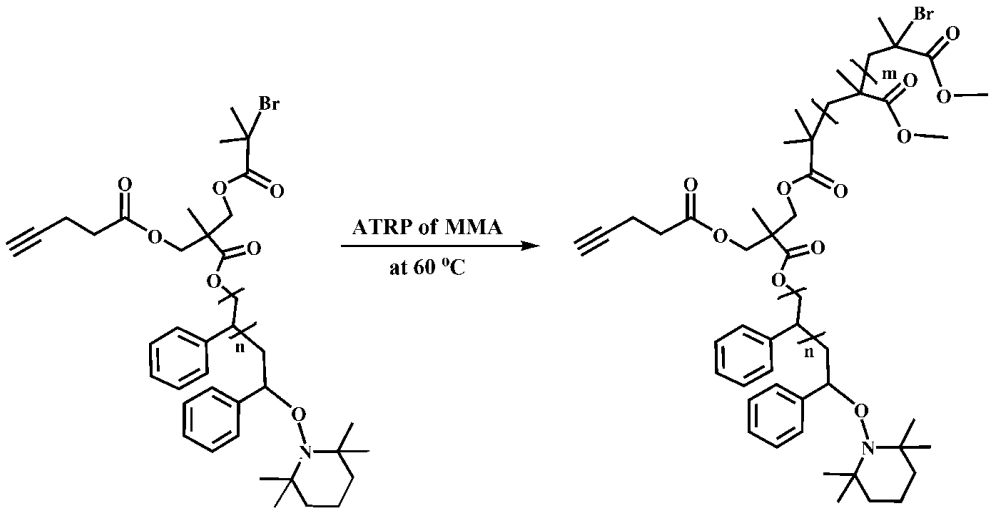

(4.10)

The GPC traces of PS precursor and PS-*b*-PMMA copolymer are shown in the Figure 4.10. The molecular weight increased with styrene conversion in NMP, comfiring the introduction of PS block to the PCL precursor. Moreover, dissappearance of the precursor peak indicating that efficient block copolymer formation. GPC analysis shows monomodal traces for both polymer. The $M_{n,NMR}$ of the resulting block copolymer was determined accordingly from the integration of the signals at 3.6 and 6.2-7.5 ppm related to OCH_3 of PMMA and aromatic protons of PS segments, respectively. $M_{n,NMR}$ = 78 (DP_n of PMMA) X 100.12 + 10000 ($M_{n,NMR}$ of PS macroinitiator) = 17800. The $M_{n,theo}$, $M_{n,GPC}$, and $M_{n,NMR}$ molecular weights are in fairly good agreement (Table 4.1).

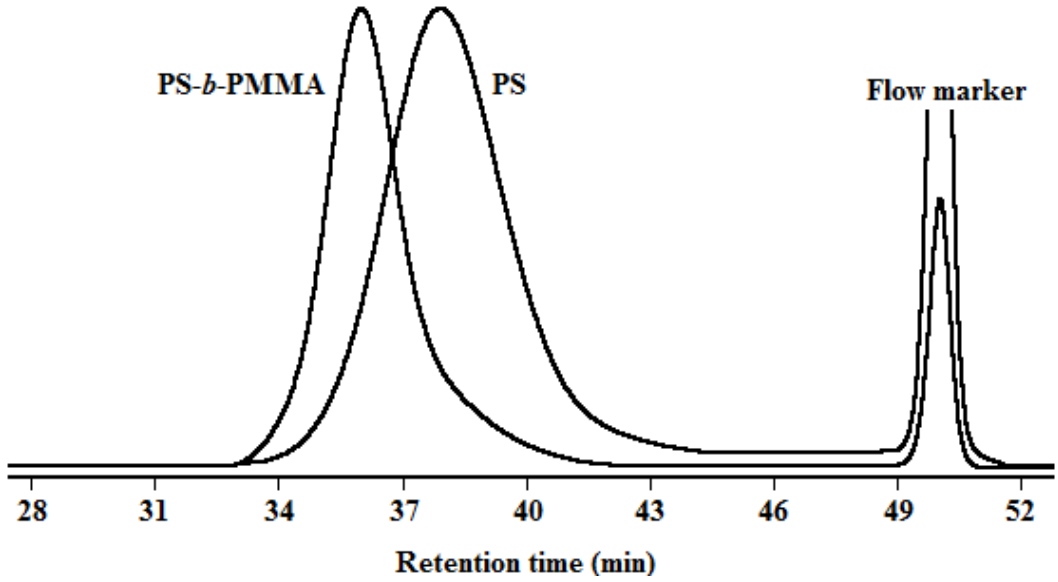

Figure 4.10: Evolution of GPC traces of PS homopolymer and PS-*b*-PMMA copolymer in THF at 30 °C.

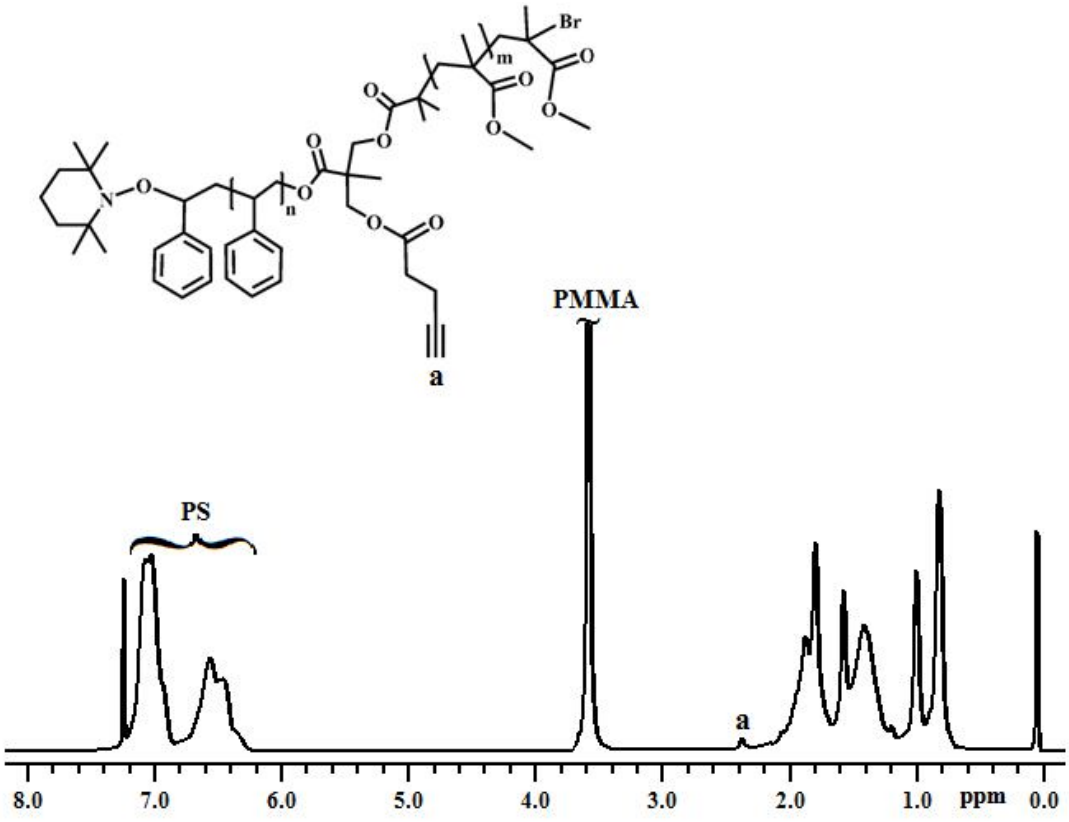

Figure 4.11: ^{1}H NMR spectrum of PS-*b*-PMMA in $CDCl_3$.

4.1.5 Synthesis of diazide end-functionalized P*t*BA and PEG

Br-P*t*BA-Br precursor was obtained from ATRP of *t*BA by using difunctional initiator (**8**) in the presence of PMDETA/CuBr catalyst system in bulk at 80 ^{o}C (reaction 4.11). Nucleophilic substitution of the dibromine terminated P*t*BA (Br-P*t*BA-Br) was achieved by the reaction with NaN_3 in DMF at room temperature (reaction 4.12).

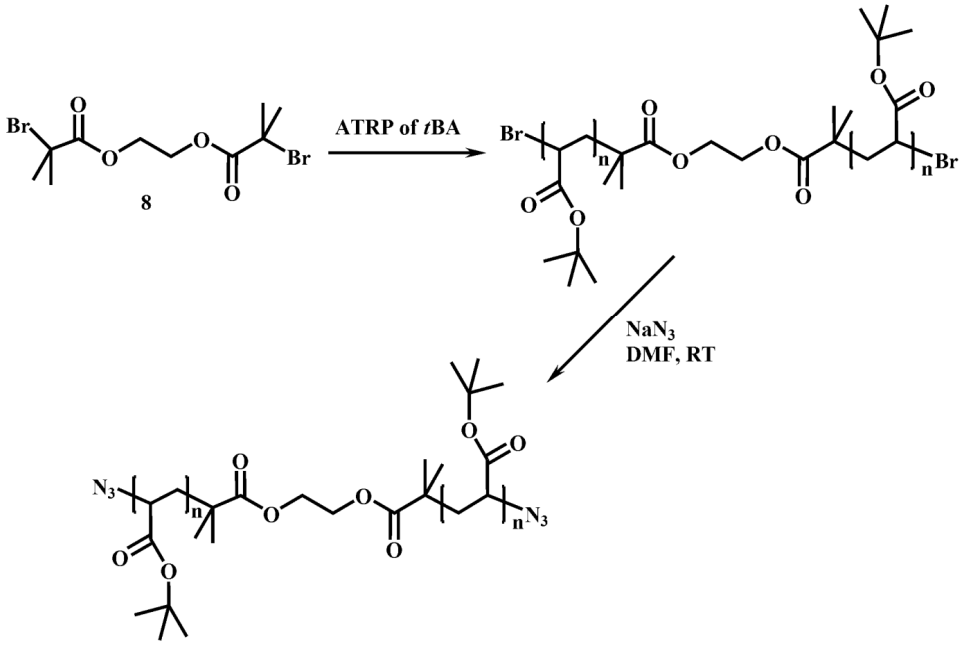

(4.11)

(4.12)

$M_{n,NMR}$ was calculated by comparison of the integrals of the C*H* units of the P*t*BA at 2.2 and that of the OCH_2CH_2O of the initiator fragment (**8**) at 4.2 ppm. $M_{n,theo}$, $M_{n,NMR}$ and $M_{n,GPC}$ values of Br-P*t*BA-Br are in good agreement (Table 4.1).

The formation of N_3-P*t*BA-N_3 precursor was monitored by ^{1}H NMR spectroscopy following the disappearing signal of the C*H*-Br end group at around 4.1 and the appearing of the new C*H*-N_3 at 3.7-3.6 ppm (Figure 4.12).

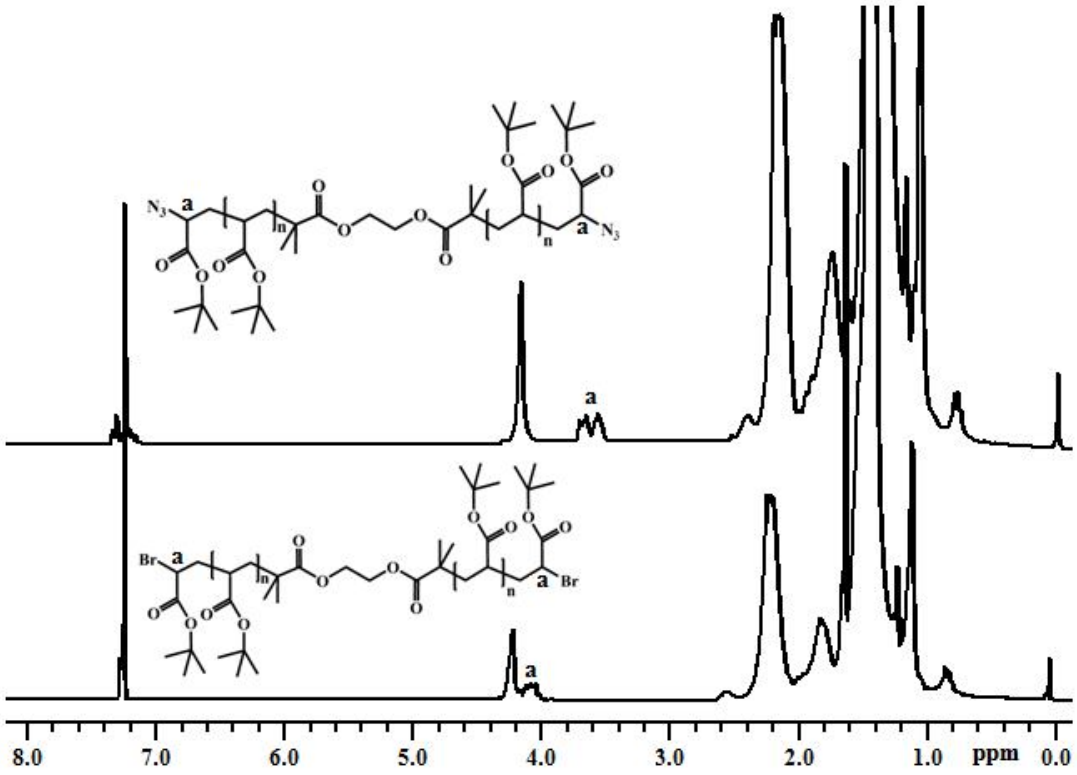

Figure 4.12: ^{1}H NMR spectra of dibromo functional P*t*BA and diazide functional P*t*BA in $CDCl_3$.

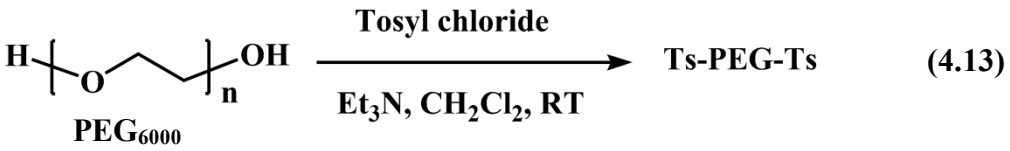

(4.13)

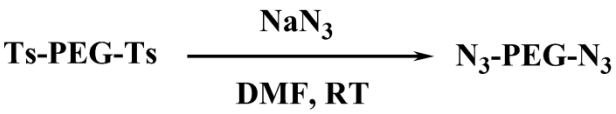

(4.14)

Moreover, dihydroxyl terminated PEG was first tosylated using tosyl chloride and then converted to diazide form by reacting NaN_3 in DMF at room temperature. (reaction 4.13 and 4.14). The structure of N_3-PEG-N_3 was confirmed ^{1}H NMR spectroscopy. The signals originating from the C*H*$_2$O end group of the PEG at 4.1 shifted to main peak of PEG at 3.6 ppm upon the azide formation. Additionally, the Ar*H* (7.8-7.3 ppm) and C*H*$_3$ (2.4 ppm) of the tosyl group disappeared from the spectrum (Figure 4.13).

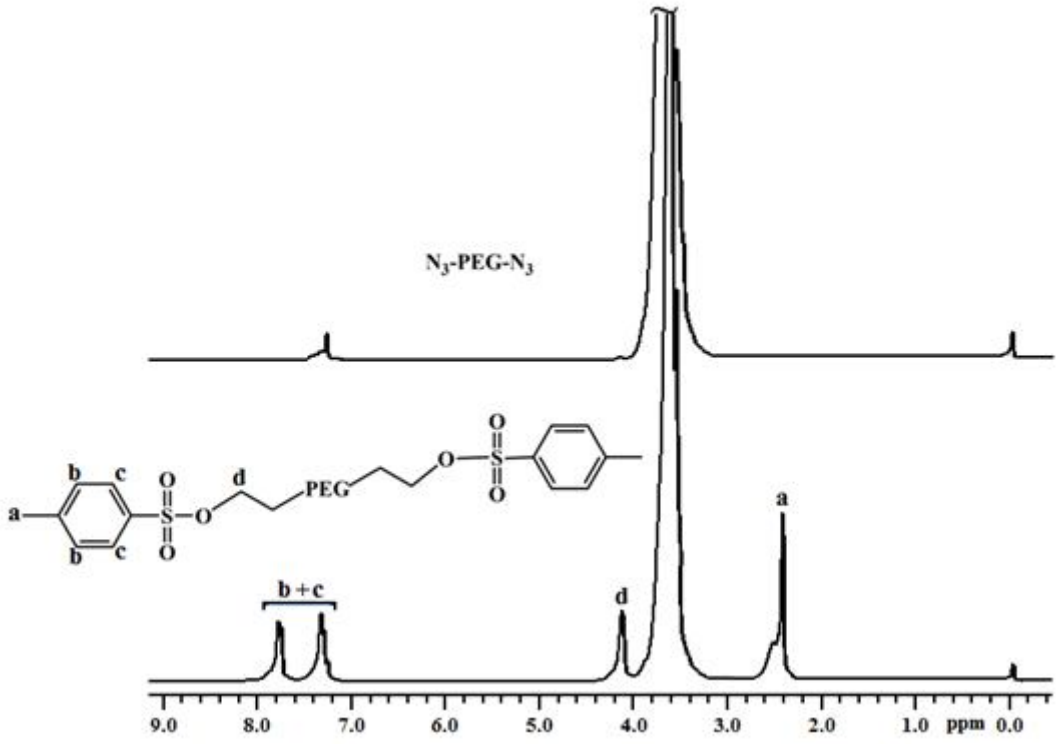

Figure 4.13: ^{1}H NMR spectra of ditosylated PEG and diazide functional PEG in $CDCl_3$.

Table 4.1: Polymers obtained from NMP and ATRP.

Polymer	Ini.	Time (h)	Conv. (%)	$M_{n,GPC}$[d] (g/mol)	M_w/M_n	$M_{n,theo}$ (g/mol)	$M_{n,NMR}$ (g/mol)
PS[a]	**7**	17	41	9800	1.20	9300[e]	10000
PS-PMMA[b]	**PS**	1	20	17000	1.17	16000[f]	17800
Br-P*t*BA-Br[c]	**8**	0.33	12	5200	1.29	5000	4300

[a] $[M]_o:[I]_o = 200$; polymerization was carried out in bulk at 125 °C.
[b] $[M]_o:[I]_o$: $[PMDETA]_o : [CuCl]_o = 300:1:1:1$; polymerization was carried out in toluene at 60 °C.
[c] $[M]_o:[I]_o$: $[PMDETA]_o : [CuBr]_o = 300:1:2:2$; polymerization was carried out at 80 °C.
[d] Molecular weigths were calculated according to linear PS standards.
[e] $M_{n,theo}$ = ($[M]_o/[I]_o$) X conversion X 104.15 + MW of **7** (622.6).
[f] $M_{n,theo}$ = ($[M]_o/[I]_o$) X conversion X 100.12 + $M_{n,NMR}$ of PS precursor.

4.1.6 H-shaped terpolymers through click reactions

The CuAAC reaction was accomplished between alkyne mid-functionalized PS-PMMA copolymers and diazide terminated P*t*BA or PEG in the presence of CuBr/PMDETA as the catalyst at room temperature, leading to H-shaped heteroarm terpolymers (reaction 4.15).

As given in the experimental part, the coupling reaction of H-shaped terpolymers were carried out by using 2-fold molar excess of alkyne mid-functionalized PS-PMMA copolymer per azide functional group of P*t*BA, since the separation of the unreacted PS-PMMA precursor would cause a problem. The formation of H-shaped heteroarm terpolymers was confirmed by NMR and GPC measurements.

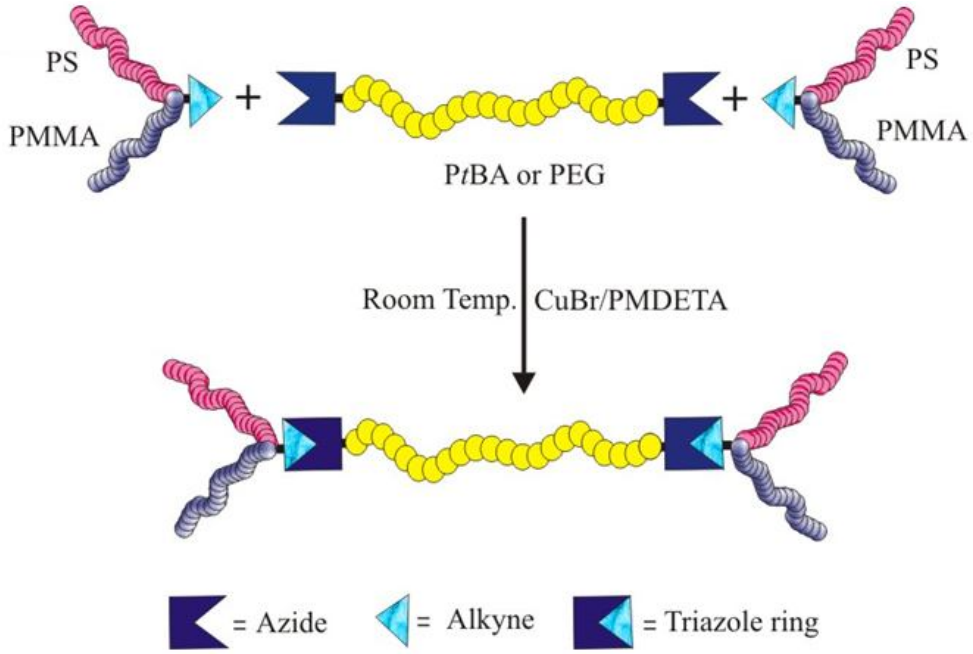

(4.15)

^{1}H NMR spectrum of (PS)(PMMA)-P*t*BA-(PMMA)(PS) H-shaped polymer displays characteristic signals at 6.5-7.2, 3.6 and 1.4 ppm assignable to the Ar*H* of the PS, the OCH_3 of the PMMA and the C(CH_3)$_3$ of the P*t*BA segments, respectively (Figure 4.14). Moreover, an analysis on the integration values of the segments (P*t*BA and PS-PMMA) obtained from the ^{1}H NMRspectrum of the H-shaped polymer displayed that click reaction occurred quantitatively between PS-PMMA and P*t*BA precursors (Table 4.2).

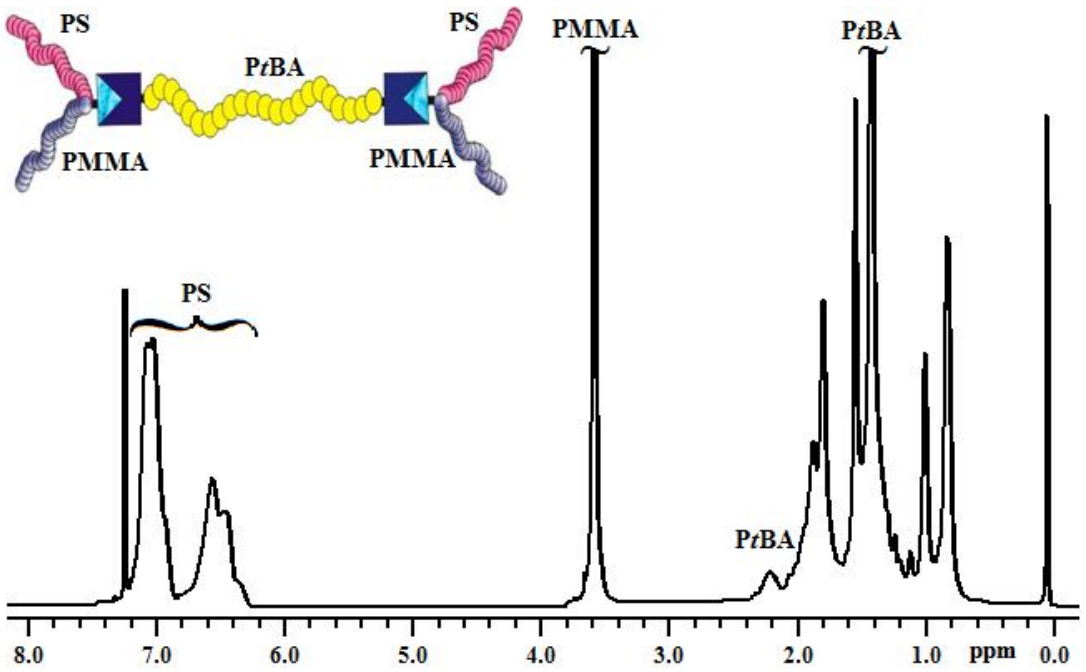

Figure 4.14: ^{1}H NMR spectrum of (PS)(PMMA)-P*t*BA-(PS)(PMMA) H-shaped polymer in $CDCl_3$.

Table 4.2: The results of H-shaped polymers obtained from CuAAC click reaction.

H-shaped polymers	**Precursors**	$M_{n,GPC}$[c] **(g/mol)**	M_w/M_n	$M_{n,theo}$[d] **(g/mol)**	$M_{n,NMR}$[e] **(g/mol)**
(PS)(PMMA)-P*t*BA-(PMMA)(PS)	N_3-P*t*BA-N_3 + PS-PMMA[a]	32000	1.33	39900	34800
(PS)(PMMA)-PEG-(PMMA)(PS)	N_3-PEG-N_3 + PS-PMMA[b]	22000	1.16	41600	36500

[a] $[N_3\text{-P}t\text{BA-}N_3]_o$/ $[\text{PS-}b\text{-PMMA}]_o$ / $[\text{CuBr}]_o$/$[\text{PMDETA}]_o$= 1/2/5/5, the click reaction was carried out in DMF at 25°C.
[b] $[N_3\text{-PEG-}N_3]_o$ / $[\text{PS-}b\text{-PMMA}]_o$ / $[\text{CuBr}]_o$/$[\text{PMDETA}]_o$= 1/2/5/5, the click reaction was carried out in DMF at 25°C.
[c] Molecular weigths were calculated according to linear PS standards.
[d] $M_{n,theo} = M_{n,NMR}$ (P*t*BA or PEG) + 2 X $M_{n,NMR}$ (PS-PMMA).
[e] Calculated from ^{1}H NMR spectrum of the H-shaped polymer taking into consideration the ratio of the integrated values of the main chain (P*t*BA or PEG) to that of the side chain (PS and PMMA).

Here, $M_{n,theo}$ of the H-shaped polymer containing P*t*BA segment is calculated according to the equation: $M_{n,theo}$ = $M_{n,NMR}$ of P*t*BA + 2 X $M_{n,NMR}$ of PS-*b*-PMMA. Moreover, $M_{n,NMR}$ is derived from the ^{1}H NMR spectrum of the H-shaped polymer taking into account the ratio of the integrated values of the main chain (P*t*BA) to the side chain (PS and PMMA). From GPC analysis, it was clearly observed that traces for both PMMA-PS and P*t*BA segments disappeared and a new monomodal trace in the higher molecular weight region appeared revealing the incorporation of the P*t*BA segment into the H-shaped polymer (Figure 4.15).

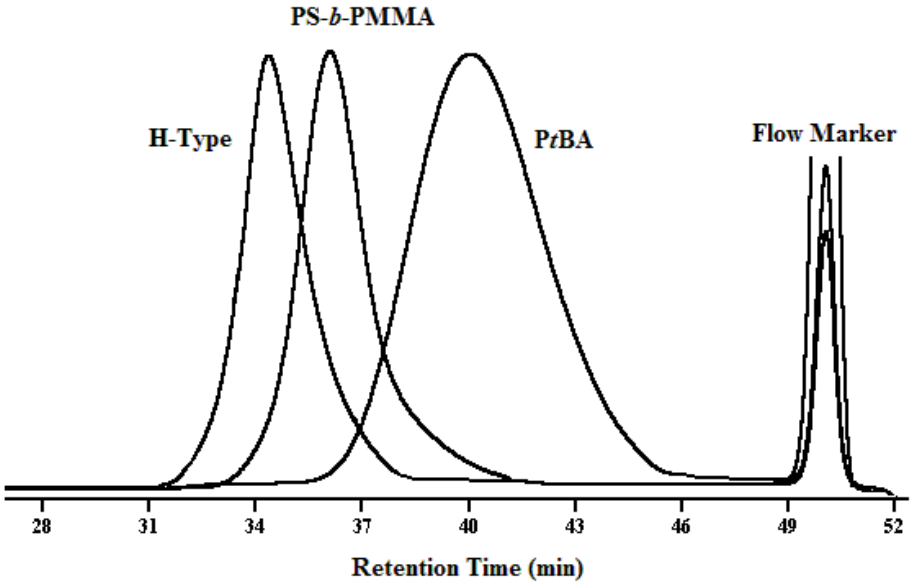

Figure 4.15: The evolution of GPC traces of P*t*BA, PS-*b*-PMMA precursors and (PS)(PMMA)-P*t*BA-(PS)(PMMA) H-shaped polymer.

^{1}H NMR spectrum of (PS)(PMMA)-PEG-(PMMA)(PS) H-shaped polymer shows a characteristic signal of the PEG at 3.63 ppm affording the incorporation of PEG into PMMA-PS copolymer (Figure 4.16). A quantitative analysis of the corresponding segments also indicated that $M_{n,theo}$ of H-shaped polymer was rather close to that of $M_{n,NMR}$ (Table 4.2).

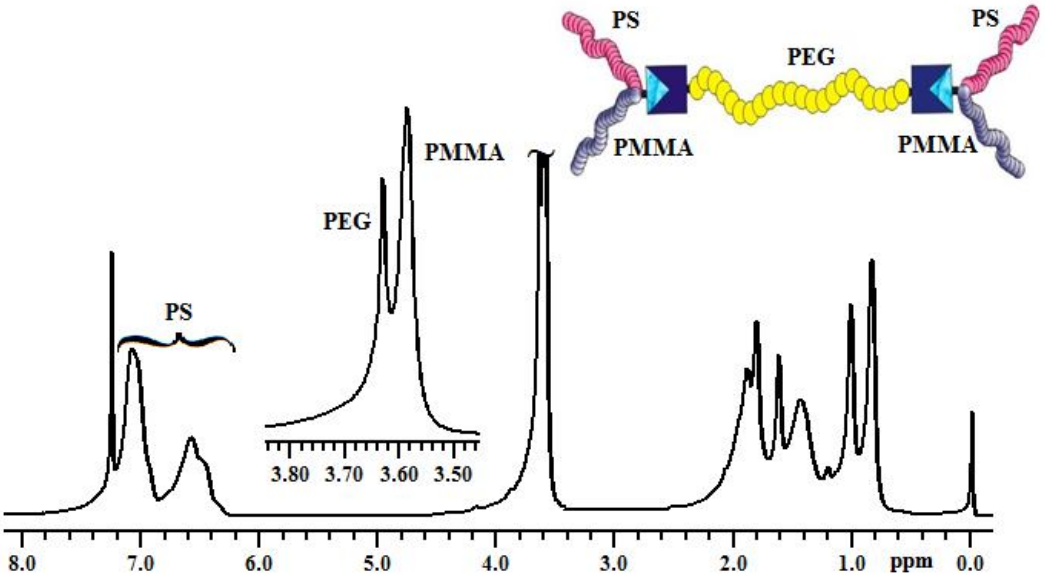

Figure 4.16: ^{1}H NMR spectrum of (PS)(PMMA)-P*EG*-(PS)(PMMA) H-shaped polymer in $CDCl_3$.

Figure 4.17 shows the evolution of GPC traces of diazide terminated PEG, alkyne mid-functionalized PS-PMMA copolymer and H-shaped terpolymer.

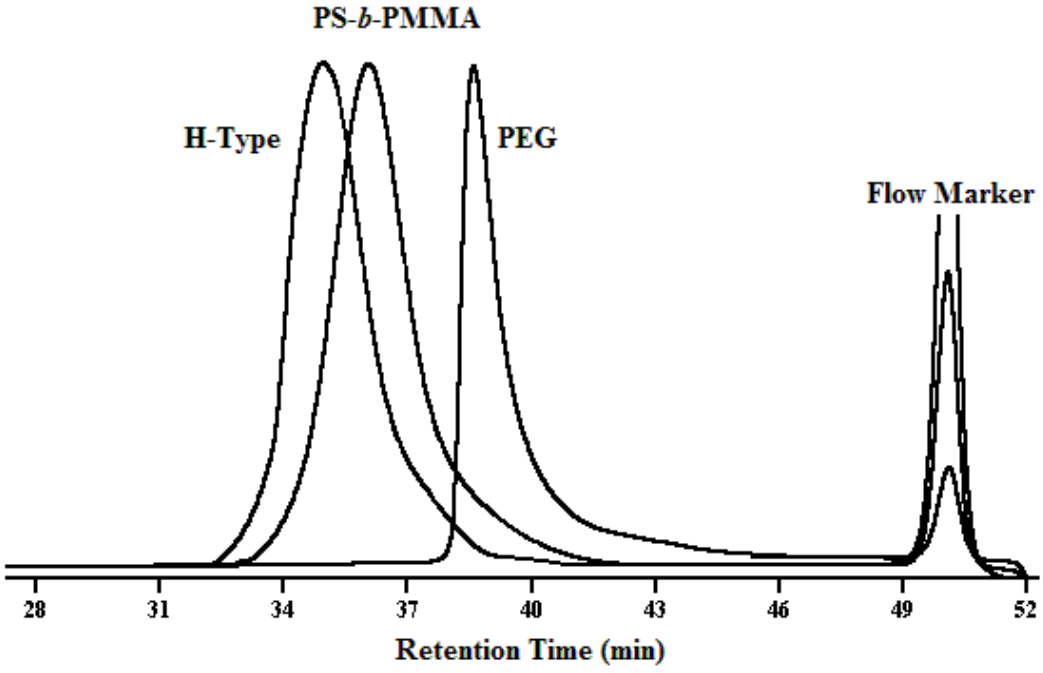

Figure 4.17: The evolution of GPC traces of PEG, PS-*b*-PMMA precursors and (PS)(PMMA)PEG-(PS)(PMMA) H-shaped polymer.

A clear shift to the higher molecular weight region was observed, and moreover the GPC trace of (PS)(PMMA)-PEG-(PMMA)(PS) H-shaped polymer was monomodal and displays almost no tail in the lower molecular weight region indicating an efficient click reaction between PEG and PS-PMMA precursors.

4.1.7 Thermal and morphological properties H-shaped polymers

Thermal properties of H-shaped polymers were probed by DSC. (PS)(PMMA)-PEG-(PMMA)(PS) H-shaped polymer showed a T_m = 22 and T_g = 88 ^oC, corresponding to the PEG and PS/PMMA precursors, respectively. However, a T_g for PEG segment is not apparent from DSC analysis. For the case of (PS)(PMMA)-P*t*BA-(PMMA)(PS) H-shaped polymer, two T_gs are evident: one at 45 ^oC corresponding to P*t*BA and at 100 ^oC corresponding to PS/PMMA precursors.

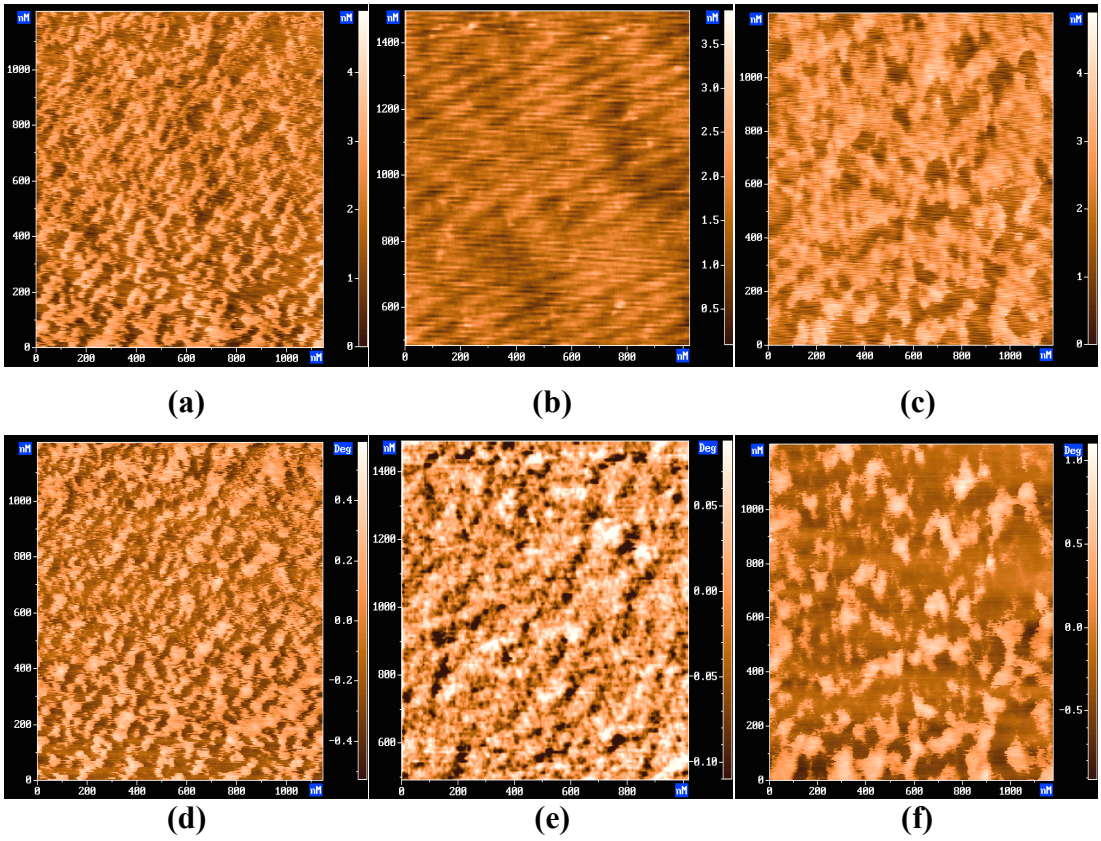

Figure 4.18: Morphology of polymers PS-*b*-PMMA, (PS)(PMMA)-PEG-(PMMA)(PS), and (PS)(PMMA)-P*t*BA-(PMMA)(PS) as determined by AFM. AFM height pictures are seen in the top row: (a) PS-*b*-PMMA, (b) (PS)(PMMA)-PEG-(PMMA)(PS), (c) (PS)(PMMA)-P*t*BA-(PMMA)(PS). Corresponding phase pictures are seen in the bottom row: (d) PS-*b*-PMMA, (e) (PS)(PMMA)-PEG-(PMMA)(PS), (f) (PS)(PMMA)-P*t*BA-(PMMA)(PS).

AFM investigations confirmed the phase separation between PS and PMMA blocks in the polymers and showed different morphologies for the two H-type polymers. Figure 4.18 shows the AFM height pictures (Figure 4.18 a-c) and phase pictures (Figure 4.18 d-f), respectively, for PS-*b*-PMMA, (PS)(PMMA)-PEG-(PMMA)(PS) and (PS)(PMMA)-P*t*BA-(PMMA)(PS). AFM height picture of PS-*b*-PMMA diblock copolymer (Figure 4.18 a) showed 2-3 nm height irregularly distributed surface undulations. The corresponding phase picture (Figure 4.18 d) shows a clear phase contrast between the lower and higher parts on the surface. The lower parts are bright in the phase picture and the higher parts are dark. This indicates a clear phase separation between the PS and PMMA blocks such that the lower surface energy PS block stays higher on the surface. In fact, annealing this film above the glass transition temperatures of both blocks (~100 ^{o}C) allowed PS to cover the top surface resulting in a smooth surface in height picture and a uniform phase in phase picture.

The height and phase picture of the H-type polymer (PS)(PMMA)-P*t*BA-(PMMA)(PS) (Figure 4.18 c and Figure 4.18 f, respectively) showed similar features to those of PS-*b*-PMMA. The height difference between the lower and higher parts was 2-3 nm and appeared bright and dark, respectively, in phase picture. The size of the higher regions was larger than that of PS-*b*-PMMA. This may be due to the increased density of PS blocks in the H-type polymer as two PS-*b*-PMMA chains were attached to a central P*t*BA block.

The surface morphology of (PS)(PMMA)-PEG-(PMMA)(PS) was significantly different than (PS)(PMMA)-P*t*BA-(PMMA)(PS). A very smooth surface is seen in the height picture of Figure 4.18 b. But the phase picture of Figure 4.18 e shows ordered regions of rods that extend from lower right corner to upper left corner of the picture. The average width of these rods is approximately 30 nm. We attribute the observed rods to the self assembly of (PS)(PMMA)-PEG-(PMMA)(PS) into cylinders in which the central PEG blocks form the core of the cylinder with the PS and PMMA blocks on the shell. The phase picture of Figure 4.18e shows the organization of the PS and PMMA blocks in the shell on the top surface.

The high resolution AFM picture of Figure 4.19 clearly shows the microphase separation and the self-assembly of the thermodynamically incompatible PEG, PS, and PMMA blocks on the top surface. Our investigations of the detailed structure of this morphology have been continuing. The driving force for the morphology of

ordered cylinders is the strong phase separation between the central PEG block and PS and PMMA. The tendency of PEG to crystallize may also contribute to the morphology formation. In the case of (PS)(PMMA)-P*t*BA-(PMMA)(PS), the three – CH_3 in the side group of P*t*BA may be preventing the strong segregation with the PS groups and hindering the formation of such an ordered morphology.

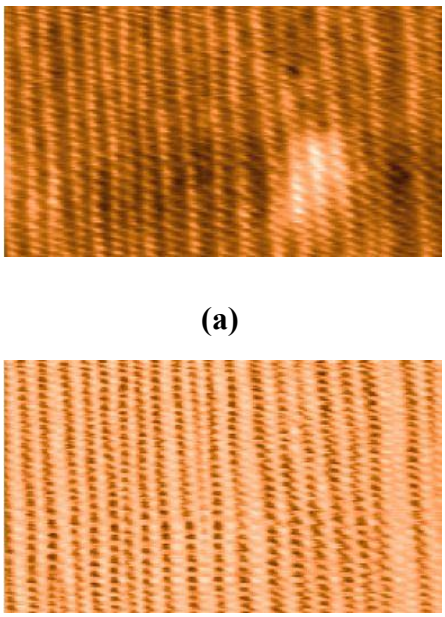

(a)

(b)

Figure 4.19: High resolution AFM height pictures of (PS)(PMMA)-PEG-(PMMA)(PS).

4.2 H-Shaped (ABCDE Type) Quintopolymer via CuAAC Strategy

H-shaped quintopolymer was prepared efficiently by applying CuAAC strategy to a reaction of azide end-functionalized miktoarm star polymer (PCL-PS-P*t*BA-N_3) with block copolymer having alkyne at the junction point (PEG-PMMA-alkyne).

4.2.1 Synthesis of azide end-functionalized miktoarm star polymer (PCL-PS-P*t*BA-N_3)

Azide end-functionalized miktoarm star polymer (PCL-PS-P*t*BA-N_3) was obtained via sequential living polymerizations such as ROP of ε-CL, NMP of St and ATRP of *t*BA, respectively starting from the initiator **6**. Firstly, PCL-macroinitiator was obtained by ROP of ε-CL in bulk in the presence of $Sn(Oct)_2$ as catalyst and **6** as initiator at 110 ^{o}C for 10.5 h (reaction 4.16).

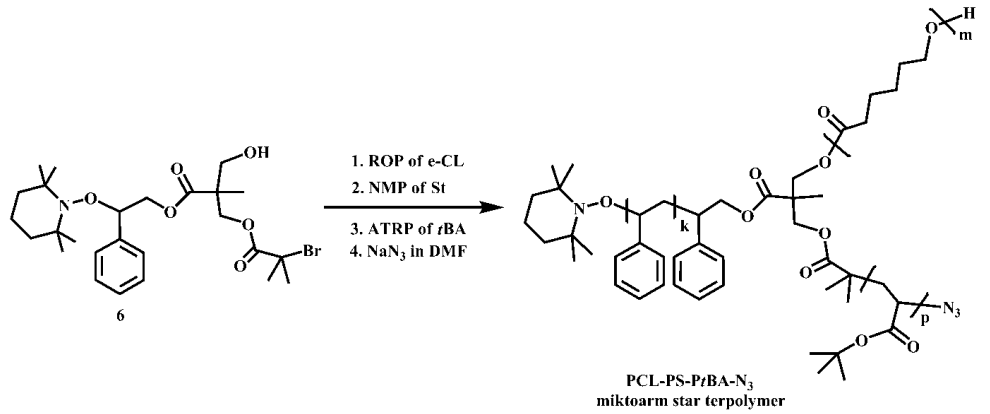

(4.16)

From ^{1}H NMR spectrum (Figure 4.20), it was observed that signals at 2.2 and 4.04 corresponding to CH_2OC=O of PCL and CH_2OH end-group of PCL, methyl protons adjacent to bromine at 1.9 ppm. $M_{n,NMR}$ was determined by using the following equation: $M_{n,NMR}$ = DP_n of PCL + MWof **6** = 52 X 114.1 + 542.5 = 6500.

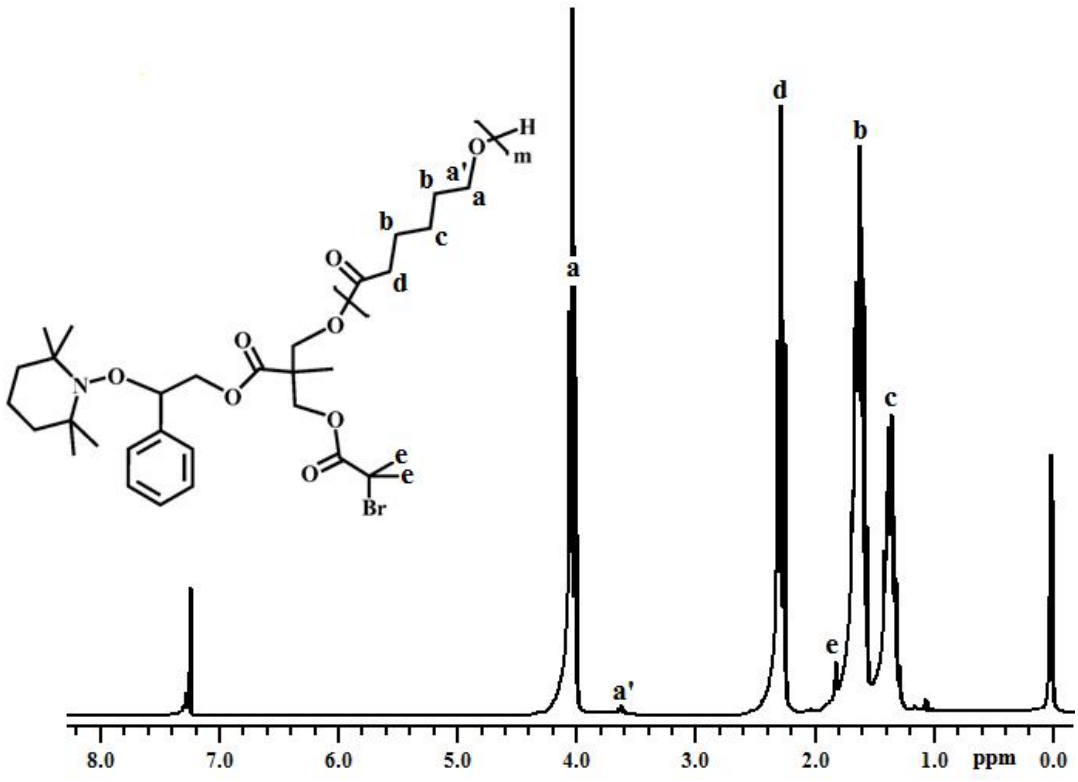

Figure 4.20: ^{1}H NMR spectrum of PCL macroinitiator in $CDCl_3$.

$M_{n,GPC}$ and M_w/M_n values were acquired to be 15000 and 1.13, respectively using GPC calibrated with linear PS standards in THF. $M_{n,GPC}$ value based on PS standards was simply converted to $M_{n,PCL}$ = 0.259 X $M_{n,GPC}^{1.073}$ = 7800 [315]. However, a small

shoulder was detected in the high molecular weight region of chromatogram that belongs to PCL (Figure 4.22). This was attributed to inadequate kinetic control and occurrence of side reactions, particularly polyester transesterifications during ROP process [316]. $M_{n,theo}$ of PCL macroinitiator was estimated using $M_{n,theo} = ([M]_0/[I]_0)$ X conv. % X MW of ε-CL + MW of **6** = 100 X 0.71 X 114.15 + 542.5 = 8600.

Next, PCL-macroinitiator was employed in NMP of St in bulk for 3 h at 125 ^oC in order to obtain PCL-*b*-PS copolymer with bromide functionality at the junction point (reaction 4.16). $M_{n,theo}$ of the PCL-*b*-PS copolymer was determined using a following equation, $M_{n,theo} = ([M]_0/[I]_0)$ X conv. % X MW of St + $M_{n,NMR}$ of PCL macroinitiator = 200 X 0.3 X 104.15 + 6500 = 12750. GPC analysis (Figure 4.23) showed a single peak shifting to a higher molecular weight compared to PCL, $M_{n,GPC}$ (22900) and poldispersity index (1.13) remained rather low.

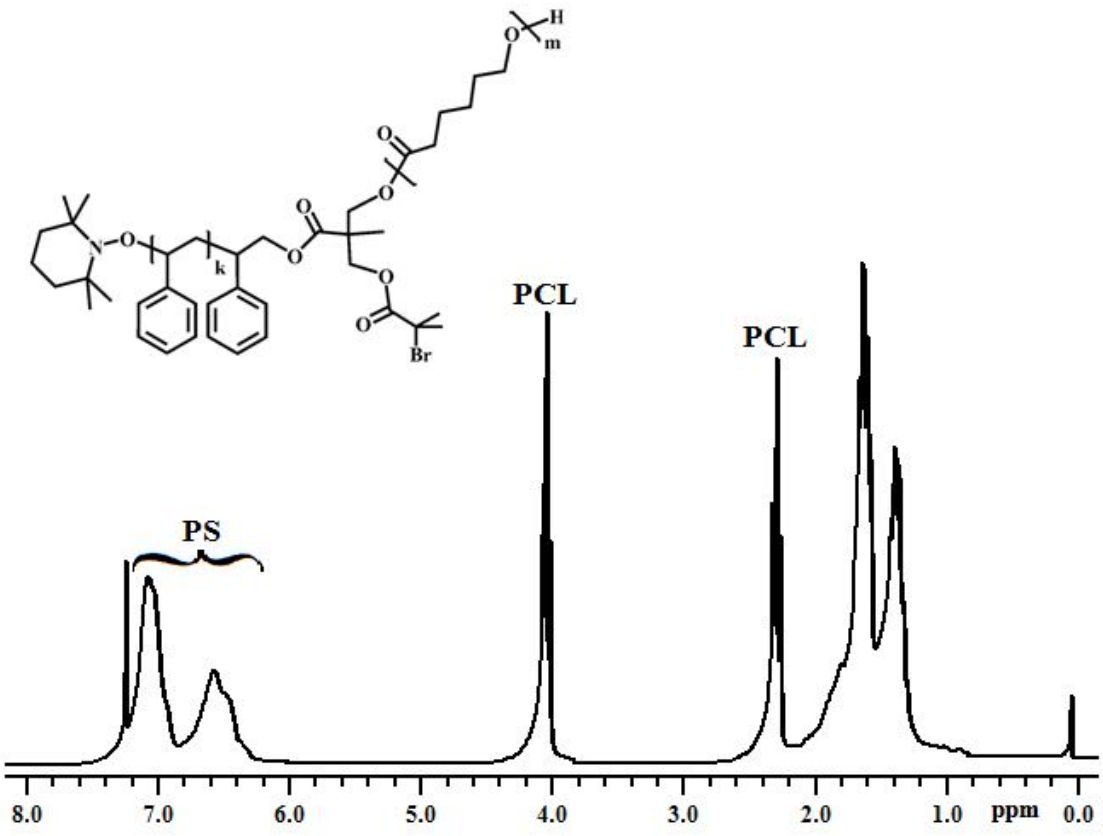

Figure 4.21: ^1H NMR spectrum of PCL-*b*-PS copolymer in $CDCl_3$.

The ^1H NMR spectrum of PS-*b*-PCL copolymer shows the presence of both blocks and a comparison of integrated values of aromatic protons of PS with $CH_2OC{=}O$ of PCL gave a DP_n = 60 of PS block (Figure 4.21). Thus, $M_{n,NMR}$ value of PS-*b*-PCL

copolymer was found to use this equation: $M_{n,NMR}$ = DP_n of PS + $M_{n,NMR}$ of PCL macroinitiator = 60 X 104.15 + 6500= 13000 (Table 4.3).

The previously obtained PCL-*b*-PS copolymer with bromide functionality was employed as a macroinitiator in subsequent ATRP of *t*BA using CuBr/PMDETA catalyst in toluene for 5 h, yielding the miktoarm star polymer (PCL-PS-P*t*BA-Br) (reaction 4.16). $M_{n,theo}$ = ($[M]_0/[I]_0$) X conv. % X MW of *t*BA + $M_{n,NMR}$ of PCL-PS precursor = 300 X 0.12 X 128.1 + 13000 = 18400 was used to calculate $M_{n,theo}$ of PCL-PS-P*t*BA-Br. The ^{1}H NMR spectrum of the resulting PCL-PS-P*t*BA miktoarm star polymer displays characteristic signals of PCL arm at 4.05 and 2.3 ppm, PS arm at 7.2 and 6.5 ppm and P*t*BA arm at 2.2 and 1.4 ppm. A comparison of the integrals of the CH_2OC=O of PCL (4.04 ppm) with the sum of the C=OCH_2 of PCL (2.3 ppm) and C*H*(C=O) of P*t*BA (2.2 ppm) revealed the P*t*BA arm with DP_n = 42 (Figure 4.22). Subsequently, PCL-PS-P*t*BA miktoarm star polymer was determined to have $M_{n,NMR}$ of 18400.

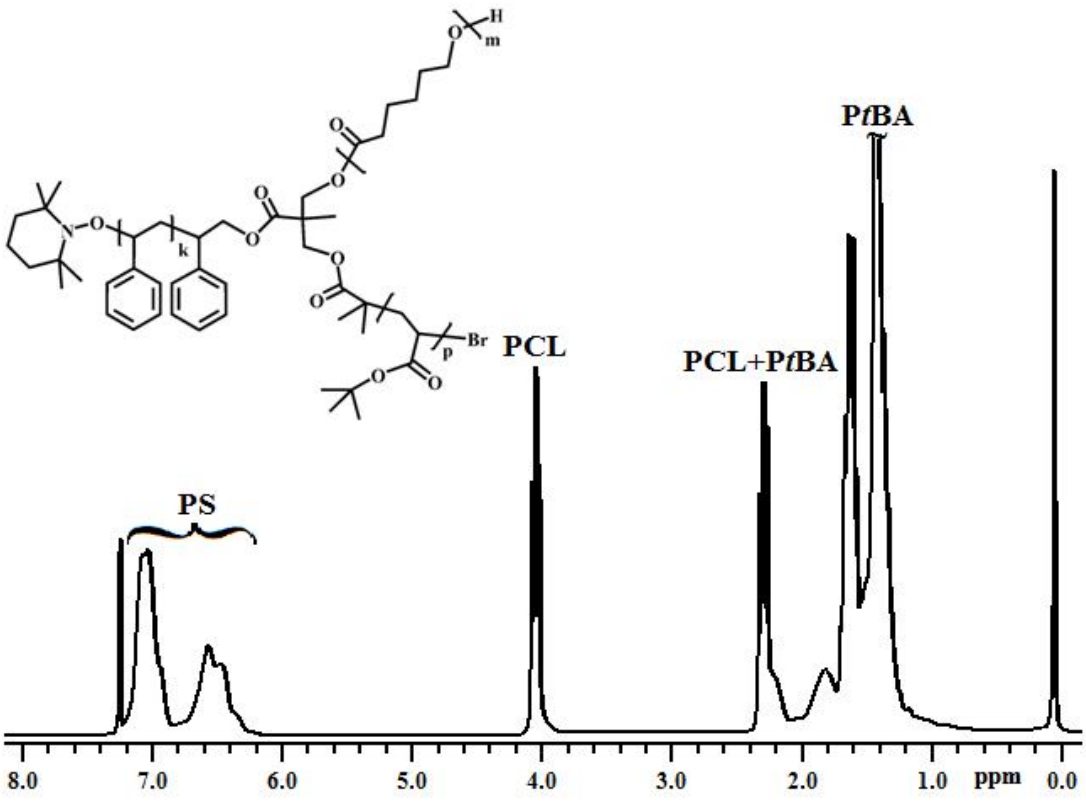

Figure 4.22: ^{1}H NMR spectrum of PCL-PS-P*t*BA miktoarm star terpolymer in $CDCl_3$.

According to GPC measurements, a clear shift in molecular weight distributions to lower retention times was observed indicating an efficient miktoarm star formation. PCL-PS-P*t*BA miktoarm star polymer was found to have a $M_{n,GPC}$ = 28000 and M_w/M_n = 1.18 (Figure 4.23). Obtained results are presented in Table 4.3. The bromide end functionality of PCL-PS-P*t*BA miktoarm star polymer was converted to azide by a reaction of NaN_3 in DMF overnight at room temperature (reaction 4.16). The structure of PCL-PS-P*t*BA-N_3 was further supported by an observation of the azide stretching band at 2094 cm^{-1} from FT-IR spectrum.

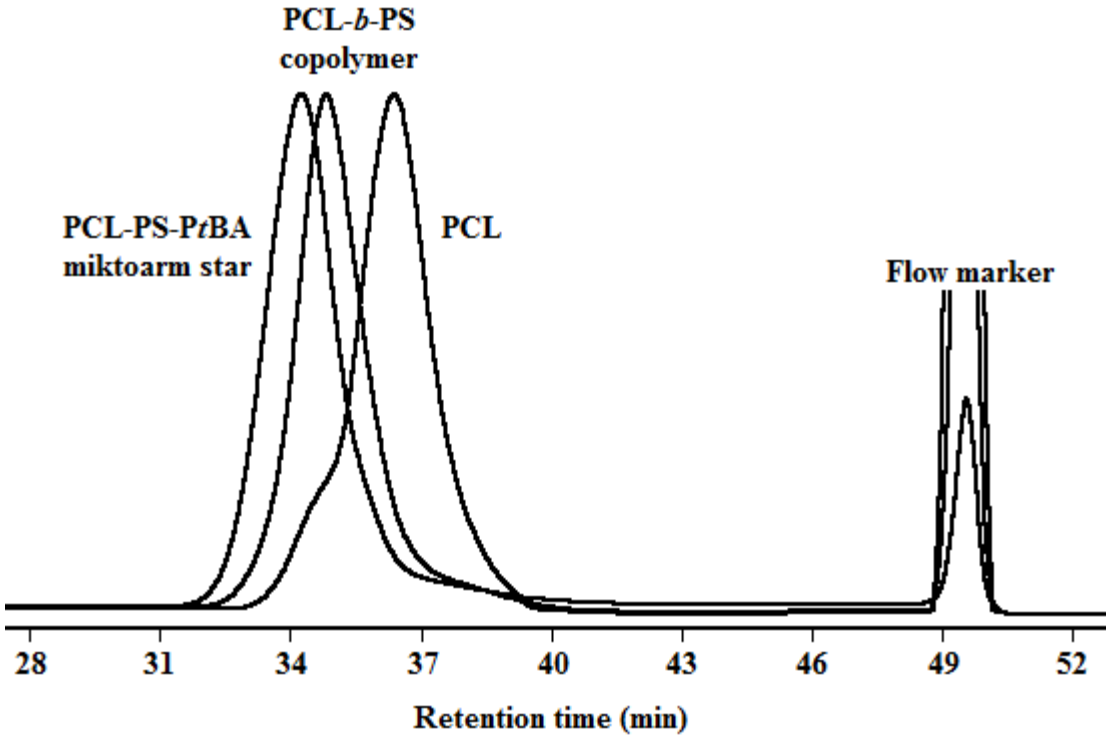

Figure 4.23: The evolution of GPC traces of PCL, PCL-*b*-PS and PCL-PS-P*t*BA miktoarm star polymers.

Table 4.3: The conditions and results of precursors for the synthesis of H-shaped quintopolymer and H-shaped polymer obtained from CuAAC.

Entry	Polymer	Initiator	Time (h)	Conv. (%)	$M_{n,GPC}$[e] (g/mol)	M_w/M_n	$M_{n,theo}$ (g/mol)	$M_{n,NMR}$[k] (g/mol)
1	**PCL-macroinitiator**[a]	**6**	10.5	71	7800[f]	1.13	8600[g]	6500
2	**PCL-*b*-PS copolymer**[b]	PCL-macroinitiator	3	30	22900	1.13	12750[h]	13000
3	**PCL-PS-P*t*BA-Br miktoarm star polymer**[c]	PCL-*b*-PS copolymer	5	12	28000	1.18	17600[i]	18400
4	**PEG-*b*-PMMA-alkyne copolymer**[d]	PEG-macroinitiator	1	31	13700	1.08	8800[j]	11300
5	**PCL-PS-P*t*BA-PEG-PMMA H-shaped polymer**	PCL-PS-P*t*BA-N_3 + PEG-PMMA-alkyne	24	Yield (75%)	32100	1.2	29700	22400[m]

[a] $[M]_0:[I]_0:[Sn(Oct)_2]$ = 2000:20:1 at 110 °C. [b] $[M]_0:[I]_0$ = 200 in bulk at 125 °C. [c] $[M]_0:[I]_0:[PMDETA]_0:[CuBr]_0$ = 300:1:1:1; *t*BA/ toluene = 1/1 (v/v) at 80 °C.
[d] $[M]_0:[I]_0$: $[PMDETA]_0:[CuCl]_0$ = 200:1:1:1; MMA/ toluene = 1/1 (v/v) at 60 °C. [e] Calculated from GPC calibrated with linear PS standards.
[f] $M_{nPCL} = 0.259 \times M_{nGPC}^{1.073}$. [g] $M_{n,theo} = ([M]_0/[I]_0)$ X conv. % X MW of ε-CL + MW of **6**.
[h] $M_{n,theo} = ([M]_0/[I]_0)$ X conv. % X MW of St + $M_{n,NMR}$ of PCL precursor. [i] $M_{n,theo} = ([M]_0/[I]_0)$ X conv. % X MW of *t*BA + $M_{n,NMR}$ of PCL-*b*-PS precursors.
[j] $M_{n,theo} = ([M]_0/[I]_0)$ X conv. % X MW of MMA + $M_{n,NMR}$ of PEG precursor
[k] $M_{n,NMR} = DP_n$ of Polymer + MW of **6** or $M_{n,NMR}$ of macroinitiator. [m] $M_{n,NMR}$ calculated from the composition of H-shaped quintopolymer.

4.2.2 Synthesis of alkyne mid-functionalized PEG-*b*-PMMA copolymer

Esterification was realized between 2,2,5-trimethyl-[1,3]dioxane-5-carboxylic acid (**3**) and propargyl alcohol to produce the alkyne functional compound **9** using DCC and DMAP ina fairly high yield (67%) (reaction 4.17).

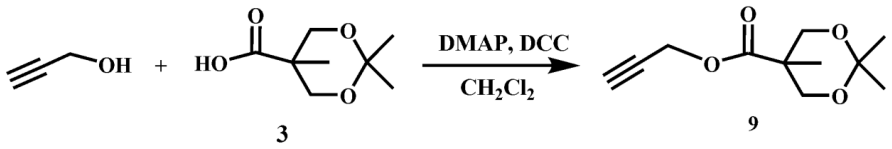

3 9 **(4.17)**

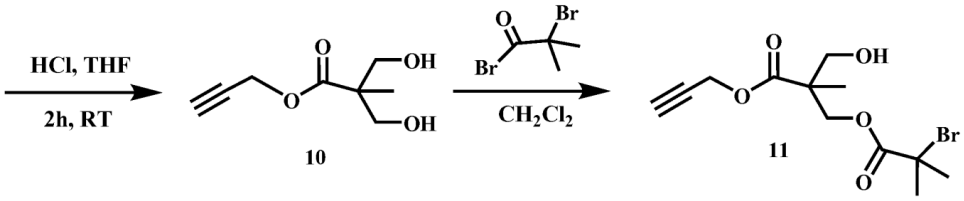

10 11 **(4.18)**

^{1}H NMR spectrum of compound **9** clearly shows the signals of alkyne appeared at 2.5 ppm, methylene protons adjacent to alkyne group and acetonide groups at 4.7 ppm and 3.6-4.2 ppm, respectively. Also, the methyl protons were detected at 1.2 and 1.35-1.5 ppm. These results confirmed that **9** was successfully synthesized (Figure 4.24).

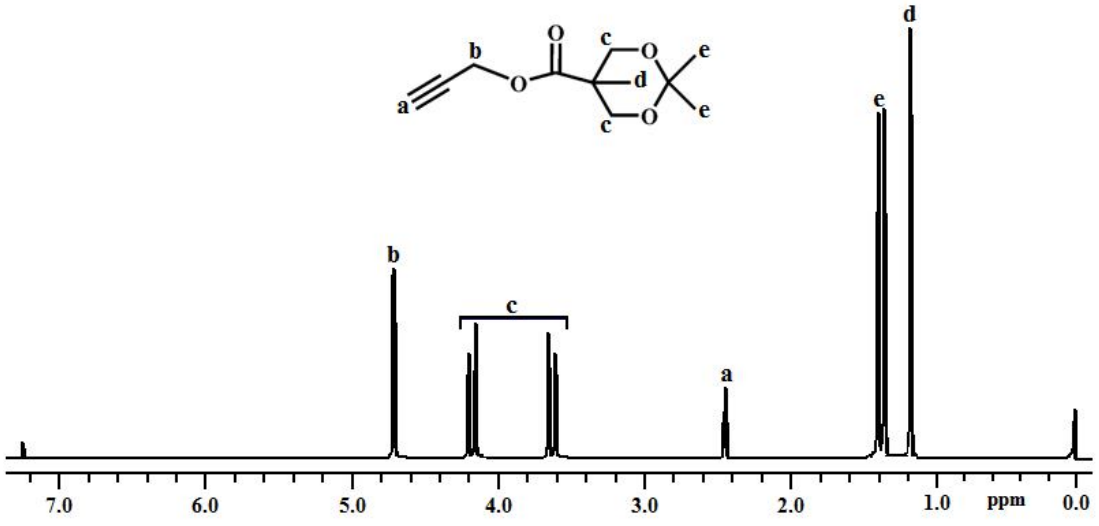

Figure 4.24: ^{1}H NMR spectrum of propargyl-2,2,5-trimethyl-1,3-dioxane-5-carboxylate (**9**) in $CDCl_3$.

Acetal protected this compound **9** was deprotected by using 1 M HCL to yield **10** (reaction 4.18). The hydroxyl groups of **10** can be seen at 2.93 ppm together with the

signals associated with alkyne functionality and core compound (Figure 4.25). Those signals disappeared after D_2O treatment.

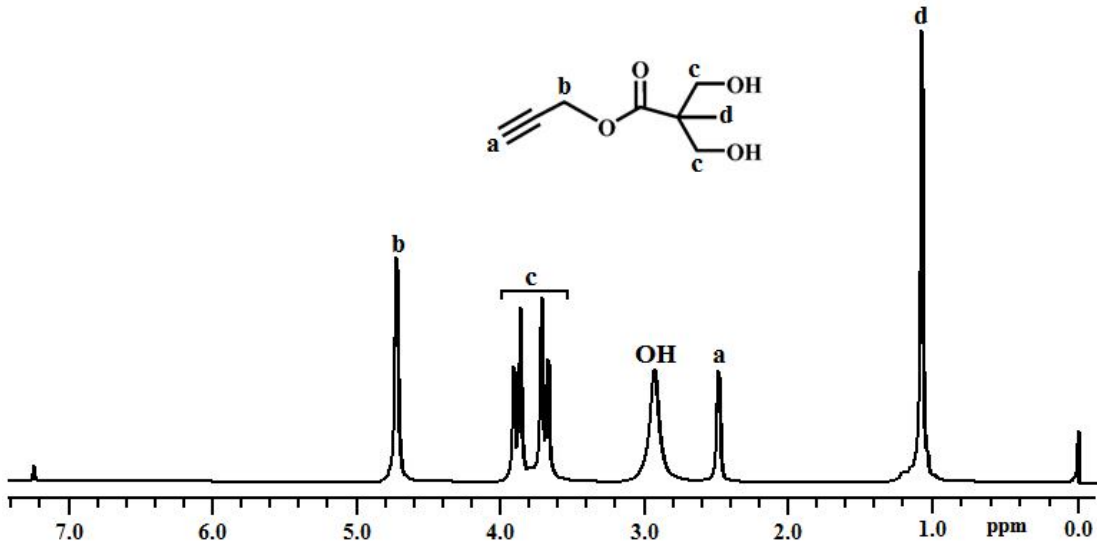

Figure 4.25: ^{1}H NMR spectrum of propargyl-3-hydroxy-2-(hydroxymethyl)-2-methyl propanoate (**10**) in $CDCl_3$.

ATRP initiator was prepared by esterfication between one hydroxyl group of **10** and 2-bromoisobutyrylbromide (reaction 4.18). ^{1}H NMR spectrum of miktofunctional initiator (**11**) clearly shows a characteristic triplet signal of methylene protons (b) adjacent to ester group at 4.71 and doublet signal methine proton of alkyne (*H*C≡CCH_2) at 2.48 ppm. O*H* protons of propargyl-2,2-bis(hydroxymethyl) propionate at 3.18 ppm completely shifted to 2.36 ppm indicating monofunctional hydroxyl group. Additionally, a new signal for methylene protons (d) adjacent to ester appeared at 4.2-4.4 ppm together with methyl protons at 1.90 ppm of ATRP functionality (Figure 4.26). Integrated values of related signals proved that esterification reaction was carried out successfully. Mono carboxylic acid functional PEG (PEG-COOH) was synthesized with a reaction of PEG-OH in the presence of succinic anhydride. When DMAP, TEA and CH_2Cl_2 were used as the catalysts and the solvent respectively, the reaction proceeded efficiently, and PEG-COOH were obtained in high yield. Figure 4.27 depicts the ^{1}H NMR spectrum of PEG with a COOH end group. The methylene proton of PEG is assigned as 4.25 ppm because of the introduction of succinic anhydride. The methylene proton formed by the ring opening of succinic anhydride is assigned as 2.65 ppm.

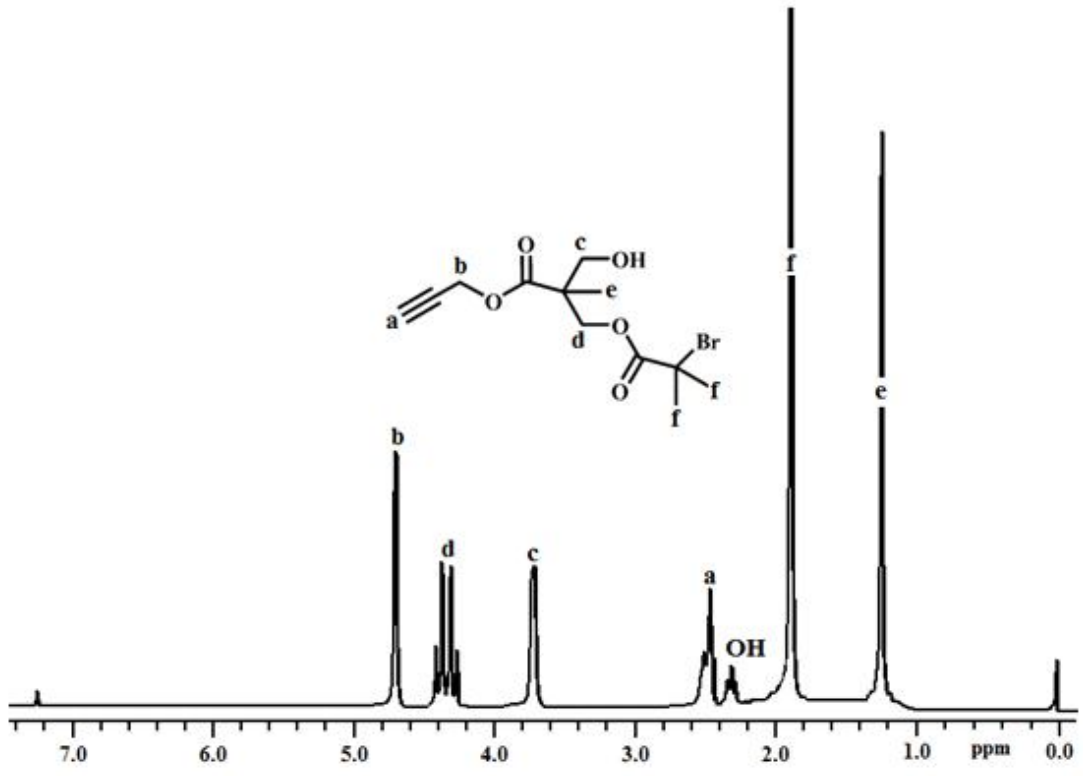

Figure 4.26: ^{1}H NMR spectrum of propargyl-3-[(2-bromo-2-methylpropanoyl)oxy]-2-(hydroxy methyl)-2-methylpropanoate (**11**) in $CDCl_3$.

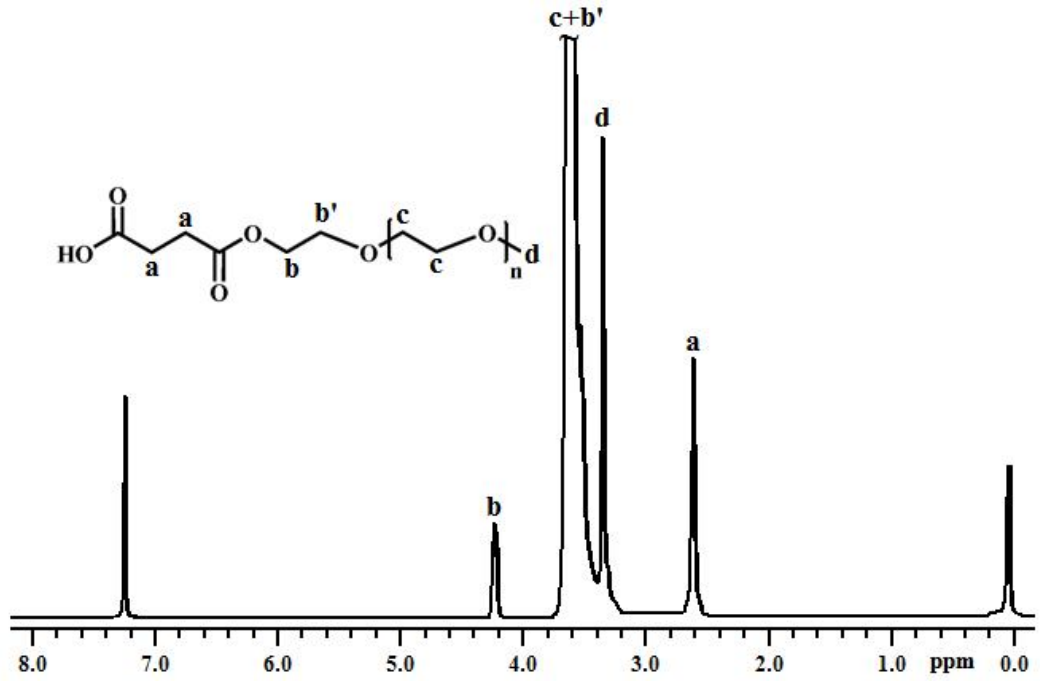

Figure 4.27: ^{1}H NMR spectrum of PEG-COOH in $CDCl_3$.

Next **11** was allowed to react with PEG-COOH to give PEG-macroinitiator with both alkyne and bromide end functionalities (reaction 4.19) The raw product was precipitated in cold diethyl ether and further purified after two times dissolution-precipitation cycle. Later has an initiation capability for ATRP. ^{1}H NMR spectrum of PEG-macroinitiator clearly shows the signal of PEG units at 3.63 ppm, alkyne proton at 2.5 ppm and methyl protons at 1.90 ppm of ATRP functionality (Figure 4.28).

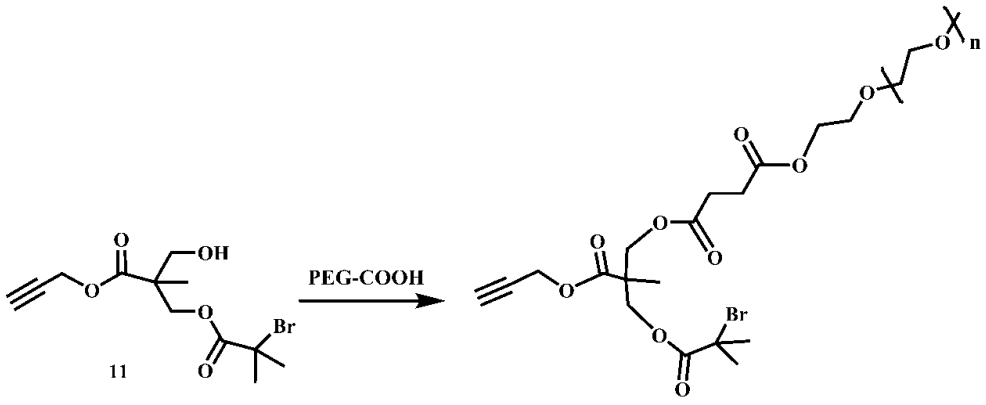

(4.19)

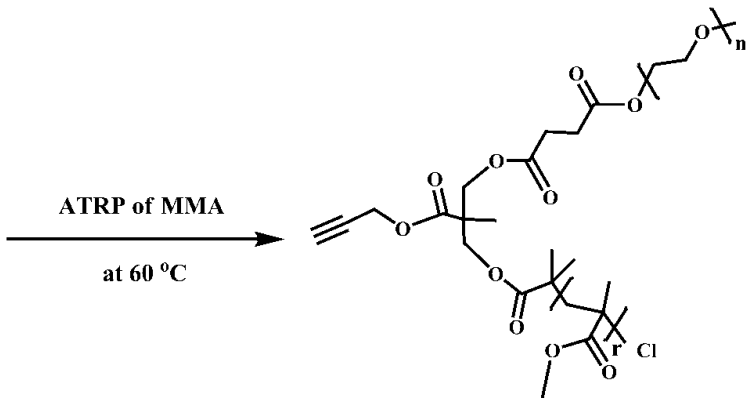

(4.20)

Thus PEG-*b*-PMMA copolymer with alkyne at the junction point was acquired by ATRP of MMA using PEG-macroinitiator in the presence of CuCl/PMDETA in toluene at 60 ^{o}C for 1 h (reaction 4.20).

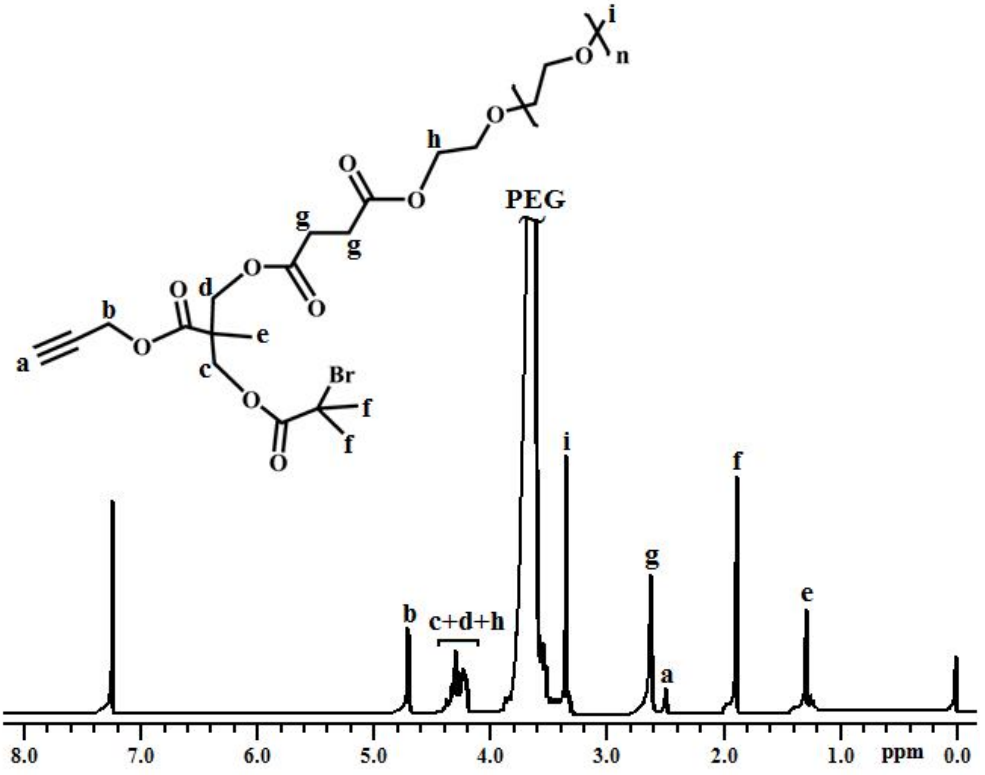

Figure 4.28: ^{1}H NMR spectrum of PEG macroinitiator in $CDCl_3$.

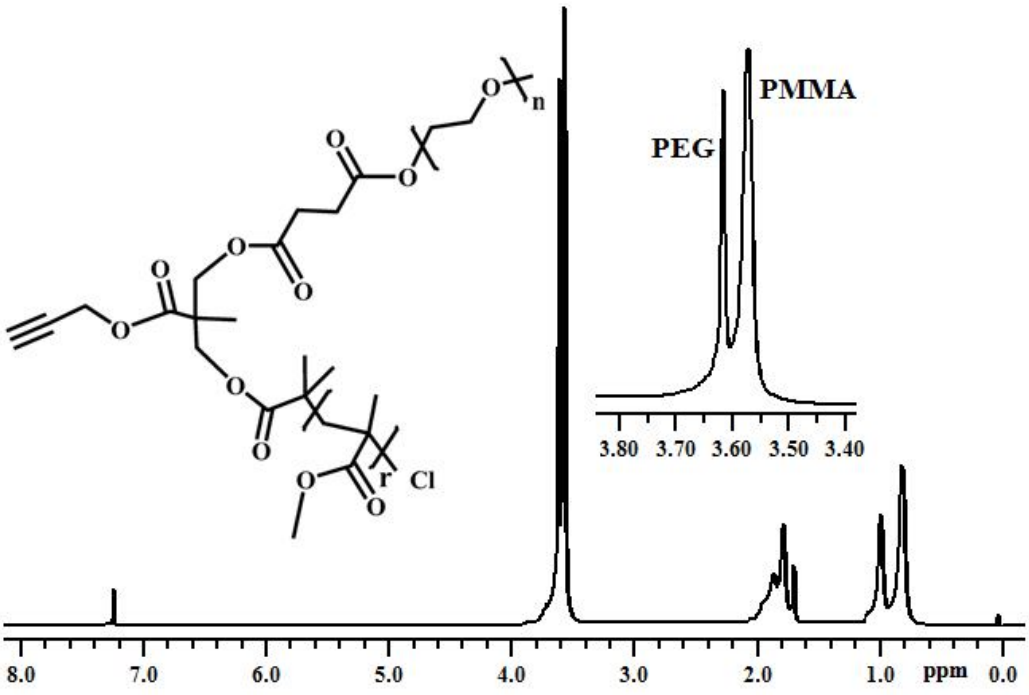

Figure 4.29: ^{1}H NMR spectrum of PEG-*b*-PMMA in $CDCl_3$.

$M_{n,NMR}$ = 11300 g/mol was measured using an integrated ratio of peaks appeared at 3.61 and 3.57 ppm, corresponding to CH_2CH_2O of PEG and OCH_3 of PMMA, respectively (Figure 4.29), while $M_{n,NMR}$ of PEG-macroinitiator ($M_{n,NMR}$ = 2150 g/mol) was being added. The obtained PEG-PMMA-alkyne block copolymer has PEG and PMMA blocks with DP_n= 45 and 87, respectively. It was found good agreement between $M_{n,theo}$, $M_{n,NMR}$ and $M_{n,GPC}$. (Table 4.3).

$M_{n,theo}$ of PEG–PMMA–alkyne was calculated using the formula $M_{n,theo} = ([M]_0/[I]_0)$ X conv. % X MW of MMA + $M_{n,NMR}$ of PEG macroinitiator = 200 X 0.31 X 100 + 2600 = 8800. GPC curves of PEG-PMMA-Alkyne and the corresponding precursor display monomodal and narrow molecular weight distribution (1.08), and a tail was not observed in the molecular weight region of the precursor (Figure 4.30). The number average molecular weight of GPC ($M_{n,GPC}$) 13700 g/mol.

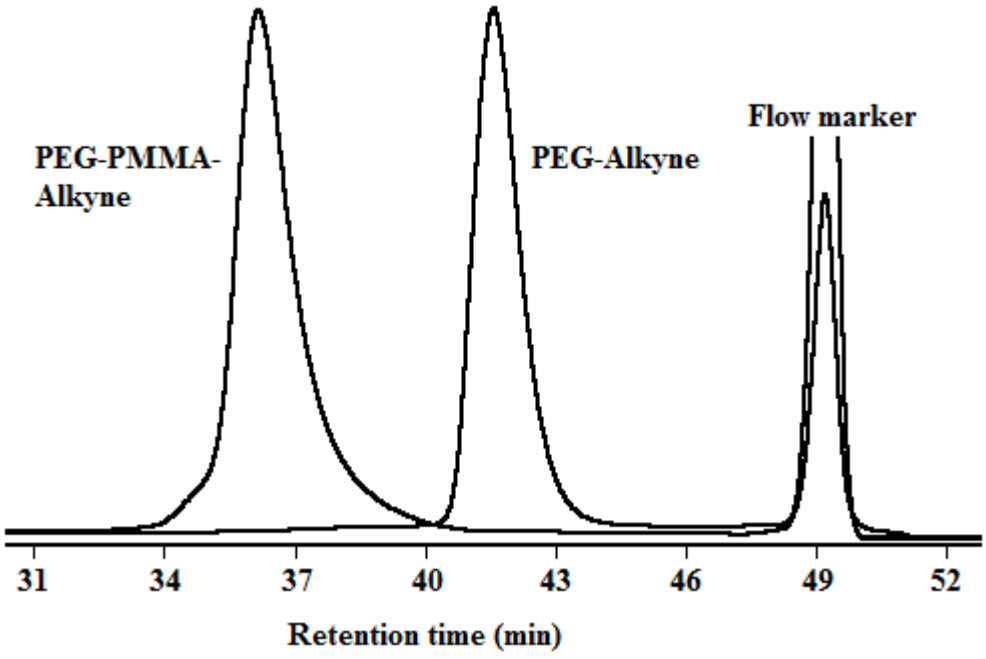

Figure 4.30: The GPC traces of PEG-macroinitiator (PEG-Alkyne) and PEG-PMMA-Alkyne.

4.2.3 H-shaped quintopolymer by using CuAAC

A click reaction between PCL-PS-P*t*BA-N_3 miktoarm star polymer and PEG-PMMA-alkyne copolymer afforded (PCL)(PS)-(P*t*BA)-(PEG)(PMMA) H-shaped quintopolymer in DMF in the presence of CuBr/PMDETA at room temperature for 20 h (reaction 4.21). For the click reaction, molar ratio of PEG-PMMA-alkyne to

PCL-PS-P*t*BA-N_3 was deliberately taken ca. 1.5 due to that the former was soluble in precipitation solvent methanol at room temperature. However, target H-shaped polymer was sequentially treated with Merrifield's-azide and -alkyne resins in order to get rid of unreacted PEG-PMMA-alkyne and PCL-PS-P*t*BA-N_3 precursors, respectively. After these treatments, H-shaped quintopolymer was characterized by ^{1}H NMR and GPC measurements. (Table 4.3)

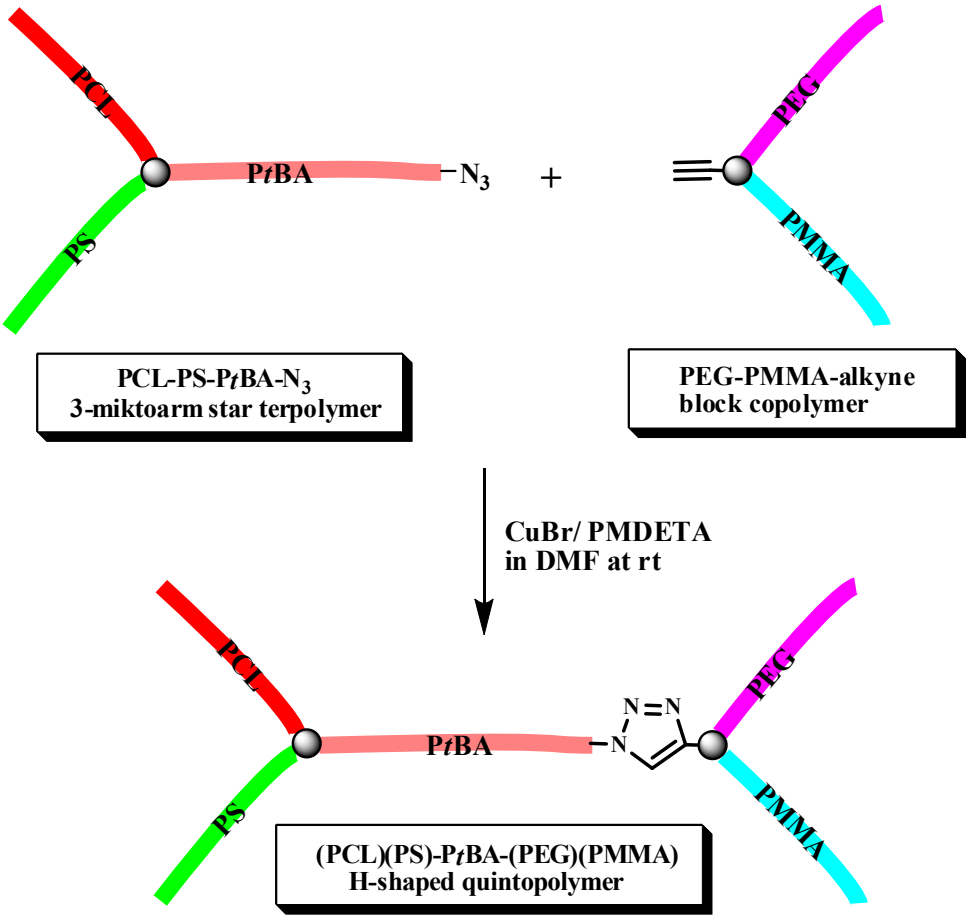

(4.21)

^{1}H NMR spectrum of H-shaped quintopolymer displays clearly the characteristic signals of PS at 7.2-6.5 ppm, PCL at 4.04 and 2.3 ppm, PEG at 3.63 ppm, PMMA at 3.58 ppm and P*t*BA segments at 2.2 and 1.4 ppm, thus indicating that the click reaction was successful (Figure 4.31).

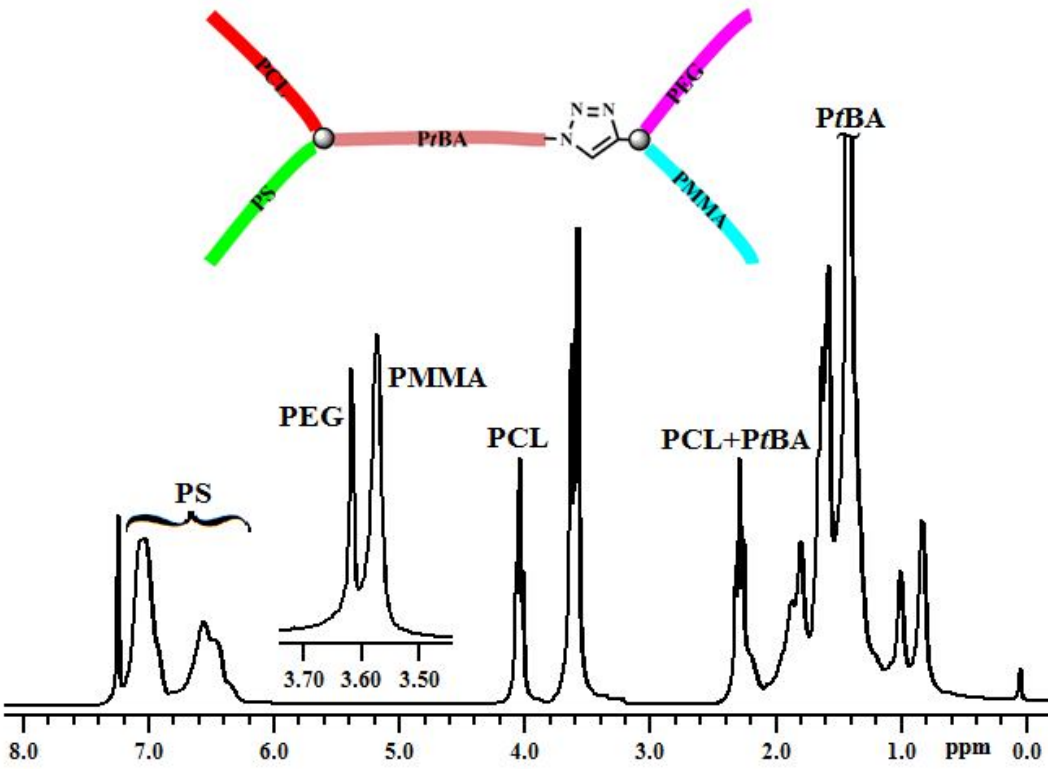

Figure 4.31: ^{1}H NMR spectrum of (PCL)(PS)-(P*t*BA)-(PEG)(PMMA) H-shaped quintopolymer in $CDCl_3$.

The click reaction between the precursors PCL-PS-P*t*BA-N_3 and PEG-PMMA-alkyne gave the H-shaped quintopolymer. From ^{1}H NMR spectrum of H-shaped quintopolymer, DP_n values of PCL, PS and P*t*BA arms in H-shaped quintopolymer were calculated to have 48, 56 and 39, respectively assuming that DP_ns of PEG and PMMA segments were as identical as in the miktoarm star terpolymer prior to click reaction. Thus $M_{n,NMR}$ of H-shaped quintopolymer was found according to a formula $M_{n,NMR}$ = DP_n (PEG) X 44 + DP_n (PMMA) X 100 + DP_n (PS) X 104.15 + DP_n (PCL) X 114.15 + DP_n (P*t*BA) X 128.1 + MW of initiators = 45 X 44 + 87 X 100 + 48 X 144.15 + 56 X 104.15 + 39 X 128.1 + 864 = 22400. Therefore, click efficiency was calculated from the $M_{n,NMR}$ ratio of H-shaped quintopolymer and $M_{n,theo}$ (22400/29700 = 0.75). The efficiency of about 75% was obtained displaying the moderate efficiency in the synthesis of H-shaped quintopolymer by click reaction. It was in close agreement with recent literature regarding nonlinear polymeric structures such as miktoarm star graft to polymeric backbone obtained by click reactions [317, 318].

H-shaped quintopolymer was obtained with $M_{n,GPC}$ of 32100 and low PDI of 1.20 as determined by GPC in THF (Table 4.3). As can be seen from Figure 4.32, monomodal GPC trace was observed for H-shaped polymer with a clear shift respect to the PCL-PS-P*t*BA miktoarm star and PEG-PMMA block copolymer precursors.

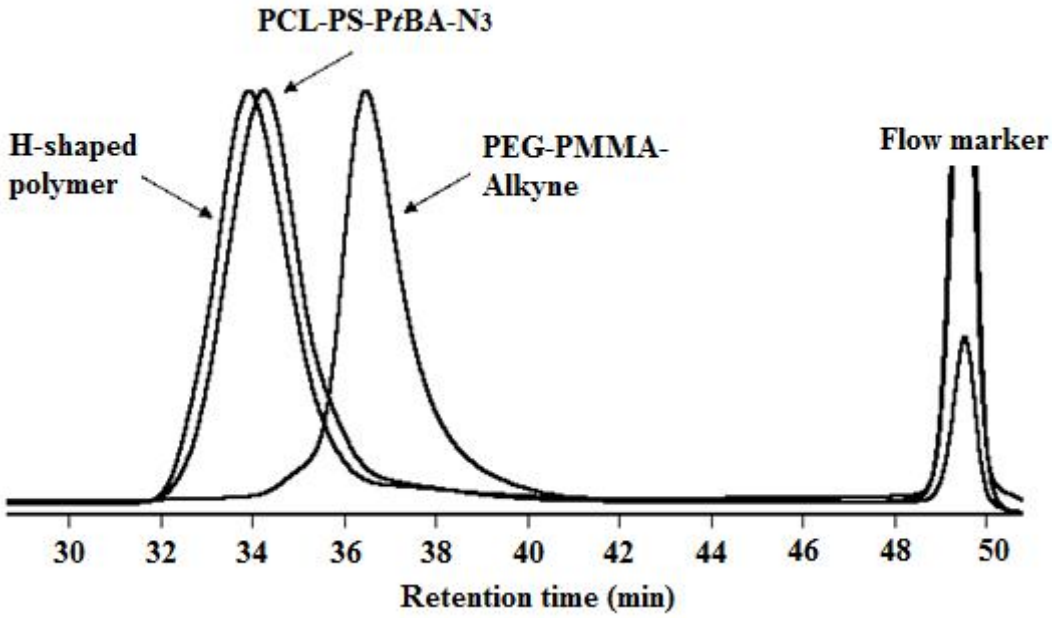

Figure 4.32: The evolution of GPC curves PEG-PMMA-alkyne block copolymer, PCL-PS-P*t*BA-N_3 miktoarm star terpolymer and (PCL)(PS)-(PtBA)-(PEG)(PMMA) H-shaped quintopolymer in THF using RI detector.

4.3 One-Pot Double Click Reactions for the Preparation of H-Shaped ABCDE-Type Quintopolymer

The first time two click reaction strategies involving CuAAC and Diels-Alder reactions were used for the preparation of H-type polymer having different pentablock (quintopolymer) in one-pot technique. This was a simple and a versatile synthetic technique when compared to previous work, due to having a lesser reaction steps and more well-defined polymeric precursors. For this task, PEG-*b*-PMMA and PCL-*b*-PS polymeric side arms having maleimide and alkyne at their centers, respectively and P*t*BA main chain with α-anthracene and ω-azide were separately prepared and simultaneously reacted in one pot technique affording the target H-shaped (PEG)(PMMA)-P*t*BA-(PS)(PCL) quintopolymer.

4.3.1 Preparation of PEG-*b*-PMMA-MI copolymer as a side arm

The initiator with proper functionalities for Diels-Alder reaction was first prepared. 4-(2-Hydroxyethyl)-10-oxa-4-azatricyclo[5.2.1.$0^{2,6}$]dec-8-ene-3,5-dione, (**13)** was first synthesized within two steps. Furan and maleic anhydride were reacted in toluene at 80 ^{o}C, then the formed adduct (**12)** (reaction 4.22)**,** was utilized for the synthesis of **13** by adding the solution 2-amino ethanol in methanol into dispersion of **12** in methanol (reaction 4.23).

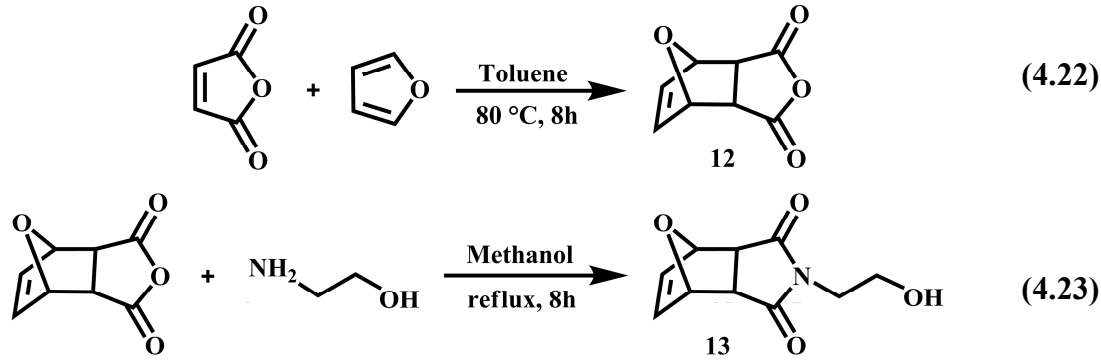

(4.22)

(4.23)

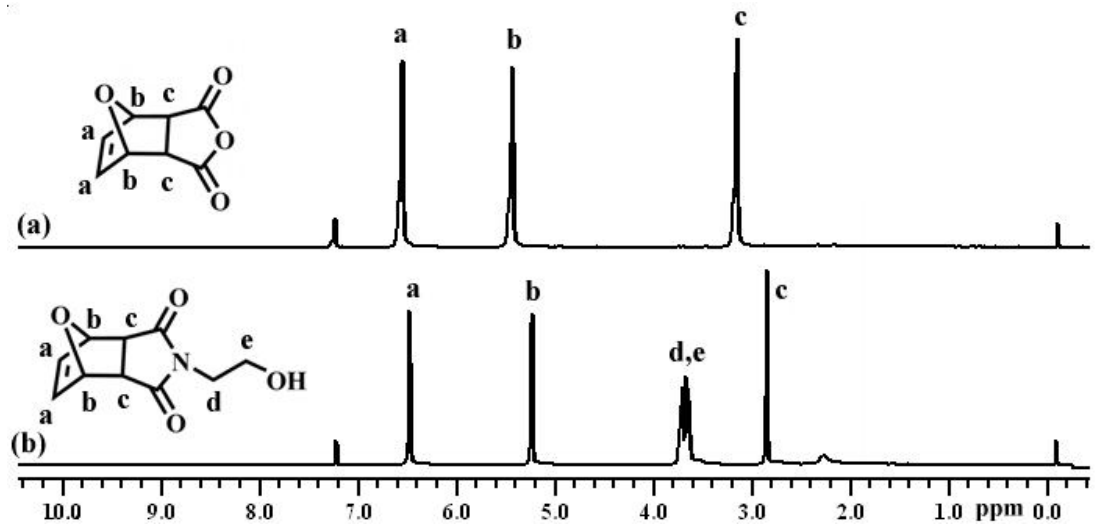

Figure 4.33: ^{1}H NMR spectra of: **a**)3-acetyl-N-(2-hydroxyethyl)-7-oxabicyclo [2.2.1]hept-5-ene-2-carboxylic acid **(12)**; **b**) 3-acetyl-N-(2-hydroxyethyl)-7-oxabicyclo[2.2.1]hept-5-ene-2-carboxamide (**13)** in $CDCl_3$.

From overlay ^{1}H NMR spectra of **12** and **13** (Figure 4.33), it was clearly seen that the methylene protons next to OH were detected at 3.6-3.8 ppm. Moreover, the characteristic protons of the adduct were also detected at 6.49 ppm (bridge vinyl

protons), 5.24 ppm (bridge-head protons) and 2.85 ppm (bridge protons) respectively. These results confirmed that the synthesis of **13** was accomplished.

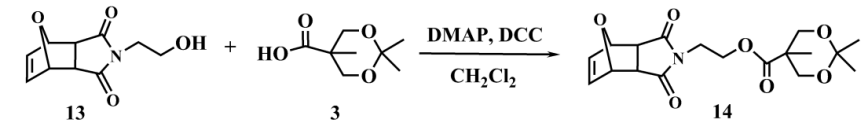

(4.24)

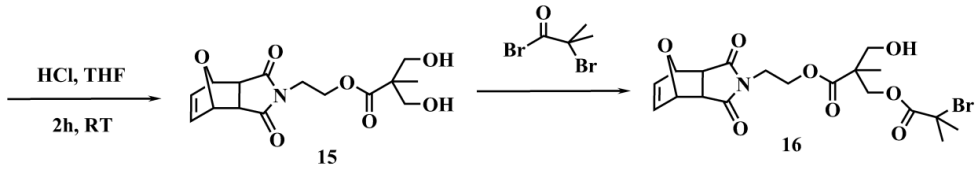

(4.25)

For the preparation of PEG-*b*-PMMA with maleimide at its center, the initiator **16** was synthesized starting from an esterification reaction of 4-(2-Hydroxyethyl)-10-oxa-4-azatricyclo[5.2.1.$0^{2,6}$] dec-8-ene-3,5-dione (**13**) with 2,2,5-trimethyl-[1,3]dioxane-5-carboxylic acid (**3**) in the presence of DMAP/DCC at room temperature (reaction 4.24), in order to give **14** followed by deprotection (**15**) and monoesterification of -CH_2OH with 2-bromoisobutrylbromide (reaction 4.25).

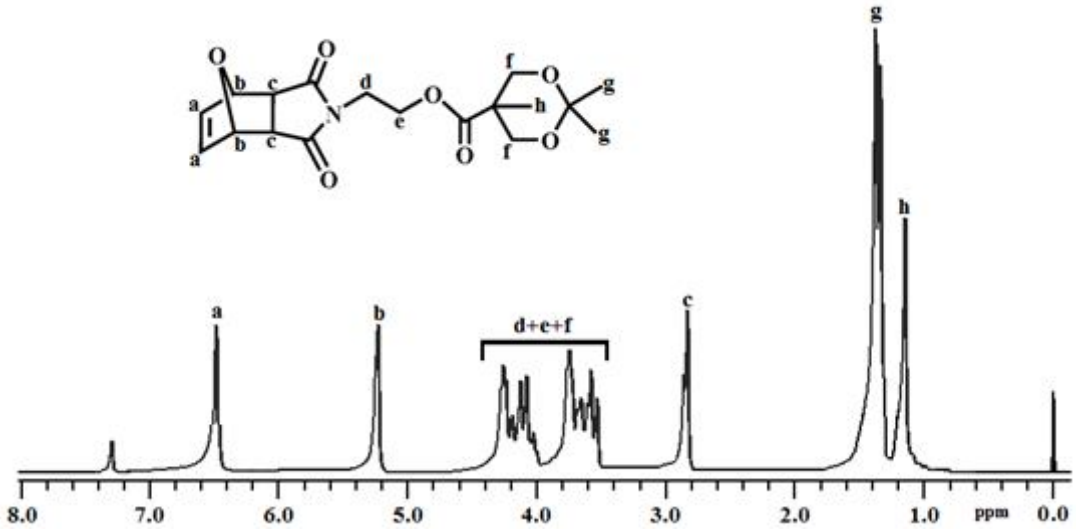

Figure 4.34: ^{1}H NMR spectrum of 2,2,5-trimethyl-[1,3]dioxane-5-carboxylic acid 4-(2-ethyl)-10-oxa-4-azatricyclo[5.2.1.$0^{2,6}$] dec-8-ene-3,5-dione ester (**14**) in $CDCl_3$.

^{1}H NMR spectrum of **14** showed characteristic triplet signal of ester CH_2 at 4.25 ppm. Notably, the signals matching the furan-protected maleimide can also be distinguished along with the others. Moreover, the characteristic protons of the adduct were also detected at 6.49 ppm (bridge vinyl protons), 5.24 ppm (bridge-head

protons) and 2.85 ppm (bridge protons) respectively (Figure 4.34). These results confirmed that the synthesis of **14** was accomplished.

The deprotection of acetal group of **14** led to the double CH_2OH functional groups in the presence of HCl in dry THF for 2 h affording the synthesis of **15** (reaction 4.25). ^1H NMR analysis confirmed the structure of **15** displaying the disappearance of acetonide groups at 1.37-1.34 and appearance of broad OH at 2.67 ppm (Figure 4.35).

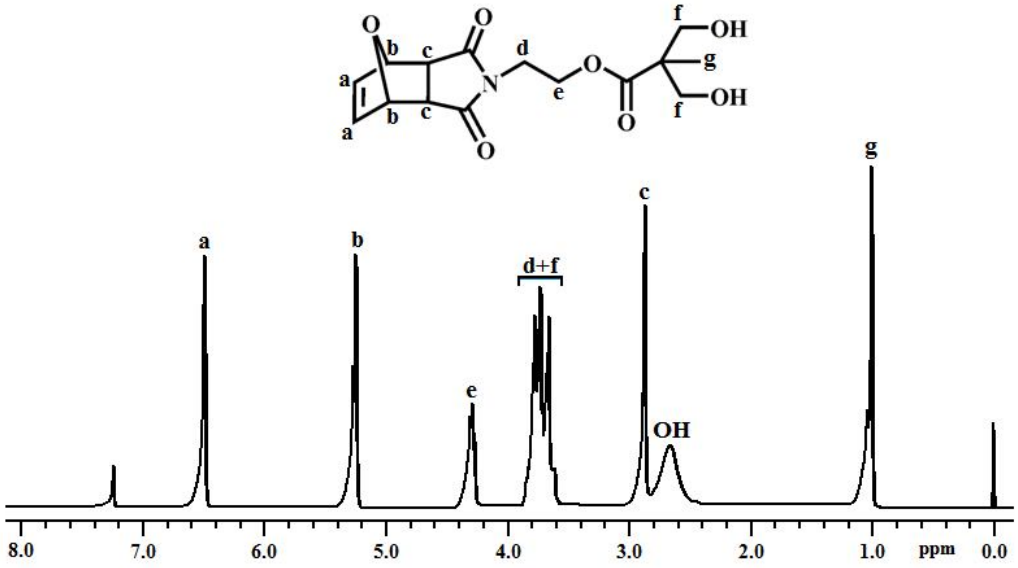

Figure 4.35: ^1H NMR spectrum of 3-hydroxy-2-hydroxymethyl-2-methyl-propionic acid 4-(2-ethyl)-10-oxa-4-azatricyclo [5.2.1.$0^{2,6}$]dec-8-ene-3,5-dione ester (**15**) in $CDCl_3$.

Next, the initiator **16** was obtained via monoesterification of -CH_2OH of **15** with 2-bromoisobutrylbromide (reaction 4.25) and successive purification via column chromatography. The ^1H NMR spectrum of **16** exhibited a new signal at 1.88 ppm that can be ascribed to the methyl protons adjacent to bromide (Figure 4.36). The integrated ratios have also supported the monoesterification of -CH_2OH.

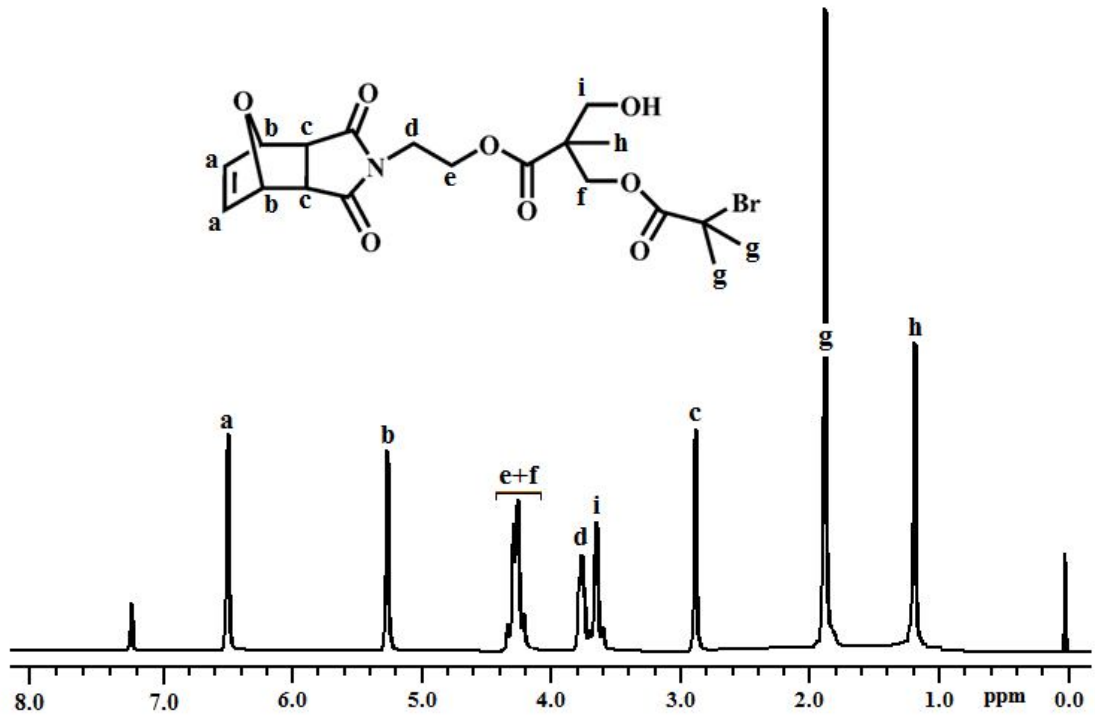

Figure 4.36: ^{1}H NMR spectrum of 2-(2-bromo-2-methyl-propionyloxymethyl)-3-hydroxy-2-methyl propionic acid 4-(2-ethyl)-10-oxa-4-azatricyclo [5.2.1.$0^{2,6}$]dec-8-ene-3,5-dione ester (**16**) in $CDCl_3$.

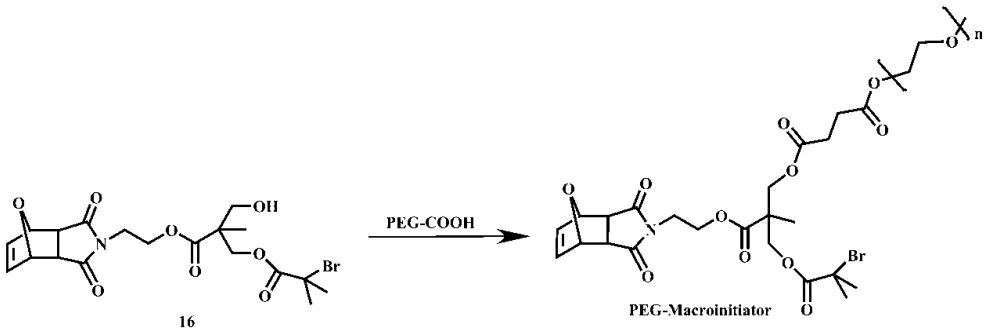

(4.26)

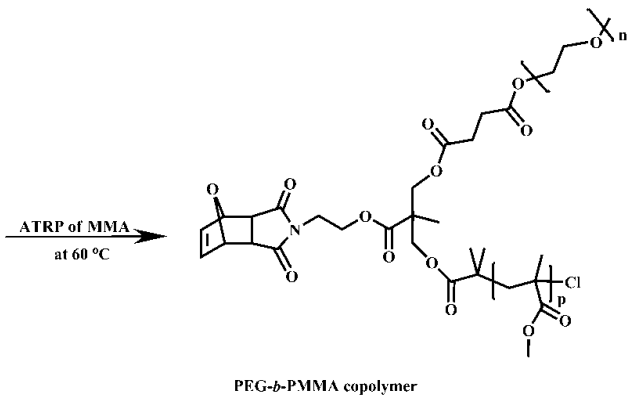

(4.27)

PEG-macroinitiator was obtained from a reaction of PEG-COOH ($M_{n,NMR}$ = 2150) with **16** using DMAP/DCC catalyst system in CH_2Cl_2 at room temperature (reaction 4.26). The raw product was precipitated in cold diethyl ether and further purified after two times dissolution-precipitation cycle.

^{1}H NMR spectrum of PEG-macroinitiator clearly displays a characteristic signal of PEG repeating unit together with those of both furan protected maleimide and bromide, thus strongly confirming the target structure was obtained (Figure 4.37). DP_n of PEG-macroinitiator was calculated to be 48 from NMR by comparing integration areas of signal at 6.5 ppm (C*H*=C*H*) to at 3.63 ppm (CH_2CH_2O of PEG). Thus, NMR number-average molecular weight ($M_{n,NMR}$) is determined to be 48 X 44 + molecular weight (MW) of **14** ≈ 2590. Moreover, theoretical molecular weight ($M_{n,theo}$) of PEG-macroinitiator was estimated by using the formula $M_{n,theo}$ = $M_{n,NMR}$ of PEG-COOH + MW of **14** = 2150 + 474 ≈ 2620.

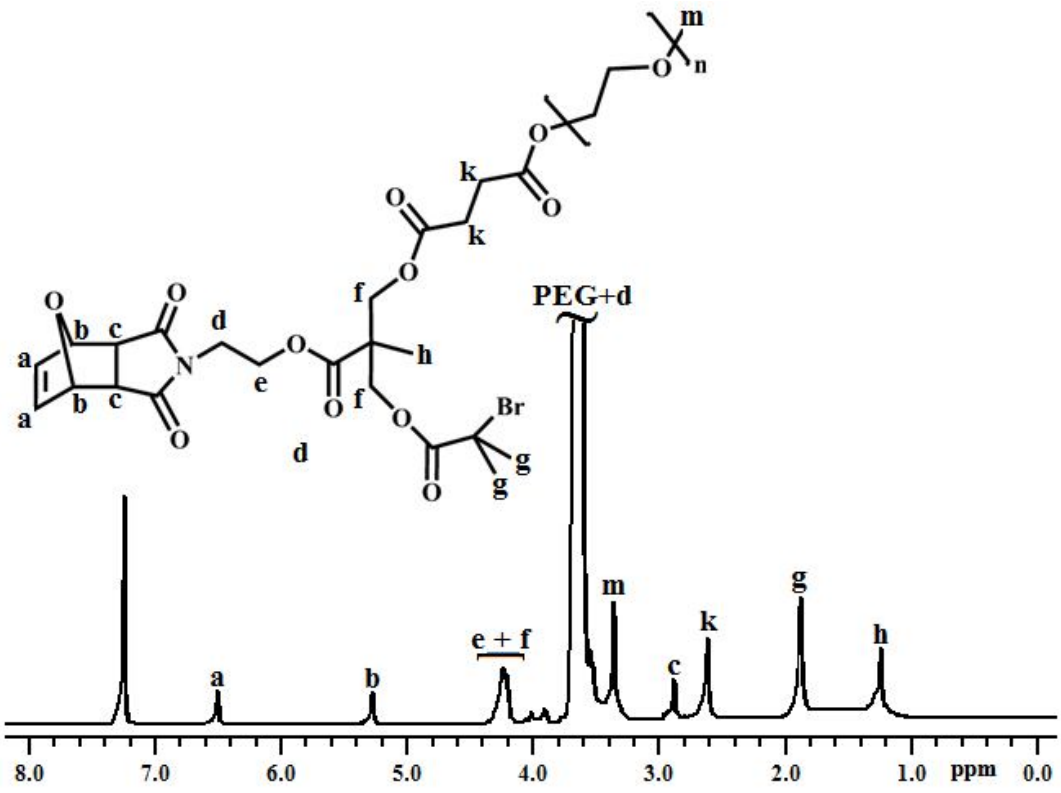

Figure 4.37: ^{1}H NMR spectrum of PEG-MI macroinitiator in $CDCl_3$.

Next, PEG-*b*-PMMA copolymer with furan-protected maleimide (PEG-*b*-PMMA-MI) was obtained by ATRP of MMA using PEG-macroinitiator and CuCl/PMDETA in toluene at 50 ^{o}C for 1.5 h (reaction 4.27). $M_{n,theo}$ of PEG-PMMA-MI was

calculated using the formula: $M_{n,theo}$ = ($[M]_0/[I]_0$) X conv. % X MW of MMA + $M_{n,NMR}$ of PEG-macroinitiator = 200 X 0.20 X 100 + 2590 = 6600. $M_{n,GPC}$ = 9900 and M_w/M_n = 1.1 (polydispersity index) values were determined from GPC calibrated with PS standards in THF. Figure 4.38 depicts the ^{1}H NMR spectrum of PEG-PMMA-MI showing resonances at 3.62 ppm and 3.58 ppm corresponding to CH_2CH_2O of PEG and OCH_3 of PMMA. Moreover, the characteristic protons of the adduct were also detected at 6.5 ppm (bridge vinyl protons), 5.24 ppm (bridge-head protons) and 295 ppm (bridge protons) respectively. $M_{n,NMR}$ = 55 (DP_n of PMMA) X 100 + 2590 ($M_{n,NMR}$ of PEG-macroinitiator) = 8100, which was measured using an integrated ratio of peaks appeared at 3.62 and 3.58 ppm corresponding to CH_2CH_2O of PEG and OCH_3 of PMMA, respectively, assuming the DP_n of PEG to be 48, fairly agreed with $M_{n,NMR}$ (Table 4.4).

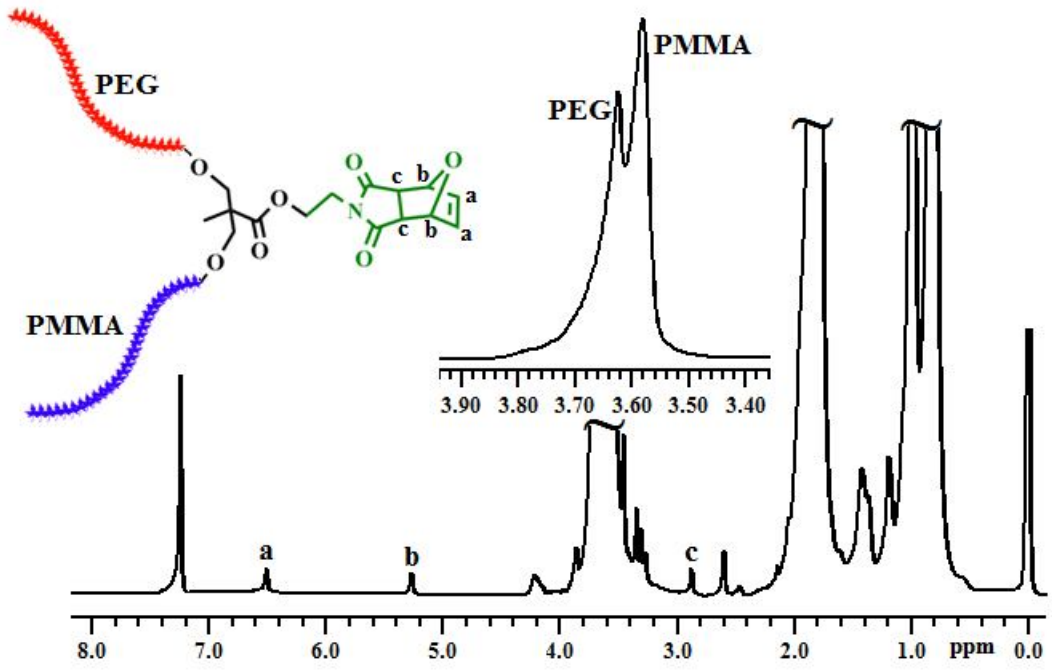

Figure 4.38: ^{1}H NMR spectrum of PEG-*b*-PMMA in $CDCl_3$.

Figure 4.39 shows GPC traces of PEG-MI and PEG-*b*-PMMA-MI. The monomodal GPC trace was observed for PEG-PMMA-MI polymer with a clear shift with respect to the PEG precursor.

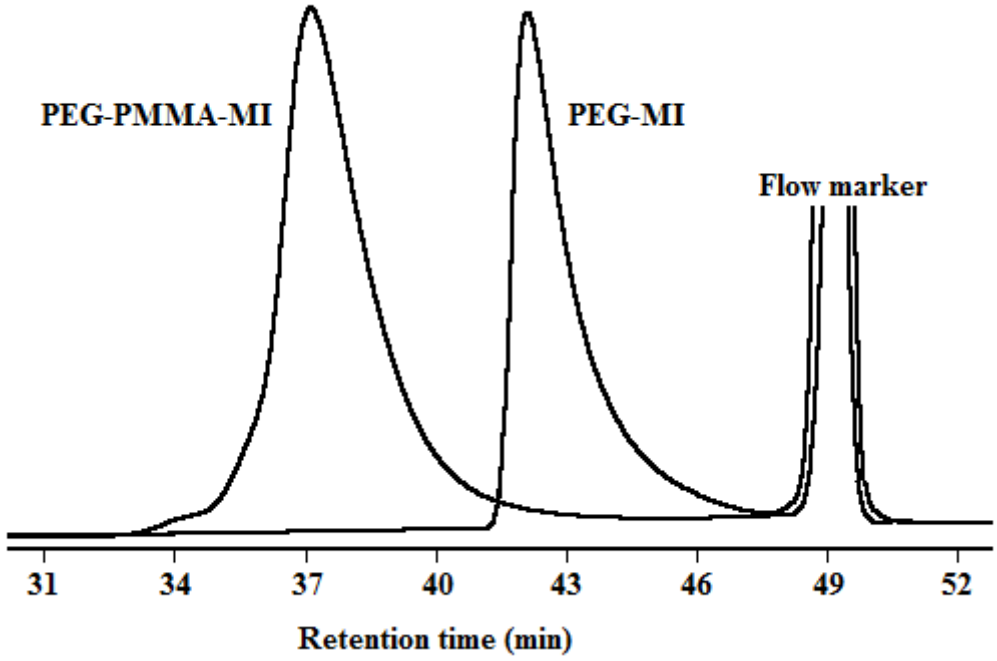

Figure 4.39: GPC traces of PEG-MI and PEG-*b*-PMMA-MI.

Figure 2.14: The conditions and results of side and main chain precursors and target H-shaped quintopolymer.

Entry	Polymer	Initiator	Time (h)	Conversion (%)	$M_{n,GPC}$ (g/mol)	M_w/M_n	$M_{n,theo}$ (g/mol)	$M_{n,NMR}$ (g/mol)
Side chain	PEG-*b*-PMMA-MI[a]	PEG-macroinitiator ($M_{n,NMR}$= 2590)	1.5	20	9860[f]	1.10[f]	6590	8090
Side chain	PCL-macroinitiator[b]	**17**	2	53	4260[h]	1.03[f]	6500	5000
Side chain	PCL-*b*-PS-alkyne[c]	PCL-macroinitiator	15	33	18600[f]	1.26[f]	11900	12840
Main chain	Anth-P*t*BA-Br (Anth-P*t*BA-N_3)[d]	**18**	2	11	5000[f]	1.10[f]	4600	8700
H-shaped quintopolymer	(PEG)(PMMA)-P*t*BA-(PCL)(PS)[e]	-	48	Yield (86 %)	39400[g]	1.26[g]	29600	33500

[a] $[M]_0$:$[I]_0$: $[PMDETA]_0$:$[CuCl]_0$ = 200:1:1:1; MMA/toluene = 1/1 (v/v) at 50 °C.
[b] $[M]_0$:$[I]_0$: $[Sn(Oct)_2]_0$ = 2000:20:1 at 110 °C.
[c] $[M]_0$:$[I]_0$ =200 in bulk at 125 °C.
[d] $[M]_0$:$[I]_0$: $[PMDETA]_0$:$[CuBr]_0$ = 300:1:1:1; *t*BA/ethylene carbonate = 1/10 (wt/wt) at 80 °C, and NaN_3 in DMF at RT.
[e] [MI]/[Alkyne]/[Anth-N_3]= 1.2/1/1.2; CuBr/PMDETA in DMF at 120 °C for 48 h.
[f] Determined from RI detection GPC using linear PS standards in THF at 30 °C.
[g] Obtained from Viscotek three-detection GPC (TD-GPC) using d*n*/d*c* = 0.101 mL/g in THF at 35 °C.
[h] M_{nPCL}= 0.259 x $M_{nGPC}^{1.073}$

4.3.2 Preparation of PCL-*b*-PS copolymer side arm

The synthesis of alkyne and hydroxyl functionalized initiator (**17**) for the preparation of other side arm was realized between **5** and 4-pentynoic acid in the presence of DCC/DMAP in CH_2Cl_2 (reaction 4.28).

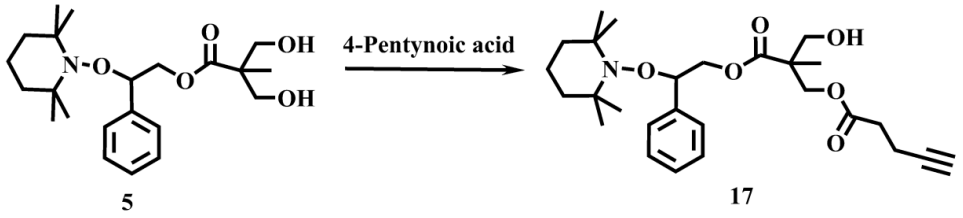

(4.28)

^{1}H NMR spectrum of **17** clearly shows a characteristic signal of methylene protons (d) adjacent to ester group at 4.7 and methine proton of alkyne (*H*C≡CCH$_2$) at 1.9 ppm. O*H* protons at 2.8-2.4 ppm completely shifted to 2.36 ppm indicating monofunctional hydroxyl group. Additionally, a new signal for methylene protons (f) adjacent to ester appeared at 4.0-4.2 ppm. Integrated values of related signals proved that esterification reaction was carried out successfully (Figure 4.40).

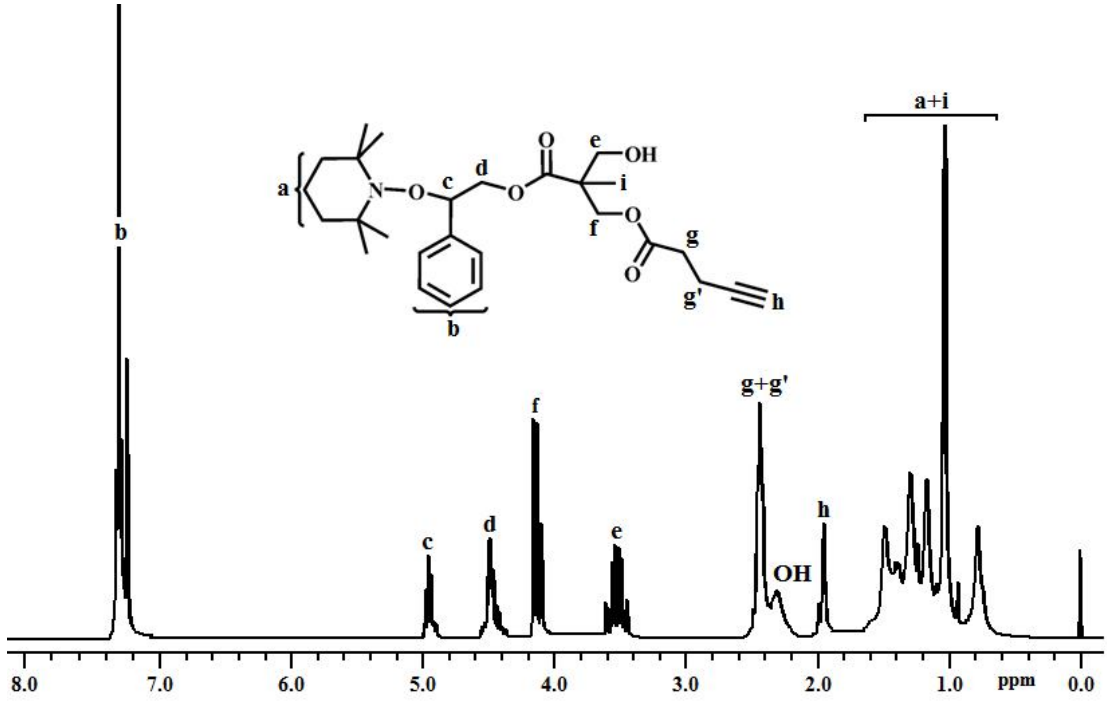

Figure 4.40: ^{1}H NMR spectrum of 2-(hydroxymethyl)-2-methyl-3-oxo-3-(2-phenyl-2-(2,2,6,6-tetramethylpiperidin -1-yloxy)ethoxy)propyl pent-4-ynoate (17) in $CDCl_3$.

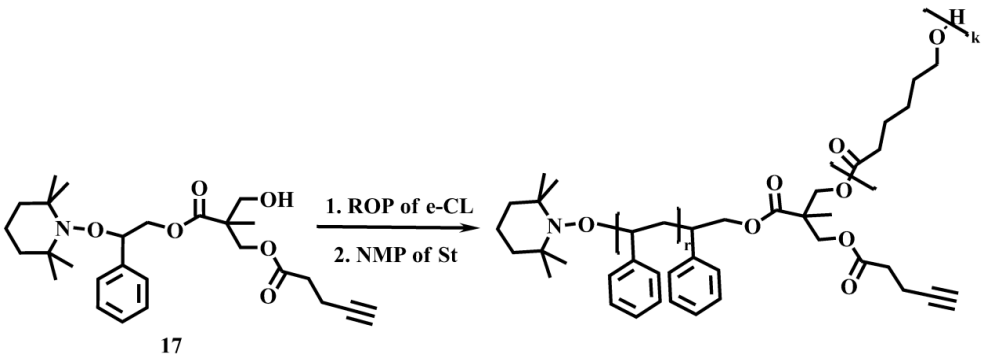

(4.29)

First, using **17** as an initiator in the ROP of ε-CL in the presence of $Sn(Oct)_2$ at 110 ^oC for 2h afforded the synthesis of PCL-macroinitiator with terminal alkyne moiety (reaction 4.29).

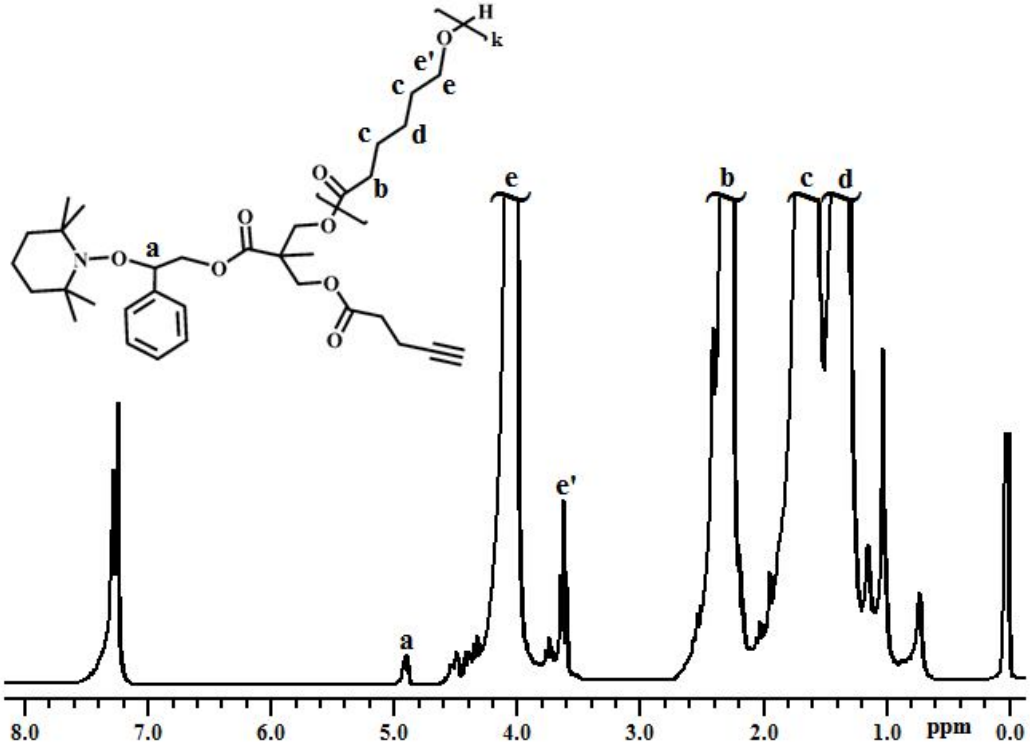

Figure 4.41: ^1H NMR spectrum of PCL macroinitiator in $CDCl_3$.

$M_{n,GPC}$ value based on PS standards was simply converted to $M_{n,PCL}$ = 0.259 X $M_{n,GPC}^{1.073}$ = 8500 [315]. However, a small shoulder was detected in the high molecular weight region of chromatogram that belongs to PCL (Figure 4.42). This was attributed to inadequate kinetic control and occurrence of side reactions, particularly polyester transesterifications during ROP process [316].

From the ^{1}H NMR spectrum (Figure 4.41), it was observed that signals at 4.9, 4.04 and 3.65 corresponding to methine proton adjacent to aromatic group, CH_2OC=O of PCL and CH_2OH end-group of PCL ($M_{n,NMR}$ = 5000 and DP_n = 40).

Next, PCL-macroinitiator was employed in NMP of St in bulk at 125 ^{o}C for 15h in order to obtain PCL-*b*-PS with alkyne at its center (reaction 4.29). $M_{n,theo}$ of the block copolymer sample is determined using a following equation, $M_{n,theo}$=($[M]_0/[I]_0$) X conv. % X MW of St + $M_{n,NMR}$ of PCL-macroinitiator = 200 X 0.33 X 104.1 + 5000 ≈ 11900 g/mol. $M_{n,GPC}$ (18600 g/mol) and poldispersity index (1.26) (Table 4.4) are determined from a monomodal GPC trace in THF using PS standards as calibrant (Figure 4.42).

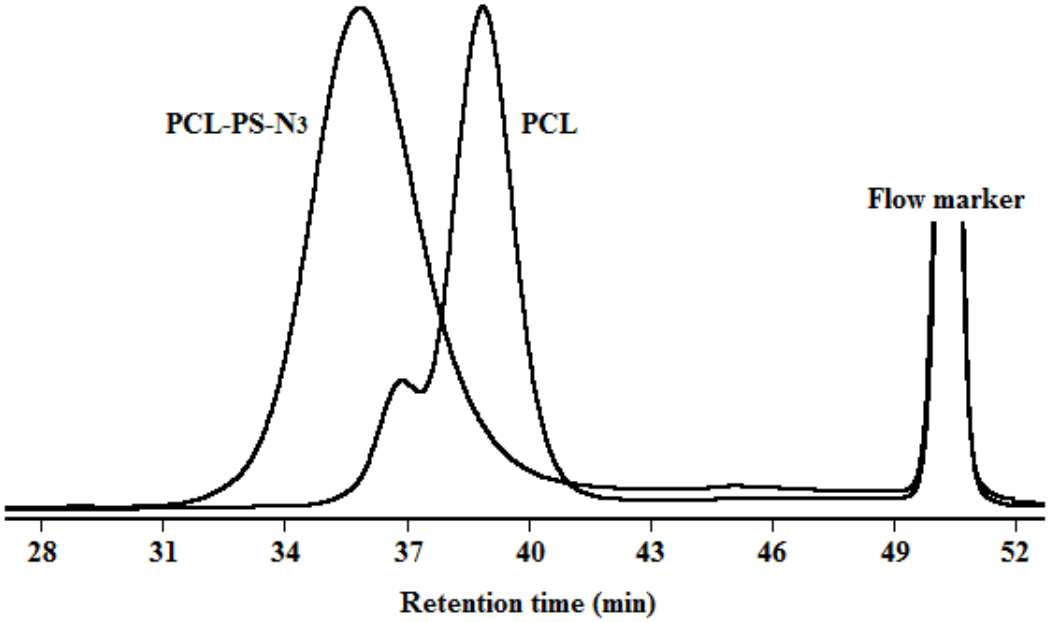

Figure 4.42: GPC traces of PCL-Macroinitiator and PCL-*b*-PS copolymer.

The ^{1}H NMR spectrum of PS-*b*-PCL copolymer shows the presence of both blocks and a comparison of integrated values of aromatic protons of PS with CH_2OC=O of PCL gave a DP_n = 75 of PS block, assuming the DP_n of PCL = 40 (Figure 4.43). Therefore, $M_{n,NMR}$ of PS-*b*-PCL copolymer was calculated to be 12800 g/mol using a formula: $M_{n,NMR}$= 75 (DP_n of PS) X 104 + 5000 ($M_{n,NMR}$ of PCL) and agreed quite well with $M_{n,theo}$ (Table 4.4).

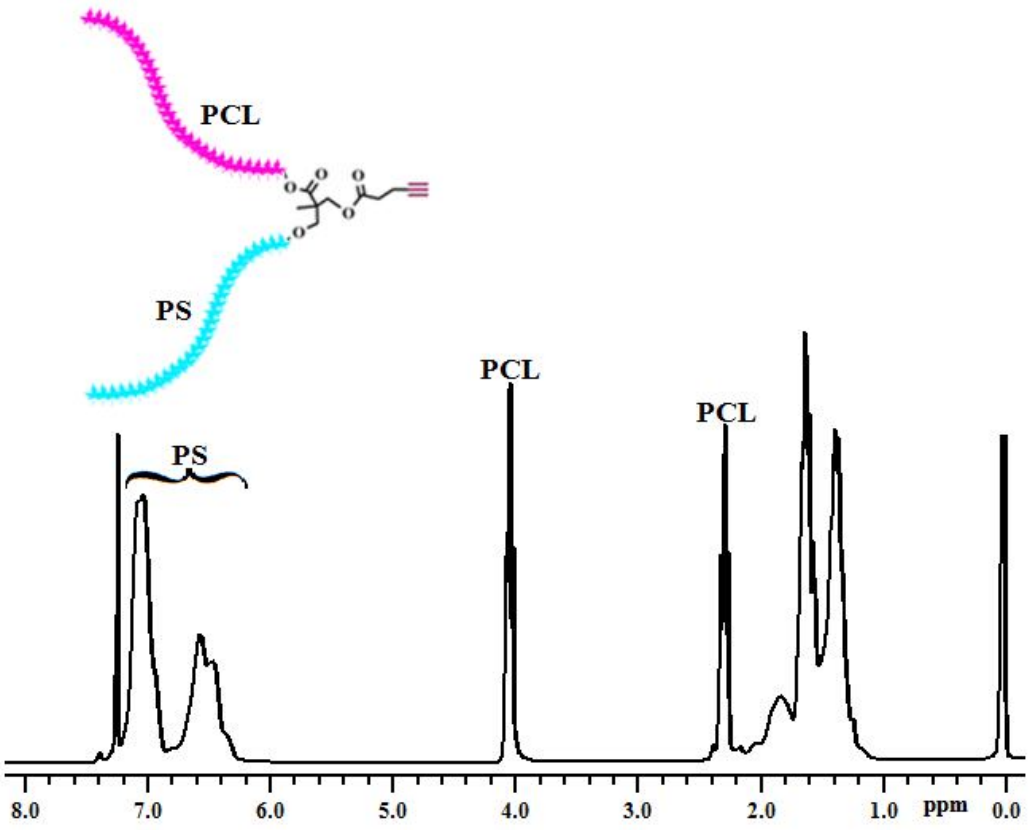

Figure 4.43: ^{1}H NMR spectrum of PCL-*b*-PS copolymer in $CDCl_3$.

4.3.3 Preparation of P*t*BA with α-anthracene-ω-azide (Anth-P*t*BA-N_3) main chain

9-Anthyrylmethyl 2-bromo-2-methyl propanoate (**18)** (reaction 4.5), was synthesized by a similar way as described previously (reaction 4.30).

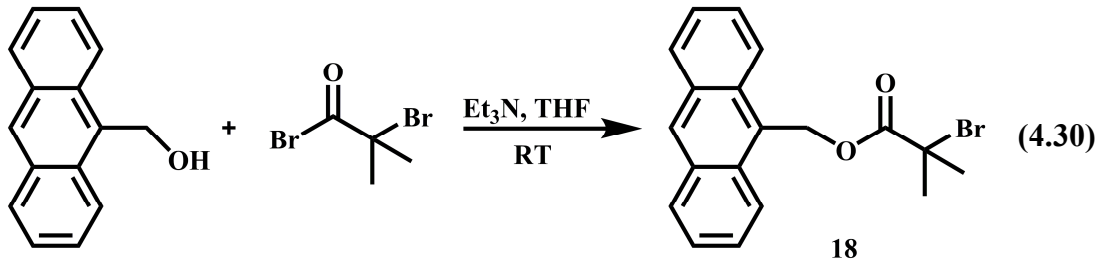

(4.30)

From ^{1}H NMR spectrum along with anthracene protons between 8.51 and 7.45 ppm, methylene protons adjacent to the anthracene and methyl protons next to Br were detected at 6.21 ppm and 1.86 ppm, respectively (Figure 4.44). These results confirmed that **18** was successfully prepared.

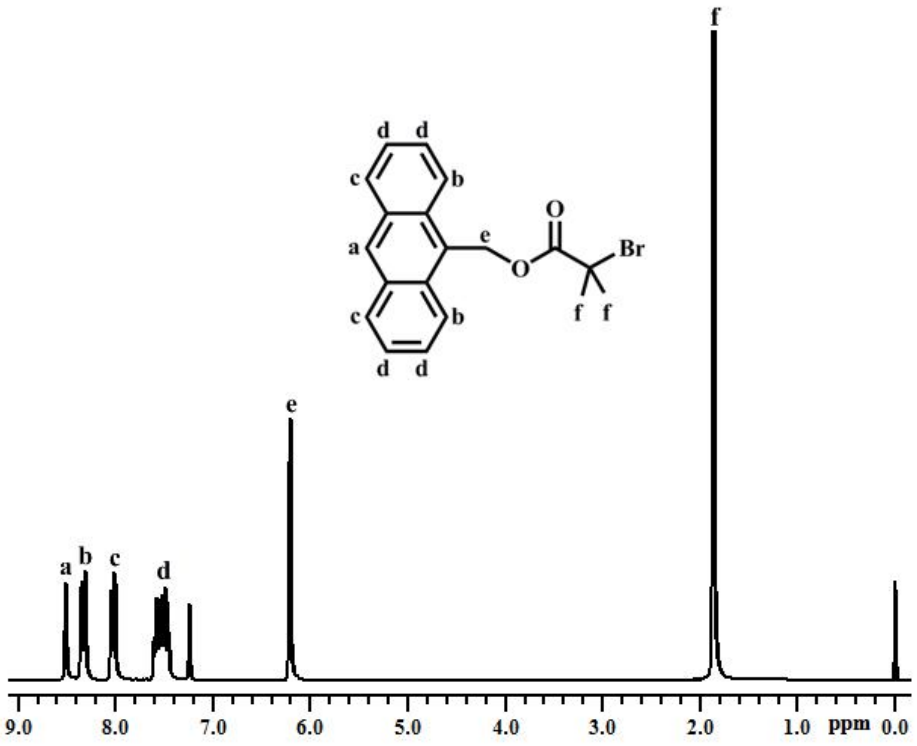

Figure 4.44: ^{1}H NMR spectrum of 9-anthyrylmethyl 2-bromo-2-methyl propanoate in $CDCl_3$.

As a last step, P*t*BA with α-anthracene-ω-bromide was obtained by ATRP of *t*BA using **18** as an initiator and CuBr/PMDETA as catalyst in ethylene carbonate at 80 ^{o}C for 2h (reaction 4.31).

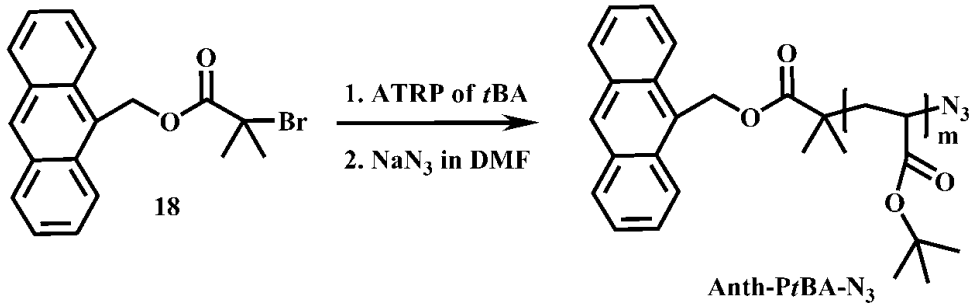

(4.31)

$M_{n,NMR}$ was determined by comparing integration areas of resonance signal of C*H* repeating unit of P*t*BA at 2.2 to that of CH_2 linked to anthracene unit at 6.1 ppm ($M_{n,NMR}$ = 65 (DP_n of *t*BA) X 128.17 + 358 (MW of **18**) = 8700) (Table 4.4). $M_{n,theo}$ of Anth-P*t*BA-N_3 was calculated using the formula: $M_{n,theo} = ([M]_0/[I]_0)$ X conv. % X MW of *t*BA + MW of **18** = 300 X 0.11 X 128.17 + 358 = 4600. It was clearly observed that $M_{n,NMR}$ deviated from $M_{n,theo}$ due to low *t*BA conversion (11 %) in ATRP (Table 4.4). The subsequent nucleophilic substitution bromide terminated

P*t*BA with NaN_3 in DMF at room temperature gave Ant-P*t*BA-N_3 (reaction 4.31). After azidation, from ^{1}H NMR spectrum, it was clearly evidenced that terminal C*H*Br proton signal at 4.1 disappeared and a new signal for C*H*N_3 at 3.7-3.6 ppm emerged (Figure 4.45). Moreover, the presence of azide end-groups of Anth-P*t*BA-N_3 was also confirmed by observing the azide stretching band at 2109 cm^{-1} using FTIR. It should be noted that azidation reaction did not resulted in a change in both $M_{n,NMR}$ and $M_{n,GPC}$ of P*t*BA.

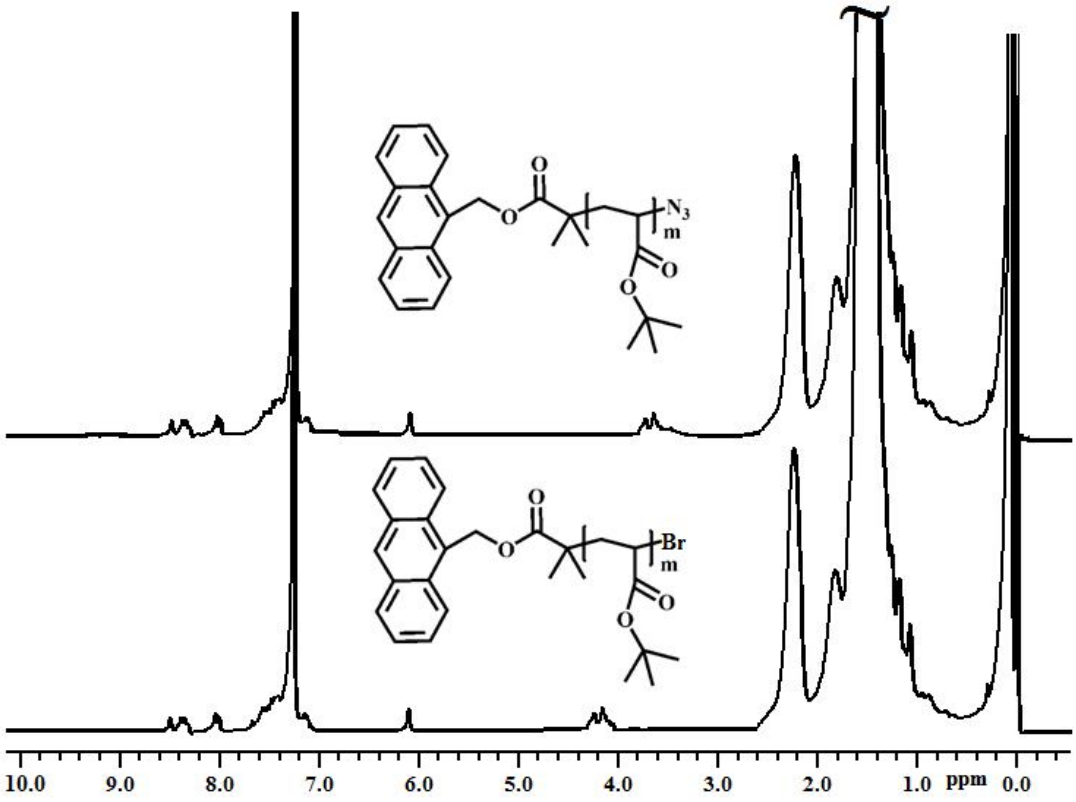

Figure 4.45: ^{1}H NMR spectra of Ant-P*t*BA-Br and Ant-P*t*BA-N_3 polymers in $CDCl_3$.

4.3.4 One-pot double click reactions for the preparation of H-shaped (PEG)(PMMA)-P*t*BA-(PCL)(PS) quintopolymer

As depicted in reaction 4.32, PEG-*b*-PMMA-MI and PCL-*b*-PS-alkyne, as side chains and Anth-P*t*BA-N_3 as a main chain were simply reacted in one-pot manner via simultaneously conducting double click reactions, CuAAC and Diels-Alder reactions, in order to obtain target (PEG)(PMMA)-P*t*BA-(PCL)(PS) H-shaped quintopolymer in the presence of CuBr/PMDETA as catalyst in DMF at 120 ^oC for

48 h. It is interesting to note that it is provided imbalances in the stoichiometric ratio of the reactants: i.e./ [MI]/[Alkyne]/[Anth-N_3]= 1.2/ 1/1.2, taking an advantage of the solubility of PEG-*b*-PMMA-MI and Anth-PtBA-N_3 precursors in precipitation solvent methanol under studied molecular weight region.

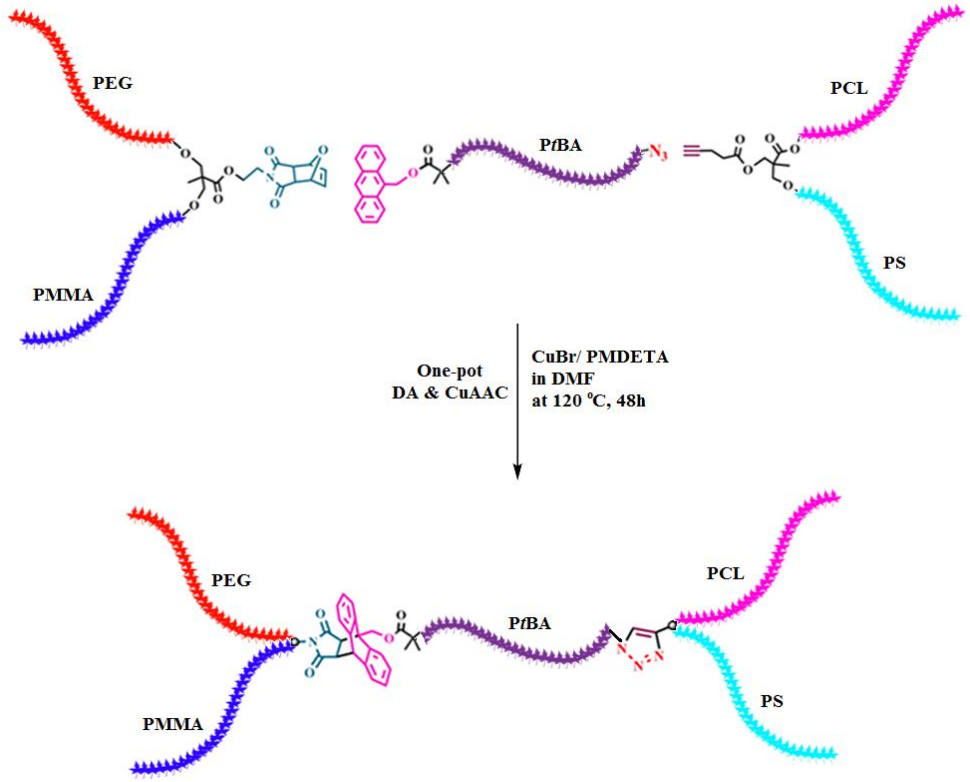

(4.32)

^{1}H NMR spectrum displays clearly characteristic signals of PEG, PMMA, P*t*BA, PCL and PS segments (Figure 4.46). $M_{n,NMR}$ of (PEG)(PMMA)-P*t*BA-(PCL)(PS) H-shaped quintopolymer was calculated to be 33500 g/mol using the integration areas of signals at 6.6 (*ortho*-position Ar*H* of PS), 4.02 (CH_2OC=O of PCL), 3.6 (OCH_3 of PMMA + CH_2CH_2O of PEG) and 1.43 ppm (C(CH_3)$_3$ of P*t*BA, based on the DP_n of PCL and PEG segments to be 40 and 48, respectively, while adding the MW of initiators ($M_{n,NMR}$ = 123 (DP_n of PS) X 104 + 36 (DP_n of PMMA) X 100 + 74 (DP_n of P*t*BA) X 128.1 + 40 (DP_n of PCL) X 114.1 + 48 (DP_n of PEG) X 44 + 1306 (MW of initiators) =33500 g/mol (Table 4.4). Meanwhile, $M_{n,theo}$ was considered to be 29600 as a sum of $M_{n,NMR}$ of individual segments and is fairly in agreement with $M_{n,NMR}$ (Table 4.4).

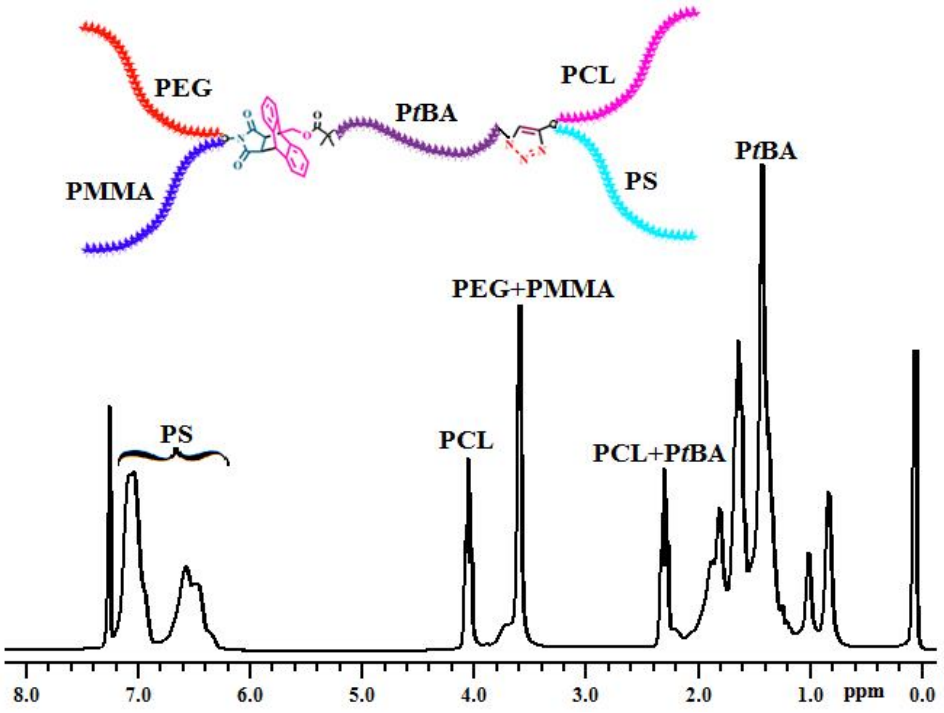

Figure 4.46: ^{1}H NMR spectrum of H-shaped quintopolymer (PEG)(PMMA)-P*t*BA-(PCL)(PS) in $CDCl_3$.

The evolution of TD-GPC traces of H-shaped quintopolymer and its precursors display in Figure 4.47.

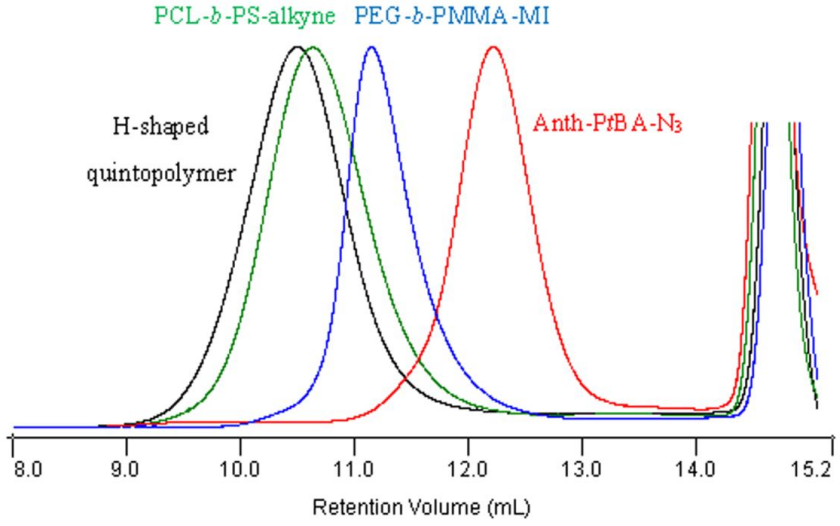

Figure 4.47: The evolution of GPC traces of the side chain precursors: PEG-*b*-PMMA-MI and PCL-*b*-PS-alkyne; main chain precursor Anth-P*t*BA-N_3 and target H-shaped quintopolymer (PEG)(PMMA)-P*t*BA-(PCL)(PS) determined by TD-GPC in THF using RI detector at 35 ^{o}C.

Compared to its precursors, the target H-shaped quintopolymer displayed a clear shift to lower elution volumes. Remarkably, a symmetric and monomodal shape of the trace suggested a successful formation of the target H-shaped quintopolymer.

An absolute molecular weight of the target (PEG)(PMMA)-P*t*BA-(PCL)(PS) H-shaped quintopolymer was obtained from Viscotek three-detection GPC (TD-GPC). The d*n*/d*c* value of the H-shaped quintopolymer was found to be 0.101 mL/g by introducing three different polymer concentration values to the GPC instrument using graphical calculation method (RI area-concentration). Next, an introducing the calculated d*n*/d*c* value to OmniSec software (Viscotek), M_n and polydispersity index for H-shaped quintopolymer were found to be 39400 and 1.26, respectively (Figure 4.47). It should be noted that M_n obtained from TD-GPC is reasonably in agreement with $M_{n,NMR}$.

Moreover, Diels-Alder click reaction progress was monitored by UV spectroscopy following decrease in the characteristic absorbance of anthracene chromophore at 368 nm by sampling at time interval. After 48 h, although a nonstoichiometric amount of Anth-P*t*BA-N_3 was available in the reaction medium, Diels-Alder click reaction efficiency was calculated to be 91 % (Figure 4.48).

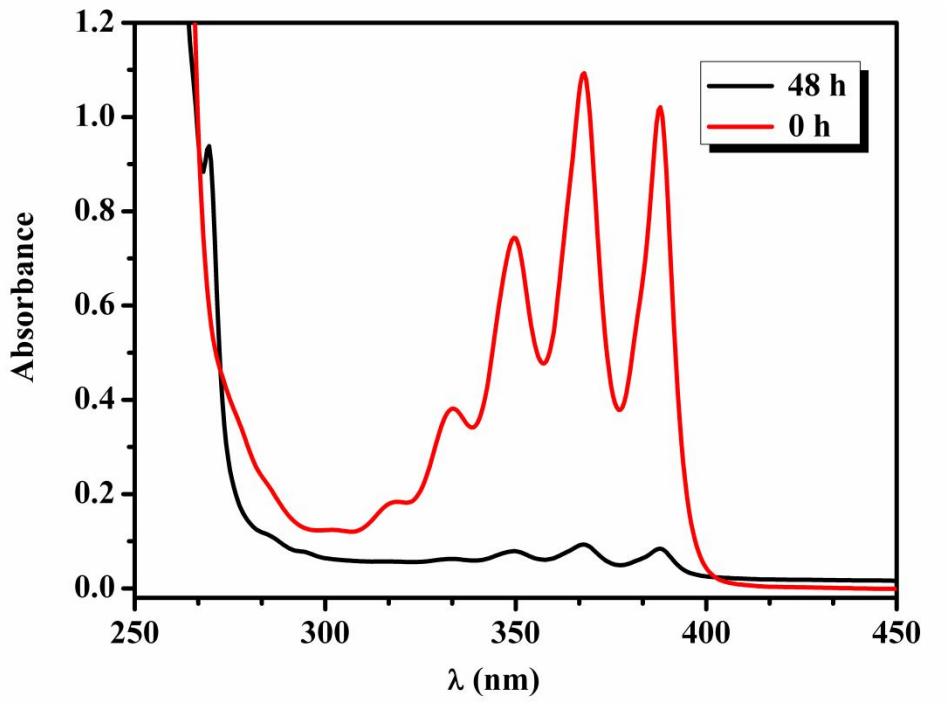

Figure 4.48: UV spectra of H-shaped quintopolymer (C_0= 1.5 X 10^{-6} mol/L in CH_2Cl_2).

Further evidence for H-shaped quintopolymer formation was obtained by FT-IR spectroscopy. The weak strechings due to azide and alkyne at 2094 and 3300 cm^{-1} disappeared after azide-alkne click reaction (Figure 4.49).

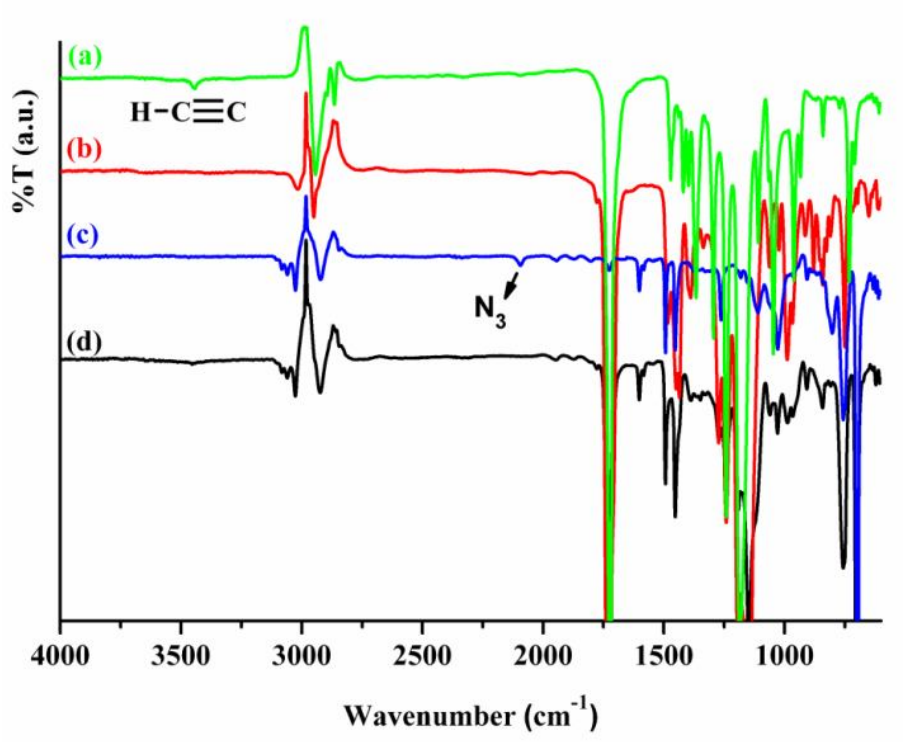

Figure 4.49: FT-IR spectra of Alkyne-PCL-*b*-PS (green) (**a**), MI-PEG-*b*-PMMA (red) (**b**), Anth-P*t*BA-N_3 (blue) (**c**) and H-shaped ABCDE quintopolymer (black) (**d**).

4.3.5 Thermal properties of H-shaped ABCDE quintopolymer

Thermal analysis of H-shaped quintopolymer was performed by using DSC under nitrogen at a heating rate of 10 ^{o}C/min. Three thermal transitions for H-shaped quintopolymer (PEG)(PMMA)-PtBA-(PCL)(PS) were detected as a sharp T_m = 58 ^{o}C of PCL, and a weak T_g = 23 ^{o}C of PtBA and T_g = 86 ^{o}C of both PMMA and PS blocks. A transition for PEG block could not be determined, although in the literature it is found that homo PEG (M_n = 2000) gave a T_m = 52 ^{o}C. Therefore, the T_m of PEG ($M_{n,NMR}$ = 2590) migth be overlapped by the Tm of PCL block.

5. CONCLUSION

In this PhD thesis, novel miktofuntional initiators having proper functionalities for controlled polymerization processes such as ATRP, NMP or ROP and click reactions such as CuAAC and Diels-Alder were used for the preparation of H-shaped polymers. As a result, well-controlled H-shaped polymers with controlled molecular weights and rather narrow molecular weight distributions were achieved.

In the first study, using click chemistry strategy, two types of H-shaped polymers containing PEG or P*t*BA as a main chain and PS-*b*-PMMA as side chains were successfully prepared. It should be noted that $M_{n,NMR}$ of H-shaped polymers were very close to those of $M_{n,theo}$ because of the efficient click reaction. CuAAC click reaction used for the preparation of heteroarm H-shaped polymer displayed following advantages compared to Diels-Alder reaction click reaction can be conducted at room temperature.

The synthesis of H-shaped quintopolymers were first time synthesized by a combination of controlled/living polymerizations and CuAAC click reaction has proven to be reasonably successful. Polymeric blocks except commercial PEG prepared by various controlled polymerization routes were used to form H-shaped quintopolymer after a click reaction. CuAAC click reaaction was realized between well-defined PEG-PMMA-Alkyne copolymer and PCL-PS-P*t*BA-N_3 miktoarm star polymer to prepare H-shaped quintopolymer. Both GPC and ^{1}H NMR analysis confirmed a successful H-shaped polymer formation. The click efficiency for H-shaped quintopolymer formation was in close agreement with those obtained for nonlinear polymers.

In addition, we have demonstrated the effective use of double click reactions involving the copper catalyzed azide-alkyne and Diels–Alder cycloaddition reactions for the preparation of H-shaped polymer possessing pentablocks with different chemical nature (H-shaped quintopolymer) using one-pot technique. H-shaped quintopolymer contains well-defined PEG-PMMA and PCL-PS side chains and a P*t*BA main chain. The first time using double click reactions in a one-pot manner

enabled us to provide an alternative and a simple way for the preparation of well-defined H-shaped quintopolymer.

As a conclusion, it is obvious that controlled/living radical polymerization techniques with CuAAC and Diels-Alder click reactions are versatile and efficient synthetic methodologies described here have emerged as a robust alternative in order to obtain well-defined macromolecular architectures over traditional methods.

REFERENCE

[1] **Davis, K. A.; Matyjaszewski, K.**, 2002. Statistical, gradient, block, and graft copolymers by controlled/living radical polymerizations. In *Statistical, gradient, block and graft copolymers by controlled/living radical polymerizations*, Vol. 159, pp 1-169.

[2] **Kamigaito, M.; Ando, T.; Sawamoto, M.**, 2001. Metal-catalyzed living radical polymerization. *Chemical Reviews* 101, (12), 3689-3746.

[3] **Yagci, Y.; Atilla Tasdelen, M.**, 2006. Mechanistic transformations involving living and controlled/living polymerization methods. *Progress in Polymer Science* 31, (12), 1133-1170.

[4] **Chiefari, J.; Chong, Y. K.; Ercole, F.; Krstina, J.; Jeffery, J.; Le, T. P. T.; Mayadunne, R. T. A.; Meijs, G. F.; Moad, C. L.; Moad, G.; Rizzardo, E.; Thang, S. H.**, 1998. Living free-radical polymerization by reversible addition-fragmentation chain transfer: The raft process. *Macromolecules* 31, (16), 5559-5562.

[5] **Georges, M. K.; Veregin, R. P. N.; Kazmaier, P. M.; Hamer, G. K.**, 1993. Narrow molecular weight resins by a free-radical polymerization process. *Macromolecules* 26, (11), 2987-2988.

[6] **Kato, M.; Kamigaito, M.; Sawamoto, M.; Higashimura, T.**, 1995. Polymerization of methyl methacrylate with the carbon tetrachloride dichlorotris (triphenylphosphine) ruthenium(II) methylaluminum bis(2,6-di-tert-butylphenoxide) initiating system possibility of living radical polymerization. *Macromolecules* 28, (5), 1721-1723.

[7] **Wang, J. S.; Matyjaszewski, K.**, 1995. Living controlled radical polymerization transition metal catalyzed atom transfer radical polymerization in the presence of a conventional radical initiator. *Macromolecules* 28, (22), 7572-7573.

[8] **Percec, V.; Barboiu, B.**, 1995. Living radical polymerization of styrene initiated by arenesulfonyl chlorides and Cu-I(bpy)(n)cl *Macromolecules* 28, (23), 7970-7972.

[9] **Kolb, H. C.; Finn, M. G.; Sharpless, K. B.**, 2001. Click chemistry: Diverse chemical function from a few good reactions. *Angewandte Chemie International Edition* 40, (11), 2004-2021.

[10] **Mishra, M. K.; Kobayashi, S.**, 1999. *Star and hyperbranched polymers*. Marcel Dekker.

[11] **Roovers, J.; Toporowski, P. M.**, 1981. Preparation and characterization of h-shaped polystyrene. *Macromolecules* 14, (5), 1174-1178.

[12] **Iatrou, H.; Avgeropoulos, A.; Hadjichristidis, N.**, 1994. Synthesis of model super H-shaped block copolymers. *Macromolecules* 27, (21), 6232-6233.

[13] **Hakiki, A.; Young, R. N.; McLeish, T. C. B.**, 1996. Synthesis and characterization of H-shaped polyisoprene. *Macromolecules* 29, (10), 3639-3641.

[14] **Gido, S. P.; Lee, C.; Pochan, D. J.; Pispas, S.; Mays, J. W.; Hadjichristidis, N.**, 1996. Synthesis, characterization, and morphology of model graft copolymers with trifunctional branch points. *Macromolecules* 29, (22), 7022-7028.

[15] **Perny, S. b.; Allgaier, J. r.; Cho, D.; Lee, W.; Chang, T.**, 2001. Synthesis and structural analysis of an H-shaped polybutadiene. *Macromolecules* 34, (16), 5408-5415.

[16] **Ball, R. C.; McLeish, T. C. B.**, 1989. Dynamic dilution and the viscosity of star-polymer melts. *Macromolecules* 22, (4), 1911-1913.

[17] **McLeish, T. C. B.; Allgaier, J.; Bick, D. K.; Bishko, G.; Biswas, P.; Blackwell, R.; Blottiere, B.; Clarke, N.; Gibbs, B.; Groves, D. J.; Hakiki, A.; Heenan, R. K.; Johnson, J. M.; Kant, R.; Read, D. J.; Young, R. N.**, 1999. Dynamics of entangled H-polymers: Theory, rheology, and neutron scattering. *Macromolecules* 32, (20), 6734-6758.

[18] **Utracki, L. A.**, 1985. On the methods of measurement of the flow properties of polyethylenes and their blends. *Advances in Polymer Technology* 5, (1), 41-53.

[19] **Iatrou, H.; Willner, L.; Hadjichristidis, N.; Halperin, A.; Richter, D.**, 1996. Aggregation phenomena of model ps/pi super-H-shaped block copolymers. Influence of the architecture. *Macromolecules* 29, (2), 581-591.

[20] **Pispas, S.; Hadjichristidis, N.; Mays, J. W.**, 1996. Micellization of model graft copolymers of the H and π type in dilute solution. *Macromolecules* 29, (23), 7378-7385.

[21] **Cong, Y.; Li, B.; Han, Y.; Li, Y.; Pan, C.**, 2005. Self-assembly of H-shaped block copolymers. *Macromolecules* 38, (23), 9836-9846.

[22] **Hedrick, J. L.; Magbitang, T.; Connor, E. F.; Glauser, T.; Volksen, W.; Hawker, C. J.; Lee, V. Y.; Miller, R. D.**, 2002. Application of complex macromolecular architectures for advanced microelectronic materials. *Chemistry-a European Journal* 8, (15), 3308-3319.

[23] **Webster, O. W.**, 1991. Living polymerization methods. *Science* 251, (4996), 887-893.

[24] **Puskas, J. E.; Antony, P.; Kwon, Y.; Paulo, C.; Kovar, M.; Norton, P. R.; Kaszas, G.; Altstadt, V.**, 2001. Macromolecular engineering via carbocationic polymerization: Branched structures, block copolymers and nanostructures. *Macromolecular Materials and Engineering* 286, (10), 565-582.

[25] **Hedrick, J. L.; Miller, R. D.; Hawker, C. J.; Carter, K. R.; Volksen, W.; Yoon, D. Y.; Trollsas, M.**, 1998. Templating nanoporosity in thin-film dielectric insulators. *Advanced Materials* 10, (13), 1049-+.

[26] **Quirk, R. P.; Lee, Y.; Kim, J.**, 2001. Synthesis of branched polymers: An introduction (reprinted from star hyperbranched polymers, pg 1-25, 1999). *Journal of Macromolecular Science-Polymer Reviews* C41, (4), 369-390.

[27] **Grayson, S. M.; Frechet, J. M. J.**, 2001. Convergent dendrons and dendrimers: From synthesis to applications. *Chemical Reviews* 101, (12), 3819-3867.

[28] **Matyjaszewski, K.**, 2001. Macromolecular engineering by controlled/living ionic and radical polymerizations. *Macromolecular Symposia* 174, 51-67.

[29] **Matyjaszewski, K.; Gaynor, S. G.**, 2000. *In applied polymer science, . Pergamon Press: Oxford*, p 929.

[30] **Carothers, W. H.**, 1929. Studies on polymerization and ring formation. I. An introduction to the general theory of condensation polymers. *Journal of the American Chemical Society* 51, (8), 2548-2559.

[31] **Odian, G. G.**, 2004. *Principles of polymerization*. Wiley-Interscience.

[32] **Szwarc, M.**, 1956. Living polymers. *Nature* 178, 1168-1169.

[33] **Szwarc, M.; Levy, M.; Milkovich, R.**, 1956. Polymerization initiated by electron transfer to monomer. A new method of formation of block polymers1. *Journal of the American Chemical Society* 78, (11), 2656-2657.

[34] **Matyjaszewski, K.**, Controlled/living radical polymerization: State of the art in 2002. In *Advances in controlled/living radical polymerization*, Matyjaszewski, K., Ed. 2003; Vol. 854, pp 2-9.

[35] **Braunecker, W. A.; Matyjaszewski, K.**, 2007. Controlled/living radical polymerization: Features, developments, and perspectives. *Progress in Polymer Science* 32, (1), 93-146.

[36] **Matyjaszewski, K.; Davis, T. P.**, In *Handbook of radical polymerization*, John Wiley & Sons, Inc: New York 895.

[37] **Matyjaszewski, K.**, 2002.Controlled/living radical polymerization: State of the art in 2005. In *Controlled/living radical polymerization*, American Chemical Society: 2006; Vol. 944, pp 2-12.

[38] **Litvinenko, G.; Muller, A. H. E.**, 1997. General kinetic analysis and comparison of molecular weight distributions for various mechanisms of activity exchange in living polymerizations. *Macromolecules* 30, (5), 1253-1266.

[39] **Brus, L. E.**, 1992. Structure and electronic states of quantum semiconductor crystallites. *Nanostructured Materials* 1, (71), 71-75.

[40] **Hawker, C. J.; Bosman, A. W.; Harth, E.**, 2001. New polymer synthesis by nitroxide mediated living radical polymerizations. *Chemical Reviews* 101, (12), 3661-3688.

[41] **Weller, H.**, 1993. Colloidal semiconductor q-particles - chemistry in the transition region between solid-state and molecules. *Angewandte Chemie-International Edition in English* 32, (1), 41-53.

[42] **Krauss, T. D.**, 2007. Laser technology - less excitement for more gain. *Nature* 447, (7143), 385-386.

[43] **Thayer, A. M.**, 1992. Catalyst suppliers face changing industry. *Chemical & Engineering News* 70, (10), 27-&.

[44] **Haruta, M.**, 2005. Catalysis - gold rush. *Nature* 437, (7062), 1098-1099.

[45] **Hughes, M. D.; Xu, Y. J.; Jenkins, P.; McMorn, P.; Landon, P.; Enache, D. I.; Carley, A. F.; Attard, G. A.; Hutchings, G. J.; King, F.; Stitt, E. H.; Johnston, P.; Griffin, K.; Kiely, C. J.**, 2005. Tunable gold catalysts for selective hydrocarbon oxidation under mild conditions. *Nature* 437, (7062), 1132-1135.

[46] **Chiefari, J.; Chong, Y. K.; Ercole, F.; Krstina, J.; Jeffery, J.; Le, T. P. T.; Mayadunne, R. T. A.; Meijs, G. F.; Moad, C. L.; Moad, G.; Rizzardo, E.; Thang, S. H.**, 1998. Living free-radical polymerization by reversible addition-fragmentation chain transfer: The raft process. *Macromolecules* 31, (16), 5559-5562.

[47] **Otsu, T.; Yoshida, M.**, 1982. Role of initiator-transfer agent-terminator (iniferter) in radical polymerizations polymer design by organic disulfides as iniferters. *Makromolekulare Chemie-Rapid Communications* 3, (2), 127-132.

[48] **Ajayaghosh, A.; Francis, R.**, 1999, A xanthate-derived photoinitiator that recognizes and controls the free radical polymerization pathways of methyl methacrylate and styrene. *Journal of the American Chemical Society* 121, (28), 6599-6606.

[49] **Angot, S.; Taton, D.; Gnanou, Y.**, 2000. Amphiphilic stars and dendrimer-like architectures based on poly(ethylene oxide) and polystyrene. *Macromolecules* 33, (15), 5418-5426.

[50] **Devonport, W.; Michalak, L.; Malmstrom, E.; Mate, M.; Kurdi, B.; Hawker, C. J.; Barclay, G. G.; Sinta, R.**, 1997. "living" free-radical polymerizations in the absence of initiators: Controlled autopolymerization. *Macromolecules* 30, (7), 1929-1934.

[51] **Benoit, D.; Grimaldi, S.; Robin, S.; Finet, J. P.; Tordo, P.; Gnanou, Y.**, 2000. Kinetics and mechanism of controlled free-radical polymerization of styrene and n-butyl acrylate in the presence of an acyclic beta-phosphonylated nitroxide. *Journal of the American Chemical Society* 122, (25), 5929-5939.

[52] **Chong, Y. K.; Ercole, F.; Moad, G.; Rizzardo, E.; Thang, S. H.; Anderson, A. G.**, 1999. Imidazolidinone nitroxide-mediated polymerization. *Macromolecules* 32, (21), 6895-6903.

[53] **Wang, J. S.; Matyjaszewski, K.**, 1995. Controlled living radical polymerization halogen atom-transfer radical polymerization promoted by a Cu(I)-Cu(II) redox process. *Macromolecules* 28, (23), 7901-7910.

[54] **Kato, M.; Kamigaito, M.; Sawamoto, M.; Higashimura, T.**, 1995. Polymerization of methyl-methacrylate with the carbon-tetrachloride dichlorotris(triphenylphosphine)ruthenium(II) methylaluminum bis(2,6-di-tert-butylphenoxide) initiating system - possibility of living radical polymerization. *Macromolecules* 28, (5), 1721-1723.

[55] **Qiu, J.; Matyjaszewski, K.**, 1997. Metal complexes in controlled radical polymerization. *Acta Polymerica* 48, (5-6), 169-180.

[56] **Patten, T. E.; Matyjaszewski, K.**, 1998. Atom transfer radical polymerization and the synthesis of polymeric materials. *Advanced Materials* 10, (12), 901-930.

[57] **Patten, T. E.; Matyjaszewski, K.**, 1999. Copper(I)-catalyzed atom transfer radical polymerization. *Accounts of Chemical Research* 32, (10), 895-903.

[58] **Matyjaszewski, K.**, 1999. Transition metal catalysis in controlled radical polymerization: Atom transfer radical polymerization. *Chemistry-a European Journal* 5, (11), 3095-3102.

[59] **Patten, T. E.; Xia, J. H.; Abernathy, T.; Matyjaszewski, K.**, 1996. Polymers with very low polydispersities from atom transfer radical polymerization. *Science* 272, (5263), 866-868.

[60] **Matyjaszewski, K.; Coca, S.; Gaynor, S. G.; Wei, M.; Woodworth, B. E.**, 1998. Controlled radical polymerization in the presence of oxygen. *Macromolecules* 31, (17), 5967-5969.

[61] **Beers, K. L.; Matyjaszewski, K.; Woodworth, B.**, 2001. Controlled/living radical polymerization in the undergraduate laboratories. 1. Using atrp to prepare block and statistical copolymers of n-butyl acrylate and styrene. *Journal of Chemical Education* 78, (4), 544-null.

[62] **Matyjaszewski, K.; Beers, K. L.; Metzner, Z.; Woodworth, B.**, 2001. Controlled/living radical polymerization in the undergraduate laboratories. 2. Using atrp in limited amounts of air to prepare block and statistical copolymers of n-butyl acrylate and styrene. *Journal of Chemical Education* 78, (4), 547-null.

[63] **Kickelbick, G.; Paik, H. J..; Matyjaszewski, K.**, 1999. Immobilization of the copper catalyst in atom transfer radical polymerization. *Macromolecules* 32, (9), 2941-2947.

[64] **Haddleton, D. M.; Duncalf, D. J.; Kukulj, D.; Radigue, A. P.**, 1999. 3-aminopropyl silica supported living radical polymerization of methyl methacrylate: Dichlorotris(triphenylphosphine)ruthenium(II) mediated atom transfer polymerization. *Macromolecules* 32, (15), 4769-4775.

[65] **Haddleton, D. M.; Kukulj, D.; Radigue, A. P.**, 1999. Atom transfer polymerisation of methyl methacrylate mediated by solid supported copper catalysts. *Chemical Communications*, (1), 99-100.

[66] **Zhang, X.; Xia, J.; Matyjaszewski, K.**, 1998. Controlled/"living" radical polymerization of 2-(dimethylamino)ethyl methacrylate. *Macromolecules* 31, (15), 5167-5169.

[67] **Matyjaszewski, K.; Xia, J. H.**, 2001. Atom transfer radical polymerization. *Chemical Reviews* 101, (9), 2921-2990.

[68] **Haddleton, D. M.; Jasieczek, C. B.; Hannon, M. J.; Shooter, A. J.**, 1997. Atom transfer radical polymerization of methyl methacrylate initiated by alkyl bromide and 2-pyridinecarbaldehyde imine copper(I) complexes. *Macromolecules* 30, (7), 2190-2193.

[69] **Matyjaszewski, K.; Shipp, D. A.; Qiu, J.; Gaynor, S. G.**, 2000. Water-borne block and statistical copolymers synthesized using atom transfer radical polymerization. *Macromolecules* 33, (7), 2296-2298.

[70] **Granel, C.; Dubois, P.; Jerome, R.; Teyssie, P.**, 1996. Controlled radical polymerization of methacrylic monomers in the presence of a bis(ortho-chelated) arylnickel(II) complex and different activated alkyl halides. *Macromolecules* 29, (27), 8576-8582.

[71] **Uegaki, H.; Kotani, Y.; Kamigaito, M.; Sawamoto, M.**, 1998. Nibr2(pn-bu3)2-mediated living radical polymerization of methacrylates and acrylates and their block or random copolymerizations1. *Macromolecules* 31, (20), 6756-6761.

[72] **Moineau, C.; Minet, M.; Teyssie, P.; Jerome, R.**, 1999. Synthesis and characterization of poly(methyl methacrylate)-block-poly(n-butyl acrylate)-block-poly(methyl methacrylate) copolymers by two-step controlled radical polymerization (atrp) catalyzed by nibr2(pph3)(2), -1. *Macromolecules* 32, 8277-8282.

[73] **Ando, T.; Kamigaito, M.; Sawamoto, M.**, 1997. Iron(II) chloride complex for living radical polymerization of methyl methacrylate. *Macromolecules* 30, (16), 4507-4510.

[74] **Louie, J.; Grubbs, R. H.**, 2000. Highly active iron imidazolylidene catalysts for atom transfer radical polymerization. *Chemical Communications*, (16), 1479-1480.

[75] **Lecomte, P.; Drapier, I.; Dubois, P.; Teyssie, P.; Jerome, R.**, 1997. Controlled radical polymerization of methyl methacrylate in the presence of palladium acetate, triphenylphosphine, and carbon tetrachloride. *Macromolecules* 30, (24), 7631-7633.

[76] **Moineau, G.; Granel, C.; Dubois, P.; Jerome, R.; Teyssie, P.**, 1998. Controlled radical polymerization of methyl methacrylate initiated by an alkyl halide in the presence of the wilkinson catalyst. *Macromolecules* 31, (2), 542-544.

[77] **Destarac, M.; Matyjaszewski, K.; Boutevin, B.**, 2000. Polychloroalkane initiators in copper-catalyzed atom transfer radical polymerization of (meth)acrylates. *Macromolecular Chemistry and Physics* 201, (2), 265-272.

[78] **Destarac, M.; Boutevin, B.; Matyjaszewski, K.**, 2000. Polychloroalkanes as atrp initiators: Fundamentals and application to the synthesis of block copolymers from the combination of conventional radical polymerization and atrp. In *Controlled/living radical polymerization*, American Chemical Society: Vol. 768, pp 234-247.

[79] **Kotani, Y.; Kato, M.; Kamigaito, M.; Sawamoto, M.**, 1996. Living radical polymerization of alkyl methacrylates with ruthenium complex and synthesis of their block copolymers1. *Macromolecules* 29, (22), 6979-6982.

[80] **Zhang, X.; Xia, J. H.; Matyjaszewski, K.**, 1998. Controlled/"Living" Radical polymerization of 2-(dimethylamino)ethyl methacrylate. *Macromolecules* 31, (15), 5167-5169.

[81] **Beers, K. L.; Boo, S.; Gaynor, S. G.; Matyjaszewski, K.**, 1999. Atom transfer radical polymerization of 2-hydroxyethyl methacrylate. *Macromolecules* 32, (18), 5772-5776.

[82] **Beers, K. L.; Gaynor, S. G.; Matyjaszewski, K.; Sheiko, S. S.; Moller, M.**, 1998, The synthesis of densely grafted copolymers by atom transfer radical polymerization. *Macromolecules* 31, (26), 9413-9415.

[83] **Xia, J. H.; Zhang, X.; Matyjaszewski, K.**, 2000. In *Transition metal catalysis in macromolecular design;*, L. S. Boffa, B. N., M.,, Ed. ACS Symposium Series 760; American Chemical Society:: Washington, DC, Vol. 13.

[84] **Zhang, X.; Matyjaszewski, K.**, 1999. Synthesis of functional polystyrenes by atom transfer radical polymerization using protected and unprotected carboxylic acid initiators. *Macromolecules* 32, (22), 7349-7353.

[85] **Ashford, E. J.; Naldi, V.; O'Dell, R.; Billingham, N. C.; Armes, S. P.**, 1999. First example of the atom transfer radical polymerisation of an acidic monomer: Direct synthesis of methacrylic acid copolymers in aqueous media. *Chemical Communications*, (14), 1285-1286.

[86] **Matyjaszewski, K.; Mu Jo, S.; Paik, H. J.; Gaynor, S. G.**, 1997. Synthesis of well-defined polyacrylonitrile by atom transfer radical polymerization. *Macromolecules* 30, (20), 6398-6400.

[87] **Matyjaszewski, K.; Gaynor Scott, G.; Qiu, J.; Beers, K.; Coca, S.; Davis, K.; Muhlebach, A.; Xia, J.; Zhang, X.**, 2000. The preparation of well-defined water soluble-swellable (co)polymers by atom transfer radical polymerization. In *Associative polymers in aqueous media*, American Chemical Society: Vol. 765, pp 52-71.

[88] **Matyjaszewski, K.; Ziegler, M. J.; Arehart, S. V.; Greszta, D.; Pakula, T.**, 2000. Gradient copolymers by atom transfer radical copolymerization. *Journal of Physical Organic Chemistry* 13, (12), 775-786.

[89] **Millard, P. E.; Barner, L.; Stenzel, M. H.; Davis, T. P.; Barner-Kowollik, C.; Muller, A. H. E.**, 2006. Raft polymerization of n-isopropylacrylamide and acrylic acid under gamma-irradiation in aqueous media. *Macromolecular Rapid Communications* 27, (11), 821-828.

[90] **Convertine, A. J.; Lokitz, B. S.; Vasileva, Y.; Myrick, L. J.; Scales, C. W.; Lowe, A. B.; McCormick, C. L.**, 2006. Direct synthesis of thermally responsive dma/nipam diblock and dma/nipam/dma triblock copolymers via aqueous, room temperature raft polymerizationâ€ *Macromolecules* 39, (5), 1724-1730.

[91] **Moad, G.; Rizzardo, E.; Thang, S. H.**, 2009. Living radical polymerization by the raft process - a second update. *Australian Journal of Chemistry* 62, (11), 1402-1472.

[92] **McCormick, C. L.; Lowe, A. B.**, 2004. Aqueous raft polymerization: recent developments in synthesis of functional water-soluble (co)polymers with controlled structures. *Accounts of Chemical Research* 37, (5), 312-325.

[93] **Boyer, C.; Bulmus, V.; Priyanto, P.; Teoh, W. Y.; Amal, R.; Davis, T. P.**, 2009. The stabilization and bio-functionalization of iron oxide nanoparticles using heterotelechelic polymers. *Journal of Materials Chemistry* 19, (1), 111-123.

[94] **Boyer, C.; Liu, J.; Bulmus, V.; Davis, T. P.; Barner-Kowollik, C.; Stenzel, M. H.**, 2008. Direct synthesis of well-defined heterotelechelic polymers for bioconjugations. *Macromolecules* 41, (15), 5641-5650.

[95] **Liu, J.; Bulmus, V.; Barner-Kowollik, C.; Stenzel, M. H.; Davis, T. P.**, 2007. Direct synthesis of pyridyl disulfide-terminated polymers by raft polymerization. *Macromolecular Rapid Communications* 28, (3), 305-314.

[96] **Postma, A.; Davis, T. P.; Evans, R. A.; Li, G.; Moad, G.; O'Shea, M. S.**, 2006. Synthesis of well-defined polystyrene with primary amine end groups through the use of phthalimido-functional raft agents. *Macromolecules* 39, (16), 5293-5306.

[97] **Scales, C. W.; Convertine, A. J.; McCormick, C. L.**, 2006. Fluorescent labeling of raft-generated poly(n-isopropylacrylamide) via a facile maleimide-thiol coupling reaction. *Biomacromolecules* 7, (5), 1389-1392.

[98] **Wong, L.; Boyer, C.; Jia, Z.; Zareie, H. M.; Davis, T. P.; Bulmus, V.**, 2008. Synthesis of versatile thiol-reactive polymer scaffolds via raft polymerization. *Biomacromolecules* 9, (7), 1934-1944.

[99] **York, A. W.; Scales, C. W.; Huang, F. Q.; McCormick, C. L.**, 2007. Facile synthetic procedure for omega, primary amine functionalization directly in water for subsequent fluorescent labeling and potential bioconjugation of raft-synthesized (co)polymers. *Biomacromolecules* 8, (8), 2337-2341.

[100] **Perrier, S. b.; Takolpuckdee, P.; Westwood, J.; Lewis, D. M.**, 2004. Versatile chain transfer agents for reversible addition fragmentation chain transfer (raft) polymerization to synthesize functional polymeric architectures. *Macromolecules* 37, (8), 2709-2717.

[101] **Gemici, H.; Legge, T. M.; Whittaker, M.; Monteiro, M. J.; Perrier, S.**, 2007. Original approach to multiblock copolymers via reversible addition–fragmentation chain transfer polymerization. *Journal of Polymer Science Part A: Polymer Chemistry* 45, (11), 2334-2340.

[102] **Stenzel, M. H.; Davis, T. P.**, 2002. Star polymer synthesis using trithiocarbonate functional β-cyclodextrin cores (reversible addition–fragmentation chain-transfer polymerization). *Journal of Polymer Science Part A: Polymer Chemistry* 40, (24), 4498-4512.

[103] **Quinn, J. F.; Chaplin, R. P.; Davis, T. P.**, 2002. Facile synthesis of comb, star, and graft polymers via reversible addition–fragmentation chain transfer (raft) polymerization. *Journal of Polymer Science Part A: Polymer Chemistry* 40, (17), 2956-2966.

[104] **Liu, J. Q.; Liu, H. Y.; Jia, Z. F.; Bulmus, V.; Davis, T. P.**, 2008. An approach to biodegradable star polymeric architectures using disulfide coupling. *Chemical Communications*, (48), 6582-6584.

[105] **Setijadi, E.; Tao, L.; Liu, J. Q.; Jia, Z. F.; Boyer, C.; Davis, T. P.**, 2009. Biodegradable star polymers functionalized with beta-cyclodextrin inclusion complexes. *Biomacromolecules* 10, (9), 2699-2707.

[106] **Xu, J. T.; Tao, L.; Liu, J. Q.; Bulmus, V.; Davis, T. P.**, 2009. Synthesis of functionalized and biodegradable hyperbranched polymers from novel ab(2) macromonomers prepared by raft polymerization. *Macromolecules* 42, (18), 6893-6901.

[107] **Tao, L.; Liu, J.; Tan, B. H.; Davis, T. P.**, 2009. Raft synthesis and DNA binding of biodegradable, hyperbranched poly(2-(dimethylamino)ethyl methacrylate. *Macromolecules* 42, (14), 4960-4962.

[108] **Dong, Z.-m.; Liu, X.-h.; Tang, X.-l.; Li, Y.-s.**, 2009. Synthesis of hyperbranched polymers with pendent norbornene functionalities via raft polymerization of a novel asymmetrical divinyl monomer. *Macromolecules* 42, (13), 4596-4603.

[109] **Rosselgong, J.; Armes, S. P.; Barton, W.; Price, D.**, 2009. Synthesis of highly branched methacrylic copolymers: Observation of near-ideal behavior using raft polymerization. *Macromolecules* 42, (16), 5919-5924.

[110] **Biasutti, J. D.; Davis, T. P.; Lucien, F. P.; Heuts, J. P. A.**, 2005. Reversible addition–fragmentation chain transfer polymerization of methyl methacrylate in suspension. *Journal of Polymer Science Part A: Polymer Chemistry* 43, (10), 2001-2012.

[111] **Moad, G.; Chiefari, J.; Chong, Y. K.; Krstina, J.; Mayadunne, R. T. A.; Postma, A.; Rizzardo, E.; Thang, S. H.**, 2000. Living free radical polymerization with reversible addition-fragmentation chain transfer (the life of raft). *Polymer International* 49, (9), 993-1001.

[112] **Simms, R. W.; Davis, T. P.; Cunningham, M. F.**, 2005. Xanthate-mediated living radical polymerization of vinyl acetate in miniemulsion. *Macromolecular Rapid Communications* 26, (8), 592-596.

[113] **Lansalot, M.; Davis, T. P.; Heuts, J. P. A.**, 2002. Raft miniemulsion polymerization: influence of the structure of the raft agent. *Macromolecules* 35, (20), 7582-7591.

[114] **Chong, Y. K.; Krstina, J.; Le, T. P. T.; Moad, G.; Postma, A.; Rizzardo, E.; Thang, S. H.**, 2003. Thiocarbonylthio compounds [sc(ph)sr] in free radical polymerization with reversible addition-fragmentation chain transfer (raft polymerization). Role of the free-radical leaving group (r). *Macromolecules* 36, (7), 2256-2272.

[115] **Odian, G.**, 1991. In *Principles of polymerization*, John Wiley & Sons: New York.

[116] **Dechy-Cabaret, O.; Martin-Vaca, B.; Bourissou, D.**, 2004. Controlled ring-opening polymerization of lactide and glycolide. *Chemical Reviews* 104, (12), 6147-6176.

[117] **Wang, C. H.; Li, H.; Zhao, X.**, 2004. Ring opening polymerization of l-lactide initiated by creatinine. *Biomaterials* 25, (27), 5797-5801.

[118] **Drumright, R. E.; Gruber, P. R.; Henton, D. E.**, 2000. Polylactic acid technology. *Advanced Materials* 12, (23), 1841-1846.

[119] **Huisgen, R.**, 1963. 1,3-dipolar cycloadditions. Past and future. *Angewandte Chemie International Edition in English* 2, (10), 565-598.

[120] **Huisgen, R.**, 1989. Kinetics and reaction-mechanisms - selected examples from the experience of 40 years. *Pure and Applied Chemistry* 61, (4), 613-628.

[121] **Tornoe, C. W.; Christensen, C.; Meldal, M.**, 2002. Peptidotriazoles on solid phase: [1,2,3]-triazoles by regiospecific copper(I)-catalyzed 1,3-dipolar cycloadditions of terminal alkynes to azides. *Journal of Organic Chemistry* 67, (9), 3057-3064.

[122] **Rostovtsev, V. V.; Green, L. G.; Fokin, V. V.; Sharpless, K. B.**, 2002. A stepwise huisgen cycloaddition process: Copper(I)-catalyzed regioselective "ligation" of azides and terminal alkynes. *Angewandte Chemie International Edition* 41, (14), 2596-2599.

[123] **Kolb, H. C.; Finn, M. G.; Sharpless, K. B.**, 2001. Click chemistry: Diverse chemical function from a few good reactions. *Angewandte Chemie-International Edition* 40, (11), 2004-2021.

[124] **Pachón, L. D.; van Maarseveen, J. H.; Rothenberg, G.**, 2005. Click chemistry: Copper clusters catalyse the cycloaddition of azides with terminal alkynes. *Advanced Synthesis & Catalysis* 347, (6), 811-815.

[125] **Himo, F.; Lovell, T.; Hilgraf, R.; Rostovtsev, V. V.; Noodleman, L.; Sharpless, K. B.; Fokin, V. V.**, 2004. Copper(I)-catalyzed synthesis of azoles. Dft study predicts unprecedented reactivity and intermediates. *Journal of the American Chemical Society* 127, (1), 210-216.

[126] **Krivopalov, V. P.; Shkurko, O. P.**, 2005. 1,2,3-triazole and its derivatives. Development of methods for the formation of the triazole ring. *Uspekhi Khimii* 74, (4), 369-410.

[127] **Rodionov, V. O.; Presolski, S. I.; DÃ-az DÃ-az, D.; Fokin, V. V.; Finn, M. G.**, 2007. Ligand-accelerated cu-catalyzed azide-alkyne cycloaddition: a mechanistic report. *Journal of the American Chemical Society* 129, (42), 12705-12712.

[128] **Diels, O.; Alder, K.**, 1928. Synthesen in der hydroaromatischen reihe. *Justus Liebigs Annalen der Chemie* 460, (1), 98-122.

[129] **Sauer, J.**, 1966. Diels-alder-reactions part i: New preparative aspects. *Angewandte Chemie International Edition in English* 5, (2), 211-230.

[130] **Sauer, J.**, 1967. Diels-alder reactions ii: The reaction mechanism. *Angewandte Chemie International Edition in English* 6, (1), 16-33.

[131] **Sauer, J.; Sustmann, R.**, 1980. Mechanistic aspects of diels-alder reactions: A critical survey. *Angewandte Chemie International Edition in English* 19, (10), 779-807.

[132] **Pindur, U.; Lutz, G.; Otto, C.**, 1993. Acceleration and selectivity enhancement of diels-alder reactions by special and catalytic methods. *Chemical Reviews* 93, (2), 741-761.

[133] **Oppolzer, W.**, 1984. Asymmetric diels-alder and ene reactions in organic-synthesis. *Angewandte Chemie-International Edition in English* 23, (11), 876-889.

[134] **Kagan, H. B.; Riant, O.**, 1992. Catalytic asymmetric diels alder reactions. *Chemical Reviews* 92, (5), 1007-1019.

[135] **Carmona, D.; Lamata, M. P.; Oro, L. A.**, 2000. Recent advances in homogeneous enantioselective diels-alder reactions catalyzed by chiral transition-metal complexes. *Coordination Chemistry Reviews* 200, 717-772.

[136] **Corey, E. J.**, 2002. Catalytic enantioselective diels-alder reactions: Methods, mechanistic fundamentals, pathways, and applications. *Angewandte Chemie-International Edition* 41, (10), 1650-1667.

[137] **Olsen, S.**, 1962. Otto Diels. *Chemische Berichte* 95, (1), V-XLVI.

[138] **Nicolaou, K. C.; Snyder, S. A.; Montagnon, T.; Vassilikogiannakis, G.**, 2002. The diels–alder reaction in total synthesis. *Angewandte Chemie International Edition* 41, (10), 1668-1698.

[139] **Sustmann, R.**, 1974. Orbital energy control of cycloaddition reactivity. *Pure and Applied Chemistry* 40, (4), 569-593.

[140] **Alder, K.; Stein, G.**, 1937. Untersuchungen über den verlauf der diensynthese. *Angewandte Chemie* 50, (28), 510-519.

[141] **Woodward, R. B.; Katz, T. J.**, 1959. The mechanism of the diels-alder reaction. *Tetrahedron* 5, (1), 70-89.

[142] **Asano, T.; Le Noble, W. J.**, 1978. Activation and reaction volumes in solution. *Chemical Reviews* 78, (4), 407-489.

[143] **Jenner, G.; Papadopoulos, M.; Rimmelin, J.**, 1983. Activation parameters and location of the transition state in the retro-diels-alder reaction of a 7-oxabicylo[2.2.1]hept-5-ene derivative. *The Journal of Organic Chemistry* 48, (5), 748-749.

[144] **Gonzalez, A.; Holt, S. L.**, 1982. Effect of microemulsions on the diels-alder reaction: Endo/exo ratios in the reaction of cyclopentadiene and methyl methacrylate. *The Journal of Organic Chemistry* 47, (16), 3186-3188.

[145] **Breslow, R.; Guo, T.**, 1988. Diels-alder reactions in nonaqueous polar solvents. Kinetic effects of chaotropic and antichaotropic agents and of .Beta.-cyclodextrin. *Journal of the American Chemical Society* 110, (17), 5613-5617.

[146] **Grieco, P. A.; Galatsis, P.; Spohn, R. F.**, 1986. Aqueous intermolecular diels-alder chemistry : Reaction of (e)-2,4-pentadienyl ammonium chloride and related ammonium salts with dienophiles in water. *Tetrahedron* 42, (11), 2847-2853.

[147] **Drewes, S. E.; Grieco, P. A.; Huffman, J. C.**, 1985. A short synthesis of dl-epi-pyroangolensolide and dl-pyroangolensolide: Confirmation of the structures of pyroangolensolide and calodendrolide. *The Journal of Organic Chemistry* 50, (8), 1309-1311.

[148] **Lindsay Smith, J. R.; Norman, R. O. C.; Stillings, M. R.**, 1978. Factors affecting the endo : Exo ratio in diels-alder reactions of cyclopentadiene. *Tetrahedron* 34, (9), 1381-1383.

[149] **Posner, T.**, 1905. Beiträge zur kenntniss der ungesättigten verbindungen. Ii. Ueber die addition von mercaptanen an ungesättigte kohlenwasserstoffe. *Berichte der deutschen chemischen Gesellschaft* 38, (1), 646-657.

[150] **Mayo, F. R.; Walling, C.**, 1940. The peroxide effect in the addition of reagents to unsaturated compounds and in rearrangement reactions. *Chemical Reviews* 27, (2), 351-412.

[151] **Griesbaum, K.**, 1970. Problems and possibilities of the free-radical addition of thiols to unsaturated compounds. *Angewandte Chemie International Edition in English* 9, (4), 273-287.

[152] **v. Braun, J.; Murjahn, R.**, 1926. Haftfestigkeit organischer reste (iv). *Berichte der deutschen chemischen Gesellschaft (A and B Series)* 59, (6), 1202-1209.

[153] **Cook, W. D.; Chen, F.; Pattison, D. W.; Hopson, P.; Beaujon, M.**, 2007. Thermal polymerization of thiol-ene network-forming systems. *Polymer International* 56, (12), 1572-1579.

[154] **Carioscia, J. A.; Stansbury, J. W.; Bowman, C. N.**, 2007. Evaluation and control of thiol-ene/thiol-epoxy hybrid networks. *Polymer* 48, (6), 1526-1532.

[155] **Dondoni, A.**, 2008. The emergence of thiol–ene coupling as a click process for materials and bioorganic chemistry. *Angewandte Chemie International Edition* 47, (47), 8995-8997.

[156] **Campos, L. M.; Killops, K. L.; Sakai, R.; Paulusse, J. M. J.; Damiron, D.; Drockenmuller, E.; Messmore, B. W.; Hawker, C. J.**, 2008. Development of thermal and photochemical strategies for thiol-ene click polymer functionalization. *Macromolecules* 41, (19), 7063-7070.

[157] **Chan, J. W.; Yu, B.; Hoyle, C. E.; Lowe, A. B.**, 2009. The nucleophilic, phosphine-catalyzed thiol-ene click reaction and convergent star synthesis with raft-prepared homopolymers. *Polymer* 50, (14), 3158-3168.

[158] **Hawker, C. J.; Wooley, K. L.**, 2005. The convergence of synthetic organic and polymer chemistries. *Science* 309, (5738), 1200-1205.

[159] **Matyjaszewski, K.**, 2005. Macromolecular engineering: From rational design through precise macromolecular synthesis and processing to targeted macroscopic material properties. *Progress in Polymer Science* 30, (8-9), 858-875.

[160] **Lutz, J. F.; Borner, H. G.**, 2008. Modern trends in polymer bioconjugates design. *Progress in Polymer Science* 33, (1), 1-39.

[161] **Fournier, D.; Hoogenboom, R.; Schubert, U. S.**, 2007. Clicking polymers: A straightforward approach to novel macromolecular architectures. *Chemical Society Reviews* 36, (8), 1369-1380.

[162] **Justynska, J.; Hordyjewicz, Z.; Schlaad, H.**, 2006. New functional diblock copolymers through radical addition of mercaptans. *Macromolecular Symposia* 240, 41-46.

[163] **Wu, P.; Feldman, A. K.; Nugent, A. K.; Hawker, C. J.; Scheel, A.; Voit, B.; Pyun, J.; Frechet, J. M. J.; Sharpless, K. B.; Fokin, V. V.**, 2004. Efficiency and fidelity in a click-chemistry route to triazole dendrimers by the copper(I)-catalyzed ligation of azides and alkynes. *Angewandte Chemie-International Edition* 43, (30), 3928-3932.

[164] **Opsteen, J. A.; van Hest, J. C. M.**, 2005. Modular synthesis of block copolymers via cycloaddition of terminal azide and alkyne functionalized polymers. *Chemical Communications*, (1), 57-59.

[165] **Opsteen, J. A.; van Hest, J. C. M.**, 2007. Modular synthesis of abc type block copolymers by "click" chemistry. *Journal of Polymer Science Part A: Polymer Chemistry* 45, (14), 2913-2924.

[166] **Vogt, A. P.; Sumerlin, B. S.**, 2008. Tuning the temperature response of branched poly(n-isopropylacrylamide) prepared by raft polymerization. *Macromolecules* 41, (20), 7368-7373.

[167] **Vogt, A. P.; Gondi, S. R.; Sumerlin, B. S.**, 2007. Hyperbranched polymers via raft copolymerization of an acryloyl trithiocarbonate. *Australian Journal of Chemistry* 60, (6), 396-399.

[168] **Ranjan, R.; Brittain, W. J.**, 2007. Combination of living radical polymerization and click chemistry for surface modification. *Macromolecules* 40, (17), 6217-6223.

[169] **Gondi, S. R.; Vogt, A. P.; Sumerlin, B. S.**, 2007. Versatile pathway to functional telechelics via raft polymerization and click chemistry. *Macromolecules* 40, (3), 474-481.

[170] **De, P.; Gondi, S. R.; Sumerlin, B. S.**, 2008. Folate-conjugated thermoresponsive block copolymers: Highly efficient conjugation and solution self-assembly. *Biomacromolecules* 9, (3), 1064-1070.

[171] **Ting, S. R. S.; Granville, A. M.; Quemener, D.; Davis, T. P.; Stenzel, M. H.; Barner-Kowollik, C.**, 2007. Raft chemistry and huisgen 1,3-dipolar cycloaddition: A route to block copolymers of vinyl acetate and 6-o-methacryloyl mannose? *Australian Journal of Chemistry* 60, (6), 405-409.

[172] **Sinnwell, S.; Inglis, A. J.; Stenzel, M. H.; Barner-Kowollik, C.**, 2008. Access to three-arm star block copolymers by a consecutive combination of the copper(I)-catalyzed azide-alkyne cycloaddition and the raft hetero diels-alder concept. *Macromolecular Rapid Communications* 29, (12-13), 1090-1096.

[173] **Quemener, D.; Davis, T. P.; Barner-Kowollik, C.; Stenzel, M. H.**, 2006. Raft and click chemistry: A versatile approach to well-defined block copolymers. *Chemical Communications*, (48), 5051-5053.

[174] **Magenau, A. J. D.; Martinez-Castro, N.; Storey, R. F.**, 2009. Site transformation of polyisobutylene chain ends into functional raft agents for block copolymer synthesis. *Macromolecules* 42, (7), 2353-2359.

[175] **Ranjan, R.; Brittain, W. J.**, 2008. Synthesis of high density polymer brushes on nanoparticles by combined raft polymerization and click chemistry. *Macromolecular Rapid Communications* 29, (12-13), 1104-1110.

[176] **Li, Y.; Yang, J.; Benicewicz, B. C.**, 2007. Well-controlled polymerization of 2-azidoethyl methacrylate at near room temperature and click functionalization. *Journal of Polymer Science Part A: Polymer Chemistry* 45, (18), 4300-4308.

[177] **Li, Y.; Benicewicz, B. C.**, 2008. Functionalization of silica nanoparticles via the combination of surface-initiated raft polymerization and click reactions. *Macromolecules* 41, (21), 7986-7992.

[178] **Briquel, R.; Mazzolini, J.; Le Bris, T.; Boyron, O.; Boisson, F.; Delolme, F.; D'Agosto, F.; Boisson, C.; Spitz, R.**, 2008. Polyethylene building blocks by catalyzed chain growth and efficient end functionalization strategies, including click chemistry. *Angewandte Chemie International Edition* 47, (48), 9311-9313.

[179] **Gungor, E.; Cote, G.; Erdogan, T.; Durmaz, H.; Demirel, A. L.; Hizal, G.; Tunca, U.**, 2007. Heteroarm H-shaped terpolymers through click reaction. *Journal of Polymer Science Part a-Polymer Chemistry* 45, (6), 1055-1065.

[180] **Gungor, E.; Durmaz, H.; Hizal, G.; Tunca, U.**, 2008. H-shaped (abcde type) quintopolymer via click reaction [3+2] strategy. *Journal of Polymer Science Part a-Polymer Chemistry* 46, (13), 4459-4468.

[181] **Gungor, E.; Hizal, G.; Tunca, U.**, 2009. One-pot double click reactions for the preparation of h-shaped abcde-type quintopolyrner. *Journal of Polymer Science Part a-Polymer Chemistry* 47, (13), 3409-3418.

[182] **Binder, W. H.; Gloger, D.; Weinstabl, H.; Allmaier, G. N.; Pittenauer, E.**, 2007. Telechelic poly(n-isopropylacrylamides) via nitroxide-mediated controlled polymerization and "click" chemistry: livingness and "grafting-from" methodology. *Macromolecules* 40, (9), 3097-3107.

[183] **Fleischmann, S.; Komber, H.; Voit, B.**, 2008. Diblock copolymers as scaffolds for efficient functionalization via click chemistry. *Macromolecules* 41, (14), 5255-5264.

[184] **Gress, A.; VÃlkel, A.; Schlaad, H.**, 2007. Thio-click modification of poly[2-(3-butenyl)-2-oxazoline]. *Macromolecules* 40, (22), 7928-7933.

[185] **Tasdelen, M. A.; Van Camp, W.; Goethals, E.; Dubois, P.; Du Prez, F.; Yagci, Y.**, 2008. Polytetrahydrofuran/clay nanocomposites by in situ polymerization and "Click" Chemistry processes. *Macromolecules* 41, (16), 6035-6040.

[186] **Luxenhofer, R.; Jordan, R.**, 2006. Click chemistry with poly(2-oxazoline)s. *Macromolecules* 39, (10), 3509-3516.

[187] **Thomsen, A. D.; Malmström, E.; Hvilsted, S.**, 2006. Novel polymers with a high carboxylic acid loading. *Journal of Polymer Science Part A: Polymer Chemistry* 44, (21), 6360-6377.

[188] **Parrish, B.; Breitenkamp, R. B.; Emrick, T.**, 2005. PEG- and peptide-grafted aliphatic polyesters by click chemistry. *Journal of the American Chemical Society* 127, (20), 7404-7410.

[189] **Li, H. Y.; Riva, R.; Jerome, R.; Lecomte, P.**, 2007. Combination of ring-opening polymerization and "Click" Chemistry for the synthesis of an amphiphilic tadpole-shaped poly(epsilon-caprolactone) grafted by peo. *Macromolecules* 40, (4), 824-831.

[190] **Hoogenboom, R.; Moore, B. C.; Schubert, U. S.**, 2006. Synthesis of star-shaped poly(epsilon-caprolactone) via 'click' chemistry and 'supramolecular click' chemistry. *Chemical Communications*, (38), 4010-4012.

[191] **Yang, S. K.; Weck, M.**, 2007. Modular covalent multifunctionalization of copolymers. *Macromolecules* 41, (2), 346-351.

[192] **Xia, Y.; Verduzco, R.; Grubbs, R. H.; Kornfield, J. A.**, 2008. Well-defined liquid crystal gels from telechelic polymers. *Journal of the American Chemical Society* 130, (5), 1735-1740.

[193] **Murphy, J. J.; Nomura, K.; Paton, R. M.**, 2006. Synthesis of isoxazolino norbornene derivatives containing sugar residues by 1,3-dipolar cycloaddition and their application to the synthesis of neoglycopolymers by living ring-opening metathesis polymerization. *Macromolecules* 39, (9), 3147-3153.

[194] **Rodionov, V. O.; Fokin, V. V.; Finn, M. G.**, 2005. Mechanism of the ligand-free cui-catalyzed azide–alkyne cycloaddition reaction. *Angewandte Chemie International Edition* 44, (15), 2210-2215.

[195] **Bock, V. D.; Hiemstra, H.; van Maarseveen, J. H.**, 2006. Cu-(I)-catalyzed alkyne-azide "Click" Cycloadditions from a mechanistic and synthetic perspective. *European Journal of Organic Chemistry*, (1), 51-68.

[196] **Nolte, C.; Mayer, P.; Straub, B.**, 2007. Isolation of a copper(I) triazolide: A “click” intermediate. *Angewandte Chemie International Edition* 46, (12), 2101-2103.

[197] **Lutz, J. F.**, 2007. 1,3-dipolar cycloadditions of azides and alkynes: A universal ligation tool in polymer and materials science. *Angewandte Chemie-International Edition* 46, (7), 1018-1025.

[198] **Binder, W. H.; Sachsenhofer, R.**, 2007. ‘Click’ chemistry in polymer and materials science. *Macromolecular Rapid Communications* 28, (1), 15-54.

[199] **Sen Gupta, S.; Raja, K. S.; Kaltgrad, E.; Strable, E.; Finn, M. G.**, 2005. Virus-glycopolymer conjugates by copper(I) catalysis of atom transfer radical polymerization and azide-alkyne cycloaddition. *Chemical Communications*, (34), 4315-4317.

[200] **Wang, Q.; Chan, T. R.; Hilgraf, R.; Fokin, V. V.; Sharpless, K. B.; Finn, M. G.**, 2003. Bioconjugation by copper(I)-catalyzed azide-alkyne [3 + 2] cycloaddition. *Journal of the American Chemical Society* 125, (11), 3192-3193.

[201] **Dirks, A. J. T.; van Berkel, S. S.; Hatzakis, N. S.; Opsteen, J. A.; van Delft, F. L.; Cornelissen, J.; Rowan, A. E.; van Hest, J. C. M.; Rutjes, F.; Nolte, R. J. M.**, 2005. Preparation of biohybrid amphiphiles via the copper catalysed huisgen [3+2] dipolar cycloaddition reaction. *Chemical Communications*, (33), 4172-4174.

[202] **Ladmiral, V.; Mantovani, G.; Clarkson, G. J.; Cauet, S.; Irwin, J. L.; Haddleton, D. M.**, 2006. Synthesis of neoglycopolymers by a combination of "click chemistry" and living radical polymerization. *Journal of the American Chemical Society* 128, (14), 4823-4830.

[203] **Lutz, J.-F. o.; BÃrner, H. G.; Weichenhan, K.**, 2006. Combining atrp and "click" chemistry: a promising platform toward functional biocompatible polymers and polymer bioconjugates. *Macromolecules* 39, (19), 6376-6383.

[204] **Devaraj, N. K.; Miller, G. P.; Ebina, W.; Kakaradov, B.; Collman, J. P.; Kool, E. T.; Chidsey, C. E. D.**, 2005. Chemoselective covalent coupling of oligonucleotide probes to self-assembled monolayers. *Journal of the American Chemical Society* 127, (24), 8600-8601.

[205] **Jang, H.; Fafarman, A.; Holub, J. M.; Kirshenbaum, K.**, 2005. Click to fit: versatile polyvalent display on a peptidomimetic scaffold. *Organic Letters* 7, (10), 1951-1954.

[206] **Sun, X.-L.; Stabler, C. L.; Cazalis, C. S.; Chaikof, E. L.**, 2005. Carbohydrate and protein immobilization onto solid surfaces by sequential diels-alder and azide-alkyne cycloadditions. *Bioconjugate Chemistry* 17, (1), 52-57.

[207] **Bodine, K. D.; Gin, D. Y.; Gin, M. S.**, 2004. Synthesis of readily modifiable cyclodextrin analogues via cyclodimerization of an alkynyl-azido trisaccharide. *Journal of the American Chemical Society* 126, (6), 1638-1639.

[208] **Bock, V. D.; Perciaccante, R.; Jansen, T. P.; Hiemstra, H.; van Maarseveen, J. H.**, 2006. Click chemistry as a route to cyclic tetrapeptide analogues: synthesis of cyclo-[pro-val-(triazole)-pro-tyr]. *Organic Letters* 8, (5), 919-922.

[209] **Punna, S.; Kuzelka, J.; Wang, Q.; Finn, M. G.**, 2005. Head-to-tail peptide cyclodimerization by copper-catalyzed azide–alkyne cycloaddition. *Angewandte Chemie International Edition* 44, (15), 2215-2220.

[210] **Sumerlin, B. S.; Tsarevsky, N. V.; Louche, G.; Lee, R. Y.; Matyjaszewski, K.**, 2005. Highly efficient "click" functionalization of poly(3-azidopropyl methacrylate) prepared by atrp. *Macromolecules* 38, (18), 7540-7545.

[211] **Gao, H.; Louche, G.; Sumerlin, B. S.; Jahed, N.; Golas, P.; Matyjaszewski, K.**, 2005. Gradient polymer elution chromatographic analysis of dihydroxypolystyrene synthesized via atrp and click chemistry. *Macromolecules* 38, (22), 8979-8982.

[212] **Gierlich, J.; Burley, G. A.; Gramlich, P. M. E.; Hammond, D. M.; Carell, T.**, 2006. Click chemistry as a reliable method for the high-density postsynthetic functionalization of alkyne-modified DNA. *Organic Letters* 8, (17), 3639-3642.

[213] **Vogt, A. P.; Sumerlin, B. S.**, 2006. An efficient route to macromonomers via atrp and click chemistry. *Macromolecules* 39, (16), 5286-5292.

[214] **Liu, Q.; Chen, Y.**, 2006. Synthesis of well-defined macromonomers by the combination of atom transfer radical polymerization and a click reaction. *Journal of Polymer Science Part A: Polymer Chemistry* 44, (20), 6103-6113.

[215] **Durmaz, H.; Dag, A.; Altintas, O.; Erdogan, T.; Hizal, G.; Tunca, U.**, 2007. One-pot synthesis of abc type triblock copolymers via in situ click [3+2] and diels-alder [4+2] reactions. *Macromolecules* 40, (2), 191-198.

[216] **Gao, H.; Matyjaszewski, K.**, 2006. Structural control in atrp synthesis of star polymers using the arm-first method. *Macromolecules* 39, (9), 3154-3160.

[217] **Altintas, O.; Hizal, G.; Tunca, U.**, 2006. Abc-type hetero-arm star terpolymers through “click” chemistry. *Journal of Polymer Science Part A: Polymer Chemistry* 44, (19), 5699-5707.

[218] **Joralemon, M. J.; O'Reilly, R. K.; Matson, J. B.; Nugent, A. K.; Hawker, C. J.; Wooley, K. L.**, 2005. Dendrimers clicked together divergently. *Macromolecules* 38, (13), 5436-5443.

[219] **Fernandez-Megia, E.; Correa, J.; RodrÃ-guez-Meizoso, I.; Riguera, R.**, 2006. A click approach to unprotected glycodendrimers. *Macromolecules* 39, (6), 2113-2120.

[220] **Tsarevsky, N. V.; Bencherif, S. A.; Matyjaszewski, K.**, 2007. Graft copolymers by a combination of atrp and two different consecutive click reactions. *Macromolecules* 40, (13), 4439-4445.

[221] **Gao, H.; Matyjaszewski, K.**, 2007. Synthesis of molecular brushes by "grafting onto" method: combination of atrp and click reactions. *Journal of the American Chemical Society* 129, (20), 6633-6639.

[222] **Joralemon, M. J.; O'Reilly, R. K.; Hawker, C. J.; Wooley, K. L.**, 2005. Shell click-crosslinked (scc) nanoparticles: a new methodology for synthesis and orthogonal functionalization. *Journal of the American Chemical Society* 127, (48), 16892-16899.

[223] **Jim, C. K. W.; Qin, A. J.; Lam, J. W. Y.; Haussler, M.; Tang, B. Z.**, 2007. Synthesis of ferrocene-containing polyacetylenes by click chemistry. *Journal of Inorganic and Organometallic Polymers and Materials* 17, (1), 289-293.

[224] **Voit, B.**, 2007. The potential of cycloaddition reactions in the synthesis of dendritic polymers. *New Journal of Chemistry* 31, (7), 1139-1151.

[225] **McElhanon, J. R.; Wheeler, D. R.**, 2001. Thermally responsive dendrons and dendrimers based on reversible furan-maleimide diels-alder adducts. *Organic Letters* 3, (17), 2681-2683.

[226] **Kose, M. M.; Yesilbag, G.; Sanyal, A.**, 2008. Segment block dendrimers via dielsâ^'alder cycloaddition. *Organic Letters* 10, (12), 2353-2356.

[227] **Morgenroth, F.; Reuther, E.; Müllen, K.**, 1997. Polyphenylene dendrimers: From three-dimensional to two-dimensional structures. *Angewandte Chemie International Edition in English* 36, (6), 631-634.

[228] **Szalai, M. L.; McGrath, D. V.; Wheeler, D. R.; Zifer, T.; McElhanon, J. R.**, 2007. Dendrimers based on thermally reversible furan maleimide diels-alder adducts. *Macromolecules* 40, (4), 818-823.

[229] **Durmaz, H.; Dag, A.; Hizal, A.; Hizal, G.; Tunca, U.**, 2008. One-pot synthesis of star-block copolymers using double click reactions. *Journal of Polymer Science Part A-Polymer Chemistry* 46, (21), 7091-7100.

[230] **Dag, A.; Durmaz, H.; Hizal, G.; Tunca, U.**, 2008. Preparation of 3-arm star polymers (a3) via diels–alder click reaction. *Journal of Polymer Science Part A: Polymer Chemistry* 46, (1), 302-313.

[231] **Dag, A.; Durmaz, H.; Tunca, U.; Hizal, G.**, 2009. Multiarm star block copolymers via diels-alder click reaction. *Journal of Polymer Science Part A: Polymer Chemistry* 47, (1), 178-187.

[232] **Durmaz, H.; Karatas, F.; Tunca, U.; Hizal, G.**, 2006. Preparation of abc miktoarm star terpolymer containing poly(ethylene glycol), polystyrene, and poly(tert-butylacrylate) arms by combining diels–alder reaction, atom transfer radical, and stable free radical polymerization routes. *Journal of Polymer Science Part A: Polymer Chemistry* 44, (1), 499-509.

[233] **Gacal, B.; Durmaz, H.; Tasdelen, M. A.; Hizal, G.; Tunca, U.; Yagci, Y.; Demirel, A. L.**, 2006. Anthracene-maleimide-based diels-alder "Click chemistry" As a novel route to graft copolymers. *Macromolecules* 39, (16), 5330-5336.

[234] **Sinnwell, S.; Inglis, A. J.; Davis, T. P.; Stenzel, M. H.; Barner-Kowollik, C.**, 2008. An atom-efficient conjugation approach to well-defined block copolymers using raft chemistry and hetero diels-alder cycloaddition. *Chemical Communications*, (17), 2052-2054.

[235] **Inglis, A.; Sinnwell, S.; Stenzel, M.; Barner-Kowollik, C.**, 2009. Ultrafast click conjugation of macromolecular building blocks at ambient temperature. *Angewandte Chemie International Edition* 48, (13), 2411-2414.

[236] **Nebhani, L.; Sinnwell, S.; Inglis, A. J.; Stenzel, M. H.; Barner-Kowollik, C.; Barner, L.**, 2008. Efficient surface modification of divinylbenzene microspheres via a combination of raft and hetero diels-alder chemistry. *Macromolecular Rapid Communications* 29, (17), 1431-1437.

[237] **Inglis, A. J.; Sinnwell, S.; Davis, T. P.; Barner-Kowollik, C.; Stenzel, M. H.**, 2008. Reversible addition fragmentation chain transfer (raft) and hetero-diels-alder chemistry as a convenient conjugation tool for access to complex macromolecular designs. *Macromolecules* 41, (12), 4120-4126.

[238] **Sinnwell, S.; Lammens, M.; Stenzel, M. H.; Du Prez, F. E.; Barner-Kowollik, C.**, 2009. Efficient access to multi-arm star block copolymers by a combination of atrp and raft-hda click chemistry. *Journal of Polymer Science Part A: Polymer Chemistry* 47, (8), 2207-2213.

[239] **Koo, S. P. S.; Stamenović, M. M.; Prasath, R. A.; Inglis, A. J.; Du Prez, F. E.; Barner-Kowollik, C.; Van Camp, W.; Junkers, T.**, Limitations of radical thiol-ene reactions for polymer–polymer conjugation. *Journal of Polymer Science Part A: Polymer Chemistry* 48, (8), 1699-1713.

[240] **Gao, C.; Yan, D.**, 2004. Hyperbranched polymers: From synthesis to applications. *Progress in Polymer Science* 29, (3), 183-275.

[241] **Teertstra, S. J.; Gauthier, M.**, 2004. Dendrigraft polymers: Macromolecular engineering on a mesoscopic scale. *Progress in Polymer Science* 29, (4), 277-327.

[242] **Wang, C. C.; Guo, Z. X.; Fu, S. K.; Wu, W.; Zhu, D. B.**, 2004. Polymers containing fullerene or carbon nanotube structures. *Progress in Polymer Science* 29, (11), 1079-1141.

[243] **Hadjichristidis, N.**, 2003. Polymer chemists/polymer physicists: A constructive partnership. *European Physical Journal E* 10, (1), 83-86.

[244] **Davis, K. A.; Matyjaszewski, K.**, 2002. Statistical, gradient, block, and graft copolymers by controlled/living radical polymerizations. *Advances in Polymer Science* 159, 1-169.

[245] **Mori, H.; Muller, A. H. E.**, 2003. New polymeric architectures with (meth)acrylic acid segments. *Progress in Polymer Science* 28, (10), 1403-1439.

[246] **Hadjichristidis, N.; Pitsikalis, M.; Pispas, S.; Iatrou, H.**, 2001. Polymers with complex architecture by living anionic polymerization. *Chemical Reviews* 101, (12), 3747-3792.

[247] **Kanaoka, S.; Sawamoto, M.; Higashimura, T.**, 1991. Star-shaped polymers by living cationic polymerization. 1. Synthesis of star-shaped polymers of alkyl and vinyl ethers. *Macromolecules* 24, (9), 2309-2313.

[248] **Zioga, A.; Sioula, S.; Hadjichristidis, N.**, 2000. Synthesis and morphology of model 3-miktoarm star terpolymers of styrene, isoprene and 2-vinyl pyridine. *Macromolecular Symposia* 157, 239-249.

[249] **Hückstädt, H.; Göpfert, A.; Abetz, V.**, 2000. Synthesis and morphology of abc heteroarm star terpolymers of polystyrene, polybutadiene and poly(2-vinylpyridine). *Macromolecular Chemistry and Physics* 201, (3), 296-307.

[250] **Beyer, F. L.; Gido, S. P.; Velis, G.; Hadjichristidis, N.; Tan, N. B.**, 1999. Morphological behavior of a5b miktoarm star block copolymers. *Macromolecules* 32, (20), 6604-6607.

[251] **Sioula, S.; Hadjichristidis, N.; Thomas, E. L.**, 1998. Novel 2-dimensionally periodic non-constant mean curvature morphologies of 3-miktoarm star terpolymers of styrene, isoprene, and methyl methacrylate. *Macromolecules* 31, (16), 5272-5277.

[252] **Floudas, G.; Reiter, G.; Lambert, O.; Dumas, P.**, 1998. Structure and dynamics of structure formation in model triarm star block copolymers of polystyrene, poly(ethylene oxide), and poly(ε-caprolactone). *Macromolecules* 31, (21), 7279-7290.

[253] **Pispas, S.; Hadjichristidis, N.; Potemkin, I.; Khokhlov, A.**, 2000. Effect of architecture on the micellization properties of block copolymers: A_2B miktoarm stars vs ab diblocks. *Macromolecules* 33, (5), 1741-1746.

[254] **Pispas, S.; Avgeropoulos, A.; Hadjichristidis, N.; Roovers, J.**, 1999. Hydrodynamic properties of A(8)B(8) type miktoarm (vergina) stars. *Journal of Polymer Science Part B-Polymer Physics* 37, (12), 1329-1335.

[255] **Vlahos, C.; Hadjichristidis, N.**, 1998. Second virial coefficient of axby miktoarm star copolymers in common good, and selective solvents. *Macromolecules* 31, (19), 6691-6696.

[256] **Lambert, O.; Jada, A.; Dumas, P.**, 1998. Adsorption of triarm starblock copolymers based on polystyrene, poly(ethylene oxide) and poly(epsilon-caprolactone) at the solid-solution interface. *Colloids and Surfaces a-Physicochemical and Engineering Aspects* 136, (3), 263-272.

[257] **Bellon-Maurel, V.; Calmon-Decriaud, A.; Chandrasekhar, V.; Hadjichristidis, N.; Mays, J.; Pispas, S.; Pitsikalis, M.; Silvestre, F.; Pitsikalis, M.; Pispas, S.; Mays, J.; Hadjichristidis, N.**, 1998. Nonlinear block copolymer architectures. In *Blockcopolymers - polyelectrolytes - biodegradation*, Springer Berlin / Heidelberg: Vol. 135, pp 1-137.

[258] **Roovers, J.; Hadjichristidis, N.; Pispas, S.; Pitsikalis, M.; Iatrou, H.; Vlahos, C.**, 1999. Asymmetric star polymers: Synthesis and properties. In *Branched polymers i*, Springer Berlin / Heidelberg: Vol. 142, pp 71-127.

[259] **Hadjichristidis, N.**, 1999. Synthesis of miktoarm star (μ-star) polymers. *Journal of Polymer Science Part A: Polymer Chemistry* 37, (7), 857-871.

[260] **Yamauchi, K.; Takahashi, K.; Hasegawa, H.; Iatrou, H.; Hadjichristidis, N.; Kaneko, T.; Nishikawa, Y.; Jinnai, H.; Matsui, T.; Nishioka, H.; Shimizu, M.; Furukawa, H.**, 2003. Microdomain morphology in an abc 3-miktoarm star terpolymer: a study by energy-filtering tem and 3d electron tomography. *Macromolecules* 36, (19), 6962-6966.

[261] **Mavroudis, A.; Avgeropoulos, A.; Hadjichristidis, N.; Thomas, E. L.; Lohse, D. J.**, 2003. Synthesis and morphological behavior of model linear and miktoarm star copolymers of 2-methyl-1,3-pentadiene and styrene. *Chemistry of Materials* 15, (10), 1976-1983.

[262] **Li, Z. B.; Hillmyer, M. A.; Lodge, T. P.**, 2006. Morphologies of multicompartment micelles formed by abc miktoarm star terpolymers. *Langmuir* 22, (22), 9409-9417.

[263] **Khan, I. M.; Gao, Z.; Khougaz, K.; Eisenberg, A.**, 1992. Synthesis of three-arm poly(styrene-arm-styrene-arm-2-vinylpyridine) star copolymers. *Macromolecules* 25, (11), 3002-3004.

[264] **Guo, Y. M.; Xu, J.; Pan, C. Y.**, 2001. Block and star block copolymers by mechanism transformation. Iv. Synthesis of s-(pst)2(pdop)2 miktoarm star copolymers by combination of atrp and crop. *Journal of Polymer Science Part A: Polymer Chemistry* 39, (3), 437-445.

[265] **Cai, Y.; Armes, S. P.**, 2004. Synthesis of well-defined y-shaped zwitterionic block copolymers via atom-transfer radical polymerization. *Macromolecules* 38, (2), 271-279.

[266] **Cho, D.; Park, S.; Chang, T.; Avgeropoulos, A.; Hadjichristidis, N.**, 2003. Characterization of a 4-miktoarm star copolymer of the (ps-b-pi)3 ps type by temperature gradient interaction chromatography. *European Polymer Journal* 39, (11), 2155-2160.

[267] **Kricheldorf, H. R.; Kreiser-Saunders, I.; Stricker, A.**, 2000. Polylactones 48. Snoct2-initiated polymerizations of lactide: A mechanistic study. *Macromolecules* 33, (3), 702-709.

[268] **Fragouli, P.; Iatrou, H.; Hadjichristidis, N.; Sakurai, T.; Matsunaga, Y.; Hirao, A.**, 2006. Synthesis of well-defined miktoarm star polymers of poly(dimethylsiloxane) by the combination of chlorosilane and benzyl chloride linking chemistry. *Journal of Polymer Science Part A: Polymer Chemistry* 44, (22), 6587-6599.

[269] **Tunca, U.; Ozyurek, Z.; Erdogan, T.; Hizal, G.**, 2004. Novel miktofunctional initiator for the preparation of an abc-type miktoarm star polymer via a combination of controlled polymerization techniques. *Journal of Polymer Science Part a-Polymer Chemistry* 42, (17), 4228-4236.

[270] **Zhao, Y.; Higashihara, T.; Sugiyama, K.; Hirao, A.**, 2006. Synthesis of asymmetric star-branched polymers having two polyacetylene arms by means of living anionic polymerization using 1,1-diphenylethylene derivatives. *Macromolecules* 40, (2), 228-238.

[271] **Zhang, W.; Zhu, J.; Zhang, Z.; Zhu, X.**, 2009. Controlled synthesis of ph-responsive amphiphilic a2b2 miktoarm star block copolymer by combination of set-lrp and raft polymerization. *Journal of Polymer Science Part A: Polymer Chemistry* 47, (24), 6908-6918.

[272] **Priftis, D.; Pitsikalis, M.; Hadjichristidis, N.**, 2007. Miktoarm star copolymers of poly(ϵ-caprolactone) from a novel heterofunctional initiator. *Journal of Polymer Science Part A: Polymer Chemistry* 45, (22), 5164-5181.

[273] **Breland, L. K.; Storey, R. F.**, 2008. Polyisobutylene-based miktoarm star polymers via a combination of carbocationic and atom transfer radical polymerizations. *Polymer* 49, (5), 1154-1163.

[274] **Heise, A.; TrollsÃ¥s, M.; Magbitang, T.; Hedrick, J. L.; Frank, C. W.; Miller, R. D.**, 2001. Star polymers with alternating arms from miktofunctional initiators using consecutive atom transfer radical polymerization and ring-opening polymerization. *Macromolecules* 34, (9), 2798-2804.

[275] **Wang, G.; Huang, J.**, 2008. Synthesis and characterization of well-defined abc 3-miktoarm star-shaped terpolymers based on poly(styrene), poly(ethylene oxide), and poly(ϵ-caprolactone) by combination of the "living" anionic polymerization with the ring-opening polymerization. *Journal of Polymer Science Part A: Polymer Chemistry* 46, (3), 1136-1150.

[276] **Miura, Y.; Sakai, Y.; Yamaoka, K.**, 2005. Synthesis of ab(2) 3- and ab(4) 5-miktoarm star copolymers initiated from dendritic tri- and penta-functional initiators by combination of ring-opening polymerization of epsilon-caprolactone and nitroxide-mediated radical polymerization of styrene. *Macromolecular Chemistry and Physics* 206, (4), 504-512.

[277] **Celik, C.; Hizal, G.; Tunca, U.**, 2003. Synthesis of miktoarm star and miktoarm star block copolymers via a combination of atom transfer radical polymerization and stable free-radical polymerization. *Journal of Polymer Science Part A: Polymer Chemistry* 41, (16), 2542-2548.

[278] **Yamazaki, Y.; Ajioka, N.; Yokoyama, A.; Yokozawa, T.**, 2009. Synthesis of well-defined miktoarm star copolymers of aromatic polyether and polystyrene by chain-growth condensation polymerization and atom transfer radical polymerization. *Macromolecules* 42, (3), 606-611.

[279] **Liu, C.; Zhang, Y.; Huang, J.**, 2007. Well-defined star polymers with mixed-arms by sequential polymerization of atom transfer radical polymerization and reverse additionâˆ'fragmentation chain transfer on a hyperbranched polyglycerol core. *Macromolecules* 41, (2), 325-331.

[280] **Erdogan, T.; Gungor, E.; Durmaz, H.; Hizal, G.; Tunca, U.**, 2006. Photoresponsive poly(methyl methacrylate)(2)-(polystyrene)(2) miktoarm star copolymer containing an azobenzene moiety at the core. *Journal of Polymer Science Part A-Polymer Chemistry* 44, (4), 1396-1403.

[281] **Li, C.; Ge, Z.; Liu, H.; Liu, S.**, 2009. Synthesis of amphiphilic and thermoresponsive abc miktoarm star terpolymer via a combination of consecutive click reactions and atom transfer radical polymerization. *Journal of Polymer Science Part A: Polymer Chemistry* 47, (16), 4001-4013.

[282] **Gungor, E.; Bilir, C.; Hizal, G.; Tunca, U.**, 2010. Multiarm star polymers with poss at the periphery. *Journal of Polymer Science Part A: Polymer Chemistry* 48, (21), 4835-4841.

[283] **Durmaz, H.; Dag, A.; Gursoy, D.; Demirel, A. L.; Hizal, G.; Tunca, U.**, 2010. Multiarm star triblock terpolymers via sequential double click reactions. *Journal of Polymer Science Part A-Polymer Chemistry* 48, (7), 1557-1564.

[284] **Durmaz, H.; Dag, A.; Erdogan, E.; Demirel, A. L.; Hizal, G.; Tunca, U.**, 2010. Multiarm star block and multiarm star mixed-block copolymers via azide-alkyne click reaction. *Journal of Polymer Science Part A-Polymer Chemistry* 48, (1), 99-108.

[285] **Dag, A.; Durmaz, H.; Kirmizi, V.; Hizal, G.; Tunca, U.**, 2010. An easy way to the preparation of multi-miktoarm star block copolymers via sequential double click reactions. *Polymer Chemistry* 1, (5), 621-623.

[286] **Altintas, O.; Hizal, G.; Tunca, U.**, 2008. Abcd 4-miktoarm star quarterpolymers using click [3 + 2] reaction strategy. *Journal of Polymer Science Part A: Polymer Chemistry* 46, (4), 1218-1228.

[287] **Altintas, O.; Demirel, A. L.; Hizal, G.; Tunca, U.**, 2008. Dendrimer-like miktoarm star terpolymers: A3-(b-c)3 via click reaction strategy. *Journal of Polymer Science Part A: Polymer Chemistry* 46, (17), 5916-5928.

[288] **Gungor, E.; Bilir, C.; Durmaz, H.; Hizal, G.; Tunca, U.**, 2009. Star polymers with poss via azide-alkyne click reaction. *Journal of Polymer Science Part a-Polymer Chemistry* 47, (22), 5947-5953.

[289] **Altintas, O.; Yankul, B.; Hizal, G.; Tunca, U.**, 2007. One-pot preparation of 3-miktoarm star terpolymers via click [3 + 2] reaction. *Journal of Polymer Science Part A: Polymer Chemistry* 45, (16), 3588-3598.

[290] **Gungor, E.; Hizal, G.; Tunca, U.**, 2008. A(2)b(2) type miktoarm star copolymers via alkyne homocoupling reaction. *Journal of Polymer Science Part a-Polymer Chemistry* 46, (20), 6703-6711.

[291] **Christodoulou, S.; Driva, P.; Iatrou, H.; Hadjichristidis, N.**, 2008. Synthesis and micellization behavior of janus H-shaped a2bc2 terpolymers. *Macromolecules* 41, (7), 2607-2615.

[292] **Hadjichristidis, N.; Iatrou, H.; Pitsikalis, M.; Pispas, S.; Avgeropoulos, A.**, 2005. Linear and non-linear triblock terpolymers. Synthesis, self-assembly in selective solvents and in bulk. *Progress in Polymer Science* 30, (7), 725-782.

[293] **Knauss, D. M.; Huang, T.**, 2002. Star-block-linear-block-star triblock (pom-pom) polystyrene by convergent living anionic polymerization. *Macromolecules* 35, (6), 2055-2062.

[294] **Knauss, D. M.; Huang, T.**, 2003. ((ps)nps)m star-shaped polystyrene with star-shaped branches at the terminal chain ends by convergent living anionic polymerization. *Macromolecules* 36, (16), 6036-6042.

[295] **Haraguchi, N.; Hirao, A.**, 2003. Synthesis of well-defined star-linear block polystyrenes by coupling reaction of chain-functionalized polystyrenes with a definite number of benzyl bromide moieties with polystyryllithiums. *Macromolecules* 36, (25), 9364-9372.

[296] **Lee, J. S.; Quirk, R. P.; Foster, M. D.**, 2005. Synthesis and characterization of well-defined, regularly branched polystyrenes utilizing multifunctional initiators. *Macromolecules* 38, (13), 5381-5392.

[297] **Tao, L.; Luan, B.; Pan, C. Y.**, 2003. Block and star block copolymers by mechanism transformation. synthesis and characterization of triblock poly(lla-b-st-b-mma) by combination of atrp and rop. *Polymer* 44, (4), 1013-1020.

[298] **Yuan, J.-Y.; Pan, C.-Y.; Tang, B. Z.**, 2000. "Living" free radical ring-opening polymerization of 5,6-benzo-2-methylene-1,3-dioxepane using the atom transfer radical polymerization method. *Macromolecules* 34, (2), 211-214.

[299] **Feng, X.-S.; Pan, C.-Y.**, 2002. Synthesis of amphiphilic miktoarm abc star copolymers by raft mechanism using maleic anhydride as linking agent. *Macromolecules* 35, (13), 4888-4893.

[300] **Johnson, R. M.; Fraser, C. L.**, 2004. Iron tris(bipyridine)-centered star block copolymers: chelation of triblock macroligands generated by rop and atrp. *Macromolecules* 37, (8), 2718-2727.

[301] **Lutz, J.-F. o.; Neugebauer, D.; Matyjaszewski, K.**, 2003. Stereoblock copolymers and tacticity control in controlled/living radical polymerization. *Journal of the American Chemical Society* 125, (23), 6986-6993.

[302] **Tong, J.-D.; Zhou, C.; Ni, S.; Winnik, M. A.**, 2001. Synthesis of meth(acrylate) diblock copolymers bearing a fluorescent dye at the junction using a hydroxyl-protected initiator and the combination of anionic polymerization and controlled radical polymerization. *Macromolecules* 34, (4), 696-705.

[303] **Francis, R.; Taton, D.; Logan, J. L.; Masse, P.; Gnanou, Y.; Duran, R. S.**, 2003. Synthesis and surface properties of amphiphilic star-shaped and dendrimer-like copolymers based on polystyrene core and poly(ethylene oxide) corona. *Macromolecules* 36, (22), 8253-8259.

[304] **Li, Y. G.; Shi, P. J.; Pan, C. Y.**, 2004. Synthesis, characterization, and thermal behavior of h-shaped copolymers prepared by atom transfer radical polymerization. *Macromolecules* 37, (14), 5190-5195.

[305] **Han, D. H.; Pan, C. Y.**, 2006. Simple route for synthesis of h-shaped copolymers. *Journal of Polymer Science Part A: Polymer Chemistry* 44, (9), 2794-2801.

[306] **Han, D. H.; Pan, C. Y.**, 2007. Preparation and characterization of heteroarm h-shaped terpolymers by combination of reversible addition-fragmentation transfer polymerization and ring-opening polymerization. *Journal of Polymer Science Part A: Polymer Chemistry* 45, (5), 789-799.

[307] **Whittaker, M. R.; Urbani, C. N.; Monteiro, M. J.**, 2006. Synthesis of 3-miktoarm stars and 1st generation mikto dendritic copolymers by "living" radical polymerization and "click" chemistry. *Journal of the American Chemical Society* 128, (35), 11360-11361.

[308] **Hawker, C. J.; Barclay, G. G.; Orellana, A.; Dao, J.; Devonport, W.**, 1996. Initiating systems for nitroxide-mediated "living" free radical polymerizations: Synthesis and evaluation. *Macromolecules* 29, (16), 5245-5254.

[309] **Karanam, S.; Goossens, H.; Klumperman, B.; Lemstrat, P.**, 2003. "Controlled" Synthesis and characterization of model methyl methacrylate/tert-butyl methacrylate triblock copolymers via atrp. *Macromolecules* 36, (9), 3051-3060.

[310] **Mantovani, G.; Lecolley, F.; Tao, L.; Haddleton, D. M.; Clerx, J.; Cornelissen, J. J. L. M.; Velonia, K.**, 2005. Design and synthesis of n-maleimido-functionalized hydrophilic polymers via copper-mediated living radical polymerization: A suitable alternative to pegylation chemistry. *Journal of American Chemical Society* 127, (9), 2966-2973.

[311] **Erdogan, M.; Hizal, G.; Tunca, U.; Hayrabetyan, D.; Pekcan, O.**, 2002. Molecular weight effect on swelling of polymer gels in homopolymer solutions: A fluorescence study. *Polymer* 43, (6), 1925-1931.

[312] **Lee, S.-H.; Kim, S. H.; Han, Y.-K.; Kim, Y. H.**, 2002. Synthesis and characterization of poly(ethylene oxide)/polylactide/poly(ethylene oxide) triblock copolymer. *Journal of Polymer Science Part A: Polymer Chemistry* 40, (15), 2545-2555.

[313] **Ihre, H.; Hult, A.; Frechet, J. M. J.; Gitsov, I.**, 1998. Double-stage convergent approach for the synthesis of functionalized dendritic aliphatic polyesters based on 2,2-bis(hydroxymethyl)propionic acid. *Macromolecules* 31, (13), 4061-4068.

[314] **Hawker, C. J.; Frechet, J. M. J.**, 1992. Unusual macromolecular architectures: The convergent growth approach to dendritic polyesters and novel block copolymers. *Journal of the American Chemical Society* 114, (22), 8405-8413.

[315] **Vion, J. M.; Jerome, R.; Teyssie, P.; Aubin, M.; Prudhomme, R. E.**, 1986. Synthesis, characterization, and miscibility of caprolactone random copolymers. *Macromolecules* 19, (7), 1828-1838.

[316] **Dubois, P.; Ropson, N.; Jerome, R.; Teyssie, P.**, 1996. Macromolecular engineering of polylactones and polylactides. 19. Kinetics of ring-opening polymerization of îµ-caprolactone initiated with functional aluminum alkoxides. *Macromolecules* 29, (6), 1965-1975.

[317] **Riva, R.; Schmeits, S.; Jerome, C.; Jerome, R.; Lecomte, P.**, 2007. Combination of ring-opening polymerization and "Click chemistry": Toward functionalization and grafting of poly(epsilon-caprolactone). *Macromolecules* 40, (4), 796-803.

[318] **Luo, X.; Wang, G.; Pang, X.; Huang, J.**, 2008. Synthesis of a novel kind of amphiphilic graft copolymer with miktoarm star-shaped side chains. *Macromolecules* 41, (7), 2315-2317.

CURRICULUM VITAE

Candidate's full name : Eda GÜNGÖR

Place and date of birth : Istanbul, 17/07/1982

Permanent Address : Istanbul, Turkey

Universities and Colleges attended:

2006-2011 *Philosophy of Doctorate* (Polymer Science and Technology), Istanbul Technical University, Istanbul, Turkey.

2004-2006 *Master of Science* (Polymer Science and Technology), Istanbul Technical University, Istanbul, Turkey

1999–2003 *Bachelor of Science* (Chemistry), Trakya University, Edirne, Turkey

1996-1999 Sehremini High school, Istanbul, Turkey

Publications:

- Multiarm Star Polymers with POSS at the Periphery, **E. Gungor**, C. Bilir, G. Hizal**,** U. Tunca, *J. Polym Sci, Part A Poly. Chem. Ed.*, 48, 4835-4841 (**2010**).
- Star polymers with POSS via Azide-Alkyne Click Reaction, **E. Gungor**, C. Bilir, H. Durmaz, G. Hizal**,** U. Tunca, *J. Polym Sci, Part A Poly. Chem. Ed.*, 47, 5947-5953 (**2009**).
- One-pot Double Click Reactions for the Preparation of H-Shaped ABCDE-Type Quintopolymer, **E. Gungor**, G. Hizal**,** U. Tunca, *J. Polym Sci, Part A Poly. Chem. Ed.*, 47, 3409–3418 (**2009**)
- A_2B_2 Type Miktoarm Star Copolymers via Alkyne Homocoupling Reaction, **E. Gungor**, G. Hizal**,** U. Tunca, *J. Polym Sci, Part A Poly. Chem. Ed.*, 46, 6703-6711 (**2008**).
- H-Shaped (ABCDE Type) Quintopolymer via Click Reaction [3+2] Strategy, **E. Gungor**, H. Durmaz, G. Hizal**,** U. Tunca, *J. Polym Sci, Part A Poly. Chem. Ed.*, 46, 4459-4468 (**2008**).

- Heteroarm H-Shaped Terpolymers Through Click Reaction, **E. Gungor**, G. Cote, T. Erdogan, H. Durmaz, A. L. Demirel, G. Hizal**,** U. Tunca, *J. Polym Sci, Part A Poly. Chem. Ed.*, 45, 1055–1065 (**2007**)
- Photoresponsive (poly(methyl methacrylate)$_2$-(polystyrene)$_2$, (PMMA)$_2$-(PSt)$_2$, Miktoarm Star Copolymer Containing an Azobenzene Moiety at the Core, T. Erdogan, **E. Gungor**, H. Durmaz, G. Hizal**,** U. Tunca, *J. Polym Sci, Part A Poly. Chem. Ed.*, 44, 1396-1403 (**2006**).